Univerzita Karlova v Praze
Přírodovědecká fakulta

Studijní program: Imunologie

Mgr. Jarmila Králová

New leukocyte membrane adaptor proteins
Nové membránové adaptorové proteiny leukocytů

Doktorská dizertační práce

Školitel:

Mgr. Tomáš Brdička, Ph.D.
Laboratoř leukocytární signalizace
Ústav molekulární genetiky, AV ČR

Praha, 2018

Prohlášení

Prohlašuji, že jsem závěrečnou práci vypracovala samostatně a uvedla jsem veškeré použité informační zdroje a literaturu. Tato práce ani žádná její část nebyla předložena k získání jiného nebo stejného akademického titulu.

V Praze 20.9.2018

Acknowledgement

My special thanks go to Dr. Tomáš Brdička, for his guidance and help and kind personal approach. Further, I would like to thank to all my colleagues for their contribution to the articles in this thesis, as well as for a very pleasant and stimulating working atmosphere. I also thank to Prof. Václav Hořejší for his support and Dr. Meritxell Alberich Jorda and her laboratory for a friendly and collaborative approach when sharing laboratory space.

1. Content

2. Abstract

Membrane adaptor proteins are characterized by the lack of enzymatic activity and the presence of various interaction sites for other proteins and cellular membranes. They typically function as scaffolds connecting receptors or other adaptors with proximal signaling molecules at cellular membranes. Their overall effects on signaling can be activating or inhibiting depending on the nature of the effector molecules they recruit.

SCIMP is one of the membrane adaptors discussed in this thesis. It is expressed in antigen-presenting cells and it has been previously shown to enhance MHCII signaling in B cells. This thesis covers the analysis of SCIMP functions beyond B cells and describes the first analysis of SCIMP deficient mice. Although the results of this analysis did not show any alterations in immune cell populations, the novel function of SCIMP in dendritic cell signaling downstream of DECTIN-1 was uncovered. DECTIN-1 is a pattern recognition receptor involved in antifungal immunity. The data presented in this thesis describe the role of SCIMP in sustaining DECTIN-1 signaling over relatively long periods of time and the contribution of SCIMP signaling to maintaining prolonged production of pro-inflammatory cytokines.

PSTPIP2 is another interesting adaptor discussed in this thesis. It is expressed in myeloid cell lineage and is crucial for the regulation of inflammatory responses. Unlike SCIMP deficient mice, mice with mutation in PSTPIP2 are well characterized and develop autoinflammatory osteomyelitis (CMO). As a typical adaptor, PSTPIP2 can bind more interaction partners at once. We identified three novel PSTPIP2-binding proteins, including two important inhibitory phosphatases (SHIP1 and PEST family phosphatase PEP/LYP) and an inhibitory kinase CSK. In addition, we found a role for PSTPIP2 in the regulation of reactive oxygen species in primary murine granulocytes. This regulation proved to be physiologically important for the prevention of inflammatory bone damage during the course of the disease in the CMO mouse strain.

3. Abstrakt

Membránové adaptorové proteiny nemají samy o sobě žádnou enzymatickou aktivitou. Je však pro ně typická přítomnost různých interakčních domén umožňujících vazbu na další proteiny a buněčné membrány. Jejich funkcí je spojovat receptory nebo jiné adaptory s proximálními signalizačními molekulami. Zda jejich vliv na přenos signálu bude aktivační nebo inhibiční závisí zejména na povaze efektorových molekul, které váží.

Jedním z membránových adaptorových proteinů, kterými se zabývá tato práce je adaptor SCIMP. Je exprimován v buňkách prezentujících antigen a zesiluje signalizaci MHCII v B buňkách. Tato dizertační práce se zabývá analýzou funkce proteinu SCIMP v primárních myších B lymfocytech a v dalších buňkách prezentujících antigen. Její hlavní součástí je podrobná analýza SCIMP deficientních myší. I přesto, že změny v zastoupení imunitních buněčných populací u SCIMP deficientních myší nebyly signifikantní, podařilo se nám najít funkci proteinu SCIMP v dendritických buňkách, kde se uplatňuje jako signalizační adaptor v dráze receptoru DECTIN-1 důležitého pro antifungální imunitu. Data prezentovaná v této práci popisují signalizaci zprostředkovanou adaptorem SCIMP v pozdních časových bodech aktivace receptoru DECTIN-1, která je také důležitá pro produkci anti-fungálních cytokinů.

Dalším zajímavým adaptorovým proteinem diskutovaným v této práci je PSTPIP2. PSTPIP2 je exprimován v myeloidní buněčné linii a plní důležitou funkci v regulaci zánětlivé odpovědi. Na rozdíl od myší s deficiencí v adaptoru SCIMP, myši kmene CMO s mutací v PSTPIP2 jsou dobře charakterizovány a dochází u nich k rozvoji autoinflmatorní osteomyelitidy (CMO). Jako typický adaptorový protein může PSTPIP2 vázat více interakčních partnerů najednou. Nám se podařilo identifikovat tři nové vazebné partnery proteinu PSTPIP2, dvě důležité inhibiční fosfatázy (SHIP1 a fosfatázu z PEST rodiny LYP/PEP) a inhibiční kinázu CSK. Kromě toho jsme objevili novou funkci PSTPIP2 při regulaci produkce reaktivních kyslíkových intermediátů u primárních myších granulocytů. Tato regulace se ukázala jako fyziologicky důležitá pro zabránění rozvoji zánětlivého poškození kostí doprovázejícího autoinflamatorní osteomyelitidu u myšího kmene CMO.

4. Introduction

4.1. Mechanisms of infection sensing by innate immune system

4.1.1. Innate immune system characteristics

Immune system is critical for host defense against various pathogens, as well as for tissue homeostasis. Innate immune system represents its oldest part. It is found already in the primitive multicellular organisms, plants, fungi and all metazoans [1] [2] [3]. Innate immune cells form the first and fast line of defense against pathogens. Innate immune cells generally do not possess highly specific receptors distinguishing individual pathogen species, but they sense more ubiquitous structures present in whole groups of them (eg. lipopolysacharide from gram-negative bacteria, fungal cell wall components, viral double stranded RNA etc.)[4]. Important feature of the innate immunity is the recognition of self from non-self, or altered self [5]. To achieve this, innate immune system employs an array of specialized receptors called pattern recognition receptors (PRRs). Other general characteristic of the innate immune system is the absence of immunological memory. However, this concept is currently being revised as a few exceptions emerged [6] [7]. The memory of innate immune cells is now described by a term "trained immunity" and has been first studied in the context of NK cells [8] [9] [10]. However, this type of memory is more general and present in other innate immune cells as well [11] [12].

4.1.2. Pattern recognition receptors (PRRs)

Innate immune cells sense infection by their pattern recognition receptors, which recognize common structural and molecular features of various classes of pathogens called pathogen-associated molecular patterns (PAMPs). On a similar basis, PRRs also sense damage-associated molecular patterns (DAMPs), which are host intracellular molecules released during cell death, damage or stress [13]. PRR activations trigger signaling cascades leading to phagocytosis, production of reactive oxygen species (ROS) and transcription of proteins important for host defense against pathogens [14] [15] [16]. Among them, pro-inflammatory cytokines are the most important. Their effect is often pleiotropic. They, for example, induce migration to the site of inflammation, enhance phagocytosis and killing of

infectious agents and activate anti-infection immunity in cells that have not encountered the infection yet [17] [18]. Dysregulation or improper activation of PRRs can lead to diseases (e.g. chronic inflammatory conditions, autoimmunity or immunodeficiency) or life-threatening complications of infections (e.g. septic shock) [19] [20]. In the following chapters I will briefly describe four main families of PRRs: Toll-like receptors (TLRs), C-type lectin receptors, NOD-like receptors (NLRs), and (RIG- I)-like receptors (RLR), with emphasis on their physiological importance in anti-infection defense.

Toll-like receptors (TLRs)

TLRs were the first discovered PRRs. In mice, 12 distinct TLRs (TLR1-9, TLR11-TLR13) have been identified, while humans have just 10 (TLR1-TLR10) [21] [22]. They are broadly expressed in both immune cells and non-immune tissues. TLRs can be divided into two groups according to their localization: plasma membrane localized TLRs (TLR1, TLR2, TLR4-6, TLR10-13) or endosomal TLRs (TLR3, TLR7, TLR8 and TLR9) [21]. Variety of PAMPs sensed by TLRs is huge, ranging from lipopolysaccharide of Gramm negative bacteria, peptidoglycan from Gramm positive bacteria, β-Glucan and mannan from fungal cell walls to viral DNA/RNA, heat shock proteins and many others [4] [23]. Structure of TLRs is characterized by an extracellular/luminal ligand-binding domain containing leucine-rich repeat (LRR) motifs and a cytoplasmic signaling Toll/interleukin-1 (IL-1) receptor homology (TIR) domain [24]. TLR signaling is important for synthesis and secretion of pro-inflammatory and antiviral cytokines such as TNF-α, IL-1β, IL-12, IL-6, IL-10 and interferons [25] [26] [27], antimicrobial peptides [28] and expression of adhesion molecules [29]. TLRs are thus crucial part of the innate immunity. Additionally, by promoting antigen-presentation they enhance adaptive immunity as well [30]. Clinical importance of TLRs is substantiated by the effects of various mutations or deficiencies in TLRs or their signaling components in mice and humans. As an example, patients with mutations in MYD88 adaptor protein or IRAK4, which are common signaling components downstream of most TLRs, are highly susceptible to invasive bacterial infections by *S. pneumoniae, S. aureus*, and *P. aeruginosa* occurring before the 2nd year of life [31]. These patients are usually life-long treated with prophylactic antibiotics even though bacterial infections may be less invasive with older age [32].

C-type lectin receptors (CLRs)

CLRs were originally described as calcium dependent lectin (carbohydrate-binding) proteins. They contain the carbohydrate recognition domain C-type lectin domain (CTLD) which is present in all of these PRRs [33]. However, the binding of many proteins containing CTLD seems to be not dependent on calcium and/or their carbohydrate ligand is not known. CLRs are mostly studied for their involvement in antifungal immunity [34] [35], although they can recognize other pathogens as well [36] (e.g. *Leishmania* [37], *Mycobacterium tuberculosis* [38] *or Salmonella* [39]).

The best characterized CLRs include DECTIN-1 and DECTIN-2, CLEC9A (DNGR-1), MCL, mannose receptor (MR), Mincle and DC-SIGN. Although they recognize different ligands, they share similarities in their signaling cascades that result in phagocytosis, ROS production, cytokine release (e.g. IL-1β , IL-6, IL-12, IL-17) and synthesis of proteins involved in antifungal and antibacterial responses [40] [41]. Probably the most studied receptor in this group is DECTIN-1. Patients bearing mutation in CTLD region of DECTIN-1 gene suffer from recurrent mucocutaneous fungal infections and are hyporesponsive to *C. albicans* [42]. Mutations in CARD9, an important signaling adaptor for many CLRs, have even more serious manifestations in affected humans. Clinical picture ranges from mucosal fungal infections to lethal systemic fungal infections caused by commensal species like *Candida* or *Exophiala* [43] [44] [45].

Retinoic acid-inducible gene I (RIG- I)-like receptors (RLRs)

RLRs recognize viral antigens based on viral PAMPs and their activation mounting type I interferon response is important for anti-viral defense. RLRs comprise three members (RIG-I, MDA5, LGP2) which all recognize viral RNA or DNA in the cytoplasm [46]. RIG-I and MDA5 are activating, while LGP2 functions as a negative regulator of RIG-I signaling [47]. High levels of interferons are implicated in the development of autoimmunity [48]. Type I interferon transcriptional signatures were reported for type 1 diabetes, systemic lupus erythematosus and other autoimmune diseases [49] [50]. Single-nucleotide polymorphisms of gene encoding MDA5 are associated with a risk of autoimmune diseases [51]. Mice with gain of function mutations in MDA5 suffer from lupus-like symptoms [52].

NOD-like receptors (NLRs)

NLR family contains many PRRs sensing strictly intracellular PAMPs. The Structure of NLRs consists of nucleotide binding oligomerization domain (NOD or NACHT) promoting signaling via oligomerization, leucine-rich repeats (LRR) for PAMP recognition and an N-terminal protein-protein interaction domain [53] [54]. The N-terminal domain contains either the caspase recruitment domain (CARD), pyrin domain (PYD), or the baculovirus inhibitor domain (BIR) to recruit signaling molecules [55]. NOD1 and NOD2 were the first described NLRs [56]. They sense bacterial peptidoglycan and are involved in autophagy as well [54]. As there are more than 30 NLR genes in mice [57], they can respond to many different PAMPs varying from bacterial muramyl dipeptide (MDP), RNA/DNA of viruses, fungal β-glucans to cell metabolites [58] [59].

Some of the NLRs form a multiprotein cytoplasmic complex involved in the processing of pro-inflammatory cytokines from the IL-1β family. As IL-1β is a very potent mediator of inflammation, its upregulation is described in variety of human diseases ranging from localized diseases such as osteoarthritis to systemic diseases such as familial mediterranean fever or PAPA syndrome [60]. Elevated IL-1β levels are often caused by activating mutations in NLRs or inflammasome signaling components. Diseases associated with these mutations are called autoinflammatory diseases and I will describe them in more detail in the chapter 4.4. [61].

4.2. Leukocyte signaling

Leukocyte signaling or signal transduction is one of the key processes that enable leukocytes to adequately react to extracellular signals. It encompasses processes occurring after ligand recognition by the receptor that connect it to the cellular response to this stimulus.

4.2.1. Basic principles of signal transduction

Signal transduction from the extracellular immune receptors involves the transmission of information about the ligand recognition through the plasma membrane towards the cytoplasm, where signaling effector molecules are activated. This is followed by a cascade of events leading to changes in gene expression, metabolic activity, and cell behavior. However, many PRRs are located in intracellular vesicles (TLRs) or cytoplasmatically (RLRs and NLRs). Signaling from these receptors is analogous, only the place of stimulus recognition is different [4].

The proximal effector molecules are typically activated by phosphorylation, ubiquitinations or by homotypic interactions (e.g. via DD, CARD, PYD domains). These modifications/interactions are at the beginning of signaling cascades, leading to the recruitment of other proteins with specific functions further propagating the signaling [62].

Phosphorylation is a posttranslational protein modification executed by protein kinases. Proximal parts of immune signaling rely mainly on tyrosine phosphorylations, while serine/threonine phosphorylations play roles in later steps when the signal is propagated or translated into activation of specific transcription factors. Activation of protein tyrosine kinases is thus the key for initiation of signaling cascades leading to appropriate responses to stimuli. These kinases are either integral parts of the signaling receptors [63, 64] or are non-covalently associated with receptors. In both cases, protein tyrosine kinases are activated by dimerization or oligomerization of the receptor or by conformational changes as a consequence of ligand binding. Signaling mediated by protein tyrosine kinases is essential in TCR or BCR signaling or signaling via DECTIN-1, and other CLRs.

Ubiquitination is another important posttranslational protein modification in signal transduction. Ubiquitin is a small protein that can be conjugated to the lysine residue of target

protein. The process of ubiquitination involves three enzymes: ubiquitin-activating enzymes (E1s), ubiquitin-conjugating enzymes (E2s) and ubiquitin ligases (E3s), which transfer ubiquitin to a target protein. E3-ubiquitin ligases that belong to RING or HECT family are often found in signaling complexes [65]. Outcome of ubiquitination depends on which lysine residue is modified and nature of ubiquitin chain (monoubiquitination vs. polyubiquitin chains). Ubiquitinated proteins are recognized by ubiquitin-binding domains (UBDs) of interacting proteins that further propagate signaling. Ubiquitination-dependent interactions are involved in TLRs, RLRs as well as in NLR-mediated signaling [66]. Moreover, ubiquitination plays an important role in activation of NF-κB, which is transcription factor activated by various PRRs and by pro-inflammatory cytokines (IL-1β and TNFα) [67].

Besides phosphorylation and ubiquitination, proximal signaling can be initiated by homotypic interactions of certain protein domains. Proteins containing death domain (DD), caspase recruitment domain (CARD), pyrin domain (PYD) or death effector domain (DED) are classical examples of proteins undergoing such interactions [62]. This type of activation is important in signaling via the TNF receptor superfamily, as well as for the assembly of the inflammasome complex.

Further signal propagation includes amplification of signal by other kinases, phosphatases, ubiquitin ligases, phospholipases, GTPases, caspases and other proteins with specific enzymatic activities. Increased levels of second messengers (e.g. cAMP, calcium) via induced synthesis or ion channel opening is also a very efficient way how the signal can be propagated and amplified.

The result of the signal transduction is a response to the initial stimuli. This response could be mediated by conformational changes in proteins leading e.g. to enhanced binding of ligands (integrins), proteolytic cleavages (activation of IL-1β) and to activation of specific transcription factors (e.g. AP1, NFAT, NFκB, STATs) and their binding to responsive gene regulatory elements, which results in new synthesis of proteins necessary for the response [68]. Depending on the nature of stimuli and type of immune cells involved, signaling can result into proliferation, differentiation, cell death, phagocytosis, migration, release of intracellular granules and many other processes.

Tight spatiotemporal regulation of signaling cascades is thus essential for the proper function of immune cells. The process leading to turning the signaling off and returning the cell to the original non-activated state involves disassembly of signaling complexes. This is often mediated by dephosphorylation of phosphoproteins/phospholipids by phosphatases, deubiquitination or ubiquitination followed by degradation by proteasome or sequestration of the signaling molecules into their original stores (e.g. calcium into ER). Some signaling molecules can be recycled, other need to be synthesized de novo [69].

During the signal transduction, large multiprotein signaling complexes are formed. Within these complexes, proteins with enzymatic activity act together with another important group of proteins called the adaptor proteins or signaling adaptors [70].

4.2.2. Signaling via adaptor proteins

While the adaptor proteins lack enzymatic activity, they possess various domains enabling protein-protein interactions and thus function as scaffolds that bring the interacting proteins into the target compartments [70].

Transmembrane adaptor proteins

Transmembrane adaptor proteins (TRAPs) constitute a subset of adaptor proteins characterized by a single span transmembrane domain, a short extracellular domain and a larger cytoplasmic tail containing various interaction motifs [71]. Interaction with other proteins is typically dependent on phosphorylation of specific residues [72].

Some of the TRAPs are part of the immunoreceptor complexes and contain immunoreceptor tyrosine-based activation motifs (ITAMs) with typical consensus sequence YxxI/L$x_{(6–12)}$YxxI/L, which after phosphorylation by SRC family kinases activate signaling via recruiting SYK family kinases. The two SH2 domains of SYK family kinases bind to the pair of phosphorylated tyrosines in the ITAM motif [71] [73]. A motif similar to ITAM is known as hemITAM. It contains only a single tyrosine phosphorylation motif and SYK kinase is activated by the recruitment to a dimer of the hemITAM-containing proteins [33]. Some TRAPs on the other hand contain immunoreceptor tyrosine-based inhibitory motifs (ITIMs) with consensus sequence (I/V/L/S)-X-Tyr-X-X-(L/V), which is phosphorylated by

SRC family kinases as well. After phosphorylation these negative regulators of signaling bind phosphatases like tyrosine phosphatases SHP1, SHP2 and the inositol 5'-phosphatase SHIP [74, 75].

Transmembrane adaptor proteins may also contain other protein interacting domains, such as the proline rich motifs PxxP, which interact with SH3 domains of the other proteins. Moreover, a number of TRAPs contain tyrosine phosphorylation motifs different from ITAMs or ITIMs, through which they often bind cytoplasmic adaptors, such as SLP76/65, GRB2, Gads, signaling enzymes (e.g. PLCγ, PI3-kinase) and others [71].

According to Stepanek et al. (2014), all TRAPs belong to one of three distinct groups. First group involves immunoreceptor-associated TRAPs (e.g. TCRζ, FcRγ, DAP12) and the second group consists of palmitoylated TRAPs (e.g. LAT, SCIMP, LST1, PAG, NTAL), which are concentrated within certain parts of plasma membranes, such as lipid rafts or tetraspanin-enriched microdomains. The last group contains TRAPs that fall into neither the first nor the second group (e.g. LAX, SIT, TRIM) [76].

Peripheral membrane phospholipid-binding adaptor proteins

This interesting group of proteins does not cross both leaflets of the plasma membrane as TRAPs do, but directly interacts with phospholipids (often with phosphatidylinositol 4,5-bisphosphate) of the inner leaflet of the plasma membrane. Here, I mention only two groups, which are employed as signaling adaptors. The first group includes proteins containing the F-BAR domain [77]. F-BAR domain proteins are generally involved in membrane dynamics, vesicle trafficking and cytoskeleton reorganization. They often contain SH3 domain interacting with other proteins (e.g. WASP) [78]. For example, the F-BAR proteins PSTPIP1, PSTPIP2, NOSTRIN and FBP17 act as signaling adaptors [77]. Other signaling adaptor proteins like STAP-2 or BAM32/DAPP1 utilize PH domain to interact with the plasma membrane [79] [80] [81].

More groups of peripheral membrane phospholipid-binding proteins exist, e.g. proteins containing PTB- and FERM, PDZ, FYVE and PX domains. They often function as adaptors for cytoskeleton [82].

Cytoplasmic adaptors

Cytoplasmic adaptors do not have any transmembrane or membrane interacting domain. They bind directly to the activated receptors or to other adaptor proteins. The function of the cytoplasmic adaptors is either to enable and amplify signaling or to restrain it and turn it off. The outcome depends on the function of the proteins binding to their interaction motifs. They can often be positive or negative regulators. The best established cytoplasmic adaptors enhancing signaling include e.g. MYD88 and TRIF involved in TLR signaling [83], CARD9 in DECTIN-1 signaling pathway [84] and SLP76/65 in T cell/B cell signaling [85]. Another well-known cytoplasmic adaptor is ASC, which is involved in inflammasome assembly and activation of caspasese-1 [86]. Examples of cytoplasmic adaptors which can have negative regulatory function include DOK1, DOK2 [87].

However, the complexity of the system is much greater, as many cytoplasmic adaptors have dual positive and negative regulatory functions that become apparent under various circumstances. Some adaptors function just for one receptor in the cell (e.g. Igα/β), while others are more promiscuous (e.g. MYD88 or SCIMP). Generally, the final outcome of signaling depends on character and concentration of the initial stimulus, the type of receptors engaged, adaptor proteins involved and on the cell environment.

Signaling via adaptor proteins SCIMP and PSTPIP2

In the next section I will introduce transmembrane adaptor protein SCIMP and peripheral membrane phospholipid-binding adaptor PSTPIP2 in more detail as characterization of these two adaptors is a central part of the results presented in this thesis.

SCIMP as a novel regulator of MHCII signaling in B cells

SCIMP is a small (145 amino acids) palmitoylated transmembrane adaptor protein, which was discovered relatively recently and the first article about SCIMP was published in 2011. The abbreviation stands for **S**LP65/SLP76, **C**SK-**I**nteracting **M**embrane **P**rotein after its main binding partners [88].

In both humans and mice, SCIMP is highly enriched in spleen and lymph nodes, while other immune organs have lower SCIMP content. Non-immune tissues have negligible

SCIMP expression. Moreover, expression of human SCIMP correlates with major histocompatibility complex type II glycoproteins (MHCII) expression in human blood leukocyte subsets, which implicates SCIMP's role in antigen-presentation.

The initial report on SCIMP focused on its involvement in MHCII signaling in B cells [88]. Importantly, SCIMP localized into the immunological synapse between B and T cells. Synapse localization of SCIMP can be explained by its association with tetraspanin-enriched microdomains, which are known to interact with MHCII [89] [90].

In its intracellular domain, SCIMP contains four potential tyrosine phosphorylation sites and proline-rich sequence. In primary murine B cells, SCIMP is tyrosine phosphorylated after MHCII crosslinking. Using Myc-tagged SCIMP transfected into the Ramos B cell line, interaction partners SLP65, GRB2 and CSK were found upon pervanadate activation, while LYN kinase was constitutively associated with the proline-rich sequence of SCIMP.

Even though SCIMP can bind molecules propagating signaling (SLP65, GRB2, LYN), as well as CSK, which is a negative regulator of SRC family kinase signaling, its overall effect on signaling is positive. Cross-linking of SCIMP (using CD25-SCIMP fusion protein as a tool) elicited strong calcium response and ERK activation mediated by SLP65 adaptor in Raji B cell line. In K46 murine B cell line, SCIMP downregulation by shRNAs disabled sustained ERK and MEK phosphorylation after MHCII cross-linking. However, SCIMP downregulation had no effect on calcium response. The effects of SCIMP on MAP kinase activation was dependent on SLP65 [88].

Overall, the data suggested an important role for SCIMP in enhancing MHCII signaling in B cells which is mediated by its binding partner SLP65. SLP65 is a cytoplasmic adaptor protein known mainly for its function downstream of B cell receptor. It enhances calcium signaling via binding PLCγ and is involved in regulation of cytoskeleton reorganization upon B cell activation via recruiting VAV1 and NCK [85].

Proline-serine-threonine phosphatase-interacting protein 2 (PSTPIP2) and chronic multifocal osteomyelitis (CMO) mouse strain

PSTPIP2 is an adaptor protein containing N-terminal F-bar domain binding phosphoinositides and C-terminal domain binding protein tyrosine phosphatases from PEST family [91]. PSTPIP2 was reported to be expressed mainly by myeloid cells [92, 93].

Missense mutation (L98P) in PSTPIP2 leading to the loss of PSTPIP2 protein causes autoinflammatory disease chronic multifocal osteomyelitis (CMO) in CMO mouse strain. The phenotype of these mice resembles the human disease chronic recurrent multifocal osteomyelitis (CRMO) [94] [95]. CMO mouse strain is a well-established mouse model of autoinflammatory disease. CMO mice suffer from severe bone destruction and tissue inflammation especially near the area of the affected bones. The disease affect preferentially the hind paws and vertebrae in the tail. Cytokine IL-1β is implicated in CMO disease development as CMO mice deficient in IL-1R remain healthy [96] [97].

Macrophages were for a long time suspected to cause this disease [92]. However, more recent publications have revealed hyperactive neutrophils as CMO disease initiators and overproduction of cytokine IL-1β by these cells was established as the most likely cause of the disease [98]. Later, more knowledge about the processing of IL-1β in CMO neutrophils that is linked to the disease development was obtained. The processing involves cleavage by either NLRP3 inflammasome dependent caspase-1 or NLRP3 independent caspase-8 pathway. These pathways thus have redundant role in IL-1β activation. IL-1β is then sensed by the radioresistant non-hematopoietic cells in the bone marrow, which potentiate the inflammatory bone destruction [96] [98]. Bone destruction per se is most likely performed by osteoclasts, whose hyperactivity in CMO disease has been reported [99] [100] [101].

Interestingly, the most recent findings implicate a strong involvement of gut microbiota in the development of the CMO disease, specifically *Prevotella* species. In agreement with this, microbiota changing diet (high fat diet) and antibiotics markedly protected CMO mice from the development of osteomyelitis [102]. However, the exact mechanism how the gut microbiota could activate neutrophils which in response produce IL-1β and mediate bone destruction is currently largely unknown.

4.3. Examples of PRRs and their signaling pathways

With the main groups of PRRs described in chapter 4.1.2., I will further focus more narrowly on selected PRR signaling pathways important for understanding of the research discussed in this thesis.

My first-author article is focused on the regulation of DECTIN-1 signaling by the transmembrane adaptor protein SCIMP and my other first-author manuscript is focusing on the mechanism of how adaptor protein PSTPIP2 regulates inflammation. DECTIN-1 signaling will be described in more detail in the following chapter, which will be succeeded by the chapter on inflammasomes, key components of the pathway regulated by PSTPIP2. I will focus mainly on the NLRP3 inflammasome, which is the most studied one and also demonstrably involved in osteomyelitis development in CMO mice. IL-1β processing as well as the importance of the regulation of this very strong pro-inflammatory stimulus will be outlined as well.

4.3.1. DECTIN-1 signaling

DECTIN-1 (CLEC7A) is a well-characterized CLR involved in antifungal immunity. DECTIN-1 shares common downstream signaling molecules with other CLRs and many principles of its activation are relevant for the whole group of CLRs. DECTIN-1 is CLR expressed in myeloid cells. It recognizes carbohydrates found in fungal cell wall known as β-glucans and is necessary for phagocytosis of β-glucan particles as well as the whole yeasts [103]. DECTIN-1 activation depends on the size of β-glucan particles, as only particulate β-glucan can induce formation of a phagocytic synapse by excluding CD45 and CD148 phosphatases and thus fully activate the DECTIN-1 receptor [41]. Many studies of DECTIN-1, used zymosan as a typical DECTIN-1 ligand [104], even though it can also stimulate other PRRs since it contains not only β-glucans but also mannans, mannoproteins, and chitin [105]. DECTIN-1 is required for antifungal immunity against many pathogens like *Candida* [106], *Aspergillus* [107] [108], *Coccoidiodes* [109] or *Pneumocystis* [110].

DECTIN-1 is type II transmembrane protein containing CTLD in its extracellular part and hemITAM as the intracellular signaling component. Binding of β-glucans by DECTIN leads to SYK-dependent activation of canonical (IKK-mediated) NF-κB pathway via CARD9/BCL10/MALT-1 complex [111], activation of p38, ERK and JNK MAPKs [112] [113] [114] and activation of NFAT and EGR2/3 transcription factors [115] [41]. Activation of these transcription factors results in the synthesis of pro-inflammatory cytokines pro-IL-1β, TNF-α, IL-6, IL-12/23 p40, and other cytokines like IL-2 and IL-10, as well as bioactive molecules like COX-2 and PGE-2 [41, 116].

Apart from activation of transcription, DECTIN-1 elicits SYK-dependent ROS production [117], which can prime/activate NLRP3/caspase-1 classical inflammasome pathway resulting in IL-1β cleavage and secretion. Processing of IL-1β upon DECTIN-1 stimulation can be attributed to activation of non-canonical caspase-8 inflammasome as well [118]. Cytokine IL-1β acts as an important antifungal defense mediator [119] [120] [121] .

In human dendritic cells, DECTIN-1 further activates non-canonical NF-κB pathway (RelB) in SYK independent manner through Raf-1 kinase [122].

Interestingly, besides the SYK kinase the phosphatases SHP-2 and SHIP-1 bind the hemITAM of DECTIN-1 as well [123] [124]. Phosphatase SHIP-1 regulates ROS and limits the oxidative tissue damage [124].

Furthermore, DECTIN-1 receptor can cooperate with other PRRs in order to activate antifungal defense. Recently, DECTIN-1 mediated TLR9 trafficking to β-glucan phagosomes and regulation of TLR9-dependent gene expression was described [125]. Other scientific papers emphasize cooperation of DECTIN-1 and TLR4 or TLR2 [126] [127].

Some features of DECTIN-1 pathway are shared by pathways of other CLRs. Majority of CLRs signal via phosphorylation of ITAM-like/ITAM motifs in the intracellular part of the receptor or on their signaling adaptors [128] [129], which leads to the recruitment of SYK kinase [130], followed by PKCδ mediated activation of the CARD9/BCL10/MALT-1 complex [131]. This results in NF-κB nuclear translocation [132] followed by synthesis of cytokines (IL-1β , IL-6, IL-12 etc.) and other proteins involved in antifungal response [40].

4.3.2. Inflammasome

At the center of inflammasome activation is another group of PRRs, receptors from the NLR family. After their activation, some of NLRs containing pyrin domain (PYD) or CARD form a multiprotein cytoplasmic complex (inflammasome) involved in caspase-1 or caspase-11 activation and pro-inflammatory cytokine IL-1β and IL-18 processing. The inflammasome-forming NLRs include mainly NLRs from the NLRP (=NALP) protein family [133]. Inflammasomes are usually named according to the NLRs involved e.g. NLRP1, NLRP3, NAIP/NLRC4, NLRP6, NLRP7, NLRP12 and AIM2 inflammasome [134]. Assembly of an inflammasome is based on homotypic domain interactions. NLRs containing CARD domain recruit CARD domain of caspase-1 and thus activate it. An example of such activation is the NAIP/NLRC4 inflammasome. Inflammasomes containing pyrin domain use an adaptor protein ASC for caspase recruitment. ASC (PYCARD) contains both PYD and CARD domains. It binds to NLRs with PYD and it recruits caspases by CARD [135].

NLRP3 (NALP3 or cryopyrin) inflammasome

The NLRP3 inflammasome is one of the most studied inflammasome species. It responds to a large variety of PAMPs and DAMPs (e.g. muramyl dipeptide (MDP), bacterial RNA, DNA and RNA viruses, ROS, fungi, protozoa, ATP, uric acid crystals, silica, aluminium salts, nigericin, fatty acid and many others) [136] [59] [137]. The variety of structural features sensed by NLRP3 inflammasome implies that NLRP3 does not recognize these structures directly, but through some common mediator or process that they trigger. The role of both oxidative and metabolic cellular stress in NLRP3 inflammasome activation was proposed [138] [139]. [140] [141] [142]. However, the exact mechanism of how NLP3 senses the stress is currently unknown.

With the exception of human monocytes [143] [144], inflammasome activation is divided into two steps. The first one is called priming and is typically achieved by LPS or TNFα signaling, which leads to NF-κB-mediated increase in NLRP3 [145, 146] and pro-IL-1β expression [145] [146, 147]. The second signal is triggered by NLPR3 inflammasome activators (PAMPs and DAMPs, listed above) and leads to the assembly of a large protein complex triggering autoactivation of caspases and cleavage of biologically inactive

precursors of IL-1β and IL-18 into biologically active molecules secreted out of the cell [148].

NLRP3 inflammasome signaling can be further divided into a canonical pathway, which is dependent on NF-κB-mediated priming and NLRP3-ASC-caspase-1 activation [149], and a non-canonical pathway, which involves NF-κB, IRF-3 and IRF7 mediated expression of type I interferons and caspase-11 activation followed by activation of caspase-1 [150] [151]. Caspase-8, originally studied in apoptotic and necroptotic cell death pathways, is another important player in the IL-1β processing [152].

It is also necessary to mention that inflammasome mediated IL-1β cleavage is not the only way how IL-1β is processed. Neutrophils secrete proteases (e.g. cathepsin G and proteinase-3) that can cleave and thus activate IL-1β extracellularly [153]. However, a recent paper showed that IL-1β cleaved this way is biologically inactive and that neutrophil proteases even inactivate the IL-1β processed by caspase-1 [154]. On the other hand, genetic deletion of cathepsin C in CMO mice resulted in partial alleviation of disease symptoms suggesting, that these proteases contribute to the IL-1β activation in these mice [96].

Since IL-lβ is a very potent pro-inflammatory cytokine, its synthesis, processing and signaling must be tightly regulated. Dysregulation of the IL-lβ pathway causes severe human/murine disorders with possible fatal consequences. The same is true for the NLRP3 inflammasome, since mutations in its pathway lead to autoinflammatory diseases, including Pyogenic Arthritis-Pyoderma Gangrenosum-Acne (PAPA) Syndrome, Familial Cold Autoinflammatory Syndrome, Muckle-Wells Syndrome, Neonatal Onset Multisystem Inflammatory Disease (NOMID) etc. [155] [156] On the other hand, the loss of NLRP3 inflammasome function leads to a high susceptibility to infections [137].

4.4. Innate immune system disorders

As previously discussed, activation of innate immune system is important for defense against pathogens, however its hyper-activation leads to the diseases. The innate immunity thus must be properly regulated. Any disruption of the balance between adequate reaction against infection and excessive inflammatory response could result in a disease. Defects in the innate immune system are caused by either insufficient or excessive activation of the innate immune cells. Diseases discussed in the following paragraphs are most relevant for the research presented in this thesis.

Chronic Granulomatous Disease (CGD)

CGD patients suffer from severe primary immunodeficiency, which is caused by mutations in any of the NADPH oxidase subunits. Phagocytes from CGD patients do not produce ROS, an important agent for killing ingested bacteria. Majority of CGD patients have mutated $gp91^{phox}$ subunit, which is encoded by the *CYBB* gene [157] [158]. A mouse model with *Cybb* deficiency exists and recapitulates the symptoms of CGD patients, which typically include susceptibility to bacterial and fungal infections and granuloma formation [159].

Autoinflammatory diseases

Autoinflammatory diseases are disorders of the innate immune system without any involvement of adaptive immunity components. They are characterized by recurrent bursts of inflammation without any obvious infectious stimuli. This process can also be termed as "sterile inflammation" and is usually caused by activating mutations of inflammatory pathway components, typically NLP3 inflammasome, IL-1β and TNFα processing and signaling machinery. Disease manifestations range from systemic fever attack to localized inflammation of the bones [160] [161]. Pro-inflammatory cytokines, most importantly IL-1β and TNFα, are often highly upregulated, together with other inflammatory proteins (such as IL-6, CRP). High success in the treatment of autoinflammatory diseases occurred with establishment of IL-1β receptor antagonist (anakinra) and TNFα blocking agents as tools for treatment of these diseases in clinical praxis [162] [163] [164]. Examples of monogenic

autoinflammatory diseases include familial Mediterranean fever (FMF), Pyrogenic arthritis pyoderma gangrenosum (PAPA) and TNF receptor-associated periodic syndrome (TRAPS) and others [165].

Interestingly, not all tissues are equally affected by these diseases and the symptoms of various autoinflammatory disorders may differ profoundly despite similar underlying causes. How tissue selectivity of autoinflammatory diseases is achieved is one of the open questions in the field. An example widely discussed in this thesis is murine osteomyelitis resulting from the mutation in the gene encoding PSTPIP2 adaptor protein. Why the diseases attacks mainly the bones and surrounding tissues in the hind paws and tails of these animals and not many other tissues and organs where dysregulated neutrophils could have an equally good access has been unclear [98].

5. Aims of the study

The aim of this PhD thesis was to study novel membrane adaptor proteins and their role in signaling events in the innate immune system.

- The main project of my PhD thesis was to phenotypically characterize mice deficient in transmembrane adaptor protein SCIMP. The focus was on potential defects in B cell MHCII signaling, as well as on signaling regulated by SCIMP in other antigen-presenting cells, especially DECTIN-1 signaling in dendritic cells and macrophages.

- My second project focused on the adaptor protein PSTPIP2 and mechanisms of its negative regulatory role in inflammatory signaling. More specifically, it aimed at identification of new binding partners of PSTPIP2 and determination of their possible roles in the suppression of inflammation by PSTPIP2. It also included an analysis of the processes dysregulated in mice and cells with inactivating mutation in PSTPIP2 with major focus on the role of elevated ROS production on CMO autoinflammatory disease development and progression.

- The aim of my second first-author paper was to establish and describe a protocol for expression of the protein of interest in bone marrow derived macrophages and dendritic cells. As an example proteins, adaptors PSTPIP2 and OPAL1 fused with eGFP were used.

6. Results and discussion

6.1. The Transmembrane Adaptor Protein SCIMP Facilitates Sustained DECTIN-1 Signaling in Dendritic Cells

Based on the results of the previously published article which implicated SCIMP in enhancing MCHII signaling in B cell lines [88], we wanted to study the role of SCIMP in B cell antigen-presentation in a more physiologically relevant model using SCIMP knock-out mouse. An important part of this article was an analysis of SCIMP-deficient mouse strain Scimptm1a(KOMP)Wtsi. These mice were obtained from the International Knockout Mouse Consortium and further bred in the IMG animal facility. The SCIMP$^{-/-}$ and control wild type (WT) mice used for the analysis were outbred from the same heterozygous parents.

6.1.1. SCIMP knock-out mouse analysis

The lack of SCIMP at the protein level was confirmed in primary mouse immune tissues, as well as in cultured BMDCs. Next, we performed a thorough analysis of various immune tissues (bone marrow, spleen, lymph nodes, peritoneal cavity and blood) using flow cytometry. Staining panels to reliably detect majority of mature and immature immune cell types in these tissues were set up and optimized. First, we focused on B cell developmental stages in the bone marrow (pre-B cells, pro-B cells, mature B cells), as well as various subtypes of B cells in the lymph nodes and spleen (germinal center B cells, marginal zone B cells, T1 B cells, T2 and follicular mature B cells). We also analyzed the peritoneal cavity (detecting B1 vs. B2 cells). Other immune cell populations were analyzed as well (CD4 and CD8 T cells, monocytes, macrophages and granulocytes). However, no significant differences between SCIMP$^{-/-}$ and wild type (WT) mice in the numbers and frequencies of analyzed leukocyte populations were found. While the analysis was performed in steady state, we also tested a few basic challenges (among them LPS or zymosan) in a limited number of animals. These experiments did not reveal any significant differences either.

6.1.2. SCIMP is not important for B cell functions *in vivo* and *in vitro*

Since we did not see any alterations in the B cell subset percentages under steady state conditions, we next investigated the functional effects of SCIMP deficiency in B cells when challenged by relevant stimuli. Due to the high expression of SCIMP in germinal center B cells, we decided to test antibody production after immunization with foreign antigens. Despite significant increase in serum levels of IgM and IgG after immunization, the amount of immunoglobulins was practically identical in $SCIMP^{-/-}$ and wild type mice. Since SCIMP was implicated in MHCII signaling in B cells, another *in vivo* assay was focused on B cell antigen presentation to antigen-specific T cells. This assay also did not reveal any dysfunction of $SCIMP^{-/-}$ B cells. We also performed a series of experiments with purified $SCIMP^{-/-}$ and WT B cells *in vitro*. The results showed that SCIMP deficient B cells responded normally in terms of calcium signaling as well as ERK activation after MHCII crosslinking or B cell receptor engagement. Together, these data show that although SCIMP deficiency results in compromised ERK signaling after MHCII crosslinking in B cell lines, this effect cannot be observed in primary B cells and SCIMP deficient primary B cells appear to function normally.

6.1.3. SCIMP is expressed in myeloid cells and upregulated upon GM-CSF treatment

Since the initial report suggested that SCIMP expression correlates with the expression of MHCII, we decided to obtain more detailed information on SCIMP levels in antigen presenting cells. The highest SCIMP expression was found in bone marrow derived dendritic cells (BMDCs), which are routinely differentiated using GM-CSF cytokine. To test whether GM-CSF causes high SCIMP expression or if it is an intrinsic characteristic of dendritic cells, we differentiated BMDCs by an alternative method using Flt3L. We also directly sorted primary murine dendritic cells from mouse spleens. All dendritic cells expressed SCIMP. However, its expression was highest in dendritic cells differentiated in the presence of GM-CSF. Accordingly, in bone marrow derived macrophages (BMDMs), which are routinely differentiated using M-CSF cytokine and express very low levels of SCIMP, its expression was substantially enhanced by GM-CSF treatment.

6.1.4. SCIMP is involved in DECTIN-1 signaling

Since we had observed only mild increase in SCIMP phosphorylation after MHCII crosslinking in BMDCs, we decided to search for another receptor which could interact with SCIMP in BMDCs. We selected DECTIN-1 as a candidate, because similar to SCIMP, it is also present in tetraspanin-enriched microdomains [166] [167] and is up-regulated by GM-CSF treatment [168]. We discovered that SCIMP was strongly phosphorylated upon treatment with DECTIN-1 ligand zymosan in both BMDCs and BMDMs and this phosphorylation was sustained for up to 24 hours. Moreover, SCIMP localized to zymosan-containing phagosomes.

As zymosan does not stimulate only DECTIN-1 but also receptors for mannans and TLR signaling, we wanted to separate their pathways from DECTIN-1 signaling. To do so, we treated BMDCs with purified soluble β-glucan, which elicits very weak signaling by DECTIN-1 and can inhibit stronger activation of DECTIN-1 by particulate β-glucan. Soluble β-glucan is not known to have this inhibitory effect on signaling by other receptors. Soluble β-glucan markedly inhibited SCIMP phosphorylation elicited by Zymosan, while soluble mannan had no effect. To further exclude any involvement of TLRs, we compared SCIMP phosphorylation between BMDCs from WT and MYD88 deficient mice. The timing, as well as the level of phosphorylation, was essentially the same, which excluded the role of majority of TLRs in SCIMP phosphorylation after zymosan treatment. Collectively, these data support the conclusion that SCIMP phosphorylation is triggered by DECTIN-1 and not by other receptors recognizing Zymosan particles.

6.1.5. SCIMP sustains MAP kinase signaling and enhances cytokine production upon DECTIN-1 crosslinking

Though SCIMP deficient BMDCs did not show any alterations in zymosan-induced ERK signaling in early time points, we found significant reduction in ERK1/2 and p38 phosphorylation at late time points (24 hours) after Zymosan addition. At that time SCIMP phosphorylation in WT cells was still present and the expression of SCIMP was significantly upregulated.

In order to see whether the reduced MAP kinase signaling in SCIMP deficient BMDCs had any physiological consequences, we tested the late cytokine production triggered by zymosan treatment. Significant reduction in pro-inflammatory cytokines (TNFα and IL-6) was observed after 48-72h of zymosan stimulation of Scimp/MYD88$^{-/-}$ BMDCs when compared to MYD88$^{-/-}$ cells. MYD88$^{-/-}$ genetic background was used in these experiments to abolish the effects of TLR-mediated signaling.

Together, all our data suggest a novel role for adaptor protein SCIMP in antifungal response mediated by DECTIN-1 signaling. However, SCIMP is definitely not the only player in DECTIN-1 pathway and its role is rather minor during the early signaling events. In late time points it has a significant impact on sustaining TNFα and IL-6 cytokine production. Both of these cytokines are physiologically important for defeating fungal infections [169] [170].

6.1.6. New insight into SCIMP function

Interestingly, last year another group published an article about SCIMP functioning as an adaptor protein for TLR4 [171]. This study was performed on RAW264.7 macrophage-like cell line and shows a close association of SCIMP and TLR4 after LPS stimulation, which is LYN kinase phosphorylation dependent. Association of TLR4 with SCIMP upon LPS stimulation enhances ERK, p38 and JNK phosphorylation, as well as pro-inflammatory cytokine IL-12 and IL-6 production. This implies a novel role for SCIMP as adaptor for TLR4. As many TLRs show similarities in terms of their signaling interactions, it is probable that SCIMP can function as an adaptor downstream of other TLRs as well.

SCIMP seems to be capable of signaling downstream of structurally unrelated proteins as it contributes to MHCII signaling in B cells, DECTIN-1 signaling in dendritic cells and TLR4 signaling in macrophages. Even though SCIMP can bind also negative regulators (CSK kinase), in all cases investigated so far SCIMP mediated activations of signaling pathways. For all three mentioned interactions, activation of MAP kinases mediated by SCIMP was always observed. I consider it likely that other receptors using SCIMP as the adaptor for fine tuning of their signaling are going to be discovered in future. For example, we detected very

high SCIMP expression in plasmacytoid dendritic cells. However, function of SCIMP in these cells is so far absolutely unknown.

6.2. Expression of Fluorescent Fusion Proteins in Murine Bone Marrow-Derived Dendritic Cells and Macrophages

My second first-author paper is method oriented. In this article, we described a detailed cost-efficient high-yield protocol for differentiation of BMDCs and BMDMs from isolated murine bone marrow cells. We described all necessary steps in detail, including home-made cytokine preparation and evaluation of purity of differentiated BMDCs and BMDMs.

We further described the optimized protocol for obtaining BMDCs and BMDMs expressing fluorescently-tagged proteins of interest with the use of retroviral vectors. As an example, we have chosen myeloid membrane adaptors PSTPIP2 and OPAL1. We show localization of these adaptors in both BMDMs and in BMDCs. We found that PSTPIP2 was cytoplasmic with only a partial localization at the plasma membrane, whereas OPAL1 was partially targeted to the plasma membrane and intracellular membranes. This was the first time when localization of these proteins in BMDCs and BMDMs has been described. This article has been accepted for publication and is currently in press.

6.3. PSTPIP2, a Protein Associated with Autoinflammatory Disease, Interacts with Inhibitory Enzymes SHIP1 and CSK

Like the majority of adaptor proteins, PSTPIP2 is thought to regulate signaling via binding to other molecules, including adaptors, signaling enzymes and other effectors. This can result in alterations of their interaction networks, their localization and activity, affecting downstream signaling pathways. In this article, we have identified inhibitory enzymes CSK and SHIP1 as two new binding partners of PSTPIP2. In addition, PSTPIP2 was previously shown to bind two members of PEST family phosphatases (PTP-HSCF and PTP-PEST) [99] [91]. We have confirmed these data and expanded them by detecting an interaction with the third member of PEST phosphatase family PEP/LYP. This way we have extended the list of known binding partners of PSTPIP2 to five molecules with the potential to inhibit signal transduction.

The binding site of PEST-family phosphatases had been identified before. We found that it is also important for CSK binding. This result suggested that PEST-PTPs contribute to CSK interaction with PSTPIP2, though we were not able to define the exact mechanism of this interaction. The SHIP1 binding site we could localize more precisely to the C-terminal tyrosines of PSTPIP2 molecule. In osteoclasts, these tyrosines were shown to be important for inhibitory signaling mediated by PSTPIP2, but the reason for this effect was unknown [99]. Our data suggested that interaction with SHIP1 might be responsible for this inhibition. Moreover, we have also shown that these tyrosines are required for the inhibitory effects of PSTPIP2 on IL-1β production in neutrophils.

Inflammasome activation as well as IL-1β processing occurs in the cytoplasm and PSTPIP2 is cytoplasmic as well. PSTPIP2 can be recruited to the membrane via its F-bar domain. Importantly, SHIP1 and CSK also must be recruited to the membrane in order to access their substrates [172] [173]. It is currently not clear what is the dynamics of PSTPIP2 localization and under what conditions it is translocated to the membranes.

Deletion of PSTPIP2 in CMO mice has a strong pro-inflammatory effects leading to autoinflammatory osteomyelitis driven predominantly by neutrophils and osteoclasts. Multiple signaling pathways are upregulated in CMO neutrophils, including MAP kinase and

AKT activation as well as IL-1β processing, suggesting relatively upstream position of PSTPIP2 in signaling cascades. PSTPIP2 binds at least three different types of negative regulators of signaling (PEST phosphates, CSK and SHIP1 [172, 173]). The data obtained so far suggest that all of them participate to some extent in the signaling regulation. However, their individual contribution to PSTPIP2-mediated inhibition of inflammatory response has not been thoroughly studied. Mice with mutations in the corresponding binding sites in PSTPIP2 will be required to properly address this question.

In this article, we have substantially expanded our knowledge of PSTPIP2 phosphorylation, PSTPIP2-mediated inflammatory pathways inhibition and described its interacting partners which probably act together to control excessive production of IL-1β. We have also described general hypersensitivity of CMO neutrophils to a variety of stimuli suggesting central position of PSTPIP2 in the regulation of neutrophil pro-inflammatory signaling.

6.4. Dysregulated ROS production by neutrophil NADPH oxidase promotes bone damage in autoinflammatory osteomyelitis

This article has not been published yet, however manuscript is in its final version and the experiments are completed. We have found that CMO neutrophils produce a significantly higher amount of NADPH oxidase-dependent reactive oxygen species (ROS) compared to WT cells upon various distinct stimuli as well as in a quiescent state. Moreover, we were able to detect strong ROS production *in vivo* in the paws and tails of CMO mice. Importantly, strong *in vivo* ROS production preceded all the other detectable symptoms of the disease and was localized in an area which later shows inflammatory bone damage in CMO mice (tail and hind paws).

To investigate, what is the role of ROS in CMO pathogenesis, we have used CMO mice unable to produce NADPH oxidase dependent ROS. Our analysis of this mouse strain revealed that autoinflammatory disease is still present in these mice, as visible paw inflammation together with elevated level of IL-1β in the inflamed tissues was still clearly observable. On the other hand, CMO mice deficient in functional NADPH oxidase were almost completely protected from inflammatory bone damage. This finding suggests that NADPH oxidase-produced ROS are responsible for inflammatory bone destruction in CMO mouse model and for targeting of the autoinflammatory disease to the bones. We also report, that ROS and IL-1β dysregulation are independent of each other and the elevated ROS is not the result of ongoing inflammation. However, both ROS and IL-1β are necessary for autoinflammatory bone destruction, as dysregulated ROS do not cause any disease in the absence of IL-1β signaling.

This article shows a completely new role for PSTPIP2 in the regulation of NADPH oxidase mediated ROS production. It also describes novel mechanism of bone destruction in a well-established mouse model of autoinflammatory osteomyelitis. Since inflammatory bone damage accompanies number of diseases our findings could have potentially broader implications in pathophysiology and treatment of disorders other than CMO in mice.

7. Conclusions

All the projects presented in this dissertation thesis are related to the topic of membrane adaptor proteins and their role in innate immunity. In order to analyze the functions and signaling pathways regulated by selected adaptor proteins under physiological conditions, single or double gene knock-out mice models were employed.

The first project aimed at identification of the function of transmembrane adaptor protein SCIMP *in vivo* using flow cytometry based phenotype analysis of SCIMP deficient mice. This analysis did not show any significant alterations in the percentages of any immune cell subsets. On the other hand, we were able to find a novel function of SCIMP in dendritic cells (BMDCs). In dendritic cells we revealed the contribution of SCIMP to signaling by DECTIN-1, a PRR important for fungal recognition and phagocytosis. Upon DECTIN-1 activation, SCIMP sustained ERK and p38 MAP kinase activation and pro-inflammatory cytokine (IL-6 and TNFα) production over relatively long periods of time (more than 24 hours). These are pro-inflammatory cytokines with rather pleiotropic function, which were also reported to be important for antifungal immunity in mice and humans. Our data together with a recently published article on the role of SCIMP as an adaptor in TLR4 signaling in macrophages suggest a relatively broad role for SCIMP mediated signaling in pro-inflammatory responses downstream of multiple classes of pattern recognition receptors.

My second first-author article is methodically oriented. We have published a detailed protocol for production BMDCs and BMDMs using our modified methods optimized for cost efficiency and high yield. We also provided an optimized protocol for obtaining BMDCs and BMDMs with fluorescently-tagged proteins. To demonstrate its efficiency, we performed this procedure with two fluorescently-tagged membrane adaptor proteins (PSTPIP2 and OPAL1), followed by flow cytometry analysis of their expression, as well as visualization of their localization by confocal microscopy. This article was supplemented by a videoprotocol, where all necessary steps are filmed.

My co-author project was aiming at elucidation of the mechanism of how adaptor protein PSTPIP2 suppresses autoinflammation and chronic multifocal osteomyelitis (CMO) which develops in the CMO mouse model lacking this protein. We described two novel PSTPIP2

interaction partners, CSK and SHIP1, which are well-known negative regulators of signaling and we suggested their involvement in the suppression of inflammation by PSTPIP2. We also described PEST phosphatase PEP/LYP as a binding partner of PSTPIP2. Moreover, we showed multiple dysregulated pathways in CMO neutrophils upon variety of stimuli, which indicated general hyperactivity of these cells that contributes to pathogenesis of inflammatory disease.

The second article about PSTPIP2 has not been published yet. However, the manuscript is finalized and ready for submission. We described dysregulated ROS production by NADPH oxidase in CMO neutrophils in steady state and after many stimuli *in vitro*. We also observed elevated ROS production in CMO mice in vivo before any detectable symptoms of the disease develop. Furthermore, we evaluated pathophysiological importance for NADPH oxidase derived ROS using NADPH oxidase-deficient CMO mice. In this model we identified ROS production as an important mediator of inflammatory bone damage in CMO mice, while its influence on IL-1β production and tissue inflammation was negligible. This finding advanced our understanding of the mechanism of autoinflammatory bone damage and also addressed the question of tissue selectivity of autoinflammatory diseases.

8. Contribution

8.1. The Transmembrane Adaptor Protein SCIMP Facilitates Sustained Dectin-1 Signaling in Dendritic Cells

Transmembrane adaptor protein SCIMP was the focus of my main project during my Ph.D. studies. I designed, performed and analyzed majority of the experiments that are published in the article and managed all the mouse strains involved in this study. I also participated in writing the article.

8.2. Expression of Fluorescent Fusion Proteins in Murine Bone Marrow-Derived Dendritic Cells and Macrophages

This is the second of my first-author articles. I adjusted and optimized the protocol, performed majority of the experiments and analyzed the obtained data. I also wrote the article with patient help from my supervisor and performed the video demonstrations.

8.3. PSTPIP2, a Protein Associated with Autoinflammatory Disease, Interacts with Inhibitory Enzymes SHIP1 and CSK

This article was my side project and I participated in it by performing western blot analysis of signaling pathways and IL-1β cleavage activated upon FcR crosslinking and Silica treatment in CMO neutrophils.

8.4. Dysregulated ROS production by neutrophil NADPH oxidase promotes bone damage in autoinflammatory osteomyelitis

In this article I am one of the three shared first-authors. For this study, I performed ROS measurements, IL-1β detection, transplantation experiments and mice monitoring. As the three shared first authors, we discussed experimental design together and each of us analyzed part of the data. I also participated in writing this article.

9. References

1. Buchmann, K., *Evolution of Innate Immunity: Clues from Invertebrates via Fish to Mammals.* Front Immunol, 2014. **5**: p. 459.
2. Uehling, J., A. Deveau, and M. Paoletti, *Do fungi have an innate immune response? An NLR-based comparison to plant and animal immune systems.* PLoS Pathog, 2017. **13**(10): p. e1006578.
3. Ward, A.E. and B.M. Rosenthal, *Evolutionary responses of innate immunity to adaptive immunity.* Infect Genet Evol, 2014. **21**: p. 492-6.
4. Mogensen, T.H., *Pathogen recognition and inflammatory signaling in innate immune defenses.* Clin Microbiol Rev, 2009. **22**(2): p. 240-73, Table of Contents.
5. Medzhitov, R. and C.A. Janeway, Jr., *Decoding the patterns of self and nonself by the innate immune system.* Science, 2002. **296**(5566): p. 298-300.
6. Sun, J.C., J.N. Beilke, and L.L. Lanier, *Adaptive immune features of natural killer cells.* Nature, 2009. **457**(7229): p. 557-61.
7. Sun, J.C., S. Ugolini, and E. Vivier, *Immunological memory within the innate immune system.* EMBO J, 2014. **33**(12): p. 1295-303.
8. Netea, M.G. and J.W. van der Meer, *Trained Immunity: An Ancient Way of Remembering.* Cell Host Microbe, 2017. **21**(3): p. 297-300.
9. Netea, M.G., J. Quintin, and J.W. van der Meer, *Trained immunity: a memory for innate host defense.* Cell Host Microbe, 2011. **9**(5): p. 355-61.
10. Netea, M.G., et al., *Trained immunity: A program of innate immune memory in health and disease.* Science, 2016. **352**(6284): p. aaf1098.
11. Quintin, J., et al., *Candida albicans infection affords protection against reinfection via functional reprogramming of monocytes.* Cell Host Microbe, 2012. **12**(2): p. 223-32.
12. Kleinnijenhuis, J., et al., *Bacille Calmette-Guerin induces NOD2-dependent nonspecific protection from reinfection via epigenetic reprogramming of monocytes.* Proc Natl Acad Sci U S A, 2012. **109**(43): p. 17537-42.
13. Takeuchi, O. and S. Akira, *Pattern recognition receptors and inflammation.* Cell, 2010. **140**(6): p. 805-20.
14. Moretti, J. and J.M. Blander, *Insights into phagocytosis-coupled activation of pattern recognition receptors and inflammasomes.* Curr Opin Immunol, 2014. **26**: p. 100-10.
15. Lima-Junior, D.S., et al., *Dectin-1 Activation during Leishmania amazonensis Phagocytosis Prompts Syk-Dependent Reactive Oxygen Species Production To Trigger Inflammasome Assembly and Restriction of Parasite Replication.* J Immunol, 2017. **199**(6): p. 2055-2068.
16. Asehnoune, K., et al., *Involvement of reactive oxygen species in Toll-like receptor 4-dependent activation of NF-kappa B.* J Immunol, 2004. **172**(4): p. 2522-9.
17. Arango Duque, G. and A. Descoteaux, *Macrophage cytokines: involvement in immunity and infectious diseases.* Front Immunol, 2014. **5**: p. 491.
18. Turner, M.D., et al., *Cytokines and chemokines: At the crossroads of cell signalling and inflammatory disease.* Biochim Biophys Acta, 2014. **1843**(11): p. 2563-2582.
19. Cao, X., *Self-regulation and cross-regulation of pattern-recognition receptor signalling in health and disease.* Nat Rev Immunol, 2016. **16**(1): p. 35-50.

20. Chousterman, B.G., F.K. Swirski, and G.F. Weber, *Cytokine storm and sepsis disease pathogenesis.* Semin Immunopathol, 2017. **39**(5): p. 517-528.
21. Kawasaki, T. and T. Kawai, *Toll-like receptor signaling pathways.* Front Immunol, 2014. **5**: p. 461.
22. Vijay, K., *Toll-like receptors in immunity and inflammatory diseases: Past, present, and future.* Int Immunopharmacol, 2018. **59**: p. 391-412.
23. Mohammad Hosseini, A., et al., *Toll-Like Receptors in the Pathogenesis of Autoimmune Diseases.* Adv Pharm Bull, 2015. **5**(Suppl 1): p. 605-14.
24. O'Neill, L.A. and A.G. Bowie, *The family of five: TIR-domain-containing adaptors in Toll-like receptor signalling.* Nat Rev Immunol, 2007. **7**(5): p. 353-64.
25. Akira, S. and K. Takeda, *Toll-like receptor signalling.* Nat Rev Immunol, 2004. **4**(7): p. 499-511.
26. Piras, V. and K. Selvarajoo, *Beyond MyD88 and TRIF Pathways in Toll-Like Receptor Signaling.* Front Immunol, 2014. **5**: p. 70.
27. Pompei, L., et al., *Disparity in IL-12 release in dendritic cells and macrophages in response to Mycobacterium tuberculosis is due to use of distinct TLRs.* J Immunol, 2007. **178**(8): p. 5192-9.
28. Uehara, A., et al., *Various human epithelial cells express functional Toll-like receptors, NOD1 and NOD2 to produce anti-microbial peptides, but not proinflammatory cytokines.* Mol Immunol, 2007. **44**(12): p. 3100-11.
29. Chung, K.J., et al., *A novel pathway of rapid TLR-triggered activation of integrin-dependent leukocyte adhesion that requires Rap1 GTPase.* Mol Biol Cell, 2014. **25**(19): p. 2948-55.
30. Schenten, D. and R. Medzhitov, *The control of adaptive immune responses by the innate immune system.* Adv Immunol, 2011. **109**: p. 87-124.
31. von Bernuth, H., et al., *Pyogenic bacterial infections in humans with MyD88 deficiency.* Science, 2008. **321**(5889): p. 691-6.
32. Maglione, P.J., N. Simchoni, and C. Cunningham-Rundles, *Toll-like receptor signaling in primary immune deficiencies.* Ann N Y Acad Sci, 2015. **1356**: p. 1-21.
33. Osorio, F. and C. Reis e Sousa, *Myeloid C-type lectin receptors in pathogen recognition and host defense.* Immunity, 2011. **34**(5): p. 651-64.
34. Wevers, B.A., T.B. Geijtenbeek, and S.I. Gringhuis, *C-type lectin receptors orchestrate antifungal immunity.* Future Microbiol, 2013. **8**(7): p. 839-54.
35. Patin, E.C., A. Thompson, and S.J. Orr, *Pattern recognition receptors in fungal immunity.* Semin Cell Dev Biol, 2018.
36. Del Fresno, C., et al., *Flexible Signaling of Myeloid C-Type Lectin Receptors in Immunity and Inflammation.* Front Immunol, 2018. **9**: p. 804.
37. Lefevre, L., et al., *The C-type lectin receptors dectin-1, MR, and SIGNR3 contribute both positively and negatively to the macrophage response to Leishmania infantum.* Immunity, 2013. **38**(5): p. 1038-49.
38. Tanne, A. and O. Neyrolles, *C-type lectins in immunity to Mycobacterium tuberculosis.* Front Biosci (Schol Ed), 2011. **3**: p. 1147-64.
39. Jackson, N., et al., *Recognition of Salmonella by Dectin-1 induces presentation of peptide antigen to type B T cells.* Eur J Immunol, 2014. **44**(4): p. 962-9.
40. Hardison, S.E. and G.D. Brown, *C-type lectin receptors orchestrate antifungal immunity.* Nat Immunol, 2012. **13**(9): p. 817-22.

41. Goodridge, H.S., et al., *Activation of the innate immune receptor Dectin-1 upon formation of a 'phagocytic synapse'.* Nature, 2011. **472**(7344): p. 471-5.
42. Ferwerda, B., et al., *Human dectin-1 deficiency and mucocutaneous fungal infections.* N Engl J Med, 2009. **361**(18): p. 1760-7.
43. Drummond, R.A. and M.S. Lionakis, *Mechanistic Insights into the Role of C-Type Lectin Receptor/CARD9 Signaling in Human Antifungal Immunity.* Front Cell Infect Microbiol, 2016. **6**: p. 39.
44. Glocker, E.O., et al., *A homozygous CARD9 mutation in a family with susceptibility to fungal infections.* N Engl J Med, 2009. **361**(18): p. 1727-35.
45. Lanternier, F., et al., *Inherited CARD9 deficiency in 2 unrelated patients with invasive Exophiala infection.* J Infect Dis, 2015. **211**(8): p. 1241-50.
46. Ng, C.S., H. Kato, and T. Fujita, *Recognition of viruses in the cytoplasm by RLRs and other helicases--how conformational changes, mitochondrial dynamics and ubiquitination control innate immune responses.* Int Immunol, 2012. **24**(12): p. 739-49.
47. Quicke, K.M., M.S. Diamond, and M.S. Suthar, *Negative regulators of the RIG-I-like receptor signaling pathway.* Eur J Immunol, 2017. **47**(4): p. 615-628.
48. Buers, I., Y. Nitschke, and F. Rutsch, *Novel interferonopathies associated with mutations in RIG-I like receptors.* Cytokine Growth Factor Rev, 2016. **29**: p. 101-7.
49. Ferreira, R.C., et al., *A type I interferon transcriptional signature precedes autoimmunity in children genetically at risk for type 1 diabetes.* Diabetes, 2014. **63**(7): p. 2538-50.
50. Mohan, C. and C. Putterman, *Genetics and pathogenesis of systemic lupus erythematosus and lupus nephritis.* Nat Rev Nephrol, 2015. **11**(6): p. 329-41.
51. Kato, H. and T. Fujita, *RIG-I-like receptors and autoimmune diseases.* Curr Opin Immunol, 2015. **37**: p. 40-5.
52. Funabiki, M., et al., *Autoimmune disorders associated with gain of function of the intracellular sensor MDA5.* Immunity, 2014. **40**(2): p. 199-212.
53. Proell, M., et al., *The Nod-like receptor (NLR) family: a tale of similarities and differences.* PLoS One, 2008. **3**(4): p. e2119.
54. Philpott, D.J., et al., *NOD proteins: regulators of inflammation in health and disease.* Nat Rev Immunol, 2014. **14**(1): p. 9-23.
55. Shaw, M.H., et al., *NOD-like receptors (NLRs): bona fide intracellular microbial sensors.* Curr Opin Immunol, 2008. **20**(4): p. 377-82.
56. Caruso, R., et al., *NOD1 and NOD2: signaling, host defense, and inflammatory disease.* Immunity, 2014. **41**(6): p. 898-908.
57. Franchi, L., et al., *Function of Nod-like receptors in microbial recognition and host defense.* Immunol Rev, 2009. **227**(1): p. 106-28.
58. Guo, H., J.B. Callaway, and J.P. Ting, *Inflammasomes: mechanism of action, role in disease, and therapeutics.* Nat Med, 2015. **21**(7): p. 677-87.
59. Carneiro, L.A. and L.H. Travassos, *The Interplay between NLRs and Autophagy in Immunity and Inflammation.* Front Immunol, 2013. **4**: p. 361.
60. Dinarello, C.A., *Interleukin-1 in the pathogenesis and treatment of inflammatory diseases.* Blood, 2011. **117**(14): p. 3720-32.
61. Hoffman, H.M. and L. Broderick, *The role of the inflammasome in patients with autoinflammatory diseases.* J Allergy Clin Immunol, 2016. **138**(1): p. 3-14.

62. Park, Y.H., M.S. Jeong, and S.B. Jang, *Structural insights of homotypic interaction domains in the ligand-receptor signal transduction of tumor necrosis factor (TNF).* BMB Rep, 2016. **49**(3): p. 159-66.
63. Ullrich, A. and J. Schlessinger, *Signal transduction by receptors with tyrosine kinase activity.* Cell, 1990. **61**(2): p. 203-12.
64. Volinsky, N. and B.N. Kholodenko, *Complexity of receptor tyrosine kinase signal processing.* Cold Spring Harb Perspect Biol, 2013. **5**(8): p. a009043.
65. Rotin, D. and S. Kumar, *Physiological functions of the HECT family of ubiquitin ligases.* Nat Rev Mol Cell Biol, 2009. **10**(6): p. 398-409.
66. Zinngrebe, J., et al., *Ubiquitin in the immune system.* EMBO Rep, 2014. **15**(1): p. 28-45.
67. Iwai, K., *Diverse ubiquitin signaling in NF-kappaB activation.* Trends Cell Biol, 2012. **22**(7): p. 355-64.
68. Yang, J., et al., *Calcineurin/nuclear factors of activated T cells (NFAT)-activating and immunoreceptor tyrosine-based activation motif (ITAM)-containing protein (CNAIP), a novel ITAM-containing protein that activates the calcineurin/NFAT-signaling pathway.* J Biol Chem, 2003. **278**(19): p. 16797-801.
69. Marrack, P., J. Scott-Browne, and M.K. MacLeod, *Terminating the immune response.* Immunol Rev, 2010. **236**: p. 5-10.
70. Flynn, D.C., *Adaptor proteins.* Oncogene, 2001. **20**: p. 6270.
71. Horejsi, V., W. Zhang, and B. Schraven, *Transmembrane adaptor proteins: organizers of immunoreceptor signalling.* Nat Rev Immunol, 2004. **4**(8): p. 603-16.
72. Lindquist, J.A., L. Simeoni, and B. Schraven, *Transmembrane adapters: attractants for cytoplasmic effectors.* Immunol Rev, 2003. **191**: p. 165-82.
73. Underhill, D.M. and H.S. Goodridge, *The many faces of ITAMs.* Trends Immunol, 2007. **28**(2): p. 66-73.
74. Ravetch, J.V. and L.L. Lanier, *Immune inhibitory receptors.* Science, 2000. **290**(5489): p. 84-9.
75. Unkeless, J.C. and J. Jin, *Inhibitory receptors, ITIM sequences and phosphatases.* Curr Opin Immunol, 1997. **9**(3): p. 338-43.
76. Stepanek, O., P. Draber, and V. Horejsi, *Palmitoylated transmembrane adaptor proteins in leukocyte signaling.* Cell Signal, 2014. **26**(5): p. 895-902.
77. Liu, S., et al., *F-BAR family proteins, emerging regulators for cell membrane dynamic changes-from structure to human diseases.* J Hematol Oncol, 2015. **8**: p. 47.
78. McDonald, N.A. and K.L. Gould, *Linking up at the BAR: Oligomerization and F-BAR protein function.* Cell Cycle, 2016. **15**(15): p. 1977-85.
79. Sekine, Y., *Adaptor protein STAP-2 modulates cellular signaling in immune systems.* Biol Pharm Bull, 2014. **37**(2): p. 185-94.
80. Saitoh, K., et al., *STAP-2 interacts with Pyk2 and enhances Pyk2 activity in T-cells.* Biochem Biophys Res Commun, 2017. **488**(1): p. 81-87.
81. Marshall, A.J., T. Zhang, and M. Al-Alwan, *Regulation of B-lymphocyte activation by the PH domain adaptor protein Bam32/DAPP1.* Biochem Soc Trans, 2007. **35**(Pt 2): p. 181-2.
82. Balla, T., *Inositol-lipid binding motifs: signal integrators through protein-lipid and protein-protein interactions.* J Cell Sci, 2005. **118**(Pt 10): p. 2093-104.

83. Monie, T.P., M.C. Moncrieffe, and N.J. Gay, *Structure and regulation of cytoplasmic adapter proteins involved in innate immune signaling.* Immunol Rev, 2009. **227**(1): p. 161-75.
84. Goodridge, H.S., et al., *Differential use of CARD9 by dectin-1 in macrophages and dendritic cells.* J Immunol, 2009. **182**(2): p. 1146-54.
85. Koretzky, G.A., F. Abtahian, and M.A. Silverman, *SLP76 and SLP65: complex regulation of signalling in lymphocytes and beyond.* Nat Rev Immunol, 2006. **6**(1): p. 67-78.
86. Latz, E., T.S. Xiao, and A. Stutz, *Activation and regulation of the inflammasomes.* Nat Rev Immunol, 2013. **13**(6): p. 397-411.
87. Coppin, E., et al., *Dok1 and Dok2 Proteins Regulate Cell Cycle in Hematopoietic Stem and Progenitor Cells.* J Immunol, 2016. **196**(10): p. 4110-21.
88. Draber, P., et al., *SCIMP, a transmembrane adaptor protein involved in major histocompatibility complex class II signaling.* Mol Cell Biol, 2011. **31**(22): p. 4550-62.
89. Saiz, M.L., V. Rocha-Perugini, and F. Sanchez-Madrid, *Tetraspanins as Organizers of Antigen-Presenting Cell Function.* Front Immunol, 2018. **9**: p. 1074.
90. Rocha-Perugini, V., et al., *CD81 controls sustained T cell activation signaling and defines the maturation stages of cognate immunological synapses.* Mol Cell Biol, 2013. **33**(18): p. 3644-58.
91. Wu, Y., D. Dowbenko, and L.A. Lasky, *PSTPIP 2, a second tyrosine phosphorylated, cytoskeletal-associated protein that binds a PEST-type protein-tyrosine phosphatase.* J Biol Chem, 1998. **273**(46): p. 30487-96.
92. Grosse, J., et al., *Mutation of mouse Mayp/Pstpip2 causes a macrophage autoinflammatory disease.* Blood, 2006. **107**(8): p. 3350-8.
93. Chitu, V., et al., *Primed innate immunity leads to autoinflammatory disease in PSTPIP2-deficient cmo mice.* Blood, 2009. **114**(12): p. 2497-505.
94. Scianaro, R., et al., *Deregulation of the IL-1beta axis in chronic recurrent multifocal osteomyelitis.* Pediatr Rheumatol Online J, 2014. **12**: p. 30.
95. Cox, A.J., et al., *Recessive coding and regulatory mutations in FBLIM1 underlie the pathogenesis of chronic recurrent multifocal osteomyelitis (CRMO).* PLoS One, 2017. **12**(3): p. e0169687.
96. Gurung, P., A. Burton, and T.D. Kanneganti, *NLRP3 inflammasome plays a redundant role with caspase 8 to promote IL-1beta-mediated osteomyelitis.* Proc Natl Acad Sci U S A, 2016. **113**(16): p. 4452-7.
97. Ferguson, P.J., et al., *A missense mutation in pstpip2 is associated with the murine autoinflammatory disorder chronic multifocal osteomyelitis.* Bone, 2006. **38**(1): p. 41-7.
98. Lukens, J.R., et al., *Critical role for inflammasome-independent IL-1beta production in osteomyelitis.* Proc Natl Acad Sci U S A, 2014. **111**(3): p. 1066-71.
99. Chitu, V., et al., *PSTPIP2 deficiency in mice causes osteopenia and increased differentiation of multipotent myeloid precursors into osteoclasts.* Blood, 2012. **120**(15): p. 3126-35.
100. Sztacho, M., et al., *BAR Proteins PSTPIP1/2 Regulate Podosome Dynamics and the Resorption Activity of Osteoclasts.* PLoS One, 2016. **11**(10): p. e0164829.
101. Hentunen, T.A., et al., *A murine model of inflammatory bone disease.* Bone, 2000. **26**(2): p. 183-8.

102. Lukens, J.R., et al., *Dietary modulation of the microbiome affects autoinflammatory disease.* Nature, 2014. **516**(7530): p. 246-9.
103. Herre, J., et al., *Dectin-1 uses novel mechanisms for yeast phagocytosis in macrophages.* Blood, 2004. **104**(13): p. 4038-45.
104. Brown, J., et al., *Structure of the fungal beta-glucan-binding immune receptor dectin-1: implications for function.* Protein Sci, 2007. **16**(6): p. 1042-52.
105. Gantner, B.N., et al., *Collaborative induction of inflammatory responses by dectin-1 and Toll-like receptor 2.* J Exp Med, 2003. **197**(9): p. 1107-17.
106. Chen, S.M., et al., *Dectin-1 plays an important role in host defense against systemic Candida glabrata infection.* Virulence, 2017. **8**(8): p. 1643-1656.
107. Werner, J.L., et al., *Requisite role for the dectin-1 beta-glucan receptor in pulmonary defense against Aspergillus fumigatus.* J Immunol, 2009. **182**(8): p. 4938-46.
108. Sun, W.K., et al., *Dectin-1 is inducible and plays a crucial role in Aspergillus-induced innate immune responses in human bronchial epithelial cells.* Eur J Clin Microbiol Infect Dis, 2012. **31**(10): p. 2755-64.
109. Viriyakosol, S., et al., *Dectin-1 is required for resistance to coccidioidomycosis in mice.* MBio, 2013. **4**(1): p. e00597-12.
110. Saijo, S., et al., *Dectin-1 is required for host defense against Pneumocystis carinii but not against Candida albicans.* Nat Immunol, 2007. **8**(1): p. 39-46.
111. Gross, O., et al., *Card9 controls a non-TLR signalling pathway for innate anti-fungal immunity.* Nature, 2006. **442**(7103): p. 651-6.
112. LeibundGut-Landmann, S., et al., *Syk- and CARD9-dependent coupling of innate immunity to the induction of T helper cells that produce interleukin 17.* Nat Immunol, 2007. **8**(6): p. 630-8.
113. Slack, E.C., et al., *Syk-dependent ERK activation regulates IL-2 and IL-10 production by DC stimulated with zymosan.* Eur J Immunol, 2007. **37**(6): p. 1600-12.
114. Jia, X.M., et al., *CARD9 mediates Dectin-1-induced ERK activation by linking Ras-GRF1 to H-Ras for antifungal immunity.* J Exp Med, 2014. **211**(11): p. 2307-21.
115. Goodridge, H.S., R.M. Simmons, and D.M. Underhill, *Dectin-1 stimulation by Candida albicans yeast or zymosan triggers NFAT activation in macrophages and dendritic cells.* J Immunol, 2007. **178**(5): p. 3107-15.
116. Sancho, D. and C. Reis e Sousa, *Signaling by myeloid C-type lectin receptors in immunity and homeostasis.* Annu Rev Immunol, 2012. **30**: p. 491-529.
117. Underhill, D.M., et al., *Dectin-1 activates Syk tyrosine kinase in a dynamic subset of macrophages for reactive oxygen production.* Blood, 2005. **106**(7): p. 2543-50.
118. Gringhuis, S.I., et al., *Dectin-1 is an extracellular pathogen sensor for the induction and processing of IL-1beta via a noncanonical caspase-8 inflammasome.* Nat Immunol, 2012. **13**(3): p. 246-54.
119. Gross, O., et al., *Syk kinase signalling couples to the Nlrp3 inflammasome for anti-fungal host defence.* Nature, 2009. **459**(7245): p. 433-6.
120. Altmeier, S., et al., *IL-1 Coordinates the Neutrophil Response to C. albicans in the Oral Mucosa.* PLoS Pathog, 2016. **12**(9): p. e1005882.
121. Netea, M.G., et al., *Inflammasome-independent regulation of IL-1-family cytokines.* Annu Rev Immunol, 2015. **33**: p. 49-77.

122. Gringhuis, S.I., et al., *Dectin-1 directs T helper cell differentiation by controlling noncanonical NF-kappaB activation through Raf-1 and Syk.* Nat Immunol, 2009. **10**(2): p. 203-13.
123. Deng, Z., et al., *Tyrosine phosphatase SHP-2 mediates C-type lectin receptor-induced activation of the kinase Syk and anti-fungal TH17 responses.* Nat Immunol, 2015. **16**(6): p. 642-52.
124. Blanco-Menendez, N., et al., *SHIP-1 Couples to the Dectin-1 hemITAM and Selectively Modulates Reactive Oxygen Species Production in Dendritic Cells in Response to Candida albicans.* J Immunol, 2015. **195**(9): p. 4466-4478.
125. Khan, N.S., et al., *Dectin-1 Controls TLR9 Trafficking to Phagosomes Containing beta-1,3 Glucan.* J Immunol, 2016. **196**(5): p. 2249-61.
126. Loures, F.V., et al., *TLR-4 cooperates with Dectin-1 and mannose receptor to expand Th17 and Tc17 cells induced by Paracoccidioides brasiliensis stimulated dendritic cells.* Front Microbiol, 2015. **6**: p. 261.
127. Ferwerda, G., et al., *Dectin-1 synergizes with TLR2 and TLR4 for cytokine production in human primary monocytes and macrophages.* Cell Microbiol, 2008. **10**(10): p. 2058-66.
128. Richardson, M.B. and S.J. Williams, *MCL and Mincle: C-Type Lectin Receptors That Sense Damaged Self and Pathogen-Associated Molecular Patterns.* Front Immunol, 2014. **5**: p. 288.
129. Kerrigan, A.M. and G.D. Brown, *Syk-coupled C-type lectin receptors that mediate cellular activation via single tyrosine based activation motifs.* Immunol Rev, 2010. **234**(1): p. 335-52.
130. Hoving, J.C., G.J. Wilson, and G.D. Brown, *Signalling C-type lectin receptors, microbial recognition and immunity.* Cell Microbiol, 2014. **16**(2): p. 185-94.
131. Strasser, D., et al., *Syk kinase-coupled C-type lectin receptors engage protein kinase C-sigma to elicit Card9 adaptor-mediated innate immunity.* Immunity, 2012. **36**(1): p. 32-42.
132. Dambuza, I.M. and G.D. Brown, *C-type lectins in immunity: recent developments.* Curr Opin Immunol, 2015. **32**: p. 21-7.
133. Kufer, T.A. and P.J. Sansonetti, *Sensing of bacteria: NOD a lonely job.* Curr Opin Microbiol, 2007. **10**(1): p. 62-9.
134. Lu, A. and H. Wu, *Structural mechanisms of inflammasome assembly.* FEBS J, 2015. **282**(3): p. 435-44.
135. Lechtenberg, B.C., P.D. Mace, and S.J. Riedl, *Structural mechanisms in NLR inflammasome signaling.* Curr Opin Struct Biol, 2014. **29**: p. 17-25.
136. Hornung, V., et al., *Silica crystals and aluminum salts activate the NALP3 inflammasome through phagosomal destabilization.* Nat Immunol, 2008. **9**(8): p. 847-56.
137. Menu, P. and J.E. Vince, *The NLRP3 inflammasome in health and disease: the good, the bad and the ugly.* Clin Exp Immunol, 2011. **166**(1): p. 1-15.
138. Cruz, C.M., et al., *ATP activates a reactive oxygen species-dependent oxidative stress response and secretion of proinflammatory cytokines in macrophages.* J Biol Chem, 2007. **282**(5): p. 2871-9.
139. Munoz-Planillo, R., et al., *K(+) efflux is the common trigger of NLRP3 inflammasome activation by bacterial toxins and particulate matter.* Immunity, 2013. **38**(6): p. 1142-53.

140. Tschopp, J. and K. Schroder, *NLRP3 inflammasome activation: The convergence of multiple signalling pathways on ROS production?* Nat Rev Immunol, 2010. **10**(3): p. 210-5.
141. Schroder, K., R. Zhou, and J. Tschopp, *The NLRP3 inflammasome: a sensor for metabolic danger?* Science, 2010. **327**(5963): p. 296-300.
142. Martinon, F., *Signaling by ROS drives inflammasome activation.* Eur J Immunol, 2010. **40**(3): p. 616-9.
143. Netea, M.G., et al., *Differential requirement for the activation of the inflammasome for processing and release of IL-1beta in monocytes and macrophages.* Blood, 2009. **113**(10): p. 2324-35.
144. Gaidt, M.M., et al., *Human Monocytes Engage an Alternative Inflammasome Pathway.* Immunity, 2016. **44**(4): p. 833-46.
145. Bauernfeind, F.G., et al., *Cutting edge: NF-kappaB activating pattern recognition and cytokine receptors license NLRP3 inflammasome activation by regulating NLRP3 expression.* J Immunol, 2009. **183**(2): p. 787-91.
146. Franchi, L., T. Eigenbrod, and G. Nunez, *Cutting edge: TNF-alpha mediates sensitization to ATP and silica via the NLRP3 inflammasome in the absence of microbial stimulation.* J Immunol, 2009. **183**(2): p. 792-6.
147. Ramirez, A., et al., *Defective pro-IL-1beta responses in macrophages from aged mice.* Immun Ageing, 2012. **9**(1): p. 27.
148. Khare, S., et al., *Inflammasomes and their activation.* Crit Rev Immunol, 2010. **30**(5): p. 463-87.
149. Man, S.M. and T.D. Kanneganti, *Regulation of inflammasome activation.* Immunol Rev, 2015. **265**(1): p. 6-21.
150. Kayagaki, N., et al., *Non-canonical inflammasome activation targets caspase-11.* Nature, 2011. **479**(7371): p. 117-21.
151. Rathinam, V.A. and K.A. Fitzgerald, *Inflammasome Complexes: Emerging Mechanisms and Effector Functions.* Cell, 2016. **165**(4): p. 792-800.
152. Monie, T.P. and C.E. Bryant, *Caspase-8 functions as a key mediator of inflammation and pro-IL-1beta processing via both canonical and non-canonical pathways.* Immunol Rev, 2015. **265**(1): p. 181-93.
153. Afonina, I.S., et al., *Proteolytic Processing of Interleukin-1 Family Cytokines: Variations on a Common Theme.* Immunity, 2015. **42**(6): p. 991-1004.
154. Clancy, D.M., et al., *Extracellular Neutrophil Proteases Are Efficient Regulators of IL-1, IL-33, and IL-36 Cytokine Activity but Poor Effectors of Microbial Killing.* Cell Rep, 2018. **22**(11): p. 2937-2950.
155. Ciccarelli, F., M. De Martinis, and L. Ginaldi, *An update on autoinflammatory diseases.* Curr Med Chem, 2014. **21**(3): p. 261-9.
156. Touitou, I. and I. Kone-Paut, *Autoinflammatory diseases.* Best Pract Res Clin Rheumatol, 2008. **22**(5): p. 811-29.
157. Chiriaco, M., et al., *Chronic granulomatous disease: Clinical, molecular, and therapeutic aspects.* Pediatr Allergy Immunol, 2016. **27**(3): p. 242-53.
158. Arnold, D.E. and J.R. Heimall, *A Review of Chronic Granulomatous Disease.* Adv Ther, 2017. **34**(12): p. 2543-2557.
159. Bjorgvinsdottir, H., et al., *Retroviral-mediated gene transfer of gp91phox into bone marrow cells rescues defect in host defense against Aspergillus fumigatus in murine X-linked chronic granulomatous disease.* Blood, 1997. **89**(1): p. 41-8.

160. Henderson, C. and R. Goldbach-Mansky, *Monogenic autoinflammatory diseases: new insights into clinical aspects and pathogenesis.* Curr Opin Rheumatol, 2010. **22**(5): p. 567-78.
161. Mortimer, L., et al., *NLRP3 inflammasome inhibition is disrupted in a group of auto-inflammatory disease CAPS mutations.* Nat Immunol, 2016. **17**(10): p. 1176-86.
162. Rubartelli, A., *Autoinflammatory diseases.* Immunol Lett, 2014. **161**(2): p. 226-30.
163. Dinarello, C.A., *Blocking interleukin-1beta in acute and chronic autoinflammatory diseases.* J Intern Med, 2011. **269**(1): p. 16-28.
164. De Benedetti, F., et al., *Canakinumab for the Treatment of Autoinflammatory Recurrent Fever Syndromes.* N Engl J Med, 2018. **378**(20): p. 1908-1919.
165. Manthiram, K., et al., *The monogenic autoinflammatory diseases define new pathways in human innate immunity and inflammation.* Nat Immunol, 2017. **18**(8): p. 832-842.
166. Mantegazza, A.R., et al., *CD63 tetraspanin slows down cell migration and translocates to the endosomal-lysosomal-MIICs route after extracellular stimuli in human immature dendritic cells.* Blood, 2004. **104**(4): p. 1183-90.
167. Meyer-Wentrup, F., et al., *Dectin-1 interaction with tetraspanin CD37 inhibits IL-6 production.* J Immunol, 2007. **178**(1): p. 154-62.
168. Willment, J.A., et al., *Dectin-1 expression and function are enhanced on alternatively activated and GM-CSF-treated macrophages and are negatively regulated by IL-10, dexamethasone, and lipopolysaccharide.* J Immunol, 2003. **171**(9): p. 4569-73.
169. van Enckevort, F.H., et al., *Increased susceptibility to systemic candidiasis in interleukin-6 deficient mice.* Med Mycol, 1999. **37**(6): p. 419-26.
170. Filler, S.G., M.R. Yeaman, and D.C. Sheppard, *Tumor necrosis factor inhibition and invasive fungal infections.* Clin Infect Dis, 2005. **41 Suppl 3**: p. S208-12.
171. Luo, L., et al., *SCIMP is a transmembrane non-TIR TLR adaptor that promotes proinflammatory cytokine production from macrophages.* Nat Commun, 2017. **8**: p. 14133.
172. Pauls, S.D. and A.J. Marshall, *Regulation of immune cell signaling by SHIP1: A phosphatase, scaffold protein, and potential therapeutic target.* Eur J Immunol, 2017. **47**(6): p. 932-945.
173. Okada, M., *Regulation of the SRC family kinases by Csk.* Int J Biol Sci, 2012. **8**(10): p. 1385-97.

10. Reprints of publications

1. **Kralova J**, Fabisik M, Pokorna J, Skopcova T, Malissen B, Brdicka T. *The Transmembrane Adaptor Protein SCIMP Facilitates Sustained Dectin-1 Signaling in Dendritic Cells*, The Journal of Biological Chemistry, 2016. 291(32):16530-40

2. **Kralova J**, Glatzova D, Borna S, Brdicka T. *Expression of Fluorescent Fusion Proteins in Murine Bone Marrow-Derived Dendritic Cells and Macrophages*, 2018. In press, Journal of Visualized Experiments

3. Drobek A, **Kralova J**, Skopcova T, Kucova M, Novák P, Angelisová P, Otahal P, Alberich-Jorda M, Brdicka T. *PSTPIP2, a Protein Associated with Autoinflammatory Disease, Interacts with Inhibitory Enzymes SHIP1 and CSK.* Journal of Immunology, 2015. 195(7): p. 3416-26.

4. **Kralova J**,* Drobek A,* Prochazka J,* Spoutil F, Glatzova D, Borna S, Pokorna J, Skopcova T, Angelisova P, Sedlacek R, Brdicka T. *Dysregulated ROS production by neutrophil NADPH oxidase promotes bone damage in autoinflammatory osteomyelitis,* Unpublished, * equal contribution

THE JOURNAL OF BIOLOGICAL CHEMISTRY VOL. 291, NO. 32, pp. 16530–16540, August 5, 2016

The Transmembrane Adaptor Protein SCIMP Facilitates Sustained Dectin-1 Signaling in Dendritic Cells*[S]

Received for publication, January 21, 2016, and in revised form, June 3, 2016 Published, JBC Papers in Press, June 10, 2016, DOI 10.1074/jbc.M116.717157

Jarmila Kralova[‡1], Matej Fabisik[‡1], Jana Pokorna[§], Tereza Skopcova[‡], Bernard Malissen[¶2], and Tomas Brdicka[‡3]

From the Laboratories of [‡]Leukocyte Signaling and [§]Molecular Immunology, Institute of Molecular Genetics, Academy of Sciences of the Czech Republic, 14220 Prague, Czech Republic and the [¶]Centre d'Immunophénomique, PHENOMIN-CIPHE, Aix Marseille Université UM2, INSERM US012, CNRS UMS3367, 13288 Marseille, France

Transmembrane adaptor proteins are molecules specialized in recruiting cytoplasmic proteins to the proximity of the cell membrane as part of the signal transduction process. A member of this family, SLP65/SLP76, Csk-interacting membrane protein (SCIMP), recruits a complex of SLP65/SLP76 and Grb2 adaptor proteins, known to be involved in the activation of PLCγ1/2, Ras, and other pathways. SCIMP expression is restricted to antigen-presenting cells. In a previous cell line-based study, it was shown that, in B cells, SCIMP contributes to the reverse signaling in the immunological synapse, downstream of MHCII glycoproteins. There it mainly facilitates the activation of ERK MAP kinases. However, its importance for MHCII glycoprotein-dependent ERK signaling in primary B cells has not been analyzed. Moreover, its role in macrophages and dendritic cells has remained largely unknown. Here we present the results of our analysis of SCIMP-deficient mice. In these mice, we did not observe any defects in B cell signaling and B cell-dependent responses. On the other hand, we found that, in dendritic cells and macrophages, SCIMP expression is up-regulated after exposure to GM-CSF or the Dectin-1 agonist zymosan. Moreover, we found that SCIMP is strongly phosphorylated after Dectin-1 stimulation and that it participates in signal transduction downstream of this important pattern recognition receptor. Our analysis of SCIMP-deficient dendritic cells revealed that SCIMP specifically contributes to sustaining long-term MAP kinase signaling and cytokine production downstream of Dectin-1 because of an increased expression and sustained phosphorylation lasting at least 24 h after signal initiation.

Dectin-1 is a pattern recognition receptor from the C-type lectin receptor family (1). It is expressed in macrophages, dendritic cells, neutrophils, and a subset of T and B cells (2–4). Through its carbohydrate recognition domain, it specifically recognizes β-1,3-glucan (5), which is a typical component of fungal cell walls (6). Dectin-1 is considered a major receptor for β-glucans and plays an important role in the defense against various species of pathogenic fungi in mice, including *Candida albicans, Aspergillus fumigatus, and Pneumocystis carinii* (7–11). The importance of dectin-1 for antifungal defense has also been demonstrated by studies of human patients with disrupted dectin-1 function who display increased mucosal colonization with *Candida* species and suffer from recurrent mucocutaneous fungal infections (12, 13).

Dectin-1 signaling is initiated by phosphorylation of the hemITAM motif in its intracellular tail, leading to the recruitment and activation of the protein tyrosine kinase Syk. This is followed by sequential activation of PLCγ2 and PKCδ. Stimulation of this pathway as well as of additional Syk-independent pathways results in the activation of the transcription factors NF-κB, nuclear factor of activated T cells (NFAT), and IRF1/5 and initiation of signaling by the MAP kinases ERK, p38, and JNK, which then contribute to downstream cellular responses (14–16). Activation of Dectin-1 leads to phagocytosis of fungi or any other β-glucan-containing particles. In addition, it also triggers the production of reactive oxygen species and proinflammatory cytokines (7, 17, 18). Cytokines produced in response to Dectin-1 stimulation also promote Th1 and Th17 polarization of helper T cells necessary for defeating fungal infection (14–16). Interestingly, only β-glucan in the form of particles can elicit the full activity of Dectin-1, whereas soluble β-glucans, which also bind to the receptor, lack strong activating properties and can inhibit the responses to particulate β-glucan (19). The difference is thought to be caused by the ability of particulate β-glucan to induce the formation of a phagocytic synapse that excludes CD45 and CD148 phosphatases (19).

As any important receptor, Dectin-1 is tightly regulated. This regulation occurs not only at the level of signaling pathways but also at the level of expression. Dectin-1 is highly up-regulated after IL-4, IL-13, and GM-CSF treatment, whereas IL-10, LPS, and dexamethasone down-regulate its expression (20).

To elicit the full antifungal immune response, Dectin-1 cooperates with several TLRs[4] (most importantly TLR2) (17). Its function is also complemented by other C-type lectin receptors, such as Dectin-2, which recognizes mannan structures in

* This work was supported by Czech Science Foundation (GACR, Project P302/12/1712) and received institutional funding from IMG ASCR (RVO 68378050). The authors declare that they have no conflicts of interest with the contents of this article.
[S] This article contains supplemental Movie 1.
[1] Supported in part by the Faculty of Science, Charles University, Prague.
[2] Supported by PHENOMIN CIPHE.
[3] To whom correspondence should be addressed: Laboratory of Leukocyte Signaling, Institute of Molecular Genetics of the Academy of Sciences of the Czech Republic, Videnska 1083, 14220 Prague, Czech Republic. Tel.: 420-241062467; Fax: 420-244472282; E-mail: tomas.brdicka@img.cas.cz.

[4] The abbreviations used are: TLR, Toll-like receptor; gp, glycoprotein; SCIMP, SLP76/SLP65-interacting membrane adaptor protein; APC, antigen-presenting cell; CFSE, 5-(and 6)-carboxyfluorescein diacetate succinimidyl ester; NP, 4-hydroxy-3-nitrophenylacetyl; BMDC, bone marrow-derived dendritic cell; BMMF, bone marrow-derived macrophage; IMDM, Iscove's modified Dulbecco's medium.

fungal cell walls (1). In addition, Dectin-1 interacts with tetraspanin molecules, which form the basis of tetraspanin-enriched microdomains and were suggested to be involved in Dectin-1 trafficking (21–23). However, the effects of tetraspanins on Dectin-1 signal transduction are at present unclear.

Tetraspanin-enriched microdomains in some Dectin-1-expressing cells also interact with MHCII glycoproteins (MHCIIgp) and a small palmitoylated transmembrane adaptor protein, SCIMP (23–25). Expression of SCIMP is highly specific for the tissues of the immune system, where it is confined to the professional antigen-presenting cells (dendritic cells, B cells, and macrophages). In B cells, SCIMP is phosphorylated after MHCIIgp cross-linking, and it is thought to be involved in the reverse signaling at the APC side of the immunological synapse. In the K46 B cell line, it was shown to be mainly responsible for supporting ERK signaling upon MHCIIgp stimulation (24).

The SCIMP molecule has four potential tyrosine phosphorylation sites. When phosphorylated, it binds Grb2, SLP-65, or SLP-76 and Csk via their Src homology 2 (SH2) domains. Through a proline-rich sequence, SCIMP is constitutively associated with the Src family kinase Lyn. Despite the interaction with a negative regulator of the Src family kinases Csk, SCIMP plays an overall positive regulatory function mediated by the recruitment of the Grb2·SLP-65 complex, whereas Csk binding seems to be only responsible for negative feedback regulation of this process (24, 25).

Here we have investigated SCIMP function *in vivo* using a SCIMP-deficient mouse model. Although we did not observe any effects of SCIMP deficiency on MHCIIgp signaling, we found that it is involved in the signaling by Dectin-1 in dendritic cells and macrophages, where it is important for sustaining prolonged MAP kinase activity and pro-inflammatory cytokine production.

Results

Normal Leukocyte Development and Distribution in SCIMP-deficient Mice—To determine the physiological function of SCIMP, we obtained the SCIMP-deficient mouse strain $Scimp^{tm1a(KOMP)Wtsi}$ (hereafter termed $Scimp^{-/-}$) from the International Knockout Mouse Consortium (for details, see "Experimental Procedures"). First we verified SCIMP deficiency at the protein level. As expected, there was no detectable SCIMP protein present in the lysates of $Scimp^{-/-}$ splenocytes and dendritic cells (Fig. 1*A*).

Next, we assessed leukocyte development and leukocyte subset representation in lymphoid organs obtained from SCIMP-deficient mice. Bone marrows, spleens, lymph nodes, and peripheral blood were isolated from 6- to 8-week-old wild-type and $Scimp^{-/-}$ animals. After preparation of single cell suspensions, a multiparametric flow cytometry analysis was carried out. This analysis determined the percentages of T cells, B cells, and their subpopulations as well as the representation of major myeloid cell subsets. However, $Scimp^{-/-}$ mice did not show any statistically significant differences from wild-type animals under steady-state conditions (Fig. 1, *B–E*).

Normal Function of SCIMP-deficient B Cells—In B cells, SCIMP was shown to be involved in signal transduction downstream of MHCIIgp (24). Moreover, we found that GL7+ germinal center B cells express higher levels of SCIMP than naïve B cells (Fig. 2*A*). This suggests that SCIMP may participate in signaling in B cells during the process of obtaining antigen-specific T cell help in the germinal centers of lymphoid follicles. This eventually results in B cell differentiation into plasma cells and secretion of specific antibodies. To test the effect of SCIMP deficiency on this process, we immunized wild-type and $Scimp^{-/-}$ mice intradermally with ovalbumin. After the immunization, we collected the serum from immunized animals and measured antigen-specific IgM and IgG by ELISA. Although there was a significant increase in immunoglobulin production after immunization, there were no significant differences between wild-type and $Scimp^{-/-}$ animals in the detected levels of antigen-specific IgM or IgG (Fig. 2*B*). Similar results were also obtained when we used different antigen (a small recombinant fragment from ARHGEF4 protein, data not shown).

Another option was that SCIMP may support the function of B cells as antigen-presenting cells. To test this, we performed a B cell antigen presentation assay. $Scimp^{-/-}$ and wild-type mice were crossed with the transgenic mouse strain B1–8i expressing B cell antigen receptor (BCR) specific for 4-hydroxy-3-nitrophenylacetyl (NP) hapten. Then we isolated B cells from these mice and fed them with NP-ovalbumin to allow its processing and presentation on MHCII molecules. Next we tested the ability of these B cells to stimulate OTII T cells expressing transgenic T cell antigen receptor (TCR) specific for ovalbumin peptide. The proliferation and activation of antigen-specific T cells were measured by flow cytometry (Fig. 2*C*). Similar to the previous experiment, we did not observe any differences between WT and $Scimp^{-/-}$ B cells in their ability to activate antigen-specific T cells.

Finally, we also tested signaling downstream of MHCIIgp in SCIMP-deficient B cells. Specifically, we analyzed ERK MAP kinase activation triggered by MHCIIgp cross-linking, which was shown previously to be reduced in the K46 B cell line after SCIMP down-regulation (24). However, in contrast to the K46 B cell line, murine purified B cells isolated from $Scimp^{-/-}$ spleen did not show any defects in ERK phosphorylation when compared with wild-type B cells (Fig. 2*D*). Moreover, calcium responses after MHCIIgp and IgM cross-linking were also not altered (Fig. 2*E*). This lack of differences at the single cell level *in vitro* may explain the lack of differences during the antigen presentation assay and antigen-specific antibody response *in vivo*.

SCIMP Expression in Myeloid Cells—SCIMP is expressed not only in the B cell lineage but also in myeloid cells, such as dendritic cells and macrophages. Strong expression of SCIMP was observed in dendritic cells differentiated from human monocytes using GM-CSF- and IL-4-supplemented medium (24). Interestingly, in bone marrow-derived macrophages (BMMFs), SCIMP expression is relatively low. However, it can be strongly up-regulated after GM-CSF treatment (Fig. 3*A*). Therefore, we wanted to find out whether SCIMP expression in BMDCs prepared by culturing bone marrow cells in GM-CSF-containing medium is caused by the presence of GM-CSF or whether it is their intrinsic quality. To test this, we used another method of BMDC generation from bone marrow cells that employs Flt3L instead of GM-CSF. As Fig. 3*B* shows, SCIMP is expressed even

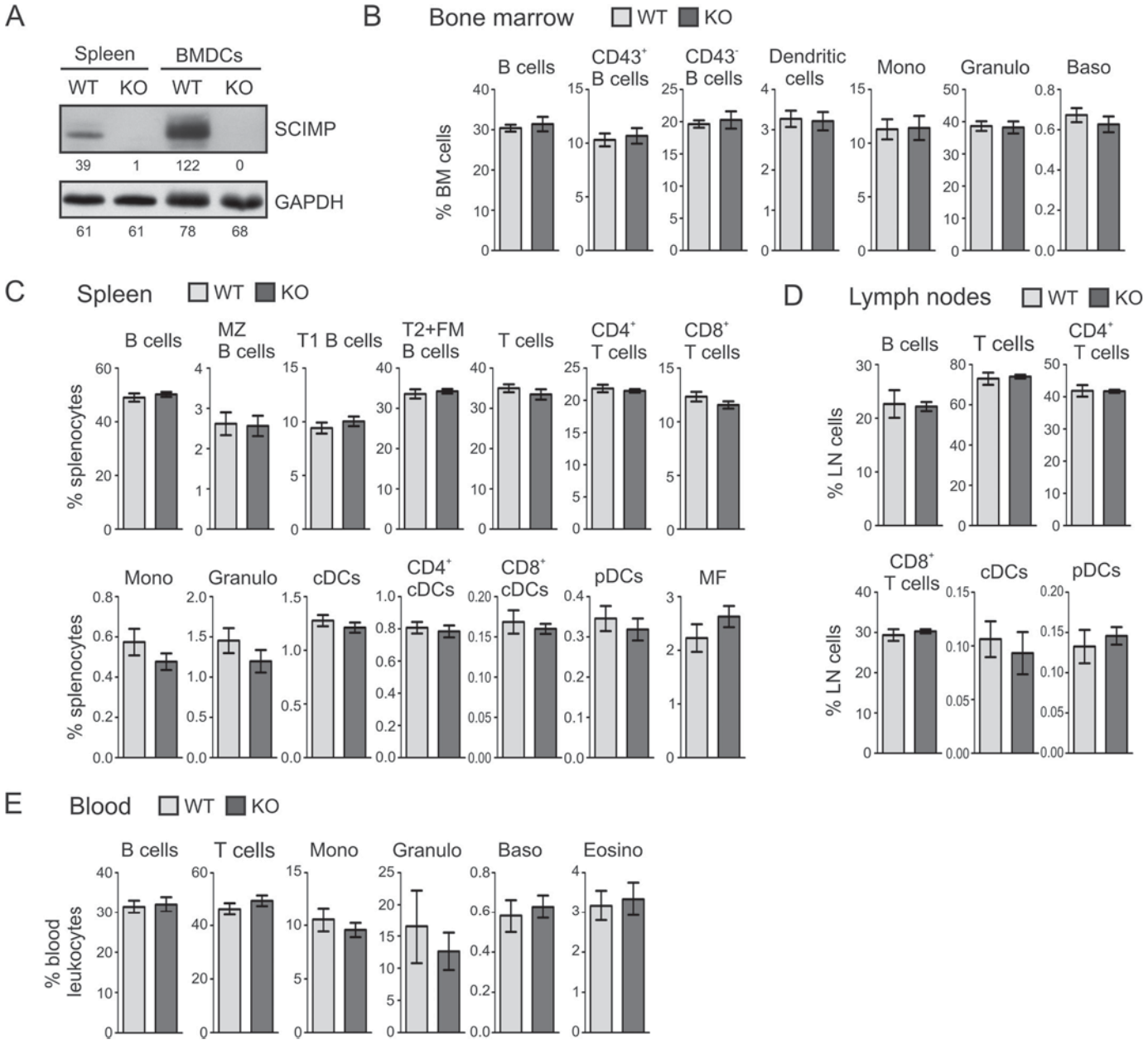

FIGURE 1. **Verification of SCIMP protein deficiency and leukocyte subset analysis in Scimp$^{-/-}$ mice.** *A*, lysates of splenocytes and BMDCs prepared from WT and Scimp$^{-/-}$ (*KO*) mice were probed for the presence of SCIMP and GAPDH (loading control) by Western blotting. *B–E*, percentages of major leukocyte subsets in the bone marrows (*B*), spleens (*C*), lymph nodes (*D*), and peripheral blood (*E*) of WT and Scimp$^{-/-}$ mice determined by flow cytometry. The individual subpopulations were gated as follows. Bone marrow: B cells (B220$^+$), CD43$^+$ B cells (B220$^+$, CD43$^+$), CD43$^-$ B cells (B220$^+$, CD43$^-$), dendritic cells (F4/80$^-$, Ly6C$^-$, CD11b^{low}, CD11c^{hi}), monocytes (*Mono*, F4/80$^-$, CD11b$^+$, Gr1^{low}, Ly6C^{hi}), granulocytes (*Granulo*, F4/80$^-$, Ly6C$^+$, Gr1^{hi}), and basophils (*Baso*, ckit$^-$, CD49b$^+$, FcεR$^+$). Spleen and lymph nodes: B cells (CD19$^+$), MZ B cells (B220$^+$, IgM^{hi}, IgD$^-$, CD1d$^+$), T1 B cells (B220$^+$, IgM$^+$, IgD$^-$), T2+FM B cells (B220$^+$, IgD$^+$), T cells (CD3$^+$), CD4 T cells (CD3$^+$, CD4$^+$), CD8 T cells (CD3$^+$, CD8$^+$), monocytes (F4/80$^-$, CD11b$^+$, Gr1^{low}, Ly6C^{hi}), granulocytes (CD3$^-$, CD19$^-$, CD11b$^+$, Gr1^{hi}), classical dendritic cells (CD11c$^+$, Ly6C$^-$), CD4$^+$ classical dendritic cells (CD11c$^+$, Ly6C$^-$,CD4$^+$), CD8$^+$ classical dendritic cells (CD11c$^+$, Ly6C$^-$,CD8$^+$), plasmacytoid dendritic cells (CD11c^{low}, Ly6C$^+$, B220$^+$), and macrophages (CD11b^{low}, F4/80$^+$). Peripheral blood: B cells (CD19$^+$), T cells (CD3$^+$), monocytes (SSA^{low}, CD11b$^+$), granulocytes (CD11b$^+$, LyG^{hi}, Ly6C^{low}), basophils (ckit$^-$, CD49b$^+$, FcεRIα$^+$), and eosinophils (*Eosino*, CD11b$^+$, Ly6C^{low}, Ly6G$^-$, SSA^{hi}).

in BMDCs differentiated by Flt3L, although it is still further up-regulated after GM-CSF exposure (Fig. 3*B*).

Finally, to assess SCIMP expression in dendritic cells *in vivo*, we sorted classical dendritic cells from murine spleens and analyzed SCIMP expression in these cells by Western blotting. These results clearly showed the presence of SCIMP in primary DCs (Fig. 3*C*). From these results we can conclude that SCIMP is expressed in dendritic cells *in vitro* and *in vivo* and that its expression is enhanced by the presence of GM-CSF.

SCIMP Is Phosphorylated After Stimulation of Dendritic Cells and Macrophages with Zymosan—Because of the strong SCIMP expression in BMDCs, we decided to search for its function in this cell type. Surprisingly, we observed only a marginal increase in SCIMP phosphorylation after MHCIIgp cross-linking on the surface of these cells (Fig. 4*A*). Thus we hypothesized that, in BMDCs, SCIMP acts downstream of a different receptor. Dectin-1 was a very good candidate because, similar to SCIMP, it is present in tetraspanin-enriched microdomains

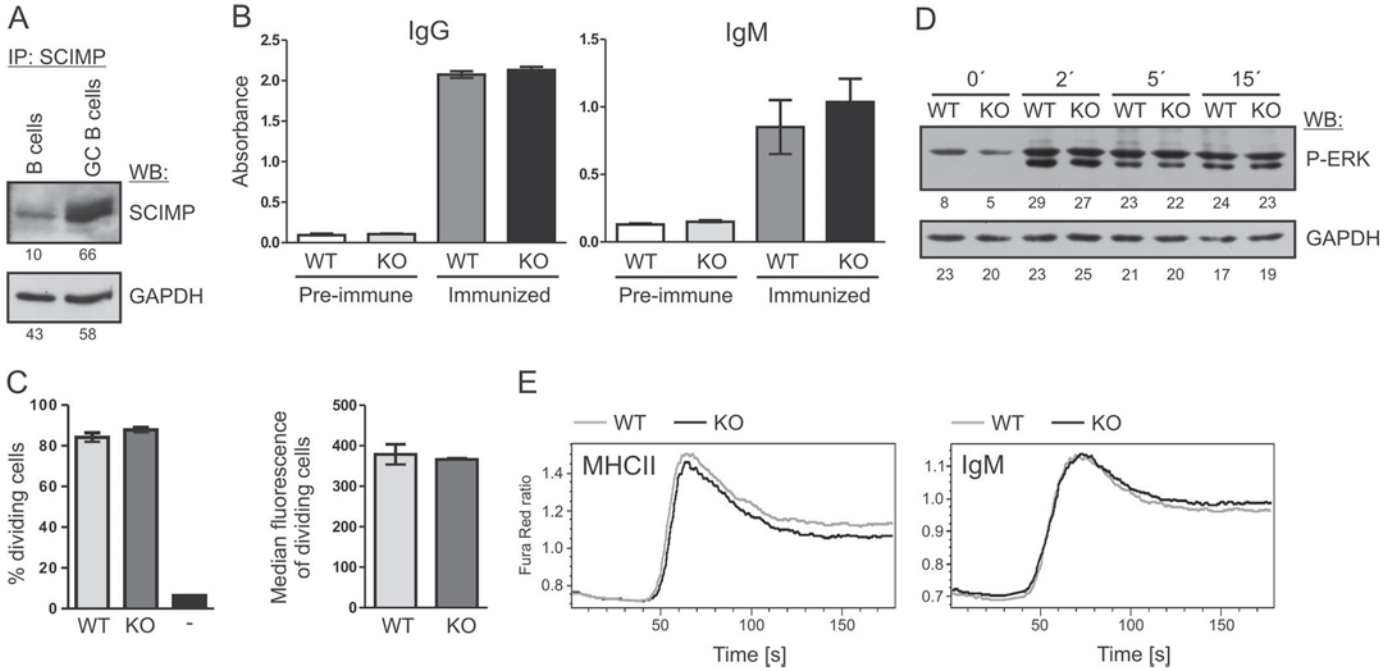

FIGURE 2. **Normal responses of Scimp$^{-/-}$ B cells.** *A*, sorted naïve mouse B cells from control mouse or GL7^{+} germinal center (*GC*) B cells from sheep red blood cell-immunized mice were lysed in SDS-PAGE sample buffer and probed for SCIMP protein by immunoblotting. GAPDH staining served as a loading control. *IP*, immunoprecipitation; *WB*, Western blotting. *B*, sera from WT ($n = 5$) or Scimp$^{-/-}$ (*KO*, $n = 6$) mice immunized intradermally with ovalbumin in incomplete Freund adjuvant were collected, and immunoglobulins specific to ovalbumin were detected by ELISA. As a control, preimmune sera from the same mice were used. *C*, proliferation of OTII transgenic T cells labeled with CFSE was measured after 48 h co-culture with NP-ovalbumin-fed B1–8i transgenic B cells (WT or Scimp$^{-/-}$) by flow cytometry. T cells cultured alone served as a negative control (−). Percentages of dividing cells and median CFSE fluorescence of cells that underwent at least one division are shown. *D*, ERK1/2 phosphorylation after MHCIIgp cross-linking in WT and Scimp$^{-/-}$ primary splenic B cells was analyzed by immunoblotting. *E*, splenocytes isolated from WT and Scimp$^{-/-}$ mice were stained with APC-conjugated anti-CD3 and anti-CD11b antibodies. The increase in calcium flux after MHCIIgp or IgM cross-linking was evaluated in B cells (gated as CD3^{-} CD11b^{-}) using a Fura Red calcium-sensitive probe.

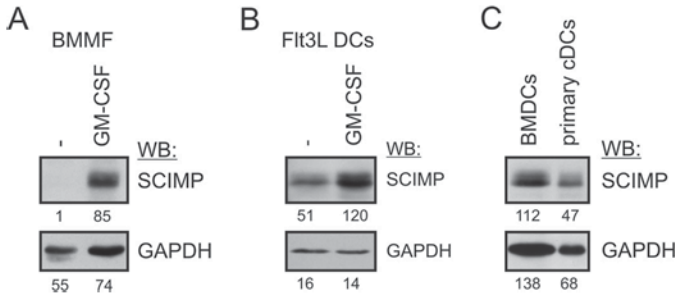

FIGURE 3. **Expression of SCIMP and its regulation in dendritic cells and macrophages.** *A*, BMMFs were differentiated from bone marrow cells for 7 days in M-CSF-containing medium. On day 7, the medium was replaced with GM-CSF-containing medium, and after an additional 24 h, cells were lysed in SDS-PAGE sample buffer. SCIMP was detected by immunoblotting. *WB*, Western blotting. *B*, dendritic cells were generated using Flt3L- and stem cell factor-containing medium. On day 8, plasmacytoid dendritic cells were removed using anti-mPDCA-1 magnetic beads, and the rest of the dendritic cells were cultured for 24 h in GM-CSF-containing medium followed by analysis of SCIMP expression by immunoblotting. *C*, splenic cDCs (CD11c^{+}, B220^{-}, Ly6C^{-}) were sorted from the spleens of wild-type mice, lysed, and subjected to immunoblotting with SCIMP and GAPDH antibodies. BMDCs served as a positive control.

(24), and it is up-regulated in the presence of GM-CSF. We used zymosan as a well established Dectin-1 activator. Zymosan is a preparation of small particles rich in the Dectin-1 ligand β-glucan, prepared from the yeast *Saccharomyces cerevisiae* (26). Strikingly, treatment of BMDCs with zymosan resulted in a strong increase of SCIMP phosphorylation (Fig. 4*B*). Moreover, SCIMP localized into zymosan-containing phagosomes and remained there for at least 30 min (Fig. 4*C* and supplemental Movie 1). SCIMP phosphorylation was very stable, with only a minor reduction during the 30-min experiment (Fig. 4*D*). A similar observation was also made with BMMFs (Fig. 4*E*).

SCIMP Is Involved in Dectin-1 Signaling—Dectin-1 signal transduction is initiated by Src family kinases and Syk (15). To test which kinases are responsible for SCIMP phosphorylation after zymosan treatment, we stimulated BMDCs with zymosan in the presence of specific inhibitors of Src family kinases and Syk. The results suggested that both Src family and Syk kinases are required for SCIMP phosphorylation after zymosan treatment because SCIMP phosphorylation was most profoundly reduced when both Src family kinase (PP2) and Syk (Syk inhibitor IV) inhibitors were combined (Fig. 5*A*).

The composition of zymosan is relatively complex. In addition to β-glucan, it also contains mannans (ligands of Dectin-2) and TLR2 ligands (26, 27). To confirm Dectin-1 involvement in the induction of SCIMP phosphorylation, we exploited the much stronger responsiveness of Dectin-1 to particulate β-glucan than to soluble β-glucan as a unique feature of this receptor. As a result, many aspects of Dectin-1 signaling after stimulation with particulate β-glucan can be inhibited by soluble forms of β-glucan (19). Thus, in the next experiment, we stimulated BMDCs with zymosan particles in the presence or absence of soluble β-glucan. Indeed, treatment with soluble β-glucan substantially inhibited SCIMP phosphorylation, whereas soluble mannan had no effect (Fig. 5*B*), suggesting that SCIMP is indeed a part of the Dectin-1 signaling pathway. To further support this conclusion, we investigated SCIMP phosphorylation in MyD88-deficient BMDCs, which have impaired function of multiple TLRs, including TLR2, the main TLR activated

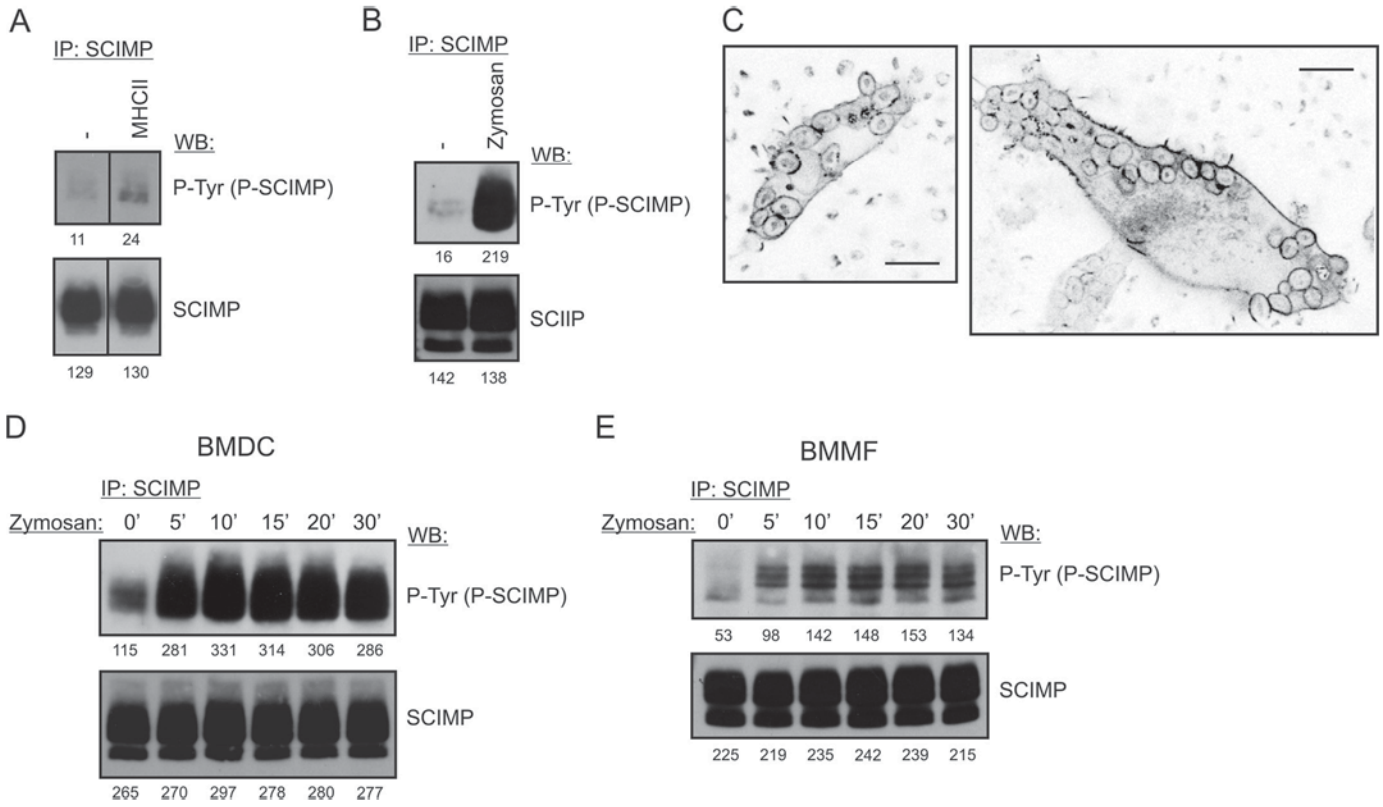

FIGURE 4. **SCIMP is phosphorylated in response to zymosan stimulation.** *A*, SCIMP phosphorylation in SCIMP immunoprecipitates (*IP*) prepared from BMDCs stimulated for 5 min by MHCIIgp cross-linking. *WB*, Western blotting. *B*, SCIMP phosphorylation in SCIMP immunoprecipitates prepared from BMDCs stimulated for 5 min with 300 μg/ml zymosan. *C*, localization of SCIMP-YFP into zymosan-containing phagosomes in BMDCs retrovirally transduced with a SCIMP-YFP coding construct. Zymosan is visible because of its strong autofluorescence. *Scale bars* = 10 μm. *D*, sustained SCIMP phosphorylation in SCIMP immunoprecipitates prepared from BMDCs stimulated for the indicated times with 300 μg/ml zymosan. *E*, sustained SCIMP phosphorylation in SCIMP immunoprecipitates prepared from BMMFs stimulated for the indicated times with 300 μg/ml zymosan.

by zymosan (17, 28, 29). SCIMP phosphorylation was not affected by the disruption of TLR signaling (Fig. 5*C*). Based on these experiments, we concluded that Dectin-1 is responsible for inducing SCIMP phosphorylation after zymosan treatment.

SCIMP Is Important for Sustained MAP Kinase Signaling and Cytokine Production After Stimulation with Zymosan—To test the functional significance of SCIMP in Dectin-1 signaling, we first measured ERK activation in zymosan-stimulated BMDCs because the ERK pathway was affected in the previous study of the SCIMP-deficient K46 B cell line (24). We stimulated BMDCs with zymosan for 30 min and followed ERK phosphorylation in the lysates prepared from these cells at various time points. Surprisingly, we could not detect any reproducible differences in ERK phosphorylation between wild-type and Scimp$^{-/-}$ BMDCs (Fig. 6*A*). Similar results were also obtained for p38 and JNK MAP kinases (Fig. 6*A* and data not shown). We also crossed Scimp$^{-/-}$ mice with a MyD88-deficient strain to avoid interference from the TLR pathways. However, even in MyD88-deficient BMDCs, no differences in signaling caused by SCIMP deficiency could be detected (data not shown).

As shown in Fig. 4*D*, SCIMP phosphorylation after zymosan activation was stable for at least 30 min. When we analyzed this further, we found that increased SCIMP phosphorylation could be observed even as late as 24 h after addition of zymosan (Fig. 6*B*). However, it also seemed that the amount of SCIMP immunoprecipitated from zymosan-treated cells was higher. Indeed, when we tested cell lysates from untreated and zymosan-activated BMDCs, we observed that SCIMP expression was up-regulated after zymosan-mediated activation (Fig. 6*C*). Therefore, we decided to investigate the signaling downstream of Dectin-1 in Scimp$^{-/-}$ BMDCs at 24 h after initiation of signaling. To avoid interference from TLR pathways, we used mice with a MyD88-deficient genetic background for this experiment. Consistent with the long-lasting SCIMP phosphorylation, we observed a significant reduction of ERK and p38 phosphorylation in SCIMP-deficient BMDCs at this late time point (Fig. 6, *D* and *E*). This effect seemed selective for MAP kinase signaling because we did not detect any differences in the phosphorylation of PKCδ in the same samples (Fig. 6*F*). We also tested the activation status of JNK and the members of the NF-κB pathway (p65 and IKKα/β), but we could not detect any phosphorylation of these proteins, which at this late stage of signaling could have already been down-regulated.

Finally, we tested whether the defects in MAP kinase signaling influence downstream functional responses in dendritic cells. In a recent study, activation of the ERK pathway was shown to be critical for inflammatory cytokine production in BMMFs (30). Because we were unable to detect any significant defects in cytokine production in Scimp$^{-/-}$ BMDCs during the typical experimental setup, where the readout was measured within the first 24 h of stimulation (data not shown), we focused our analysis on late phases of cytokine production beyond the 24-h time frame. At these late phases, the alterations to sustained MAP kinase activity observed in Scimp$^{-/-}$ BMDCs were

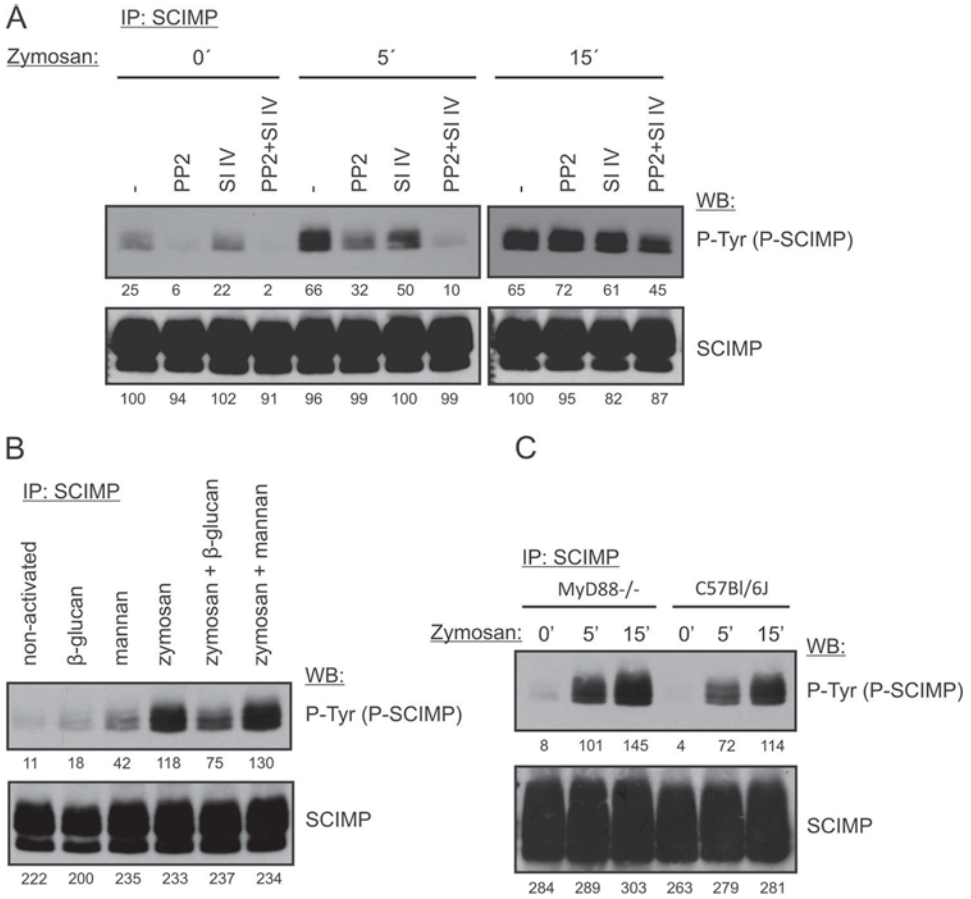

FIGURE 5. **SCIMP is part of the Dectin-1 signaling pathway.** *A*, BMDCs were incubated with 10 μM PP2 or 2 μM Syk inhibitor IV (*SI IV*) or a combination of them for 5 min. Next, 300 μg/ml zymosan was added, and cells were incubated in its presence for the indicated times, lysed, and subjected to SCIMP immunoprecipitation (*IP*) followed by immunoblotting with phosphotyrosine (*P-Tyr*) and SCIMP antibodies. *WB*, Western blotting. *B*, BMDCs were incubated at 37 °C with 600 μg/ml mannan or 600 μg/ml soluble β-glucan alone or in combination with 300 μg/ml zymosan. The level of SCIMP phosphorylation was detected as in *A*. *C*, MyD88-deficient or wild-type BMDCs were activated with 300 μg/ml zymosan for 5 or 15 min, and SCIMP phosphorylation was detected as in *A*.

more likely to have an effect. To measure the prolonged cytokine production, we washed away cytokines produced during the initial 48 h of stimulation and then cultured the cells for an additional 24 h before collecting the supernatants. This way we obtained samples containing only the cytokines produced between 48–72 h after zymosan stimulation. Under these conditions, we observed a significant reduction in the production of TNFα and IL-6 by Scimp/MyD88$^{-/-}$ BMDCs compared with MyD88$^{-/-}$ cells (Fig. 6*G*). These data are in agreement with our observations that SCIMP deficiency affects mainly the late phases of Dectin-1 signaling.

Discussion

In this article, we describe an initial analysis of SCIMP-deficient mice. Analysis of lymphocyte subsets in these mice at steady state showed that SCIMP is dispensable for leukocyte development and homeostasis. On the other hand, our results also showed that SCIMP is involved in Dectin-1 signaling, where it appears to be selectively involved in sustaining long-term ERK and p38 MAP kinase activation and pro-inflammatory cytokine production.

An earlier cell line-based study from our laboratory (24) suggested that, in B cells, SCIMP is involved in the reverse signaling at the B cell side of the immunological synapse downstream of MHCII glycoproteins. Specifically, it showed that SCIMP accumulates at the APC side of the immunological synapse and that shRNA-mediated SCIMP down-regulation results in a defect in ERK signaling downstream of MHCIIgp in the K46 murine B cell line. However, our analysis of primary murine B cells from SCIMP-deficient mice showed that, in contrast to the K46 B cell line, SCIMP deficiency has no significant impact on ERK signaling elicited by MHCIIgp cross-linking in primary mouse B cells. One possible explanation was that the K46 cell line may be more related to activated B cells, such as those present in the germinal center (31). Indeed, germinal center B cells express higher levels of SCIMP than naïve B cells and thus seem more likely to be affected by the loss of SCIMP. Nevertheless, we have not observed any effects of SCIMP deficiency on germinal center B cell numbers in Scimp$^{-/-}$ mice, and our experiments with isolated germinal center B cells did not reveal any differences in MHCIIgp signaling between WT and Scimp$^{-/-}$ GC B cells (data not shown). Moreover, intact antibody production by Scimp$^{-/-}$ mice (Fig. 2*B*) also suggested that germinal center reaction is not affected by SCIMP deficiency.

We also tested a possible involvement of SCIMP in MHCIIgp signaling in dendritic cells. However, despite the high levels of SCIMP in these cells, MHCIIgp cross-linking resulted only in a

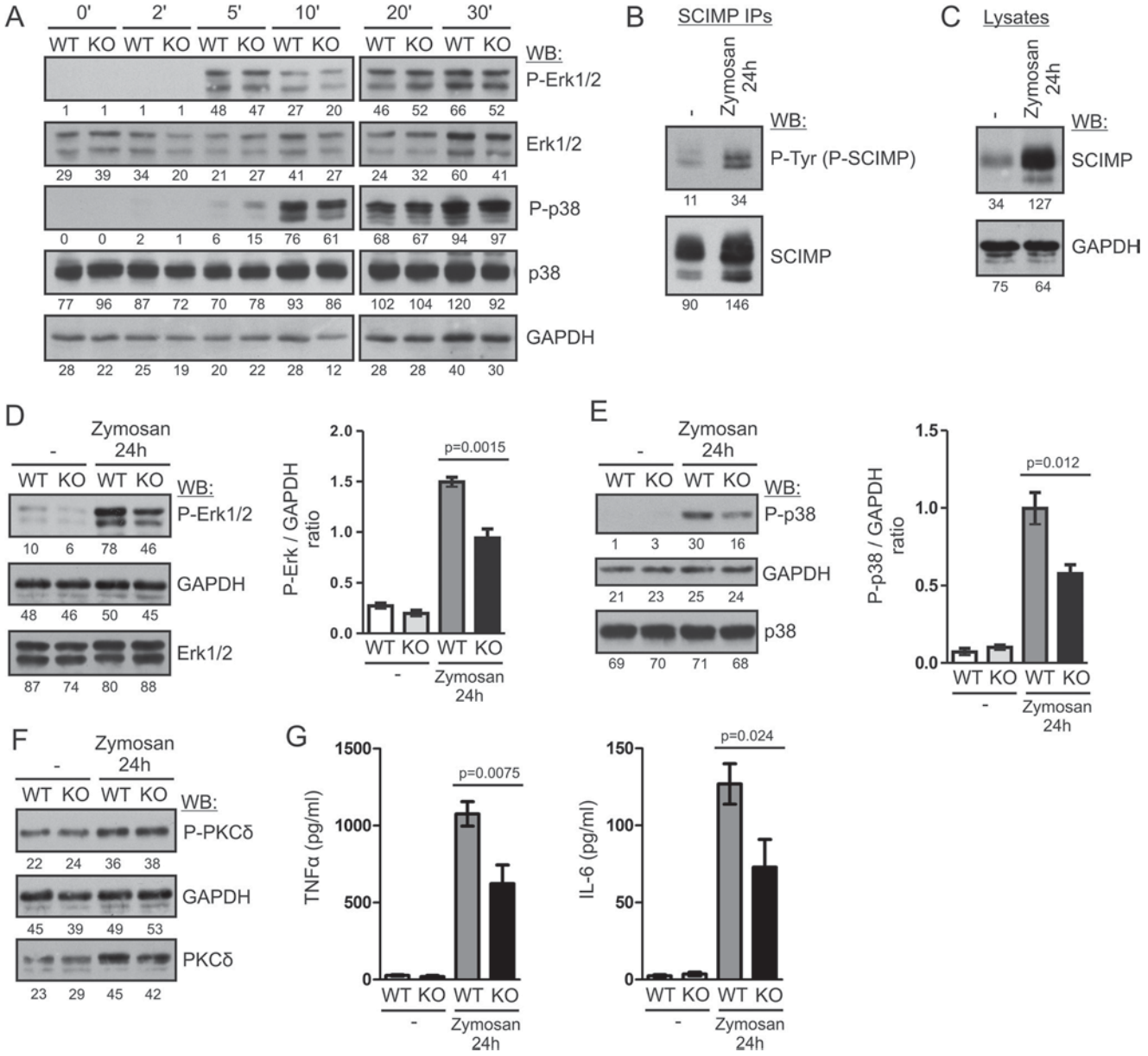

FIGURE 6. **SCIMP enhances long-term MAP kinase activation and pro-inflammatory cytokine production after stimulation with zymosan.** *A*, BMDCs from WT and Scimp$^{-/-}$ (*KO*) mice were stimulated with 300 μg/ml zymosan for the indicated times, and ERK1/2 and p38 phosphorylation was analyzed by immunoblotting. *WB*, Western blotting. *B*, BMDCs from C57Bl/6J mice were stimulated with 300 μg/ml zymosan for 24 h or left unstimulated, lysed, and subjected to SCIMP immunoprecipitation followed by immunoblotting with phosphotyrosine (*P-Tyr*) and SCIMP antibodies. *C*, levels of SCIMP protein in the lysates of BMDCs stimulated with 300 μg/ml zymosan for 24 h or left unstimulated were analyzed by immunoblotting with SCIMP antibodies. *D*, phosphorylation of ERK1/2 in the lysates of WT and Scimp$^{-/-}$ BMDCs stimulated with zymosan for 24 h or left unstimulated (*left panel*). The *right panel* shows the results of densitometric quantification of ERK phosphorylation in samples prepared from 4 mice/genotype. *E*, a similar analysis of p38 phosphorylation in the samples from *D*. *F*, a similar analysis of PKCδ phosphorylation. *G*, late production of TNFα and IL-6 by WT and Scimp$^{-/-}$ BMDCs. BMDCs were stimulated with 300 μg/ml zymosan for 48 h, washed, and cultured for an additional 24 h in the absence of stimulus. After this period, culture supernatants were collected and analyzed by ELISA for the presence of TNFα and IL-6. In the experiments shown in *B*–*G*, mice with a MyD88-deficient genetic background were used.

marginal increase in SCIMP phosphorylation, suggesting that, in dendritic cells, SCIMP may function differently from B cells and act downstream of a different receptor. Our candidate-based approach led to the identification of the β-glucan receptor Dectin-1 as a receptor employing SCIMP in its signal transduction. Because both SCIMP and Dectin-1 are associated with tetraspanins (21, 22), we hypothesized that, via tetraspanin-enriched microdomains, SCIMP and Dectin-1 may interact and, as a result, that SCIMP may be involved in coupling of Dectin-1 to downstream signaling pathways. Indeed, in both dendritic cells and GM-CSF-activated macrophages, SCIMP is strongly phosphorylated after Dectin-1 stimulation with zymosan. However, zymosan also contains ligands for additional pattern recognition receptors, and so we performed a series of experiments indicating that Dectin-1 is indeed the receptor triggering SCIMP phosphorylation. These experiments showed that SCIMP phosphorylation induced by zymosan treatment is not affected in Myd88$^{-/-}$ dendritic cells with dysfunctional TLR signaling. In addition, zymosan-triggered SCIMP phosphorylation was inhibited by soluble β-glucan, which can spe-

cifically bind to the receptor but does not fully activate it (19). In contrast, a soluble form of mannan, another major zymosan component, did not inhibit SCIMP phosphorylation after zymosan treatment. Interestingly, soluble mannan alone elicited moderate SCIMP phosphorylation, suggesting that there may be a minor contribution from a mannan receptor, such as Dectin-2 (32), to zymosan-induced SCIMP phosphorylation.

SCIMP phosphorylation lasts for many hours after the encounter with zymosan. Moreover, zymosan stimulation also enhances SCIMP expression. Because SCIMP typically displays a certain level of constitutive phosphorylation even in quiescent cells, SCIMP protein up-regulation can contribute to the increased phosphorylation observed at the very late time points. However, the relative contribution of increased SCIMP expression and Dectin-1-induced phosphorylation to global levels of phosphorylated SCIMP remains unclear. Phosphorylated SCIMP appears to be important for sustaining ERK and p38 activation for prolonged periods of time. The precise mechanism of how SCIMP mediates ERK and p38 signaling is not entirely clear. Dectin-1 activates, by an unclear mechanism, PLCγ2, which is indispensable for ERK activation (33). PLCγ2 products also activate PKCδ, which then phosphorylates the adaptor protein CARD9, resulting in activation of the NF-κB pathway (15). A recent study showed that CARD9 also plays a critical role in ERK activation by bringing together Ras and RasGRF1, resulting in the activation of Ras and ERK further downstream (30). However, the existence of CARD9-independent pathways cannot be ruled out. Previously published data showed that SCIMP binds the SLP65/SLP76 adaptor proteins, which are known to be involved in PLCγ1/2 activation (24, 34). In addition, SCIMP also binds Grb2, which can then recruit Sos proteins, well characterized exchange factors for Ras and activators of the Ras/ERK pathway. Products of PLCγ2 also activate another family of Ras exchange factors, RasGRP proteins, which activate Ras downstream of TCR, BCR, and other immunoreceptors (35). Clearly, there are multiple options of how SCIMP can contribute to Dectin-1-dependent ERK activation. It certainly is not the only player connecting Dectin-1 to the ERK pathway, and especially at the early stages of signaling, other pathways dominate the response. However, at the very late stages of Dectin-1 stimulation, SCIMP activity becomes more apparent.

In addition to ERK, SCIMP also contributes to the activation of p38 MAP kinase. The mechanism of p38 activation downstream of Dectin-1 is less well understood. In contrast to ERK, it was shown to be independent of CARD9 (30). Our observations of similar defects in ERK and p38 activation in SCIMP-deficient animals together with unperturbed PKCδ activity suggest that SCIMP affects a CARD9-independent pathway that may be involved in the activation of both of these MAP kinases.

Dectin-1 is an important innate immune receptor recognizing a number of pathogenic fungi. It supports the immune response by mediating phagocytosis of these pathogens by triggering an oxidative burst and by inducing the production of cytokines (7, 17, 18). We have analyzed all of these downstream responses in BMDCs from SCIMP-deficient mice, but we did not observe any differences between WT and SCIMP-deficient cells when stimulated by zymosan (data not shown). The only exceptions were the late phases of TNFα and IL-6 production (Fig. 6*G*). Our data are consistent with previous observations that ERK signaling is required for the production of TNFα and IL-6 downstream of Dectin-1 (30, 36). p38 signaling in macrophages and dendritic cells has also been shown to contribute to pro-inflammatory cytokine production (37, 38). Although the precise function of the late sustained production of these cytokines still remains to be clarified, the role of these cytokines in antifungal defense has already been well established. Mice deficient in TNFα or IL-6 were shown to be highly susceptible to fungal infections (39–42). Moreover, the use of agents blocking the function of TNFα or IL-6 in human patients is also associated with an increased incidence of infection with opportunistic fungi (43).

Taken together, our study describes a novel branch of Dectin-1 signaling that is driven by the small transmembrane adaptor SCIMP. Our data suggest that the early and late phases of Dectin-1 signaling are differentially regulated. The late sustained phase of Dectin-1 signaling is partly dependent on SCIMP, which in dendritic cells promotes MAP kinase signaling and production of TNFα and IL-6, important mediators of the inflammatory response during fungal infections.

Experimental Procedures

Antibodies—Antibodies to the following antigens were used for Western blotting detection: GAPDH (Sigma-Aldrich); phospho-ERK (Thr-202/Tyr-204), phospho-PKCδ/θ (Ser-643/676), PKCδ, phospho-p38 (Thr-180/182), and p38 MAPK, (Cell Signaling Technology); ERK1/2 (Promega); and phospho-tyrosine (4G10, Upstate Biotechnology). Rabbit polyclonal antibodies against murine SCIMP were described earlier (24). For the flow cytometry analysis, antibodies against the following mouse antigens conjugated to the indicated fluorophores were used: CD3-PE-Cy7, CD5-PE, CD11b-FITC, CD11b-PE, CD11b-APC, CD19-eFluor 660, CD19-FITC, CD23-Dye 647, F4/80-FITC, Gr1-PB, Ly6G-FITC, CD49b (DX5)-APC, c-kit-PE, Gr1-PE, Ly6C-PE-Cy7, B220-FITC, IgM-FITC, MHCII-FITC, FcϵRIα-PB, and CD86-APC (Biolegend); CD1d-FITC, CD4-PE, CD8-e450, CD11c-APC, CD43-PE, GL7-FITC, B220-e450, IgD-APC, and CD80-APC (eBiosciences); and CD3-APC and CD8-FITC (EXBIO). The anti-IgM-Dy547 antibody was conjugated in-house. For MACS purification, anti-CD43, anti-CD11b, anti-CD19, anti-FITC, and anti-mPDCA-1 MicroBeads (Miltenyi Biotec, Bergisch Gladbach, Germany) were used. Other antibodies used in this study were anti-mouse I-A/I-E-biotin (Biolegend), HRP-conjugated goat anti-mouse IgG (Sigma-Aldrich), HRP-conjugated goat anti-rabbit IgG Fc fragment-specific, goat anti-mouse IgM $F(ab)_2$ (Jackson ImmunoResearch Laboratories), Fc Bloc (2.4G2) (BD Biosciences), and HRP-conjugated goat anti-rabbit polyclonal antibody (Bio-Rad).

Other Reagents—We also used mannan from *S. cerevisiae* (Sigma-Aldrich), zymosan A from *S. cerevisiae* (Sigma-Aldrich), streptavidin (Jackson ImmunoResearch Laboratories), CFSE (5-(and 6)-carboxyfluorescein diacetate succinimidyl ester; eBioscience), and NP(14)-ovalbumin (Bioresearch Technologies, Inc.). Soluble β-glucan (Wellmune Soluble) was a kind gift from Bengt Hansson (Biogredia AB, Sandef-

jord, Norway). The Src family kinase inhibitor PP2 and Syk inhibitor IV (BAY 61-3606) were from Calbiochem/Merck (Darmstadt, Germany).

Mice—The SCIMP-deficient mouse strain Scimp$^{tm1a(KOMP)Wtsi}$ on the C57Bl/6J genetic background (throughout this article labeled as Scimp$^{-/-}$) was generated at the Wellcome Trust Sanger Institute (Cambridge, UK) within International Knock-out Mouse Consortium Project 24100 and was directly obtained from the Wellcome Trust Sanger Institute. B1–8i B cell antigen receptor-transgenic mice (44), the OTII transgenic mouse strain (C57BL/6-Tg(TcraTcrb)425Cbn/Crl), and the Myd88-deficient mouse strain (B6.129P2(SJL)-Myd88tm1.1Defr/J) derived from Myd88fl mice (45) were obtained from The Jackson Laboratory (Bar Harbor, ME). C57Bl/6J for comparative experiments originated from crossing Scimp$^{+/-}$ heterozygotes. Other C57Bl/6J mice were from the animal facility of the Institute of Molecular Genetics of the Academy of Sciences of the Czech Republic (IMG ASCR) (Prague, Czech Republic). All experiments in this work conducted on animals were approved by the Animal Care and Use Committee of the Institute of Molecular Genetics and were in agreement with local legal requirements and ethical guidelines.

Cell Lines and Primary Cells—Primary mouse B cells were isolated from spleens of Scimp$^{-/-}$ and C57Bl/6J mice by negative selection using anti-CD43 and anti-CD11b MicroBeads (Miltenyi Biotec) on an AutoMACS magnetic cell sorter (Miltenyi Biotec) and subsequently cultured in Iscove's modified Dulbecco's medium (IMDM). BMMFs were differentiated from mouse bone marrow cells in DMEM conditioned with 10% L929 culture supernatant containing M-CSF for 7–9 days. BMDCs were differentiated in DMEM conditioned with 3% LUTZ cell culture supernatant containing GM-CSF for 10–12 days. Ftl3L-generated dendritic cells were cultured in 100 ng/ml rmFLT3L (Peprotech) and RPMI medium supplemented with stem cell factor (supernatant from HEK293 cells transfected with a stem cell factor-coding construct) for 8 days, and then plasmacytoid dendritic cells were removed using anti-mPDCA-1 microbeads on an AutoMACS, and the rest of the dendritic cells were used further.

To prepare primary classical dendritic cells, splenocytes from C57Bl/6J mice were incubated with Fc bloc, CD3-FITC, IgM-FITC, and Ter119-FITC and precleared on an AutoMACS using anti-FITC magnetic beads (Miltenyi Biotec). The negative fraction was further stained with B220-e450, Ly6C-PE_Cy7, and CD11c-APC and sorted by BD Influx FACS (BD Biosciences) for classical DCs (CD11c$^+$, B220$^-$, Ly6C$^-$) (46). For GL7$^+$ germinal center B cell purification, all splenic B cells were first purified from mice immunized intraperitoneally with sheep red blood cells by negative selection using CD11b and CD43 microbeads on an AutoMACS magnetic cell separator. The obtained B cells were then stained with GL-7-FITC antibody, followed by positive selection with anti-FITC magnetic beads using the same AutoMACS separator. Phoenix Eco cells were obtained from Origene and cultured in DMEM. All media were supplemented with 10% fetal calf serum and antibiotics. The cells were cultured at 37 °C in 5% CO_2.

DNA Constructs, Transfection, and Transduction—The mouse SCIMP-YFP construct coding for full-length mouse SCIMP tagged at the C terminus with yellow fluorescent protein was cloned into the pMSCV-LNGFR retroviral vector. Lipofectamine 2000 (Invitrogen/Thermo Fisher Scientific) was used according to the protocol of the manufacturer for the transfection of SCIMP-YFP/pMSCV-LNGFR construct to Phoenix Eco cells to produce viral particles. Retrovirus-containing supernatants were then harvested, supplemented with Polybrene (10 mg/ml, Sigma-Aldrich), and added to the freshly isolated bone marrow cells. The cells were then centrifuged at 1250 × *g* for 90 min at 30 °C and differentiated into BMDCs or BMMFs.

Cell Activation, Lysis, and Immunoprecipitation—To test the effect of zymosan and other activators on BMDCs, fully differentiated BMDCs were plated on 6-well plates (2×10^6 cells/well) in culture medium and allowed to adhere to the plastic overnight. Then the medium was changed for DMEM without GM-CSF. After 2 h, zymosan in DMEM was added to a final concentration of 300 μg/ml. The activation of cells was stopped after the indicated time periods by lysis in SDS-PAGE sample buffer. For immunoprecipitation, the cells (BMDCs or BMMFs) were plated on 10-cm dishes and activated as above or by biotinylated anti mouse I-A/I-E antibody (Biolegend, 10 μg/ml), followed by cross-linking with 10 μg/ml streptavidin (Jackson ImmunoResearch Laboratories). They were then lysed in lysis buffer containing 1% laurylmaltoside (Calbiochem/Merck), 20 mM Tris (pH 7.5), 150 mM NaCl, 5 mM iodoacetamide, 5 mM NaF, 1 mM Na_3VO_4, 2 mM EDTA, and 100× diluted protease inhibitor mixture set III (Calbiochem) for 30 min on ice. Postnuclear supernatants were incubated for 1–2 h with anti-SCIMP rabbit antiserum followed by 1–2 h of incubation with protein A/G Plus-agarose beads (Santa Cruz Biotechnology) at 4 °C. After washing, the immunoprecipitates were eluted with 40 μl of SDS-PAGE sample buffer.

B cell stimulations were carried out in suspension. B cells were resuspended in a concentration of 5×10^7/ml in IMDM and activated by labeling with 10 μg/ml biotinylated anti-mouse I-A/I-E antibody, followed by cross-linking with 10 μg/ml streptavidin in IMDM at 37 °C for the indicated time intervals. The activation of cells was stopped by addition of an equal volume of 2× concentrated SDS-PAGE sample buffer. Western blotting quantification was performed by densitometry of scanned films using AIDA image analyzer software (Elysia-raytest, Straubenhardt, Germany), and the obtained values were inserted into the figures below the individual blots.

Flow Cytometry—Single cell suspensions were prepared from spleens, lymph nodes, bone marrow, and peripheral blood from 6- to 8-week-old mice. Erythrocytes were lysed with ACK buffer (150 mM NH_4Cl, 0.1 mM EDTA (disodium salt), and 1 mM $KHCO_3$). The remaining cells were incubated with Fc-bloc and fluorophore-conjugated antibodies and analyzed on a BD LSRII Flow cytometer. For calcium response measurement, a single cell suspension of splenocytes (after erythrocyte lysis in ACK buffer) was loaded with 2 μM calcium indicator Fura Red (Invitrogen) and subsequently stained with anti-CD3-APC and anti-CD11b-APC. Samples were analyzed using a BD LSRII flow cytometer for 30 s at rest and then another 150 s after activation (either with 10 μg/ml anti-mouse IgM F(ab)2 antibody (Jackson ImmunoResearch Laboratories) or with 10

μg/ml streptavidin, which cross-linked MHCIIgp molecules on B cells preincubated with biotinylated anti-I-A/I-E antibody (Biolegend). The relative calcium concentration was measured as a ratio of the Fura Red fluorescence intensity elicited by excitation wavelengths of 405 nm (emission measured at 635–720 nm) and 488 nm (emission measured at 655–695 nm). Data were analyzed using FlowJo software (TreeStar).

Antigen Presentation Assay—For the antigen-presentation assay, we modified a method published previously (47). $CD4^+$ T cells isolated from lymph nodes of OTII mice using negative selection (CD11b, CD8, CD19-FITC) on AutoMACS were cultured for 2 days in RPMI medium supplemented with 100 ng/ml anti-CD3 antibody and 2 units/ml IL2 for 48 h. B cells negatively selected on AutoMACS were fed for 1 h with 10 mg/ml NP-ovalbumin at 37 °C, washed with PBS, and cultured in a ratio of 1:1 with CFSE-stained T cells. After 48 h, cell proliferation was measured using a BD LSRII flow cytometer.

Immunization—For antibody detection, $Scimp^{-/-}$ and C57Bl/6J mice, 6–8 weeks old, were intradermally injected with 100 μg of ovalbumin/mouse in incomplete Freund adjuvant. The second immunization followed 21 days after the first immunization. Serum from mice was collected on day 10 after the second immunization. Antibody concentration was measured by ELISA.

Cytokine Detection—Concentrations of TNFα and IL-6 in BMDC culture supernatants were determined by Ready-SET-Go!® ELISA kits from eBioscience according to the instructions of the manufacturer.

Microscopy—For live cell microscopy, BMDCs and BMMFs expressing SCIMP-YFP were transferred into Lab-Tek chambered coverglass (Nunc, Thermo Fisher Scientific), and strongly autofluorescent zymosan particles were subsequently added. Cells were observed in a climate chamber (37 °C, 5% CO_2) under a Leica TCS SP5 confocal microscope using a ×63 objective lens (Leica Microsystems). Data were analyzed using LAS AF software (Leica Microsystems).

Author Contributions—J. K. conducted the majority of the experiments, analyzed the results, and wrote most of the paper. M. F. was involved in the preparation of BMDCs and conducted the part of the experiments addressing the expression and function of SCIMP in BMDCs. J. P. performed the analysis of antibody production by $Scimp^{-/-}$ mice. T. S. performed part of the BMDC biochemical analysis. B. M. designed and conducted part of the flow cytometry analysis. T. B. conceptualized and supervised the project, conducted some of the biochemical experiments, and wrote the paper with J. K. All authors reviewed the results and approved the final version of the manuscript.

Acknowledgments—We thank the International Knockout Mouse Consortium and the Wellcome Trust Sanger Institute for providing us with $Scimp^{-/-}$ mice. We also thank Bengt Hansson from Biogredia AB (Sandefjord, Norway) for providing us with a generous amount of soluble β-glucan (Wellmune Soluble). We also acknowledge the Microscopy Centre, IMG ASCR (Prague, Czech Republic) for support with obtaining the scientific data presented in this paper.

References

1. Hardison, S. E., and Brown, G. D. (2012) C-type lectin receptors orchestrate antifungal immunity. *Nat. Immunol.* **13,** 817–822
2. Seo, B. S., Lee, S. H., Lee, J. E., Yoo, Y. C., Lee, J., and Park, S. R. (2013) Dectin-1 stimulation selectively reinforces LPS-driven IgG1 production by mouse B cells. *Immune Netw.* **13,** 205–212
3. Taylor, P. R., Brown, G. D., Reid, D. M., Willment, J. A., Martinez-Pomares, L., Gordon, S., and Wong, S. Y. (2002) The β-glucan receptor, dectin-1, is predominantly expressed on the surface of cells of the monocyte/macrophage and neutrophil lineages. *J. Immunol.* **169,** 3876–3882
4. Willment, J. A., Marshall, A. S., Reid, D. M., Williams, D. L., Wong, S. Y., Gordon, S., and Brown, G. D. (2005) The human β-glucan receptor is widely expressed and functionally equivalent to murine Dectin-1 on primary cells. *Eur. J. Immunol.* **35,** 1539–1547
5. Brown, G. D., and Gordon, S. (2001) Immune recognition: a new receptor for β-glucans. *Nature* **413,** 36–37
6. Barreto-Bergter, E., and Figueiredo, R. T. (2014) Fungal glycans and the innate immune recognition. *Front. Cell. Infect. Microbiol.* **4,** 145
7. Brown, G. D., Herre, J., Williams, D. L., Willment, J. A., Marshall, A. S., and Gordon, S. (2003) Dectin-1 mediates the biological effects of β-glucans. *J. Exp. Med.* **197,** 1119–1124
8. Brown, G. D., Taylor, P. R., Reid, D. M., Willment, J. A., Williams, D. L., Martinez-Pomares, L., Wong, S. Y., and Gordon, S. (2002) Dectin-1 is a major β-glucan receptor on macrophages. *J. Exp. Med.* **196,** 407–412
9. Saijo, S., Fujikado, N., Furuta, T., Chung, S. H., Kotaki, H., Seki, K., Sudo, K., Akira, S., Adachi, Y., Ohno, N., Kinjo, T., Nakamura, K., Kawakami, K., and Iwakura, Y. (2007) Dectin-1 is required for host defense against *Pneumocystis carinii* but not against *Candida albicans*. *Nat. Immunol.* **8,** 39–46
10. Marakalala, M. J., Vautier, S., Potrykus, J., Walker, L. A., Shepardson, K. M., Hopke, A., Mora-Montes, H. M., Kerrigan, A., Netea, M. G., Murray, G. I., Maccallum, D. M., Wheeler, R., Munro, C. A., Gow, N. A., Cramer, R. A., *et al.* (2013) Differential adaptation of *Candida albicans in vivo* modulates immune recognition by dectin-1. *PLoS Pathog.* **9,** e1003315
11. Steele, C., Rapaka, R. R., Metz, A., Pop, S. M., Williams, D. L., Gordon, S., Kolls, J. K., and Brown, G. D. (2005) The β-glucan receptor dectin-1 recognizes specific morphologies of *Aspergillus fumigatus*. *PLoS Pathog.* **1,** e42
12. Ferwerda, B., Ferwerda, G., Plantinga, T. S., Willment, J. A., van Spriel, A. B., Venselaar, H., Elbers, C. C., Johnson, M. D., Cambi, A., Huysamen, C., Jacobs, L., Jansen, T., Verheijen, K., Masthoff, L., Morré, S. A., *et al.* (2009) Human dectin-1 deficiency and mucocutaneous fungal infections. *N. Engl. J. Med.* **361,** 1760–1767
13. Plantinga, T. S., van der Velden, W. J., Ferwerda, B., van Spriel, A. B., Adema, G., Feuth, T., Donnelly, J. P., Brown, G. D., Kullberg, B. J., Blijlevens, N. M., and Netea, M. G. (2009) Early stop polymorphism in human DECTIN-1 is associated with increased *Candida* colonization in hematopoietic stem cell transplant recipients. *Clin. Infect. Dis.* **49,** 724–732
14. Sancho, D., and Reis e Sousa, C. (2012) Signaling by myeloid C-type lectin receptors in immunity and homeostasis. *Annu. Rev. Immunol.* **30,** 491–529
15. Brubaker, S. W., Bonham, K. S., Zanoni, I., and Kagan, J. C. (2015) Innate immune pattern recognition: a cell biological perspective. *Annu. Rev. Immunol.* **33,** 257–290
16. Dambuza, I. M., and Brown, G. D. (2015) C-type lectins in immunity: recent developments. *Curr. Opin. Immunol.* **32,** 21–27
17. Gantner, B. N., Simmons, R. M., Canavera, S. J., Akira, S., and Underhill, D. M. (2003) Collaborative induction of inflammatory responses by dectin-1 and Toll-like receptor 2. *J. Exp. Med.* **197,** 1107–1117
18. Rogers, N. C., Slack, E. C., Edwards, A. D., Nolte, M. A., Schulz, O., Schweighoffer, E., Williams, D. L., Gordon, S., Tybulewicz, V. L., Brown, G. D., and Reis e Sousa, C. (2005) Syk-dependent cytokine induction by Dectin-1 reveals a novel pattern recognition pathway for C type lectins. *Immunity* **22,** 507–517
19. Goodridge, H. S., Reyes, C. N., Becker, C. A., Katsumoto, T. R., Ma, J., Wolf, A. J., Bose, N., Chan, A. S., Magee, A. S., Danielson, M. E., Weiss, A.,

Vasilakos, J. P., and Underhill, D. M. (2011) Activation of the innate immune receptor Dectin-1 upon formation of a "phagocytic synapse." *Nature* **472,** 471–475
20. Willment, J. A., Lin, H. H., Reid, D. M., Taylor, P. R., Williams, D. L., Wong, S. Y., Gordon, S., and Brown, G. D. (2003) Dectin-1 expression and function are enhanced on alternatively activated and GM-CSF-treated macrophages and are negatively regulated by IL-10, dexamethasone, and lipopolysaccharide. *J. Immunol.* **171,** 4569–4573
21. Mantegazza, A. R., Barrio, M. M., Moutel, S., Bover, L., Weck, M., Brossart, P., Teillaud, J.-L., and Mordoh, J. (2004) CD63 tetraspanin slows down cell migration and translocates to the endosomal-lysosomal-MIICs route after extracellular stimuli in human immature dendritic cells. *Blood* **104,** 1183–1190
22. Meyer-Wentrup, F., Figdor, C. G., Ansems, M., Brossart, P., Wright, M. D., Adema, G. J., and van Spriel, A. B. (2007) Dectin-1 interaction with tetraspanin CD37 inhibits IL-6 production. *J. Immunol.* **178,** 154–162
23. Berditchevski, F., and Odintsova, E. (2007) Tetraspanins as regulators of protein trafficking. *Traffic* **8,** 89–96
24. Draber, P., Vonkova, I., Stepanek, O., Hrdinka, M., Kucova, M., Skopcova, T., Otahal, P., Angelisova, P., Horejsi, V., Yeung, M., Weiss, A., and Brdicka, T. (2011) SCIMP, a transmembrane adaptor protein involved in major histocompatibility complex class II signaling. *Mol. Cell. Biol.* **31,** 4550–4562
25. Stepanek, O., Draber, P., and Horejsi, V. (2014) Palmitoylated transmembrane adaptor proteins in leukocyte signaling. *Cell. Signal.* **26,** 895–902
26. Di Carlo, F. J., and Fiore, J. V. (1958) On the composition of zymosan. *Science* **127,** 756–757
27. Underhill, D. M., Ozinsky, A., Hajjar, A. M., Stevens, A., Wilson, C. B., Bassetti, M., and Aderem, A. (1999) The Toll-like receptor 2 is recruited to macrophage phagosomes and discriminates between pathogens. *Nature* **401,** 811–815
28. Takeuchi, O., Kaufmann, A., Grote, K., Kawai, T., Hoshino, K., Morr, M., Mühlradt, P. F., and Akira, S. (2000) Cutting edge: preferentially the R-stereoisomer of the mycoplasmal lipopeptide macrophage-activating lipopeptide-2 activates immune cells through a toll-like receptor 2- and MyD88-dependent signaling pathway. *J. Immunol.* **164,** 554–557
29. Akira, S. (2000) Toll-like receptors: lessons from knockout mice. *Biochem. Soc. Trans.* **28,** 551–556
30. Jia, X. M., Tang, B., Zhu, L. L., Liu, Y. H., Zhao, X. Q., Gorjestani, S., Hsu, Y. M., Yang, L., Guan, J. H., Xu, G. T., and Lin, X. (2014) CARD9 mediates Dectin-1-induced ERK activation by linking Ras-GRF1 to H-Ras for antifungal immunity. *J. Exp. Med.* **211,** 2307–2321
31. André, P., Cambier, J. C., Wade, T. K., Raetz, T., and Wade, W. F. (1994) Distinct structural compartmentalization of the signal transducing functions of major histocompatibility complex class II (Ia) molecules. *J. Exp. Med.* **179,** 763–768
32. McGreal, E. P., Rosas, M., Brown, G. D., Zamze, S., Wong, S. Y., Gordon, S., Martinez-Pomares, L., and Taylor, P. R. (2006) The carbohydrate-recognition domain of Dectin-2 is a C-type lectin with specificity for high mannose. *Glycobiology* **16,** 422–430
33. Xu, S., Huo, J., Lee, K.-G., Kurosaki, T., and Lam, K.-P. (2009) Phospholipase Cγ2 is critical for Dectin-1-mediated Ca^{2+} flux and cytokine production in dendritic cells. *J. Biol. Chem.* **284,** 7038–7046
34. Koretzky, G. A., Abtahian, F., and Silverman, M. A. (2006) SLP76 and SLP65: complex regulation of signalling in lymphocytes and beyond. *Nat. Rev. Immunol.* **6,** 67–78
35. Jun, J. E., Rubio, I., and Roose, J. P. (2013) Regulation of ras exchange factors and cellular localization of ras activation by lipid messengers in T cells. *Front. Immunol.* **4,** 239
36. Slack, E. C., Robinson, M. J., Hernanz-Falcón, P., Brown, G. D., Williams, D. L., Schweighoffer, E., Tybulewicz, V. L., and Reis e Sousa, C. (2007) Syk-dependent ERK activation regulates IL-2 and IL-10 production by DC stimulated with zymosan. *Eur. J. Immunol.* **37,** 1600–1612
37. Zhu, W., Downey, J. S., Gu, J., Di Padova, F., Gram, H., and Han, J. (2000) Regulation of TNF expression by multiple mitogen-activated protein kinase pathways. *J. Immunol.* **164,** 6349–6358
38. Wu, Y.-J., Wu, Y.-H., Mo, S.-T., Hsiao, H.-W., He, Y.-W., and Lai, M.-Z. (2015) Cellular FLIP inhibits myeloid cell activation by suppressing selective innate signaling. *J. Immunol.* **195,** 2612–2623
39. Cenci, E., Mencacci, A., Casagrande, A., Mosci, P., Bistoni, F., and Romani, L. (2001) Impaired antifungal effector activity but not inflammatory cell recruitment in interleukin-6-deficient mice with invasive pulmonary aspergillosis. *J. Infect. Dis.* **184,** 610–617
40. Romani, L., Mencacci, A., Cenci, E., Spaccapelo, R., Toniatti, C., Puccetti, P., Bistoni, F., and Poli, V. (1996) Impaired neutrophil response and $CD4^+$ T helper cell 1 development in interleukin 6-deficient mice infected with *Candida albicans*. *J. Exp. Med.* **183,** 1345–1355
41. van Enckevort, F. H., Netea, M. G., Hermus, A. R., Sweep, C. G., Meis, J. F., Van der Meer, J. W., and Kullberg, B. J. (1999) Increased susceptibility to systemic candidiasis in interleukin-6 deficient mice. *Med. Mycol.* **37,** 419–426
42. Filler, S. G., Yeaman, M. R., and Sheppard, D. C. (2005) Tumor necrosis factor inhibition and invasive fungal infections. *Clin. Infect. Dis.* **41,** S208-S212
43. Vallabhaneni, S., and Chiller, T. M. (2016) Fungal infections and new biologic therapies. *Curr. Rheumatol. Rep.* **18,** 29
44. Sonoda, E., Pewzner-Jung, Y., Schwers, S., Taki, S., Jung, S., Eilat, D., and Rajewsky, K. (1997) B cell development under the condition of allelic inclusion. *Immunity* **6,** 225–233
45. Hou, B., Reizis, B., and DeFranco, A. L. (2008) Toll-like receptors activate innate and adaptive immunity by using dendritic cell-intrinsic and -extrinsic mechanisms. *Immunity* **29,** 272–282
46. Edwards, A. D., Diebold, S. S., Slack, E. M., Tomizawa, H., Hemmi, H., Kaisho, T., Akira, S., and Reis e Sousa, C. (2003) Toll-like receptor expression in murine DC subsets: lack of TLR7 expression by CD8 α^+ DC correlates with unresponsiveness to imidazoquinolines. *Eur. J. Immunol.* **33,** 827–833
47. Chatterjee, P., Tiwari, R. K., Rath, S., Bal, V., and George, A. (2012) Modulation of antigen presentation and B cell receptor signaling in B cells of beige mice. *J. Immunol.* **188,** 2695–2702

TITLE:
Expression of Fluorescent Fusion Proteins in Murine Bone Marrow-Derived Dendritic Cells and Macrophages

AUTHORS AND AFFILIATIONS:
Jarmila Kralova[1,2], Daniela Glatzova[1,2,3], Simon Borna[1,2], Tomas Brdicka[1]
[1]Laboratory of Leukocyte Signalling, Institute of Molecular Genetics of the ASCR, Prague, Czech Republic
[2]Faculty of Science, Charles University, Prague, Czech Republic
[3]Department of Biophysical Chemistry, J. Heyrovsky Institute of Physical Chemistry ASCR, Prague, Czech Republic

Corresponding Author:
Tomas Brdicka
tomas.brdicka@img.cas.cz
Tel: (420) 241 062 467

E-mail Addresses of Co-authors:
Jarmila Kralova (jarmilla.kralova@img.cas.cz)
Daniela Glatzova (daniela.glatzova@jh-inst.cas.cz)
Simon Borna (simon.borna@img.cas.cz)
Tomas Brdicka (tomas.brdicka@img.cas.cz)

KEYWORDS:
Dendritic cells, macrophages, myeloid cells, differentiation, murine bone marrow cells, cytokines, M-CSF, GM-CSF, viral infection, GFP tagged protein

SUMMARY:
In this article, we provide a detailed protocol for the expression of fluorescent fusion proteins in murine bone marrow derived dendritic cells and macrophages. The method is based on the transduction of bone marrow progenitors with retroviral constructs followed by differentiation into macrophages and dendritic cells *in vitro*.

ABSTRACT:
Dendritic cells and macrophages are crucial cells that form the first line of defense against pathogens. They also play important roles in the initiation of an adaptive immune response. Experimental work with these cells is rather challenging. Their abundance in organs and tissues is relatively low. As a result, they cannot be isolated in large numbers. They are also difficult to transfect with cDNA constructs. In the murine model, these problems can be partially overcome by *in vitro* differentiation from bone marrow progenitors in the presence of M-CSF for macrophages or GM-CSF for dendritic cells. In this way, it is possible to obtain large amounts of these cells from very few animals. Moreover, bone marrow progenitors can be transduced with retroviral vectors carrying cDNA constructs during early stages of cultivation prior to their differentiation into bone marrow derived dendritic cells and

macrophages. Thus, retroviral transduction followed by differentiation *in vitro* can be used to express various cDNA constructs in these cells. The ability to express ectopic proteins substantially extends the range of experiments that can be performed on these cells, including live cell imaging of fluorescent proteins, tandem purifications for interactome analyses, structure-function analyses, monitoring of cellular functions with biosensors and many others. In this article, we describe a detailed protocol for retroviral transduction of murine bone marrow derived dendritic cells and macrophages with vectors coding for fluorescently-tagged proteins. On the example of two adaptor proteins, OPAL1 and PSTPIP2, we demonstrate its practical application in flow cytometry and microscopy. We also discuss the advantages and limitations of this approach.

INTRODUCTION:

Myeloid cells represent an indispensable part of our defense mechanisms against pathogens. They are able to rapidly eliminate microbes, as well as dying cells. In addition, they are also involved in regulating tissue development and repair and in maintaining homeostasis[1-3]. All myeloid cells differentiate from common myeloid progenitors in the bone marrow. Their differentiation into many functionally and morphologically distinct subsets is to a large extent controlled by cytokines and their various combinations[4]. The most intensively studied myeloid cell subsets include neutrophilic granulocytes, macrophages and dendritic cells. Defects in any of these populations lead to potentially life-threatening consequences and cause severe dysfunctions of the immune system in humans and mice[1-3,5,6].

Unlike neutrophilic granulocytes, dendritic cells and macrophages are tissue resident cells and their abundance in immune organs is relatively low. As a result, the isolation and purification of primary dendritic cells and macrophages for experiments requiring a large number of these cells is expensive and often impossible. To solve this problem, protocols have been developed to obtain large amounts of homogenous macrophages or dendritic cells *in vitro*. These approaches are based on the differentiation of murine bone marrow cells in the presence of cytokines: macrophage colony-stimulating factor (M-CSF) for macrophages and granulocyte-macrophage colony-stimulating factor (GM-CSF) or Flt3 ligand for dendritic cells[7-12]. Cells generated by this method are commonly described in the literature as bone marrow derived macrophages (BMDMs) and bone marrow derived dendritic cells (BMDCs). They have more physiological properties in common with primary macrophages or dendritic cells than with corresponding cell lines. Another major advantage is the possibility of obtaining these cells form genetically modified mice[13]. Comparative studies between wild-type cells and cells derived from genetically modified mice are often critical for uncovering novel functions of genes or proteins of interest.

Analysis of subcellular localization of proteins in living cells requires the coupling of a fluorescent label to the protein of interest *in vivo*. This is most commonly achieved by expressing genetically encoded fusion construct composed of an analyzed protein coupled (often via a short linker) to a fluorescent protein (*e.g.*, green fluorescent protein (GFP))[14-16]. The expression of fluorescently tagged proteins in dendritic cells or macrophages is

challenging. These cells are generally difficult to transfect by standard transfection procedures and the efficiencies tend to be very low. Moreover, the transfection is transient, it generates cellular stress and achieved intensity of fluorescence might not be sufficient for microscopy[17]. In order to obtain a reasonable fraction of these cells with a sufficient level of transgene expression, the infection of bone marrow progenitor cells with retroviral vectors and their subsequent differentiation into BMDMs or BMDCs has become a very efficient approach. It has allowed for the analysis of the proteins of myeloid origin in their native cellular environment, both in a steady state or during processes that are critical for immune response such as phagocytosis, immunological synapse formation or migration. Here, we describe a protocol that allows stable expression of fluorescently tagged proteins of interest in murine bone marrow derived macrophages and dendritic cells.

PROTOCOL:

All methods described here have been approved by the Expert Committee on the Welfare of Experimental Animals of the Institute of Molecular Genetics and by the Academy of Sciences of the Czech Republic.

1. Reagent Preparation

1.1. Prepare the ammonium-chloride-potassium (ACK) buffer. Add 4.145 g of NH_4Cl and 0.5 g of $KHCO_3$ to 500 mL of ddH_2O, then add 100 µL of 0.5 M ethylenediaminetetraacetic acid (EDTA) and filter-sterilize.

1.2. Prepare polyethylenimine (PEI) solution. Add 0.1 g of PEI to 90 mL of ddH_2O. While stirring, add 1 M HCl dropwise until the pH is lower than 2.0. Stir for up to 3 h until PEI is dissolved and then adjust pH to 7.2 with 1 M NaOH. Adjust the volume to 100 mL with ddH_2O and filter-sterilize. Make 1-2 mL aliquots and store at -20°C.

Note: After thawing, PEI can be stored at 4°C for up to 2 weeks but should not be re-frozen.

1.3. Prepare cell culture supernatants containing M-CSF or GM-CSF. These supernatants can be made in advance and stored in -80°C. To make these supernatants, grow the cytokine-producing cells (J558 cells for GM-CSF [18] or CMG 14-12 cells for M-CSF [19]) in a 10 cm Petri dish in Dulbecco's modified Eagle's medium (DMEM) with 10% fetal bovine serum (FBS) to confluence. Then transfer all cells to 200 mL of media in T150 tissue culture flask and culture for additional 4 days at 5% CO_2/37 °C. Collect the supernatant and filter over 0.2 µm sterilization filter. Make aliquots and store these at -80 °C.

1.4. Prepare 100 mL of cell culture medium: DMEM supplemented with 10% heat inactivated FBS and cell culture supernatants from cells secreting GM-CSF (for BMDC differentiation) or M-CSF (for BMDM differentiation).

Note: The amount of cytokines in these supernatants can vary and the working concentration has to be determined empirically. Typically, 2-3% supernatant from cell lines

producing GM-CSF (the recommended starting concentration is 2%) or 5-10% supernatant from CMG 14-12 cells producing M-CSF (the recommended starting concentration is 10%) is used. Alternatively, purified commercially available M-CSF at 10 ng/mL and GM-CSF at 20 ng/mL can be used with results virtually identical to cytokine-containing supernatants, *i.e.*, without any effect on the rate of differentiation, infection efficiency and subcellular localization of EGFP-tagged constructs. Antibiotics, including penicillin G (100 IU/mL), streptomycin (100 µg/mL), and gentamicin (40 µg/mL), can be used for cell culture at any step of the protocol unless otherwise stated.

2. Production of Retrovirus

CAUTION: Although retroviral vectors are relatively safe when compared to other types of viral vectors, they still pose a potential safety hazard. Therefore, it is crucial to work with the utmost care and appropriate protective equipment, and to adhere to all safety regulations and legal requirements for working with viral particles.

2.1. Plate a single cell suspension of Platinum-Eco (Plat-E) packaging cells in a 10 cm Petri dish and cultivate in 15 mL of DMEM containing 10% FBS until 50-60 % confluent (~24 h). Cells should grow in a monolayer and should not form clumps in culture.

2.2. Pipette 20 µg of retroviral construct (*e.g.*, the construct expressing the fluorescently tagged protein of interest in the pMSCV vector) and 10 µg of pCL-Eco packaging vector[20] into 1 mL of DMEM (without serum and antibiotics) and gently mix.

2.3. To a second tube, add 75 µL of PEI in 1 mL of DMEM (without serum and antibiotics). Incubate 5 min at room temperature (RT) and then mix the contents of both tubes together and incubate for additional 10 min at RT.

Note: Addition of pCL-Eco is optional. It is coding for the ecotropic viral receptor and may increase the virus titer.

2.4. Carefully replace the medium on Plat-E cells with 8 mL of fresh DMEM supplemented with 2% FBS. Pre-warm the medium to 37 °C before use. Do not use antibiotics during transfection, since antibiotics may reduce the transfection efficiency.

2.5. Carefully add (in drops) the mixture prepared in Step 2.3 on the Plat-E cells, and incubate for 4 h at 37 °C.

2.6. After the incubation, exchange the medium on Plat-E cells for 10 mL of pre-warmed DMEM containing 10% FBS, and cultivate the cells for 24 h at 37 °C. During this incubation, Plat-E cells will produce virus into the media.

2.7. After 24 h, collect the medium containing retroviral particles from Platinum Eco cells

using a 10 mL serological pipette and transfer it to a 15 mL centrifuge tube (= “supernatant 1” containing ecotropic retroviral particles).

2.8. To avoid contamination by Plat-E cells in viral supernatants, spin the collected virus at 1250 × g for 5 min at 4 °C. For the best results, the virus should be used immediately for infection.

Note: Aliquots of virus can also be stored at -80 °C for later use. However, it will result in certain reduction in transduction efficiency. Avoid repetitive freezing/thawing of the virus, since it leads to virus degradation.

2.9. Add 10 mL of pre-warmed DMEM with 10% FBS to Plat-E cells and cultivate for another 24 h at 37 °C.

2.10. Repeat steps 2.7. and 2.8. to obtain “supernatant 2”.

3. Murine Bone Marrow Cell Isolation

3.1. Sacrifice the mouse using cervical dislocation or other approved method. Spray the mouse with 70% ethanol.

3.2. Using tweezers and scissors, remove the skin as well as part of muscles from hind legs. Carefully dislodge the acetabulum from the hip joint without breaking the femur. Cut the paw in the ankle joint. Spray the bones (femur connected to tibia) with 70% ethanol and remove the rest of the muscles using a paper towel.

3.3. Place the bones in a 5 cm Petri dish containing sterile phosphate buffered saline (PBS) with 2% FBS (PBS-FBS) and keep on ice until processed.

3.4. For securing cultivation sterility, perform all the following steps in a tissue culture hood.

3.5. Separate the femur from the tibia without breaking the bone ends (bend in the knee joint and carefully cut with scissors).

3.6. Process the bones one by one. Cut off a very small part of the epiphyses (approximately 1 - 2 mm) with scissors while holding the bone in tweezers.

3.7. Use a 30G needle and a 2 or 5 mL syringe filled with PBS-FBS to flush the bone marrow cells from both ends of the bone into a 15 mL centrifuge tube. Move the needle inside the bone during the flushing in order to remove all the cells. If the needle gets clogged, change it.

Note: Bones should turn from red to white during flushing. This indicates that the majority of the cells were removed from the bone. Use approximately 2-3 mL of PBS-FBS per bone.

3.8. Centrifuge the cells at 500 × g for 5 min at 4 °C.

3.9. Discard the supernatant and lyse the red blood cells by resuspending the pellet in 2.5 mL of ACK buffer for 2-3 min at room temperature. During the lysis, filter the bone marrow cells through a 100 µm cell strainer into a fresh 15 mL centrifug tube. Restore the tonicity by adding 12 mL of PBS-FBS.

Note: Do not exceed 5 min of hypotonic lysis with ACK buffer to avoid cell death.

3.10. Centrifuge immediately at 500 × g for 5 min at 4 °C.

4. Bone Marrow Cell Differentiation into Bone Marrow Derived Macrophages

4.1. Resuspend the pellet of bone marrow cells in DMEM supplemented with 10 % FBS and antibiotics (see the note after Step 1.4. for antibiotic concentration) and count the cells. For differentiation into BM derived macrophages, plate 5-10 × 10^6 of bone marrow cells in a 10 cm non-tissue culture treated (bacterial) Petri dish with 10 mL of pre-prepared DMEM media with serum and M-CSF from Step 1.4.

Note: The yield of the bone marrow cells is approximately 4 × 10^7 per 6-8 week-old C57BL/6J mouse.

4.2. Incubate the cells in cell culture incubator for 3 days at 5% CO_2, 37 °C.

Note**:** During the first 2 days, cells do not look very vital, as a large number of apoptotic cells is present (cells unable to differentiate into myeloid cells and terminally differentiated cells).

4.3. After 3 days, the bone marrow cell culture begins to look vital and clusters of dividing cells are formed. First adherent cells can already be observed. At this point, supplement the cells with fresh cytokine media.

4.4. Add 10 mL of pre-warmed DMEM media with serum and M-CSF (from Step 1.3) into each 10 cm Petri dish and return it in the cell culture incubator. There is no need to remove the old media during this step.

Note: Bone marrow macrophages are fully differentiated after 5-7 days in culture. The best time for harvesting is at day 6-8, where majority of cells are adherent and the Petri dish is completely covered.

4.5. At day 5, take the Petri dish into the cell culture hood and incline the dish until the

media is almost reaching the edge of the dish. Carefully take out 15 mL of the media from the surface near the edge, and the cells tend to stay in the middle of the dish. Add the same volume of pre-warmed media with M-CSF and place the dish back into the incubator.

Note: If media is aspirated slowly and carefully, almost no cells are lost. However, it is also possible to centrifuge the aspirated media and add the cells back to the culture, to ensure that no non-adherent (*i.e.*, incompletely differentiated) cells are lost.

4.6. For experiments, only adherent cells (macrophages) are used. To harvest cells, on day 6 or 7, remove all media and floating cells. Wash the dish once with pre-warmed PBS without serum.

4.7. Add 5 mL of 0.02% EDTA in PBS, and incubate for 3-5 min at 37 °C in tissue culture incubator.

4.8. Using a 5 mL pipette, remove the cells from the dish by a stream of PBS-EDTA and place them in a 50 mL centrifuge tube with 25 mL of PBS. If needed, pool more dishes together.

4.9. Centrifuge immediately at 500 × g for 5 min at 4 °C.

4.10. Resuspend the macrophage pellet in DMEM media and count the cells. Verify the expression of macrophage surface differentiation markers (CD11b and F4/80) by flow cytometry.

4.11. For experiments requiring the cells to be in suspension, *e.g.*, flow cytometry experiments, qPCR or western blot analysis, use the macrophages directly. For experiments with adherent macrophages, plate the cells in the tissue culture plate according to the experimental setup.

4.12. The cells are already fully differentiated. Keep them in the media suitable for the intended experiment or in the original growth and differentiation media with M-CSF.

Note: For working with adherent macrophages, transfer them into a new plate at least 6 h before use (ideally overnight) to allow for the full adhesion to the new surface. The small fraction of floating cells can be removed before experiment.

5. Bone Marrow Cell Differentiation into Bone Marrow Derived Dendritic Cells

5.1. Follow the protocol for BMDMs with adjustments specific for BMDCs described below in steps 5.2. – 5.4.

5.2. Resuspend the obtained pellet of bone marrow cells in DMEM supplemented with 10% FBS and antibiotics and count the cells (by following Steps 4.1. - 4.2. of macrophage

protocol). For differentiation into dendritic cells, plate 1 - 1.5 × 10^7 bone marrow cells in a 10 cm non-tissue culture treated (bacterial) Petri dish in 10 mL of pre-prepared DMEM media with serum and GM-CSF (from Step 1.4.).

5.3. Follow the same cultivation steps as in BMDM protocol (steps 4.3. - 4.5. of macrophage protocol). Use DMEM media with serum and GM-CSF instead of M-CSF. Since for BMDCs the cultivation time is longer (typically 10-12 days), add 1-2 additional feedings in 3 day intervals (by removing the supernatant and adding a new cultivation media as described in Step 4.5.).

5.4. This part of the protocol is virtually the same as the corresponding part of the macrophage protocol (Steps 4.6. – 4.12. of macrophage protocol). For experiments use only adherent cells. On day 10-12, collect the cells using EDTA, count and plate them on a new surface. Verify the expression of surface differentiation markers of dendritic cells (CD11c+, CD11b+, F4/80-) by flow cytometry.

.

6. Production of BMDMs and BMDCs Expressing EGFP-tagged Protein of Interest

6.1. Resuspend the pellet of bone marrow cells obtained in Step 3.10. in DMEM supplemented with 10 % FBS and antibiotics and count the cells. For the infection, use 2-5 × 10^6 of BM cells per well of a 6-well tissue culture treated plate.

6.2. Plate the cells in 1 mL of the prepared DMEM media per well, supplemented either with M-CSF for differentiation into BMDMs or with GM-CSF for differentiation in BMDCs. Keep the cells for 4-6 h in a tissue culture incubator with 5% CO_2 at 37 °C.

6.3. Add 2 mL of freshly collected virus (“supernatant 1”) supplemented with polybrene (12 µg/mL, final concentration 8 µg/mL after addition to the cells).

Note: Frozen aliquot of the virus-containing supernatant can also be used, but efficacy will be lower.

6.4. Centrifuge the plate at 1250 × g for 90 min at 30 °C (with slow acceleration and deceleration). Then, incubate for 4 h with 5% CO_2 at 37 °C.

6.5. Optional: Replace 2 mL of the culture media with fresh medium containing respective cytokine (M-CSF or GM-CSF) and culture with 5% CO_2 at 37 °C. On the second day, remove 2 mL of culture media and repeat the whole infection procedure (Step 6.3-6.4) with 2 mL of freshly collected virus (“supernatant 2”).

Note: This step may increase infection efficacy. Improvement after the second infection is dependent on the cell type and target protein and in our experience can vary from 30% increase in efficiency to no improvement at all.

6.6. Collect the non-adherent cells, transfer to a 15 mL centrifuge tube, and spin at 500 × g for 5 min (4 °C). Discard the supernatant.

6.7. Resuspend the cell pellet in 10 mL of culture media with M-CSF or GM-CSF, place the cells into a 10 cm non-tissue culture treated Petri dish and culture at 37 °C, 5% CO_2. Optimal number of cells for a 10 cm dish is 5-10 × 10^6 for BM-derived macrophages and 10-15 × 10^6 for BM-derived dendritic cell.

Note: Smaller dishes or plates can be used, but cell numbers must be adjusted accordingly.

6.8. Follow the macrophage and dendritic cell cultivation and differentiation protocol described in step 3 and 4.

REPRESENTATIVE RESULTS:

Signaling adaptor proteins are usually small proteins without any enzymatic activity. They possess various interaction domains or motifs, which mediate binding to other proteins involved in signal transduction, including tyrosine kinases, phosphatases, ubiquitin ligases and others[21]. For the demonstration of the functionality of this protocol myeloid cell adaptors PSTPIP2 and OPAL1 were selected. PSTPIP2 is a well characterized protein involved in the regulation of inflammatory response[22]. It is a cytoplasmic protein which can also be recruited to cellular membranes via its F-bar domain. Second protein is a transmembrane adaptor OPAL1, expected to be associated with cellular membranes. Its physiological function is still unknown. However, in acute lymphoblastic leukemia, expression of OPAL1 is associated with better prognosis[23].

cDNA constructs coding for PSTPIP2 or OPAL1 fused via a short linker (GSGGGS or Myc-tag, respectively) to EGFP at the C-terminus were cloned into the pMSCV retroviral vector using standard methods of cDNA cloning. This construct was then transfected into Plat-E cells together with the packaging vector pCL-Eco. The resulting supernatants containing retroviruses were used for the transduction of bone marrow cells, followed by the differentiation into BMDMs and BMDCs. The efficacy of Plat-E transfection was evaluated by flow cytometry after the collection of the second virus-containing supernatant. Mean transfection efficiency was 62% for PSTPIP2-EGFP and 53% for OPAL1 and the results were highly reproducible (**Figure 1A,** B). OPAL1 construct seemed to be more toxic for Plat-E cells (assessed by the appearance of floating/dying cells in culture), resulting in a reduction in the percentages of transfected cells.

Differentiation status of the bone marrow derived macrophages and dendritic cells (transduced with PSTPIP2-EGFP and OPAL1-EGFP retroviral constructs) was assessed by flow cytometry. Mature macrophage population is defined by CD11b and F4/80 expression, while dendritic cells express the CD11c lineage marker. More than 90% of cells in both types of culture were positive for their respective markers (**Figure 2A, B**). Finally, we determined the expression level of PSTPIP2-EGFP and OPAL1-EGFP constructs in BMDMs and BMDCs by a simple flow cytometry measurement of EGFP fluorescence. The mean percentage of

EGFP-positive macrophages was 71% for PSTPIP2-EGFP and 62% for OPAL1-EGFP (**Figure 3A**). In case of dendritic cells, the efficiency was lower, 32% for PSTPIP2 and 9% for OPAL1 (**Figure 3B**). The results of multiple experiments demonstrate the reproducibility of this method (**Figure 3C**).

We typically do not determine the virus concentration in the supernatants that we use in infections. We prefer to use the virus supernatants fresh, immediately after collection, while the virus titer determination requires three additional days. As a result, the information on virus titer can only be obtained *ex post.* However, it can still be useful when addressing technical issues and problems. To assess the virus concentration in supernatants from Plat E cells transfected with PSTPIP2-EGFP and OPAL1-EGFP constructs, we incubated NIH-3T3 cells with serially diluted virus-containing supernatants collected from these transfected Plat-E cells and determined virus titer exactly as described by Zjablovskaja *et al* in previously published JoVE article[24]. In three independent experiments, the virus titer ranged from 1.1×10^6 to 4.4×10^6 TU/mL. We did not observe any substantial differences between PSTPIP1-EGFP and OPAL1-EGFP constructs and between supernatants from day 1 and day 2. When these supernatants were used for bone marrow cell infections according to the protocol we are describing in this article, the multiplicity of infection (MOI) ranged from 1.1 to 4.4. Interestingly, within this range, we did not observe any correlation between MOI and infection efficiency.

In **Figure 4**, PSTPIP2-EGFP and OPAL1-EGFP expressed in BMDMs and BMDCs were visualized by confocal microscopy. Fully differentiated macrophages and dendritic cells have a characteristic shape. The change in morphology from small rounded progenitor cells to the large cells of irregular shapes confirms successful differentiation. In macrophages, PSTPIP2 was cytoplasmic with partial localization at the plasma membrane. OPAL1 appeared to be also partially targeted to the plasma membrane. The rest was likely associated with intracellular membranes, such as the endoplasmic reticulum and Golgi complex. However, to confirm this localization, specific organelle markers would have to be used. In dendritic cells, the membrane localization was less apparent.

FIGURE LEGENDS:

Figure 1. Efficiency of Plat-E cell transfection. For transfection of Plat-E cells, two constructs encoding adaptor proteins PSTPIP2 and OPAL1 fused with EGFP (PSTPIP2-EGFP and OPAL1-EGFP) were cloned into the pMSCV vector. Standard PEI transfection was performed. The efficacy of transfection was evaluated by flow cytometry of the Plat-E cells after the collection of the second viral supernatant. (**A**). Representative flow cytometry plot. (**B**). Graph showing results of four independent experiments.

Figure 2. Assessment of the differentiation status of BMDMs (A) and BMDCs (B). Surface expression of specific macrophage and dendritic cell lineage markers was measured by flow cytometry at day 8 of cultivation. Dead cells were gated out based on their side and forward scatter properties and staining with Hoechst 33258. The results are representative of at least 3 independent experiments.

Figure 3. Assessment of the expression of PSTPIP2-EGFP and OPAL1-EGFP. EGFP fluorescence in BMDMs (**A**) and BMDCs (**B**) retrovirally transduced with PSTPIP2-EGFP and OPAL1-EGFP constructs was measured by flow cytometry at day 8 of cultivation. (**C**)**.** Graph showing the results of multiple independent experiments. BMDMs and BMDCs were gated as in **Figure 2**.

Figure 4. Representative images of macrophages and dendritic cells expressing PSTPIP2 or OPAL1. BMDMs (**A**) and BMDCs (**B**) expressing PSTPIP2 and OPAL1 were visualized by live imaging confocal microscopy. EGFP fluorescence in green is shown on the left side of each panel, bright field image on the right. Bar = 10 µm. The results are representative of at least three independent experiments.

DISCUSSION:

The expression of protein of interest in target cells is a key step in many types of biological studies. Differentiated macrophages and dendritic cells are difficult to transfect by standard transfection and retroviral transduction techniques. Bypassing the transfection of these differentiated cells with retroviral transduction of bone marrow progenitors, followed by differentiation when they already carry the desired construct, is a critical step allowing the expression of ectopic cDNAs in these cell types. An example of successful use of this method can be found in our recent publication[25]. Here, we provide a cost-effective protocol for achieving stable expression of the construct of choice in bone marrow-derived dendritic cells and macrophages using this approach. The procedure we present is relatively inexpensive and simple, yet delivering very good results. Reagents used in this protocol allow for its routine use even under a relatively restrictive budget. The protocol for Plat-E transfection employs PEI as a transfection reagent. Compared to other chemical transfection agents, PEI is of a very low cost, while its efficiency is similar to the majority of other widely used compounds. However, PEI can be replaced with many different commercially available transfection reagents in this step without any loss of efficiency. As a guiding principle, transfection protocols known to work with commonly used HEK293 cells typically perform well with Plat-E cells, too. Another cost-effective measure is the utilization of cytokine-containing supernatants instead of purified recombinant cytokines. The use of these supernatants requires some optimization. However, when the standard protocol for their preparation is established and followed, the variability between individual batches of these supernatants becomes very low, usually requiring no changes in working concentrations between individual lots. The efficiencies of BMDM and BMDC differentiation with these supernatants are, in our experience, identical to purified cytokines.

In addition to retroviral transduction, other well-established methods of mammalian cell transfection exist, including chemical transfection (typically using cationic lipids or cationic polymers forming complexes with DNA), electroporation and the use of other types of viral vectors, mainly adenoviral and lentiviral systems[26-30]. Although very high titers and efficiencies can be achieved with adenovirus-based gene delivery, the preparation of

corresponding plasmids and viral particles are more difficult and time-consuming than in the case of retroviral systems[29]. In addition, adenovirus elicits inflammatory response in dendritic cells and macrophages[29,31,32] and for optimum performance in murine hematopoietic cells mouse strain carrying transgenic adenovirus receptor is required[33]. On the other hand, the generation of lentiviral particles carrying the gene of interest is a relatively simple process, virtually identical to the one utilized for retroviruses. In contrast to the ecotropic retroviral vectors used in this protocol, lentiviruses are capable of infecting non-proliferating cells of multiple species, including humans[34]. This may be an important advantage under specific experimental conditions. However, this feature also greatly compromises the safety of these vectors. In our opinion, for gene delivery to BMDMs and BMDCs, retroviruses provide the best balance of efficiency, safety and ease of use. Retroviral DNA constructs can be easily prepared using simple standard molecular cloning techniques. Virus is produced by packaging the cell lines directly to the culture supernatant and further virus purification is usually not necessary. Ecotropic retroviruses also do not readily infect human cells, which makes their use relatively safe. However, there also are some general disadvantages associated with the use of retroviral vectors. The major limiting factor is that these viruses infect only proliferating cells[35]. This feature does not significantly affect the protocol described here, but it limits the range of applications where retroviral vectors can be used. The size of the gene of interest that can be cloned into these vectors is also limited and the viral particle titer decreases with increasing insert size. With pMSCV vectors, we usually start seeing effects of insert size at around 3 kbp. With further increases in insert size, the infection efficiency gradually declines.

The chemical transfection and electroporation are easier to use, safer and less time-consuming than any of the virus-based procedures[26-28,30]. However, in BMDMs and BMDCs, they can stimulate responses to foreign nucleic acids[31] and they generate more cellular stress. In addition, some chemical transfection reagents increase cell auto-fluorescence that may interfere with flow cytometry or microscopy analyzes. Due to the transient nature of expression, they can only be used with mature differentiated BMDMs or BMDCs. In contrast, the sequences introduced with retroviral vectors are permanently integrated into the genome of the target cells and allow for a stable long-lasting expression compatible with the time scale of the differentiation protocols[34,35]. However, this feature also increases the risk of insertional mutagenesis. Due to the relatively random nature of the vector integration, its effects on large populations of cells are limited. However, they may be visible at the level of individual cells. Additional problems may arise when a construct expressed from the retroviral vector affects dendritic cell or macrophage differentiation, resulting in failure to generate differentiated BMDMs or BMDCs from the infected progenitors. To some extent, this may be overcome by adjusting the infection conditions to achieve low expression levels (*e.g.*, by reducing the virus titer) or through the use of an inducible expression system. The use of EGFP fused to the protein of interest or as a reporter also allows for sorting of cells with expression level corresponding to experiment goals and limitations. Finally, we should also mention problems common to all transfection/transduction procedures. These include mainly overexpression artefacts, such as protein misfolding, mislocalization and toxicity[36]. Protein toxicity could be the reason

why OPAL1 was relatively difficult to express. Its example clearly illustrates that the nature of the expressed protein can substantially affect the effectiveness of this method. However, despite this, we were able to obtain sufficient quantities of OPAL1-EGFP expressing cells for microscopy analysis with this method, demonstrating its usefulness even when dealing with difficult targets. In addition, it would be possible to increase the percentages of transduced cells by FACS sorting if required by a particular application. The low infection efficiency can also be partially overcome by increasing viral particle concentration using various methods or ready-to-use kits. In our hands, ultrafiltration of the viral supernatant on centrifugal filters with a molecular weight cut off of 100 kDa has proven to provide the best balance between efficiency and required effort.

Bone marrow derived macrophages and dendritic cells are widely used tools in phagocyte immunology. They are more physiologically relevant than available cell lines. They can be generated in relatively high numbers and, at the same time, lack the genetic heterogeneity and instability characteristic of cell lines. Another advantage is that they can be generated from genetically modified mice to study the effects of genetic modification on a relatively abundant and homogenous cell population. This is particularly useful in biochemical studies, where relatively large amounts of cells are typically required. The ability to transduce these cells with cDNA constructs opens up additional possibilities of research based on the reconstitution or complementation of genetic defects in these cells and structure-function analysis.

ACKNOWLEDGMENTS:
This work was supported by Czech Science Foundation (GACR) (project number 16-07425S), by Charles University Grant Agency (GAUK) (project number 923116) and by institutional funding from the Institute of Molecular Genetics, Academy of Sciences of the Czech Republic (RVO 68378050).

DISCLOSURES:
The authors have nothing to disclose.

REFERENCES:
1 Moghaddam, A. S. *et al.* Macrophage plasticity, polarization and function in health and disease. *Journal of Cellular Physiology.* 10.1002/jcp.26429, (2018).
2 Qian, C. & Cao, X. Dendritic cells in the regulation of immunity and inflammation. *Seminars in Immunology.* **35** 3-11, (2018).
3 Amulic, B., Cazalet, C., Hayes, G. L., Metzler, K. D. & Zychlinsky, A. Neutrophil function: from mechanisms to disease. *Annual Review of Immunology.* **30** 459-489, (2012).
4 Kondo, M. Lymphoid and myeloid lineage commitment in multipotent hematopoietic progenitors. *Immunological Reviews.* **238** (1), 37-46, (2010).
5 Andrews, T. & Sullivan, K. E. Infections in patients with inherited defects in phagocytic function. *Clinical Microbiology Reviews.* **16** (4), 597-621, (2003).
6 Wynn, T. A., Chawla, A. & Pollard, J. W. Macrophage biology in development,

homeostasis and disease. *Nature.* **496** (7446), 445-455, (2013).

7 Austin, P. E., McCulloch, E. A. & Till, J. E. Characterization of the factor in L-cell conditioned medium capable of stimulating colony formation by mouse marrow cells in culture. *Journal of Cellular Physiology.* **77** (2), 121-134, (1971).

8 Scheicher, C. *et al.* Recombinant GM-CSF induces in vitro differentiation of dendritic cells from mouse bone marrow. *Advances in Experimental Medicine and Biology.* **329** 269-273, (1993).

9 Stanley, E. R. The macrophage colony-stimulating factor, CSF-1. *Methods in Enzymology.* **116** 564-587, (1985).

10 Weischenfeldt, J. & Porse, B. Bone Marrow-Derived Macrophages (BMM): Isolation and Applications. *Cold Spring Harbor Protocols.* **2008** pdb prot5080, (2008).

11 Lutz, M. B. *et al.* An advanced culture method for generating large quantities of highly pure dendritic cells from mouse bone marrow. *Journal of Immunological Methods.* **223** (1), 77-92, (1999).

12 Inaba, K. *et al.* Generation of large numbers of dendritic cells from mouse bone marrow cultures supplemented with granulocyte/macrophage colony-stimulating factor. *Journal of Experimental Medicine.* **176** (6), 1693-1702, (1992).

13 Chamberlain, L. M., Godek, M. L., Gonzalez-Juarrero, M. & Grainger, D. W. Phenotypic non-equivalence of murine (monocyte-) macrophage cells in biomaterial and inflammatory models. *Journal of Biomedical Materials Research Part A.* **88** (4), 858-871, (2009).

14 Remington, S. J. Green fluorescent protein: a perspective. *Protein Science.* **20** (9), 1509-1519, (2011).

15 Hoffman, R. M. Strategies for In Vivo Imaging Using Fluorescent Proteins. *Journal of Cellular Biochemistry.* **118** (9), 2571-2580, (2017).

16 Telford, W. G., Hawley, T., Subach, F., Verkhusha, V. & Hawley, R. G. Flow cytometry of fluorescent proteins. *Methods.* **57** (3), 318-330, (2012).

17 Zhang, X., Edwards, J. P. & Mosser, D. M. The expression of exogenous genes in macrophages: obstacles and opportunities. *Methods in Molecular Biology.* **531** 123-143, (2009).

18 Zal, T., Volkmann, A. & Stockinger, B. Mechanisms of tolerance induction in major histocompatibility complex class II-restricted T cells specific for a blood-borne self-antigen. *Journal of Experimental Medicine.* **180** (6), 2089-2099, (1994).

19 Takeshita, S., Kaji, K. & Kudo, A. Identification and Characterization of the New Osteoclast Progenitor with Macrophage Phenotypes Being Able to Differentiate into Mature Osteoclasts. *Journal of Bone and Mineral Research.* **15** (8), 1477-1488, (2000).

20 Naviaux, R. K., Costanzi, E., Haas, M. & Verma, I. M. The pCL vector system: rapid production of helper-free, high-titer, recombinant retroviruses. *Journal of Virology.* **70** (8), 5701-5705, (1996).

21 Janssen, E. & Zhang, W. Adaptor proteins in lymphocyte activation. *Current Opinion in Immunology.* **15** (3), 269-276, (2003).

22 Ferguson, P. J. & Laxer, R. M. New discoveries in CRMO: IL-1beta, the neutrophil, and the microbiome implicated in disease pathogenesis in Pstpip2-deficient mice.

Seminars in Immunopathology. **37** (4), 407-412, (2015).

23 Holleman, A. *et al.* Expression of the outcome predictor in acute leukemia 1 (OPAL1) gene is not an independent prognostic factor in patients treated according to COALL or St Jude protocols. *Blood.* **108** (6), 1984-1990, (2006).

24 Zjablovskaja, P., Danek, P., Kardosova, M. & Alberich-Jorda, M. Proliferation and Differentiation of Murine Myeloid Precursor 32D/G-CSF-R Cells. *Journal of Visualized Experiments: JoVE.* 10.3791/57033 (132), (2018).

25 Kralova, J. *et al.* The Transmembrane Adaptor Protein SCIMP Facilitates Sustained Dectin-1 Signaling in Dendritic Cells. *Journal of Biological Chemistry.* **291** (32), 16530-16540, (2016).

26 Maess, M. B., Wittig, B. & Lorkowski, S. Highly efficient transfection of human THP-1 macrophages by nucleofection. *Journal of Visualized Experiments: JoVE.* 10.3791/51960 (91), e51960, (2014).

27 Bowles, R., Patil, S., Pincas, H. & Sealfon, S. C. Optimized protocol for efficient transfection of dendritic cells without cell maturation. *Journal of Visualized Experiments: JoVE.* 10.3791/2766 (53), e2766, (2011).

28 Siegert, I. *et al.* Electroporation of siRNA into mouse bone marrow-derived macrophages and dendritic cells. *Methods in Molecular Biology.* **1121** 111-119, (2014).

29 Lee, C. S. *et al.* Adenovirus-Mediated Gene Delivery: Potential Applications for Gene and Cell-Based Therapies in the New Era of Personalized Medicine. *Genes & Diseases.* **4** (2), 43-63, (2017).

30 Jin, L., Zeng, X., Liu, M., Deng, Y. & He, N. Current progress in gene delivery technology based on chemical methods and nano-carriers. *Theranostics.* **4** (3), 240-255, (2014).

31 Muruve, D. A. *et al.* The inflammasome recognizes cytosolic microbial and host DNA and triggers an innate immune response. *Nature.* **452** (7183), 103-107, (2008).

32 Yang, Y., Li, Q., Ertl, H. C. & Wilson, J. M. Cellular and humoral immune responses to viral antigens create barriers to lung-directed gene therapy with recombinant adenoviruses. *Journal of Virology.* **69** (4), 2004-2015, (1995).

33 Tallone, T. *et al.* A mouse model for adenovirus gene delivery. *Proceedings of the National Academy of Sciences of the United States of America.* **98** (14), 7910-7915, (2001).

34 Milone, M. C. & O'Doherty, U. Clinical use of lentiviral vectors. *Leukemia.* 10.1038/s41375-018-0106-0, (2018).

35 McTaggart, S. & Al-Rubeai, M. Retroviral vectors for human gene delivery. *Biotechnology Advances.* **20** (1), 1-31, (2002).

36 Gibson, T. J., Seiler, M. & Veitia, R. A. The transience of transient overexpression. *Nature Methods.* **10** (8), 715-721, (2013).

PSTPIP2, a Protein Associated with Autoinflammatory Disease, Interacts with Inhibitory Enzymes SHIP1 and Csk

Ales Drobek,* Jarmila Kralova,* Tereza Skopcova,* Marketa Kucova,* Petr Novák,† Pavla Angelisová,‡ Pavel Otahal,‡ Meritxell Alberich-Jorda,§ and Tomas Brdicka*

Mutations in the adaptor protein PSTPIP2 are the cause of the autoinflammatory disease chronic multifocal osteomyelitis in mice. This disease closely resembles the human disorder chronic recurrent multifocal osteomyelitis, characterized by sterile inflammation of the bones and often associated with inflammation in other organs, such as the skin. The most critical process in the disease's development is the enhanced production of IL-1β. This excessive IL-1β is likely produced by neutrophils. In addition, the increased activity of macrophages, osteoclasts, and megakaryocytes has also been described. However, the molecular mechanism of how PSTPIP2 deficiency results in this phenotype is poorly understood. Part of the PSTPIP2 inhibitory function is mediated by protein tyrosine phosphatases from the proline-, glutamic acid-, serine- and threonine-rich (PEST) family, which are known to interact with the central part of this protein, but other regions of PSTPIP2 not required for PEST-family phosphatase binding were also shown to be indispensable for PSTPIP2 function. In this article, we show that PSTPIP2 binds the inhibitory enzymes Csk and SHIP1. The interaction with SHIP1 is of particular importance because it binds to the critical tyrosine residues at the C terminus of PSTPIP2, which is known to be crucial for its PEST-phosphatase–independent inhibitory effects in different cellular systems. We demonstrate that in neutrophils this region is important for the PSTPIP2-mediated suppression of IL-1β processing and that SHIP1 inhibition results in the enhancement of this processing. We also describe deregulated neutrophil response to multiple activators, including silica, Ab aggregates, and LPS, which is suggestive of a rather generalized hypersensitivity of these cells to various external stimulants. *The Journal of Immunology*, **2015, 195: 3416–3426.**

The activity of leukocyte signaling pathways must be properly controlled to prevent excessive responses with harmful consequences. This is ensured by a number of negative regulators that limit the duration and magnitude of the signaling. One such regulatory protein is the lipid phosphatase SHIP1, which controls the activity of the PI3K pathway by dephosphorylating its key mediator, phosphatidylinositol-3,4,5-trisphosphate [PI(3,4,5)P_3]. This results in the reduced activity of some of its downstream effectors (1). A prototypical example of such an effector is Akt (also known as PKB), a serine/threonine kinase, which is involved in the regulation of cell activation, proliferation, metabolism, and survival, and which is recruited to the plasma membrane by PI(3,4,5)P_3 for further activation (2). The deletion of SHIP1 results in the increased activity of Akt in the mast cells (3) and in the increased translocation of the Akt PH domain to the plasma membrane in neutrophils, suggesting that in myeloid cells SHIP1 regulates Akt localization and activity in vivo (4). There is also ample evidence that SHIP1 negatively regulates MAPK pathways by various mechanisms, in some cases independently of SHIP1 enzymatic activity (5).

Another critical negative regulator of leukocyte signaling is the protein tyrosine kinase Csk. It is involved in the regulation of Src-family kinases (SFKs), a family of protein tyrosine kinases indispensable to the initiation of signal transduction via ITAM-bearing immunoreceptors, and with additional and important roles in signaling by cytokine, growth factor, and pattern recognition receptors, and many others (6). Csk phosphorylates an inhibitory tyrosine residue at the C terminus of SFKs. This phosphorylated tyrosine then interacts with an SH2 domain in the same molecule, resulting in an autoinhibited conformation (7–9). Csk itself is recruited to the plasma membrane and is activated by binding to the phosphorylated tyrosine motifs of transmembrane proteins such as PAG (10, 11), LIME (12), and SCIMP (13). An additional mechanism of SFK inhibition is dependent upon protein tyrosine phosphatases (PTPs) that dephosphorylate the activation loop tyrosine necessary for SFK catalytic activity. This residue can be dephosphorylated by multiple phosphatases, including the receptor tyrosine phosphatases CD45 and CD148 (14–16), PTPs of the Shp family (17), as well as PTP LYP (PTPN22, also known as PEP in mice). In T cells, LYP/PEP forms a complex with Csk.

*Laboratory of Leukocyte Signaling, Institute of Molecular Genetics, Academy of Sciences of the Czech Republic, 142 20 Prague, Czech Republic; †Laboratory of Structural Biology and Cell Signaling, Institute of Microbiology, Academy of Sciences of the Czech Republic, 142 20 Prague, Czech Republic; ‡Laboratory of Molecular Immunology, Institute of Molecular Genetics, Academy of Sciences of the Czech Republic, 142 20 Prague, Czech Republic; and §Laboratory of Hematooncology, Institute of Molecular Genetics, Academy of Sciences of the Czech Republic, 142 20 Prague, Czech Republic

Received for publication June 11, 2014. Accepted for publication July 28, 2015.

This work was supported by the Czech Science Foundation (Project P302/12/1712), institutional funding from the Institute of Molecular Genetics, Academy of Sciences of the Czech Republic (RVO 68378050), the Ministry of Education, Youth and Sport of the Czech Republic Project Navrat (Grant LK21307 to M.A.-J.), the Czech Science Foundation (Project 15-03796S to M.A.-J.), the Ministry of Education, Youth and Sports of the Czech Republic, the European Regional Development Fund (Projects CZ.1.07/2.3.00/30.0003 and CZ.1.05/1.1.00/02.0109 to P.N.), Operational Program Prague–Competitiveness (Project CZ.2.16/3.1.00/24023 to P.N.), Institutional Research Concept of the Institute of Microbiology, Academy of Sciences of the Czech Republic (RVO 61388971 to P.N.), and the Faculty of Science, Charles University, Prague (to A.D.).

Address correspondence and reprint requests to Dr. Tomas Brdicka, Laboratory of Leukocyte Signaling, Institute of Molecular Genetics, Academy of Sciences of the Czech Republic, Videnska 1083, 142 20 Prague, Czech Republic. E-mail address: tomas.brdicka@img.cas.cz

The online version of this article contains supplemental material.

Abbreviations used in this article: 3-AC, 3-α-aminocholestane; ACN, acetonitrile; BM, bone marrow; BMDM, BM-derived macrophage; FcR, Fc receptor; PEST-PTP, proline-, glutamic acid-, serine- and threonine-rich–family PTP; PI(3,4,5)P_3, phosphatidylinositol-3,4,5-trisphosphate; PTP, protein tyrosine phosphatase; SFK, Src-family kinase; WT, wild type.

www.jimmunol.org/cgi/doi/10.4049/jimmunol.1401494

Together, they simultaneously dephosphorylate the activation loop tyrosine and phosphorylate the inhibitory C-terminal tyrosine of SFKs, exerting a combined inhibitory effect (18, 19). LYP/PEP is a member of a small family of PTPs known as proline-, glutamic acid-, serine- and threonine-rich–family PTPs (PEST-PTPs), consisting of only three members: PEP/LYP, PTP-HSCF (PTPN18), and PTP-PEST (PTPN12) (reviewed in Ref. 20). All three family members bind Csk via proline-rich or tyrosine-containing motifs in their central region (18, 21, 22). In addition, a conserved C-terminal homology domain of PEST-PTPs binds two related proteins, PSTPIP1 and PSTPIP2 (23, 24). These are adaptor proteins involved in the control of inflammation, and their altered function results in the development of autoinflammatory diseases (25–27). In general, these disorders are characterized by sterile inflammation and consequential tissue damage. They are mainly the result of dysregulated activity of the innate immune system with no or limited involvement of adaptive immunity (28). The autoinflammatory disease caused by PSTPIP2 mutations is, in mice, characterized by sterile inflammatory lesions in the bones and various degrees of skin and paw inflammation (26, 27, 29). The disease closely resembles the human disorder known as chronic recurrent multifocal osteomyelitis. However, human patients with genetic alterations in the PSTPIP2 gene have not been identified yet. PSTPIP2 is a member of the F-BAR family of proteins (also known as the *pombe cdc15* homology family), characterized by the presence of N-terminal F-bar domain mediating interactions with membrane phospholipids and a C-terminal tail containing various interaction motifs (30). The F-bar domain of PSTPIP2 interacts with $PI(4,5)P_2$ (31), whereas its C-terminal tail binds PEST-PTPs via the interaction motif, which includes tryptophan 232 (24, 32). The C-terminal tail of PSTPIP2 contains several tyrosines of unknown function that are phosphorylated in macrophages after exposure to M-CSF (33). Two different mouse strains where point mutations in PSTPIP2 result in the autoinflammatory disorder have been established. As a result of these mutations, one of these strains, LUPO, displays approximately a 70% reduction in PSTPIP2 protein expression (27), whereas the other strain, CMO, shows a complete absence of PSTPIP2 (34). The disease is independent of T or B cells, and it was originally attributed to the enhanced activity of macrophages and osteoclasts (27, 32, 34). In addition, more recent work has suggested that neutrophils may also be a critical cell type in disease initiation (35, 36). Similar to several other autoinflammatory syndromes, the disease appears to be, at least in part, caused by the enhanced production of IL-1β (35, 37). The molecular mechanism of how PSTPIP2 prevents autoinflammatory disease development remains largely unknown. The effects of PSTPIP2 binding to PEST-family phosphatases have been tested recently in osteoclasts and megakaryocytes, where it had an effect on their differentiation. However, in these experiments, a profound effect was also seen after the mutation of C-terminal tyrosines, which rendered PSTPIP2 especially in the case of osteoclasts essentially nonfunctional without affecting the interaction with PEST-family phosphatases (32, 38). This suggested that the binding partners of these tyrosines are critical for PSTPIP2 function. However, their identity remained unknown.

In this article, we show that these phosphorylated tyrosine residues bind the lipid phosphatase SHIP1. In addition, we also show that PSTPIP2 interacts with Csk via a mechanism that is, at least in part, independent of PEST-PTPs. Our data also bring evidence for the involvement of these inhibitory enzymes in the PSTPIP2-mediated suppression of the inflammatory response.

Materials and Methods

Abs

Abs to the following Ags were used in this study: FLAG (M2) and GAPDH (from Sigma-Aldrich, St. Louis, MO); phospho-Erk (T202/Y204), phospho-Akt (S473, T308), and Myc (9B11) (Cell Signaling Technology, Danvers, MA); Csk (C-20) (Santa Cruz Biotechnology, Santa Cruz, CA); CD18 (YTS 213.1) (Serotec, Kidlington, U.K.); B220-biotin (RA3-6B2), TER119-biotin, Gr-1–PE (RB6-8C5), c-Kit–biotin, CD3ε-biotin, CD11b-FITC, Ly6C-PE-Cy7 (Biolegend, San Diego, CA); B220-FITC, DX5-biotin, F4/80-biotin, F4/80-PE, and F4/80-Alexa700 (eBioscience, San Diego, CA); Thy1.2-FITC, CD271-FITC, anti-FITC, and anti-biotin MicroBeads (Miltenyi Biotec, Bergisch Gladbach, Germany); HRP-conjugated goat anti-mouse L chain–specific Ab, HRP-mouse anti-rabbit L chain–specific, purified mouse IgG-whole molecule, goat anti-mouse $F(ab)_2$, goat anti-rat $F(ab)_2$ (Jackson Immunoresearch, West Grove, PA), Fc Bloc (2.4G2) (BD Biosciences, San Jose, CA). The rabbit antisera against SHIP1, PEP, PTP-PEST, and PTP-HSCF were a gift from Dr. A. Veillette (Institut de Recherches Cliniques de Montreal, University of Montreal). The Ab against human SHIP1 was from Exbio (Vestec, Czech Republic).

The mouse mAb that recognizes murine and human PSTPIP2 was generated by the immunization of mice (F1 hybrids of BALB/c × B10A) with a full-length recombinant murine PSTPIP2 produced in *Escherichia coli*. Splenocytes from immunized mice were fused with Sp2/0 myeloma cells and cloned by limiting dilution. Ab production was tested by ELISA and Western blotting.

To prepare mouse or human aggregated Ig, we first purified IgG from mouse serum (Sigma-Aldrich) or human AB serum (Invitrogen, Carlsbad, CA) on protein A-Sepharose (GE Healthcare, Uppsala, Sweden), transferred them to PBS, and concentrated them to 30 mg/ml on an Amicon Ultracel–30K unit (Millipore, Merck, Darmstadt, Germany). The aggregation was induced by heating to 63°C for 30 min.

Mice

CMO mouse strain (Cg-Pstpip2cmo/J) carrying the *c*.293T→C mutation in the *Pstpip2* gene (26, 29) on the BALB/c genetic background, resulting in an L98P change in the PSTPIP2 protein, and BALB/cByJ, were obtained from The Jackson Laboratory (Bar Harbor, ME). The BALB/c and F1 hybrids of BALB/c × B10A were from the animal facility of Institute of Molecular Genetics, Academy of Sciences of the Czech Republic (Prague, Czech Republic). All the experiments in this work that were conducted on animals were approved by the Animal Care and Use Committee of the Institute of Molecular Genetics and were in agreement with local legal requirements and ethical guidelines.

Cell lines and primary cells

All the primary cells and cell lines were cultured at 37°C with 5% CO_2 in the following media supplemented with 10% FCS and antibiotics: WEHI-231 cell line (ATCC) in RPMI 1640, HEK293FT cells (Invitrogen), Phoenix Eco cells (Origene, Rockville, MD), J774.2 (ATCC) cells, and immortalized macrophage progenitors in DMEM. IMDM was used for immortalized granulocyte progenitors and primary granulocytes.

Bone marrow (BM) was isolated from CMO and BALB/cByJ or BALB/c mice sacrificed by cervical dislocation. Full BM was cultured in DMEM conditioned with 10% L929 culture supernatant containing M-CSF to differentiate BM-derived macrophages (BMDMs). Osteoclasts were differentiated in DMEM supplemented with 20 ng/ml M-CSF and 100 ng/ml RANKL (Peprotech, Rocky Hill, NJ). Murine granulocytes were isolated from BM by negative selection using B220, F4/80, DX5, c-Kit, CD3ε, and Ter119 biotinylated Abs, and anti-biotin MicroBeads, on an AutoMACS magnetic cell sorter (Miltenyi Biotec), and the purity (>90%) was determined by flow cytometry. Human granulocytes were purified from buffy coats (purchased on a commercial basis from the Blood Bank of Thomayer Hospital, Prague, Czech Republic) by sedimentation in 2% Dextran T500 (Pharmacosmos, Holbaek, Denmark) followed by Ficoll centrifugation (Ficoll-Paque PLUS, GE Health Care) and erythrocyte lysis in an ACK buffer [150 mM NH_4Cl, 0.1 mM EDTA (disodium salt), 1 mM $KHCO_3$]. The generation of immortalized macrophage progenitors has been described previously (39); in brief, BM was centrifuged over Ficoll-Paque PLUS gradient, and mononuclear cells were directly infected with ER-Hoxb8 retrovirus by spinoculation. The cells were cultivated in a medium conditioned with 1% LUTZ culture supernatant as a source of GM-CSF and 1 μM β-estradiol (estrogen; Sigma-Aldrich). The cells could be differentiated into macrophages by the withdrawal of estrogen from the media within a week. To prepare immortalized granulocyte progenitors, we used a modified version of this protocol (39). The progenitors were first enriched by the depletion of Mac-1^+, $B220^+$, and Thy1.2^+ from mouse BM

cells and cultured in the presence of IL-3, IL-6, and SCF (supplied as culture supernatants from HEK293 cells transduced with constructs coding for respective cytokines) for 2 d. Next, they were transduced with the same ER-HoxB8 construct described earlier. The transduced cells were enriched for the GMP progenitor population by FACS (Lin^-, $Sca\text{-}1^-$, $c\text{-}Kit^+$, $Fc\gamma R^+$, $CD34^+$) and propagated in a media containing 1 μM β-estradiol and 1% SCF-containing supernatant. Granulocyte differentiation was induced by β-estradiol withdrawal and the addition of 50 ng/ml G-CSF.

DNA constructs, transfection, and transduction

The CLG construct (generated by the PCR-mediated joining of individual overlapping fragments and subcloned to MSCV-IRES-Thy1.1; Clontech, Mountain View, CA) was composed of the SH2 and SH3 domains of human Csk (aa 1–171) followed by the kinase domain from human Lck (aa 225–509) with Y505 mutated to phenylalanine and then by a Myc tag sequence and GST from *Schistosoma japonicum* lacking methionine 1 (Fig. 1A). Murine PSTPIP2 was cloned from cDNA prepared by the reverse transcription (RevertAid, Fermentas, Thermo Fisher Scientific, Waltham, MA) of RNA from WEHI-231 cells. Wild type (WT) PSTPIP2 or its various mutants generated by PCR mutagenesis were cloned into the MSCV-IRES-LNGFR vector (Clontech) with an N-terminal FLAG tag. Human PSTPIP2 was cloned from cDNA prepared from peripheral blood leukocytes. A Csk-Myc construct in a pMSCV retroviral vector and its variants with inactivating point mutations in the SH2 and SH3 domains (R107K and W47A, respectively) were prepared by PCR from the analogous Csk-Myc-OFP constructs described earlier (40). Lipofectamine 2000 (Invitrogen) was used according to the manufacturer's protocol for the transfection of Phoenix Eco cells to produce viral particles. Retrovirus-containing supernatants were then harvested, supplemented with polybrene (10 μg/ml; Sigma-Aldrich), and added to the cells. The cells were then centrifuged at 1250 × *g* for 90 min at 30°C. Infected cells were sorted based on the expression of reporter markers (Thy1.1 or LNGFR) by a BD Influx FACS (BD Biosciences).

Cell activation, lysis, and immunoprecipitation

For Western blotting, the cells were washed and resuspended in serum-free conditioned IMDM or DMEM at a concentration of 1–4 × 10^7 cells/ml. Subsequently, the cells were stimulated as indicated at 37°C. The activation of cells was stopped by the addition of an equal volume of a 2× concentrated SDS-PAGE sample buffer containing 0.1 mM diisopropyl fluorophosphate, followed by the sonication and heating of the samples (96°C for 2 min). The samples were analyzed by SDS-PAGE followed by Western blotting. For pervanadate-induced activation, the cells were incubated with 0.1 mM pervanadate for 10 min. To inhibit SHIP1 during the activation, we treated the cells with 10 μM 3-α-aminocholestane (3AC; Echelon Biosciences, Salt Lake City, UT).

For immunoprecipitation, the cells were lysed in the lysis buffer (1% lauryl maltoside [Calbiochem, Merck], 20 mM Tris [pH 7.5], 100 mM NaCl, 5 mM iodoacetamide, 50 mM NaF, 1 mM Na_3VO_4, 2 mM EDTA, 1 mM Pefabloc [Sigma-Aldrich] or 100× diluted Protease Inhibitor Cocktail set III [Calbiochem]; for neutrophil granulocyte lysis, 1 mM PMSF [Sigma-Aldrich] and 0.1 mM diisopropyl fluorophosphate [Fluka; Sigma-Aldrich] were also added) at 5 × 10^6/ml for 30 min on ice. Postnuclear supernatants were then incubated for 1 h with a primary Ab (2 μg/ml), followed by 1–2 h of incubation with Protein A/G Plus agarose beads (Santa Cruz Biotechnology) or Protein G magnetic beads (Millipore, Billerica, MA) at 4°C. After washing on chromatography columns or a magnetic stand, immunoprecipitates were eluted with a 70 μl SDS-PAGE sample buffer.

In vitro kinase assay

For the in vitro kinase assay, cells were lysed in the lysis buffer where NaF, Na_3VO_4, and EDTA were omitted. The immunoprecipitation was carried out in 96-well plates precoated with 0.1 mg/ml goat anti-mouse IgG (Sigma-Aldrich) and Myc Ab (see earlier). The immunoprecipitates were incubated with a kinase buffer (25 mM HEPES pH 7.4, 5 mM $MgCl_2$, 5 mM $MnCl_2$, 0.1% lauryl maltoside, and 0.1 μCi $\gamma[^{32}P]$-ATP per well) for 20 min at room temperature. After washing, the immunoprecipitates were eluted with a 50 μl SDS-PAGE sample buffer and subjected to SDS-PAGE and autoradiography.

Mass spectrometric analysis

Protein bands were cut from the gel, then further cut into small pieces and decolorized in a sonic bath at 60°C several times with 0.1 M 4-ethylmorpholine acetate (pH 8.1) in 50% acetonitrile (ACN). After complete destaining, proteins were reduced by 50 mM TCEP in 0.1 M 4-ethylmorpholine acetate (pH 8.1) for 5 min at 80°C and alkylated using 50 mM iodoacetamide in 0.1M 4-ethylmorpholine acetate (pH 8.1) in the dark at room temperature. Next, the gel was washed with water and ACN and was partly dried using a SpeedVac concentrator (Savant, Holbrook, NY). Finally, the gel was reconstituted with a cleavage buffer containing 0.01% 2-ME, 0.05M 4-ethylmorpholine acetate (pH 8.1), 10% ACN, and sequencing-grade trypsin (10 ng/μl; Promega). Digestion was carried out overnight at 37°C, and the resulting peptides were extracted with 30% ACN/0.1% TFA and subjected to mass spectrometric analysis. Mass spectra were acquired using the positive ion mode on a MALDI-FTMS APEX-Ultra (Bruker Daltonics, Bremen, Germany) equipped with a 9.4 T superconducting magnet and a SmartBeam laser. The acquisition mass range was 700–3500 m/z, and 512k data points were collected. The instrument was externally calibrated using the PepMix II peptide standard (Bruker Daltonics, Bremen, Germany). This results in a typical mass accuracy <2 ppm. A saturated solution of α-cyano-4-hydroxy-cinnamic acid in 50% ACN/0.2% TFA was used as a MALDI matrix. One microliter of the matrix solution was mixed with 1 μl of the sample on the target and the droplet was allowed to dry at ambient temperature. After the analysis, the spectra were apodized using square sine apodization with one zero fill. The interpretation of the mass spectra was done using the DataAnalysis version 3.4 and BioTools 3.2 software packages (Bruker Daltonics, Billerica, MA). The proteins were identified by peptide mass fingerprinting using the search algorithm MASCOT (Matrix Science).

Results

The initial goal of this study was the identification of novel Csk-interacting proteins. To achieve this, we designed a construct (hereafter termed CLG) consisting of the SH2 and SH3 domains of Csk and the kinase domain from the SFK Lck, followed by the Myc tag and GST (Fig. 1A). The construct was expressed in the murine B cell line WEHI-231 via retroviral infection. Because many Csk-binding proteins are substrates of SFKs, we expected that the Lck kinase domain would phosphorylate proteins bound to the Csk SH2/SH3 module of the construct, and we thus label them for relatively easy detection in the in vitro kinase assay or else after phosphorylation in vivo. This would allow for the subsequent optimization and scaling up of the procedure to identify these proteins by mass spectrometry. The Myc-GST module was intended for the tandem purification of CLG using glutathione Sepharose followed by the second round of affinity purification with the anti-Myc Ab. However, this approach was eventually abandoned because of the major technical difficulties caused, presumably, by the competition between the construct and the endogenous murine GST present in the cell lysates. Hence we eventually used this construct in only single-step Myc immunoprecipitations, without engaging its GST moiety. In this setup, we immunoprecipitated the CLG fusion protein from WEHI-231 lysates and incubated the immunoprecipitate with $\gamma[^{32}P]$-ATP. The proteins radioactively labeled by the CLG Lck kinase domain were then subjected to SDS-PAGE and autoradiography. This procedure revealed several proteins with molecular masses of 75, 51–55, 37, and 16 kDa in the immunoprecipitates (Fig. 1B). Whereas the 75-kDa band most likely represented the autophosphorylated CLG construct, the identity of the other proteins remained unknown. To identify these proteins, we performed a large-scale immunoprecipitation from WEHI-231 cell lysates (from 4 × 10^8 cells) infected with the CLG construct followed by SDS-PAGE and Coomassie blue detection. In this way, we were able to detect a protein of 37 kDa, which likely corresponded to a 37-kDa band from the in vitro kinase assay (Fig. 1C). Mass spectrometry identification revealed that this protein was PSTPIP2 (Fig. 1D, Supplemental Fig. 1). Although it was known to interact with PEST-PTPs (24, 32), interaction of PSTPIP2 with Csk has not yet been described.

Because of the unusual composition of the CLG construct, we wanted to confirm that nonaltered full-length endogenous Csk interacts with PSTPIP2. To achieve this, we infected a murine WEHI-231 cell line with a FLAG-tagged PSTPIP2 construct and

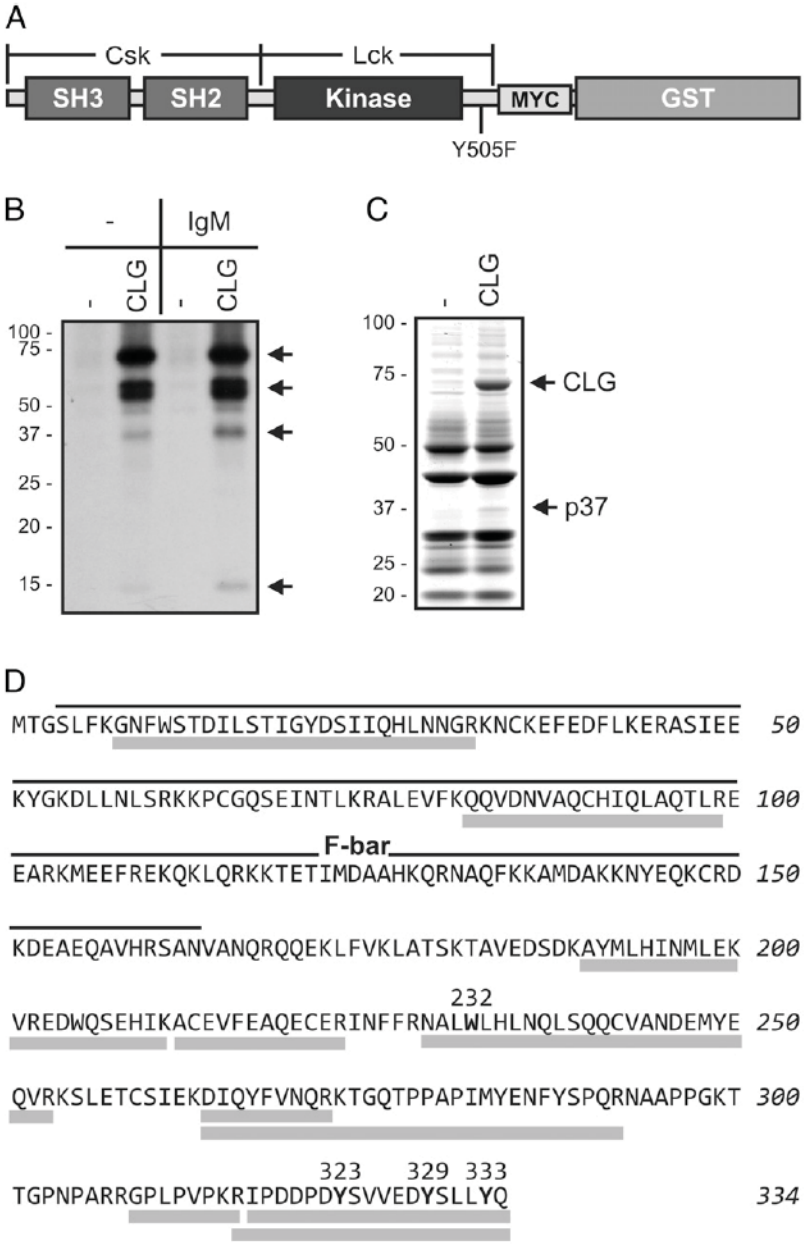

FIGURE 1. Identification of PSTPIP2 as a Csk binding protein. (**A**) Schematic representation of the CLG construct. (**B**) Anti-myc (CLG) immunoprecipitates from WEHI-231 cells transfected (or not) with the CLG construct and activated (or not) with an anti-IgM Ab were incubated with $\gamma[^{32}P]$-ATP and subjected to SDS-PAGE and autoradiography. Arrows indicate the positions of major phosphorylated species. (**C**) Large-scale anti-Myc (CLG) immunoprecipitation from lysates of WEHI-231 transfected (or not) with the CLG construct. The immunoprecipitates were separated by SDS-PAGE followed by staining with colloid Coomassie blue. Arrows show the positions of the CLG construct and p37. (**D**) Amino acid sequence of PSTPIP2. Gray bars underline the peptides identified by mass spectrometry. Functionally important sequences and residues are also labeled (F-bar domain with a black line above the sequence, important amino acid residues by numbers above the sequence).

then immunoprecipitated this protein from the lysates of infected cells. We could readily detect endogenous Csk in FLAG immunoprecipitates from PSTPIP2-FLAG–infected cells, but not from noninfected cells, demonstrating that full-length endogenous Csk interacts with PSTPIP2 (Fig. 2A). To find out which of the binding domains present in Csk is responsible for PSTPIP2 binding, we infected WEHI-231 cells with Csk constructs containing inactivating mutations in their SH2 and SH3 domains. Intriguingly, the immunoprecipitations of these mutated Csk proteins from the cell lysates revealed that the mutation of any of these domains substantially reduced or abolished the binding of PSTPIP2 to Csk, suggesting that the binding is likely cooperative, involving both the SH2 and the SH3 domains of Csk (Fig. 2B).

Because Csk is known to interact with PEST-PTPs (18, 21, 22), we wanted to find out whether the Csk–PSTPIP2 interaction is dependent on these enzymes. For this purpose, we again used WEHI-231 cells transfected with WT PSTPIP2 and its W232A mutant, which is unable to bind PEST-family phosphatases. Coprecipitation experiments revealed that the W232A mutation diminished Csk binding. However, a substantial fraction of Csk still interacted with PSTPIP2 W232A, whereas at the same time the binding of all the PEST-family phosphatases was completely abolished (Fig. 2C). These data suggested that a fraction of Csk binds to PSTPIP2 independently of PEST-PTPs, most likely via the direct interaction with PSTPIP2. In this experiment, we also demonstrated that PSTPIP2 interacts with PEP in a similar manner (requiring the presence of W232) to other PEST-family phosphatases (Fig. 2C). PEP is the last PEST-family member for which this interaction has not yet been demonstrated.

Although we identified the interaction between Csk and PSTPIP2 in the B cell line WEHI-231, macrophages were initially thought to be the critical cell type driving inflammatory disease in CMO mice (27, 34). Moreover, PSTPIP2 phosphorylation can be observed in macrophage cell line after stimulation by M-CSF (33), and the absence of PSTPIP2 resulted in an increased macrophage proliferation in response to the same stimulation (34). Thus, to study PSTPIP2 tyrosine phosphorylation and its effects on Csk binding in a more relevant cell type, we used the murine macrophage-like cell line J774. We generated constructs with phenylalanine mutations in Y323, Y329, and Y333, located in the PSTPIP2 C-terminal

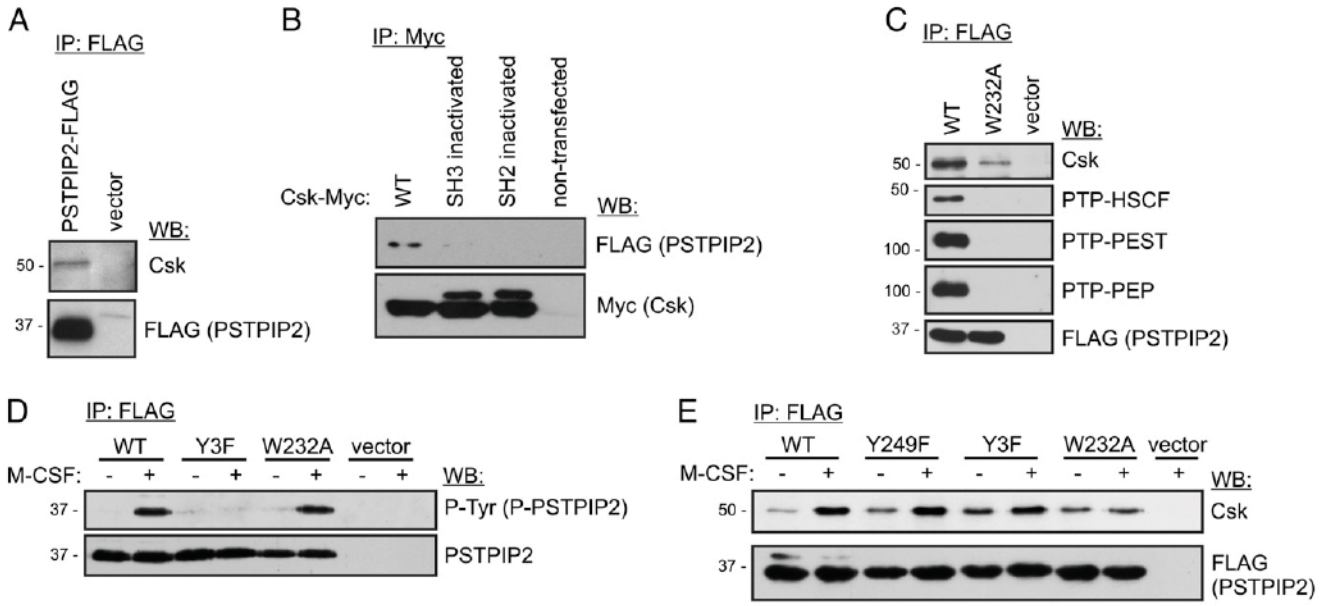

FIGURE 2. PSTPIP2 interaction with Csk. (**A**) Lysates from PSTPIP2-FLAG or vector-transduced WEHI-231 were subjected to FLAG immunoprecipitation (IP) followed by immunoblotting (WB) with indicated Abs. (**B**) Lysates from WEHI-231 transduced with PSTPIP2-FLAG and the Csk-Myc constructs with or without an inactivating mutation in the SH2 (R107K) or SH3 (W47A) domain were subjected to Myc immunoprecipitation followed by immunoblotting with FLAG and Myc Abs. (**C**) Lysates from WEHI-231 cells expressing the WT or W232A PSTPIP2-FLAG constructs were subjected to FLAG immunoprecipitation followed by immunoblotting with Abs to the indicated proteins. Empty vector-transduced cells served as a negative control. (**D**) FLAG immunoprecipitates from J774 cells transfected with indicated PSTPIP2-FLAG constructs and stimulated (or not) with M-CSF were subjected to immunoblotting with phosphotyrosine (P-Tyr) and PSTPIP2 Abs. Empty vector-transduced cells served as a negative control. (**E**) Similar immunoprecipitation as in (D) followed by immunoblotting with Csk and FLAG Abs. Only relevant parts of the blots are shown.

tail (Y3F). Y323 and Y333 have previously been reported to be responsible for the majority of PSTPIP2 tyrosine phosphorylation (24, 32), and Y329 also seemed a good candidate phosphorylation site (see *Discussion* for more details on the selection of these tyrosines). Next, we expressed these constructs, as well as the W232A construct, in J774 cells stimulated (or not) with M-CSF to induce the tyrosine phosphorylation of PSTPIP2. We observed an increase in the tyrosine phosphorylation of PSTPIP2 after M-CSF treatment, which was not affected by W232A mutation (Fig. 2D). In contrast, the mutation of all three C-terminal tyrosines (Y3F) almost completely abolished PSTPIP2 tyrosine phosphorylation (Fig. 2D), which is in agreement with previously published data (24, 32). In the next experiment, we analyzed the Csk binding to these mutants. For this purpose, we also included a mutation of Y249, which, of all PSTPIP2 tyrosines, most closely resembled the Csk-binding site (12). Similar to the previous experiment, in resting cells we observed Csk binding to WT PSTPIP2 (Fig. 2E). Moreover, upon M-CSF stimulation, Csk binding to PSTPIP2 substantially increased. However, none of the tyrosine mutations were able to reduce basal or M-CSF–induced Csk binding to PSTPIP2. In addition, when we analyzed the W232A mutant of PSTPIP2, which was unable to interact with PEST-family phosphatases, we found that in nonstimulated cells Csk binding was not altered by the W232A mutation. However, the increase in Csk binding after M-CSF stimulation was lost (Fig. 2E). We also tested a number of other mutations (Supplemental Table I), as well as their combinations with W232A, but we did not observe any additional effect on Csk binding (data not shown). Unfortunately, some of the candidate binding sites could not be analyzed because their mutations resulted in instability and degradation of the mutant protein that, as a result, could not be detected in the lysates of the transfected cells. Thus, we can conclude that, in J774 cells, PSTPIP2 constitutively binds Csk and this binding is independent of PEST-PTPs. Moreover, M-CSF stimulation results in enhanced binding, which is likely mediated by PEST-PTPs.

To better understand the function of PSTPIP2 in macrophages and to find relevant situations where the signaling pathways could be regulated by PSTPIP2, we analyzed its expression and phosphorylation in this cell type. To be able to follow the endogenous protein expression, we developed a mouse mAb specific for both human and mouse PSTPIP2. The Ab recognizes transfected (Fig. 3A) and endogenous PSTPIP2 (Fig. 3B), and works well in both Western blot analysis and immunoprecipitation experiments.

It has been previously published that PSTPIP2 expression in macrophages is increased after LPS treatment, suggesting that PSTPIP2 expression may be enhanced during inflammation. Thus, we treated BMDMs with LPS or various mostly proinflammatory cytokines and followed the PSTPIP2 expression. Interestingly, PSTPIP2 was strongly upregulated, not only by LPS but also by treatment with several proinflammatory cytokines, including IFN-γ, TNF-α, and GM-CSF, whereas treatment with IL-4 (which promotes their alternative M2 differentiation) did not change the PSTPIP2 expression (Fig. 3B). These data suggest that an increase in PSTPIP2 expression is a part of a proinflammatory differentiation program in macrophages.

To obtain the more complete information about the involvement of PSTPIP2 in the regulation of inflammatory processes in macrophages, we next tested several additional receptors involved in the macrophage inflammatory response for their ability to regulate the tyrosine phosphorylation of PSTPIP2. In this experiment, we stimulated J774 cells expressing FLAG-PSTPIP2 with M-CSF, an anti-Fc receptor (anti-FcR) Ab or an Ab against an integrin β2 subunit, as well as LPS, GM-CSF, and IFN-γ. In resting cells, we observed a low level of constitutive PSTPIP2 phosphorylation (Fig. 4A). Similar to the previously published data, M-CSF treatment resulted in increased phosphorylation. Importantly, PSTPIP2 tyrosine phosphorylation was also substantially increased after FcR

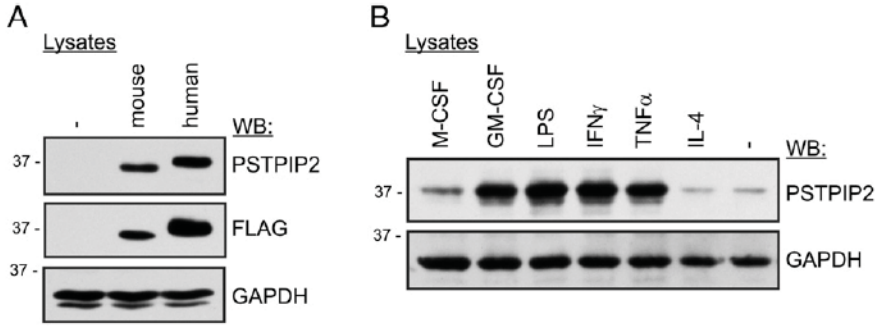

FIGURE 3. Evaluation of the PSTPIP2 Ab and regulation of PSTPIP2 expression. (**A**) HEK293 cells were transfected with FLAG-tagged mouse or human PSTPIP2. Both proteins were detected on the Western blot by the mAb to PSTPIP2. Nontransfected cells served as a negative control. (**B**) BMDMs from WT mice were treated for 24 h with LPS or indicated cytokines followed by immunoblotting with the PSTPIP2 Ab. Staining for GAPDH served as a loading control. Only relevant parts of the blots are shown.

cross-linking with more rapid kinetics (Fig. 4A). This phosphorylation peaked at 1 min and then gradually declined (Fig. 4B). It was accompanied by increased Csk binding, which was also more sustained. The binding of the PEST phosphatases PTP-PEST and PTP-HSCF did not seem to be influenced by FcR stimulation. However, the remaining family member PTP-PEP displayed a comparatively low level of binding in the resting cells, which increased substantially after FcR stimulation (Fig. 4B). Similar phosphorylation was also observed after integrin stimulation, although in this case the involvement of the FcRs could not be excluded because full-length Abs were used to cross-link the integrins in these experiments (Fig. 4A). We did not see any changes in PSTPIP2 phosphorylation after stimulation with LPS, GM-CSF, or INF-γ (data not shown).

The C-terminal tyrosines of PSTPIP2 were identified as major phosphorylation sites in PSTPIP2, and in some experiments they also appeared to be among the functionally most important residues in the PSTPIP2 protein (32, 38). In our experiments, Csk binding did not depend on the presence of these tyrosines. Therefore, we assumed that there must be an additional, unknown binding partner that interacts with these residues, and we attempted its identification. For this purpose, we used immortalized macrophage progenitors (see *Materials and Methods*). These cells are much more closely related to primary cells than tumor cell lines, and thus they are better suited for the detection of the most relevant interactions. Moreover, increased number of macrophage progenitors has been observed in CMO mice, suggesting PSTPIP2 involvement in the regulation of this population (34). Finally, these cells can be propagated in a cell culture and obtained in sufficient numbers for large-scale experiments. We infected these cells with WT PSTPIP2 and PSTPIP2 with mutated C-terminal tyrosines (Y3F) and then performed large-scale PSTPIP2 immunoprecipitations. Mass-spectrometry analysis of the proteins specifically present in the immunoprecipitates of WT, but not mutant, PSTPIP2 resulted in the identification of the lipid phosphatase SHIP1 as a novel PSTPIP2 binding partner (Fig. 5A, Supplemental Fig. 2). To confirm these data under more physiological conditions, we immunoprecipitated PSTPIP2 from the lysates of WT and CMO BMDMs stimulated with M-CSF or via FcR, and we observed a low level of constitutive SHIP1 binding that was substantially increased after both M-CSF and FcR stimulation (Fig. 5B, 5C). To verify that SHIP1 binds to the C-terminal tyrosines of PSTPIP2, we expressed WT and Y3F mutants of PSTPIP2 in CMO BMDMs and stimulated these cells with pervanadate. Indeed, we could readily observe SHIP1 binding to WT, but not to the mutant protein, confirming that functionally important C-terminal tyrosines are required for SHIP1 binding (Fig. 5D).

SHIP1 dephosphorylates the PI3K product PI(3,4,5)P_3, thus regulating a number of important pathways, whereas Csk inhibits SFKs, which are also expected to have a strong impact on macrophage signaling. Unexpectedly, we could not find any differences in the activity of M-CSF, LPS, or FcR-driven signaling pathways when comparing the BMDMs from WT and CMO mice (data not shown). This included the analysis of Akt and Erk phosphorylation, which are known to be regulated by SHIP as well as SFK phosphorylation at the inhibitory tyrosine (or in the activation loop) regulated by Csk. We also analyzed a number of other pathways in the macrophages (Jak-Stat, NF-κB, JNK, p38) (data not shown), but we did not see any defects. However, recently published work has suggested neutrophil granulocytes and IL-1β as probable driving forces behind inflammatory disease in CMO mice (35, 36). Thus, as a next step, we analyzed PSTPIP2 expression and function in granulocytes. Surprisingly, we found that

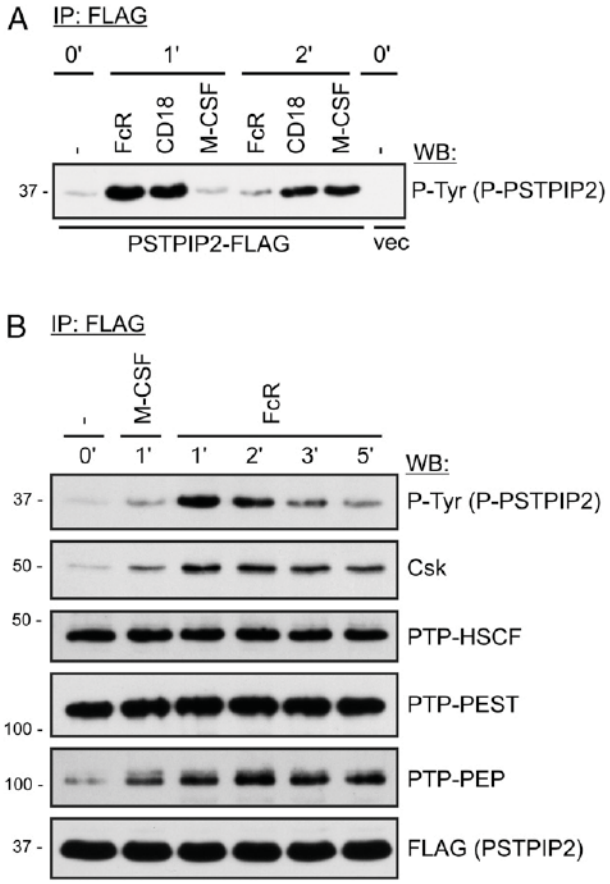

FIGURE 4. Phosphorylation and interactions of PSTPIP2. (**A**) J774 cells expressing PSTPIP2-FLAG were stimulated by M-CSF or by FcR or CD18 cross-linking for the indicated time intervals. PSTPIP2-FLAG was immunoprecipitated from the lysates of these cells and subjected to immunoblotting with the phosphotyrosine (P-Tyr) Ab. (**B**) Immunoprecipitates from M-CSF– or FcR-stimulated cells were prepared in a similar manner as in (A) and subjected to immunoblotting with the indicated Abs. Only relevant parts of the blots are shown.

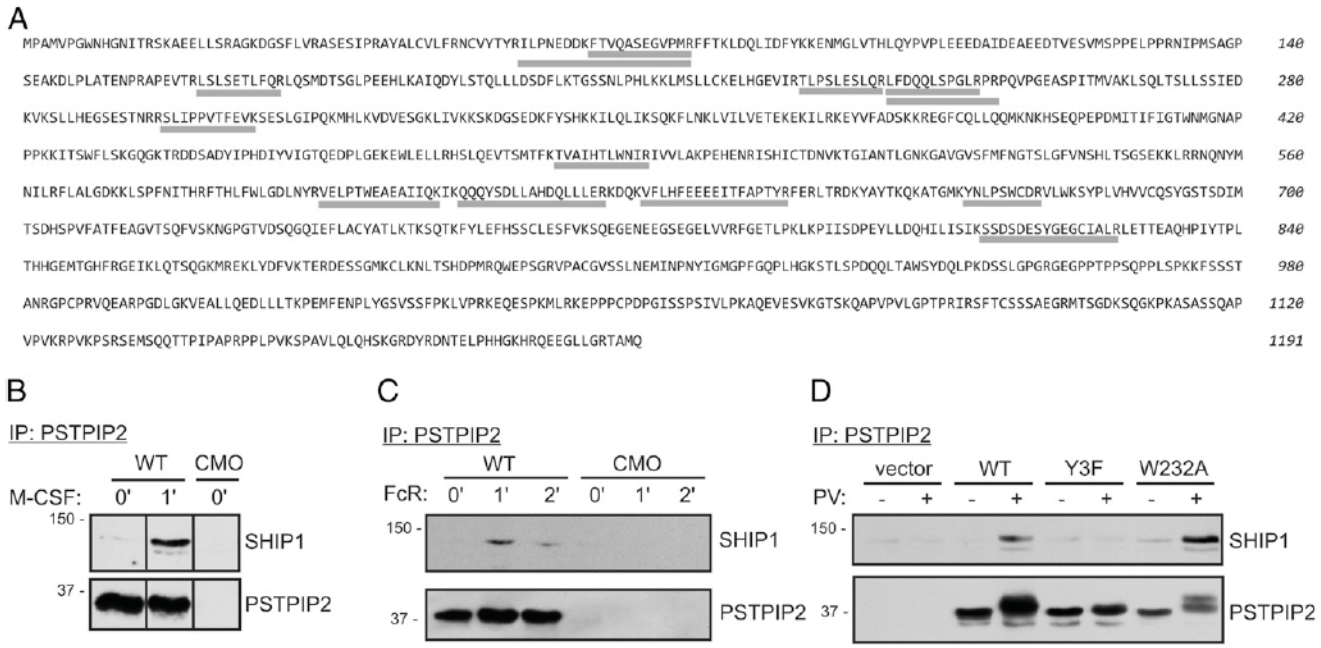

FIGURE 5. Binding of SHIP1 to PSTPIP2. (**A**) Amino acid sequence of SHIP1. Gray bars underline the peptides identified by mass spectrometry. (**B** and **C**) Lysates from WT or CMO BMDMs activated for indicated time intervals with M-CSF (B) or by FcR cross-linking (C) were subjected to PSTPIP2 immunoprecipitation followed by SHIP1 or PSTPIP2 immunoblotting. (**D**) CMO macrophages differentiated from immortalized macrophage progenitors were transduced with the indicated constructs. The cells were treated (or not) with 0.1 mM pervanadate and the lysates from these cells were subjected to PSTPIP2 immunoprecipitation followed by SHIP1 and PSTPIP2 immunoblotting. Only relevant parts of the blots are shown.

in these cells the expression of PSTPIP2 is higher than in macrophages or osteoclasts (Fig. 6A). Moreover, in contrast with our observations in the macrophages, CMO neutrophils exhibited increased FcR-triggered phosphorylation of the Erk and p38 MAPKs, as well as higher phosphorylation of Akt (Fig. 6B) and more efficient processing of IL-1β (Fig. 6C), compared with WT

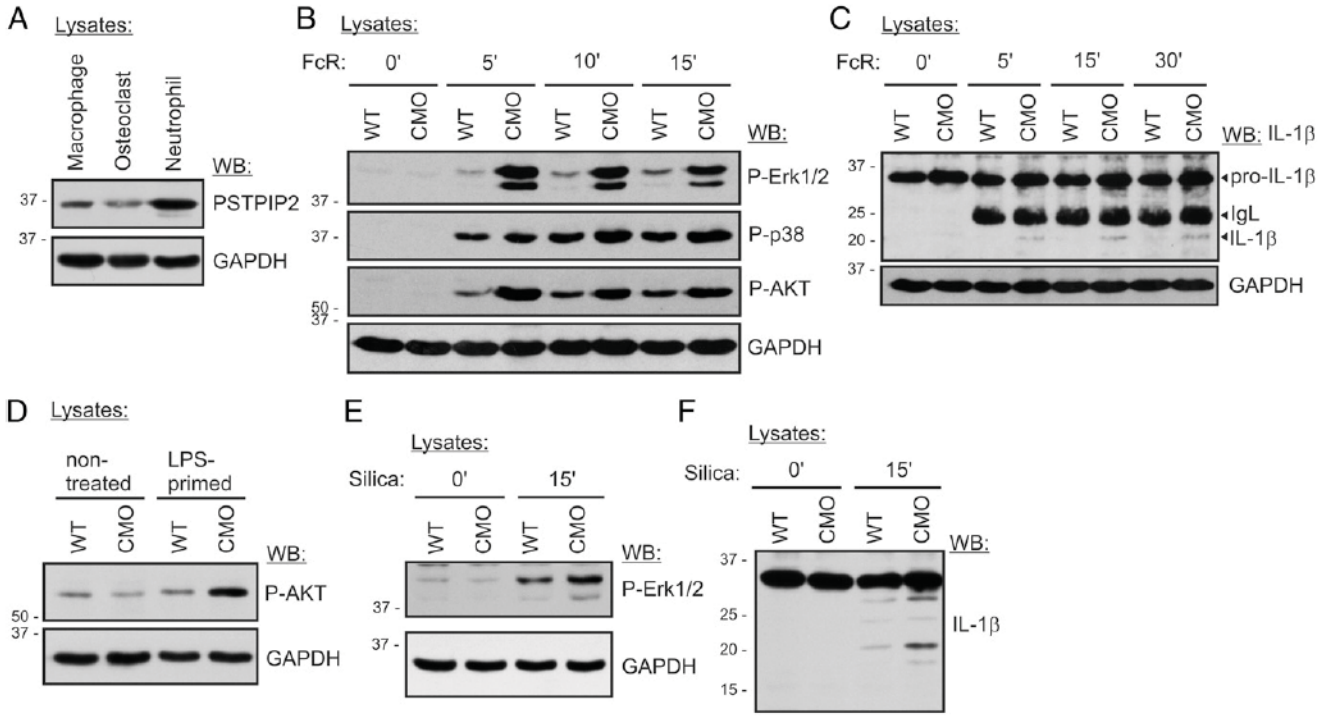

FIGURE 6. Effects of PSTPIP2 deficiency on neutrophil signaling. (**A**) Expression of the PSTPIP2 protein in the lysates of BMDMs and BM-derived osteoclasts and primary neutrophils purified from the same organ. (**B**) Erk, p38, and Akt (S473) phosphorylation in the lysates of neutrophils purified from mouse BM and treated for the indicated time intervals with mouse aggregated IgG to stimulate their FcRs. (**C**) Neutrophils were purified from mouse BM primed for 3 h with 100 ng/ml LPS and then for the indicated time intervals with aggregated mouse IgG. They were then lysed and subjected to immunoblotting with the IL-1β Ab to probe for processed IL-1β and its precursor. Note the presence of the Ig L chains from the mouse IgG used in the FcR activation. (**D**) Akt phosphorylation at S473 in the lysates of neutrophils primed for 90 min with 50 ng/ml LPS. (**E**) Erk phosphorylation in the lysates of neutrophils treated for 15 min with silica particles (50 $\mu g/cm^2$). (**F**) The same samples from (E) were probed for pro–IL-1β and its cleavage products. Only relevant parts of the blots are shown.

neutrophils. The additional analysis of signaling pathways in granulocytes isolated from CMO mice revealed that Akt phosphorylation was also increased after the relatively long (90-min) treatment of neutrophils with LPS (Fig. 6D). However, pro–IL-1β production after LPS priming did not appear to be altered in CMO neutrophils (Fig. 6C).

Finally, we also tested the effects of silica particles, a typical inflammasome activator, on CMO neutrophil signaling and IL-1β cleavage. The silica exposure in these cells resulted in the enhanced activation of MAPKs Erk1/2 (Fig. 6E), whereas no reproducible differences in Akt phosphorylation were observed in CMO mice (data not shown). To analyze IL-1β processing, we induced pro–IL-1β production in neutrophils by priming with LPS and then triggered its cleavage by subsequent incubation with silica. Although the LPS-induced pro–IL-1β production was not markedly affected in CMO neutrophils, silica exposure led to the enhanced production of mature IL-1β of 21 and 17 kDa (Fig. 6F), which are the sizes characteristic for cleavage by neutrophil serine proteases and inflammasome-dependent caspases, respectively (41). This is in agreement with the previously published data showing the enhanced secretion of IL-1β by neutrophils into the culture media under these circumstances (35, 36).

Because recent reports showed that IL-1β and inflammasome-activated caspases are critical for the disease development in CMO mice (35–37), we decided to analyze the silica-triggered IL-1β production in more detail, especially with respect to the interactions among PSTPIP2, SHIP1, and Csk described earlier. To address the question of PSTPIP2 phosphorylation under these conditions, we performed the immunoprecipitation of endogenous PSTPIP2 from unstimulated or LPS-primed and silica-stimulated BM cells. Of the cell types that express PSTPIP2 in the BM, neutrophils comprise the vast majority. Thus, we used non-separated BM cells for this experiment to increase the yield and to prevent unnecessary manipulations of these sensitive cells. Under these conditions, we observed a slight increase in PSTPIP2 phosphorylation after LPS priming followed by a much more substantial increase after silica treatment (Fig. 7A).

To study the effect of the mutations of SHIP1 binding sites in PSTPIP2 on IL-1β processing in neutrophils, we generated immortalized granulocyte progenitors by the infection of BM progenitors with the ER-HoxB8 fusion construct that, in the presence of estrogen, is maintained in the cell nucleus and blocks further differentiation. Such cells can be propagated in the cell culture and infected with retroviral constructs. The replacement of estrogen with G-CSF results in the differentiation of these progenitors into mature granulocytes. Similar to primary granulocytes, these cells are short-lived and cannot be maintained in the culture for >1 d after reaching maturity. We prepared immortalized granulocyte progenitors from CMO mice and transduced these cells with WT, Y3F, and W232A constructs of PSTPIP2. Next, we tested granulocytes differentiated from these progenitors for the processing of IL-1β. The processing of IL-1β after treatment with silica was more efficient in the cells infected with W232A and 3YF mutants when compared with WT PSTPIP2, demonstrating that despite a slightly higher expression level, the mutant proteins were unable to inhibit IL-1β cleavage as efficiently as WT PSTPIP2 (Fig. 7B). This result shows that SHIP1 and PEST phosphatase-binding sites are important for the PSTPIP2-mediated inhibition of IL-1β processing. We excluded empty-vector transfected CMO progenitors from this experiment because of their increased speed of maturation, which was not observed in PSTPIP2-infected cells (irrespective of the mutation present in PSTPIP2; data not shown). Because vector-infected cells were already progressing to apoptosis at the time when the other cell lines just reached the maturity, they could not be used as a control.

Next, to directly analyze the role of SHIP1 in IL-1β processing, we treated the WT and CMO primary granulocytes from the BM

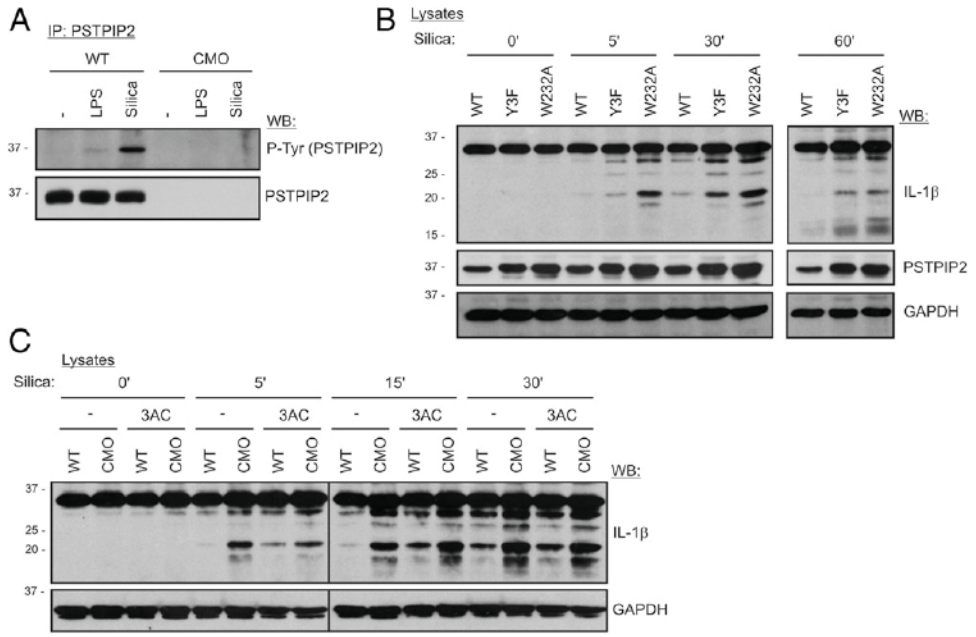

FIGURE 7. Role of SHIP1 in the PSTPIP2-mediated suppression of IL-1β processing. (**A**) BM cells were primed with 50 ng/ml LPS for 3 h followed by 15-min silica exposure (50 μg/cm^2). PSTPIP2 was immunoprecipitated from the lysates of these cells and the immunoprecipitates were subjected to immunoblotting with phosphotyrosine (P-Tyr) and PSTPIP2 Abs. Only relevant parts of the blots are shown. (**B**) Granulocytes differentiated from immortalized progenitors transduced with WT PSTPIP2 and its Y3F and W232A mutants were primed for 3 h with 100 ng/ml LPS and then stimulated by silica particles (50 μg/cm^2) for the indicated time intervals. The cells were then lysed and probed for IL-1β cleavage products. (**C**) Neutrophils purified from the mouse BM were primed with 100 ng/ml LPS for 3 h and then with silica particles (50 μg/cm^2) for the indicated time intervals in the presence or absence of the SHIP1 inhibitor 3AC (10 μM). Only relevant parts of the blots are shown.

with the specific SHIP1 inhibitor 3AC. In agreement with the proposed role of SHIP1 in PSTPIP2 function, this treatment resulted in enhanced IL-1β cleavage after exposure to silica in WT neutrophils, whereas only a very mild effect was observed in their CMO counterparts (Fig. 7C). Altogether, these data support the conclusion that interaction with SHIP1 is a part of the mechanism of how PSTPIP2 suppresses the IL-1β–mediated inflammatory response in granulocytes.

Finally, we wanted to test the expression and interactions of PSTPIP2 in primary human granulocytes. Because these cells can be obtained in relatively large numbers, they also allowed us to test the PSTPIP2 interactions. We isolated human granulocytes from fresh buffy coats and stimulated these cells with silica or human aggregated IgG (as an FcR ligand). Surprisingly, these granulocytes did not appear to interact with silica particles or to phagocytose these particles, and this treatment did not result in any PSTPIP2 tyrosine phosphorylation (data not shown). However, they vigorously responded to the FcR stimulation. This treatment resulted in the increased tyrosine phosphorylation of PSTPIP2 accompanied by the binding of Csk and SHIP1 (Fig. 8). The 100-kDa form of SHIP1 prevailing in these immunoprecipitates is likely the result of proteolytic cleavage and has been described previously (42). These results confirm that PSTPIP2 is also expressed in human granulocytes and that it participates in similar interactions as its murine counterpart.

Discussion

PSTPIP2 is known for its principal role in the development of the inflammatory disorder described as chronic multifocal osteomyelitis in mice, where its reduced expression or its complete absence is the main cause of the disease (26, 27, 34). However, the mechanism for how PSTPIP2 prevents the disease development has remained unclear. As an adaptor protein, it is likely to function via the recruitment of inhibitory enzymes and other negative regulators. The only molecules of this class previously known to bind to PSTPIP2 were the PEST-PTPs (24, 32). All three family members have been expected to bind to PSTPIP2, although the interaction has formally been proved only for PTP-HSCF and PTP-PEST (24, 32). We filled this gap by showing that PEP/LYP also interacts with PSTPIP2 in a similar manner, dependent on the residue W232 of PSTPIP2 (Fig. 2C). Mice deficient in PEP or PTP-PEST do not develop typical signs of autoinflammatory disorder (43–46), and thus it seems that the major functions of these PTPs are not related to their binding to PSTPIP2. However, if there is a redundancy among the PEST-PTPs that are associated with PSTPIP2, single family member deficiencies would probably not reveal any relevant phenotype. Moreover, additional evidence supports the importance of PEST-PTPs for the functionality of PSTPIP2. The W232A mutation in PSTPIP2, which prevented its binding to PEST-family phosphatases, diminished the ability of PSTPIP2 to inhibit the differentiation of osteoclasts and megakaryocytes (32, 38). In addition, we show in this article that this tryptophan is also important for the suppression of IL-1β processing in neutrophils. The substrate of PSTPIP2-associated PEST-PTPs remains unknown. By analogy with PSTPIP1 (47), one might speculate that their substrate would be PSTPIP2 itself, but we have not observed any increase in the phosphorylation of PSTPIP2 mutated at W232 (Fig. 2D). Thus, it seems more likely that these phosphatases dephosphorylate some of its binding partners, such as SHIP1 and Lyn or other unknown proteins in the vicinity of PSTPIP2.

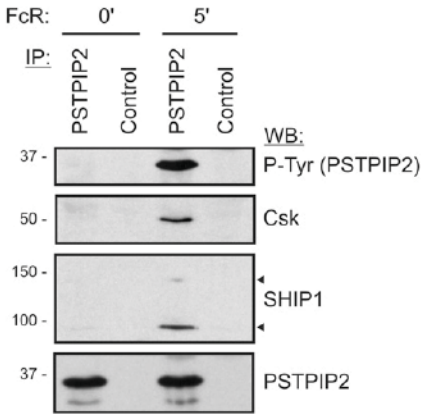

FIGURE 8. PSTPIP2 phosphorylation and interactions in human neutrophils. Human neutrophils were purified from a fresh buffy coat and activated by human aggregated IgG (300 μg/ml) for 5 min. The cells were then lysed and subjected to PSTPIP2 immunoprecipitation. The immunoprecipitates were then analyzed for the presence of the indicated molecules by immunoblotting. In the immunoprecipitations, an irrelevant isotype-matched Ab served as a negative control. Only relevant parts of the blots are shown.

Another possible role of PEST-PTPs includes the recruitment of Csk to PSTPIP2, which is further enhanced by the independent binding of Csk directly to PSTPIP2. In such a case, SFKs would be the most probable target. We did not observe any effect of PSTPIP2 deficiency on the global phosphorylation of SFKs, whether in macrophages or granulocytes. However, it is possible that PEST-PTPs together with Csk specifically inhibit the pool of SFKs associated with PSTPIP2. The interaction between PSTPIP2 and SFK Lyn was described previously in megakaryocytes (38), and we detected a similar interaction in macrophages (data not shown). The effect of Csk binding could not be fully analyzed because we were unable to identify its binding site in PSTPIP2. We suspect that the binding site is within the F-bar domain or other sequences that could not be evaluated because of the lack of mutated protein expression. Notably, the sequence integrity seems to be essential for PSTPIP2 protein stability, because other mutations, including Lupo and CMO, also result in defective protein expression (27, 34). In addition, there was a fraction of Csk that, in J774 cells, interacted with PSTPIP2 inducibly after M-CSF or FcR stimulation. The binding of the inducible Csk fraction was dependent on the interaction of PSTPIP2 with PEST-family phosphatases. The most likely candidate for bringing this additional Csk to the complex is PTP-PEP, which interacted with PSTPIP2 in an inducible manner. However, another option is that PTP-HSCF, which, unlike PTP-PEST or PTP-PEP, binds Csk via phosphorylated tyrosines in its C-terminal tail (22), is responsible for this inducible binding.

Another critical region in PSTPIP2 comprises the C-terminal tyrosines. Their mutation completely abolished the ability of PSTPIP2 to suppress the differentiation of osteoclasts and reduced its ability to inhibit megakaryocyte differentiation (32, 38). The most likely explanation was that these tyrosines recruit a negative regulatory molecule responsible for these effects. In this work, we have shown that these tyrosines are responsible for binding to the lipid phosphatase SHIP1. Indeed, Y329 and Y323 very well match the consensus binding site for the SHIP1 SH2 domain (48, 49), whereas Y333 bears a certain resemblance to the ITIM motif [hydrophobic amino acid (L) in position −2 with respect to the tyrosine], which is also known to bind the SHIP1 SH2 domain (50). All the previous work on PSTPIP2 tyrosine phosphorylation has analyzed only Y323 and Y333. It was based on the assumption that these tyrosines are analogous to the phosphorylated tyrosine residues found in the related and more thoroughly studied protein PSTPIP1 (Y344 and Y367, respectively) (24). However, our sequence analysis did not reveal any relationship between these

tyrosines. Y367 of PSTPIP1 is located inside its SH3 domain, which is not present in PSTPIP2. Moreover, it is a highly conserved residue forming a part of the SH3 domain ligand-binding pocket that is found within a number of these domains in various proteins where it is thought to regulate their interactions with respective ligands (51). The sequence surrounding Y344 of PSTPIP1 (LVYASI) is also somewhat different from Y323 of PSTPIP2 (PDYSVV), and therefore we concluded that the C-terminal tyrosines are a unique feature of PSTPIP2 not found in PSTPIP1. Notably, in the previous work, the mutation of Y323 and 333 severely reduced, but did not completely abolish, the phosphorylation of PSTPIP2, suggesting that there is an additional tyrosine phosphorylation site in PSTPIP2 (24). Y329 was shown to be phosphorylated in mast cells (52), and thus we assumed that Y329 is the most likely candidate. Therefore, we decided to mutate all three C-terminal tyrosines in PSTPIP2 at the same time for our analysis of SHIP1 binding and function. This analysis showed that these three tyrosines are required for SHIP1 binding and that the PSTPIP2 phosphorylation in their absence is negligible. Moreover, we also showed that these tyrosines are required for the maximum inhibition of IL-1β processing in neutrophils. This, together with our data demonstrating increased IL-1β cleavage in WT neutrophils in the presence of the SHIP1 inhibitor, strongly supports the idea that some of the key functions of PSTPIP2 are, at least in part, mediated by SHIP1. Additional support for this idea is also derived from the fact that the Akt and Erk pathways, which are both known to be regulated by SHIP1, are affected by PSTPIP2 absence.

When considering the role of SHIP1 in PSTPIP2 function, it is also interesting to compare the phenotypes of SHIP1-deficient mice with the phenotype caused by PSTPIP2 deficiency. Similar to CMO, SHIP1$^{-/-}$ mice develop a disease with an autoinflammatory component where inflammatory myeloid infiltrate into multiple organs and enhanced serum IL-6 levels can be observed (3, 53–55). Both strains display splenomegaly with extramedullary hematopoiesis and an increased number and proliferation of myeloid progenitor cells (3, 34, 53). In addition, they also share a phenotype of increased osteoclastogenesis and osteoclast activity, resulting in osteopenia and osteoporosis (32, 56). These features shared between SHIP1$^{-/-}$ and CMO mice suggest that they are components of a common signaling pathway. In contrast, the reduced survival of SHIP$^{-/-}$ mice because of massive myeloid cell infiltration in the lungs is not observed in CMO mice (53), and PSTPIP2 does not seem to be involved in endotoxin tolerance. This phenomenon is mainly caused by the dramatic increase in SHIP1 expression after LPS treatment (57). Despite the fact that the expression of PSTPIP2 is also increased, we did not observe any significant difference in the signaling of endotoxin-tolerized WT and CMO BMDMs, suggesting that PSTPIP2 plays no role in this process (data not shown). The more serious phenotype of SHIP1$^{-/-}$ mice is, however, not surprising, because PSTPIP2 is not the only binding partner of SHIP1, and this enzyme interacts with multiple other proteins and has an effect on other pathways.

The initial characterization of CMO and LUPO mice led to the conclusion that macrophages and osteoclasts are the major cell types responsible for the disease development (27, 32, 34). However, recent work has suggested that, in fact, granulocytes are the most important cell type triggering the disease via the increased production of IL-1β (35, 36). Indeed, we had difficulty detecting any differences in the signaling pathways between the WT and CMO macrophages. In contrast, in CMO neutrophils, we observed enhanced activity of multiple signaling pathways after LPS or silica exposure or after FcR stimulation. The CMO disease development was recently shown to require the activity of inflammasome-associated caspases (36). Indeed, we have observed increased CMO neutrophil responses to a typical inflammasome stimulator silica, which was also used in the previous studies (35, 36). Moreover, we also observed enhanced responses to FcR cross-linking, and to some extent also to TLR stimulation by LPS. This suggests that PSTPIP2 has relatively broad effects on neutrophil sensitivity to various stimuli, and that it is likely that other receptors and pathways that have not been tested yet are influenced by the absence of PSTPIP2.

Which of the receptors regulated by PSTPIP2 are responsible for disease initiation in vivo remains unclear. One possibility is that a receptor for environmental silica or other related compounds triggers the disease in living animals. Our data, as well as previous reports, show an exaggerated neutrophil response to silica treatment. However, to our knowledge, the silica receptor on granulocytes has not been identified yet, and so how silica particles initiate phagocytosis and signaling remains unclear. Fc receptors are also good candidates for triggering the disease, because they not only recognize Abs but they also bind pentraxins and pentraxin-opsonized particles (58). Pentraxins, such as C-reactive protein and serum amyloid P, are a family of acute-phase proteins involved in the recognition and opsonization of bacteria, and could well represent a link described by Lukens et al. (36) between altered bacterial microflora in the gut and inflammatory disease development in CMO mice. Moreover, FcRs use a relatively universal ITAM-dependent signaling pathway, which is also used by a number of other innate immune receptors (e.g., the C-type lectin family of pattern recognition receptors and the TREM family receptors), as well as integrins (59), and our results thus imply that signaling by these receptors will also potentially be affected. Clearly, additional research is needed to address all these possibilities, but at present our data suggest that pathways downstream of multiple receptors are affected by PSTPIP2 deficiency and, in fact, they all may contribute in concert to the CMO disease development. Our data provide evidence that SHIP1 and Csk are part of the PSTPIP2-dependent inhibitory network that regulates these pathways and prevents the development of autoinflammatory disease. Deciphering the mechanisms that govern the assembly and activity of this network will help us to understand the cause of autoinflammatory diseases, including chronic recurrent multifocal osteomyelitis and other related disorders, and will facilitate the development of successful treatments.

Acknowledgments

We thank Dr. Andre Veillette for providing Abs to SHIP1 and PEST-PTPs, Dr. Mark Kamps for DNA vector encoding ER-HoxB8, and Zdenek Cimburek for technical assistance.

Disclosures

The authors have no financial conflicts of interest.

References

1. Leslie, N. R., M. J. Dixon, M. Schenning, A. Gray, and I. H. Batty. 2012. Distinct inactivation of PI3K signalling by PTEN and 5-phosphatases. *Adv. Biol. Regul.* 52: 205–213.
2. Okkenhaug, K. 2013. Signaling by the phosphoinositide 3-kinase family in immune cells. *Annu. Rev. Immunol.* 31: 675–704.
3. Liu, Q., T. Sasaki, I. Kozieradzki, A. Wakeham, A. Itie, D. J. Dumont, and J. M. Penninger. 1999. SHIP is a negative regulator of growth factor receptor-mediated PKB/Akt activation and myeloid cell survival. *Genes Dev.* 13: 786–791.
4. Nishio, M., K. Watanabe, J. Sasaki, C. Taya, S. Takasuga, R. Iizuka, T. Balla, M. Yamazaki, H. Watanabe, R. Itoh, et al. 2007. Control of cell polarity and motility by the PtdIns(3,4,5)P3 phosphatase SHIP1. *Nat. Cell Biol.* 9: 36–44.
5. Condé, C., G. Gloire, and J. Piette. 2011. Enzymatic and non-enzymatic activities of SHIP-1 in signal transduction and cancer. *Biochem. Pharmacol.* 82: 1320–1334.
6. Lowell, C. A. 2011. Src-family and Syk kinases in activating and inhibitory pathways in innate immune cells: signaling cross talk. *Cold Spring Harb. Perspect. Biol.* 3: 3.

7. Nada, S., M. Okada, A. MacAuley, J. A. Cooper, and H. Nakagawa. 1991. Cloning of a complementary DNA for a protein-tyrosine kinase that specifically phosphorylates a negative regulatory site of p60c-src. *Nature* 351: 69–72.
8. Bergman, M., T. Mustelin, C. Oetken, J. Partanen, N. A. Flint, K. E. Amrein, M. Autero, P. Burn, and K. Alitalo. 1992. The human p50csk tyrosine kinase phosphorylates p56lck at Tyr-505 and down regulates its catalytic activity. *EMBO J.* 11: 2919–2924.
9. Sicheri, F., and J. Kuriyan. 1997. Structures of Src-family tyrosine kinases. *Curr. Opin. Struct. Biol.* 7: 777–785.
10. Brdicka, T., D. Pavlistová, A. Leo, E. Bruyns, V. Korínek, P. Angelisová, J. Scherer, A. Shevchenko, I. Hilgert, J. Cerný, et al. 2000. Phosphoprotein associated with glycosphingolipid-enriched microdomains (PAG), a novel ubiquitously expressed transmembrane adaptor protein, binds the protein tyrosine kinase csk and is involved in regulation of T cell activation. *J. Exp. Med.* 191: 1591–1604.
11. Takeuchi, S., Y. Takayama, A. Ogawa, K. Tamura, and M. Okada. 2000. Transmembrane phosphoprotein Cbp positively regulates the activity of the carboxyl-terminal Src kinase, Csk. *J. Biol. Chem.* 275: 29183–29186.
12. Brdicková, N., T. Brdicka, P. Angelisová, O. Horváth, J. Spicka, I. Hilgert, J. Paces, L. Simeoni, S. Kliche, C. Merten, et al. 2003. LIME: a new membrane Raft-associated adaptor protein involved in CD4 and CD8 coreceptor signaling. *J. Exp. Med.* 198: 1453–1462.
13. Draber, P., I. Vonkova, O. Stepanek, M. Hrdinka, M. Kucova, T. Skopcova, P. Otahal, P. Angelisova, V. Horejsi, M. Yeung, et al. 2011. SCIMP, a transmembrane adaptor protein involved in major histocompatibility complex class II signaling. *Mol. Cell. Biol.* 31: 4550–4562.
14. McNeill, L., R. J. Salmond, J. C. Cooper, C. K. Carret, R. L. Cassady-Cain, M. Roche-Molina, P. Tandon, N. Holmes, and D. R. Alexander. 2007. The differential regulation of Lck kinase phosphorylation sites by CD45 is critical for T cell receptor signaling responses. *Immunity* 27: 425–437.
15. Stepanek, O., T. Kalina, P. Draber, T. Skopcova, K. Svojgr, P. Angelisova, V. Horejsi, A. Weiss, and T. Brdicka. 2011. Regulation of Src family kinases involved in T cell receptor signaling by protein-tyrosine phosphatase CD148. *J. Biol. Chem.* 286: 22101–22112.
16. Zikherman, J., C. Jenne, S. Watson, K. Doan, W. Raschke, C. C. Goodnow, and A. Weiss. 2010. CD45-Csk phosphatase-kinase titration uncouples basal and inducible T cell receptor signaling during thymic development. *Immunity* 32: 342–354.
17. Lorenz, U., K. S. Ravichandran, S. J. Burakoff, and B. G. Neel. 1996. Lack of SHPTP1 results in src-family kinase hyperactivation and thymocyte hyperresponsiveness. *Proc. Natl. Acad. Sci. USA* 93: 9624–9629.
18. Cloutier, J. F., and A. Veillette. 1996. Association of inhibitory tyrosine protein kinase p50csk with protein tyrosine phosphatase PEP in T cells and other hemopoietic cells. *EMBO J.* 15: 4909–4918.
19. Cloutier, J. F., and A. Veillette. 1999. Cooperative inhibition of T-cell antigen receptor signaling by a complex between a kinase and a phosphatase. *J. Exp. Med.* 189: 111–121.
20. Veillette, A., I. Rhee, C. M. Souza, and D. Davidson. 2009. PEST family phosphatases in immunity, autoimmunity, and autoinflammatory disorders. *Immunol. Rev.* 228: 312–324.
21. Davidson, D., J. F. Cloutier, A. Gregorieff, and A. Veillette. 1997. Inhibitory tyrosine protein kinase p50csk is associated with protein-tyrosine phosphatase PTP-PEST in hemopoietic and non-hemopoietic cells. *J. Biol. Chem.* 272: 23455–23462.
22. Wang, B., S. Lemay, S. Tsai, and A. Veillette. 2001. SH2 domain-mediated interaction of inhibitory protein tyrosine kinase Csk with protein tyrosine phosphatase-HSCF. *Mol. Cell. Biol.* 21: 1077–1088.
23. Spencer, S., D. Dowbenko, J. Cheng, W. Li, J. Brush, S. Utzig, V. Simanis, and L. A. Lasky. 1997. PSTPIP: a tyrosine phosphorylated cleavage furrow-associated protein that is a substrate for a PEST tyrosine phosphatase. *J. Cell Biol.* 138: 845–860.
24. Wu, Y., D. Dowbenko, and L. A. Lasky. 1998. PSTPIP 2, a second tyrosine phosphorylated, cytoskeletal-associated protein that binds a PEST-type protein-tyrosine phosphatase. *J. Biol. Chem.* 273: 30487–30496.
25. Wise, C. A., J. D. Gillum, C. E. Seidman, N. M. Lindor, R. Veile, S. Bashiardes, and M. Lovett. 2002. Mutations in CD2BP1 disrupt binding to PTP PEST and are responsible for PAPA syndrome, an autoinflammatory disorder. *Hum. Mol. Genet.* 11: 961–969.
26. Ferguson, P. J., X. Bing, M. A. Vasef, L. A. Ochoa, A. Mahgoub, T. J. Waldschmidt, L. T. Tygrett, A. J. Schlueter, and H. El-Shanti. 2006. A missense mutation in pstpip2 is associated with the murine autoinflammatory disorder chronic multifocal osteomyelitis. *Bone* 38: 41–47.
27. Grosse, J., V. Chitu, A. Marquardt, P. Hanke, C. Schmittwolf, L. Zeitlmann, P. Schropp, B. Barth, P. Yu, R. Paffenholz, et al. 2006. Mutation of mouse Mayp/Pstpip2 causes a macrophage autoinflammatory disease. *Blood* 107: 3350–3358.
28. Masters, S. L., A. Simon, I. Aksentijevich, and D. L. Kastner. 2009. Horror autoinflammaticus: the molecular pathophysiology of autoinflammatory disease (*). *Annu. Rev. Immunol.* 27: 621–668.
29. Byrd, L., M. Grossmann, M. Potter, and G. L. Shen-Ong. 1991. Chronic multifocal osteomyelitis, a new recessive mutation on chromosome 18 of the mouse. *Genomics* 11: 794–798.
30. Roberts-Galbraith, R. H., and K. L. Gould. 2010. Setting the F-BAR: functions and regulation of the F-BAR protein family. *Cell Cycle* 9: 4091–4097.
31. Tsujita, K., S. Suetsugu, N. Sasaki, M. Furutani, T. Oikawa, and T. Takenawa. 2006. Coordination between the actin cytoskeleton and membrane deformation by a novel membrane tubulation domain of PCH proteins is involved in endocytosis. *J. Cell Biol.* 172: 269–279.
32. Chitu, V., V. Nacu, J. F. Charles, W. M. Henne, H. T. McMahon, S. Nandi, H. Ketchum, R. Harris, M. C. Nakamura, and E. R. Stanley. 2012. PSTPIP2 deficiency in mice causes osteopenia and increased differentiation of multipotent myeloid precursors into osteoclasts. *Blood* 120: 3126–3135.
33. Yeung, Y. G., S. Soldera, and E. R. Stanley. 1998. A novel macrophage actin-associated protein (MAYP) is tyrosine-phosphorylated following colony stimulating factor-1 stimulation. *J. Biol. Chem.* 273: 30638–30642.
34. Chitu, V., P. J. Ferguson, R. de Bruijn, A. J. Schlueter, L. A. Ochoa, T. J. Waldschmidt, Y. G. Yeung, and E. R. Stanley. 2009. Primed innate immunity leads to autoinflammatory disease in PSTPIP2-deficient cmo mice. *Blood* 114: 2497–2505.
35. Cassel, S. L., J. R. Janczy, X. Bing, S. P. Wilson, A. K. Olivier, J. E. Otero, Y. Iwakura, D. M. Shayakhmetov, A. G. Bassuk, Y. Abu-Amer, et al. 2014. Inflammasome-independent IL-1β mediates autoinflammatory disease in Pstpip2-deficient mice. *Proc. Natl. Acad. Sci. USA* 111: 1072–1077.
36. Lukens, J. R., P. Gurung, P. Vogel, G. R. Johnson, R. A. Carter, D. J. McGoldrick, S. R. Bandi, C. R. Calabrese, L. Vande Walle, M. Lamkanfi, and T.-D. Kanneganti. 2014. Dietary modulation of the microbiome affects autoinflammatory disease. *Nature* 516: 246–249.
37. Lukens, J. R., J. M. Gross, C. Calabrese, Y. Iwakura, M. Lamkanfi, P. Vogel, and T. D. Kanneganti. 2014. Critical role for inflammasome-independent IL-1β production in osteomyelitis. *Proc. Natl. Acad. Sci. USA* 111: 1066–1071.
38. Liu, L., Q. Wen, R. Gong, L. Gilles, M. J. Stankiewicz, W. Li, M. Guo, L. Li, X. Sun, W. Li, et al. 2014. PSTPIP2 dysregulation contributes to aberrant terminal differentiation in GATA-1-deficient megakaryocytes by activating LYN. *Cell Death Dis.* 5: e988.
39. Wang, G. G., K. R. Calvo, M. P. Pasillas, D. B. Sykes, H. Häcker, and M. P. Kamps. 2006. Quantitative production of macrophages or neutrophils ex vivo using conditional Hoxb8. *Nat. Methods* 3: 287–293.
40. Otáhal, P., S. Pata, P. Angelisová, V. Hořejší, and T. Brdička. 2011. The effects of membrane compartmentalization of csk on TCR signaling. Biochim. Biophys. Acta. 1813: 367–376.
41. Netea, M. G., A. Simon, F. van de Veerdonk, B. J. Kullberg, J. W. Van der Meer, and L. A. Joosten. 2010. IL-1beta processing in host defense: beyond the inflammasomes. *PLoS Pathog.* 6: e1000661.
42. Horn, S., J. Meyer, J. Heukeshoven, B. Fehse, C. Schulze, S. Li, J. Frey, S. Poll, C. Stocking, and M. Jücker. 2001. The inositol 5-phosphatase SHIP is expressed as 145 and 135 kDa proteins in blood and bone marrow cells in vivo, whereas carboxyl-truncated forms of SHIP are generated by proteolytic cleavage in vitro. *Leukemia* 15: 112–120.
43. Hasegawa, K., F. Martin, G. Huang, D. Tumas, L. Diehl, and A. C. Chan. 2004. PEST domain-enriched tyrosine phosphatase (PEP) regulation of effector/memory T cells. *Science* 303: 685–689.
44. Davidson, D., X. Shi, M. C. Zhong, I. Rhee, and A. Veillette. 2010. The phosphatase PTP-PEST promotes secondary T cell responses by dephosphorylating the protein tyrosine kinase Pyk2. *Immunity* 33: 167–180.
45. Rhee, I., D. Davidson, C. M. Souza, J. Vacher, and A. Veillette. 2013. Macrophage fusion is controlled by the cytoplasmic protein tyrosine phosphatase PTP-PEST/PTPN12. *Mol. Cell. Biol.* 33: 2458–2469.
46. Rhee, I., M. C. Zhong, B. Reizis, C. Cheong, and A. Veillette. 2014. Control of dendritic cell migration, T cell-dependent immunity, and autoimmunity by protein tyrosine phosphatase PTPN12 expressed in dendritic cells. *Mol. Cell. Biol.* 34: 888–899.
47. Shoham, N. G., M. Centola, E. Mansfield, K. M. Hull, G. Wood, C. A. Wise, and D. L. Kastner. 2003. Pyrin binds the PSTPIP1/CD2BP1 protein, defining familial Mediterranean fever and PAPA syndrome as disorders in the same pathway. *Proc. Natl. Acad. Sci. USA* 100: 13501–13506.
48. Sweeney, M. C., A. S. Wavreille, J. Park, J. P. Butchar, S. Tridandapani, and D. Pei. 2005. Decoding protein-protein interactions through combinatorial chemistry: sequence specificity of SHP-1, SHP-2, and SHIP SH2 domains. *Biochemistry* 44: 14932–14947.
49. Zhang, Y., A. S. Wavreille, A. R. Kunys, and D. Pei. 2009. The SH2 domains of inositol polyphosphate 5-phosphatases SHIP1 and SHIP2 have similar ligand specificity but different binding kinetics. *Biochemistry* 48: 11075–11083.
50. Tridandapani, S., T. Kelley, M. Pradhan, D. Cooney, L. B. Justement, and K. M. Coggeshall. 1997. Recruitment and phosphorylation of SH2-containing inositol phosphatase and Shc to the B-cell Fc gamma immunoreceptor tyrosine-based inhibition motif peptide motif. *Mol. Cell. Biol.* 17: 4305–4311.
51. Tatárová, Z., J. Brábek, D. Rösel, and M. Novotný. 2012. SH3 domain tyrosine phosphorylation–sites, role and evolution. *PLoS One* 7: e36310.
52. Cao, L., K. Yu, C. Banh, V. Nguyen, A. Ritz, B. J. Raphael, Y. Kawakami, T. Kawakami, and A. R. Salomon. 2007. Quantitative time-resolved phosphoproteomic analysis of mast cell signaling. *J. Immunol.* 179: 5864–5876.
53. Helgason, C. D., J. E. Damen, P. Rosten, R. Grewal, P. Sorensen, S. M. Chappel, A. Borowski, F. Jirik, G. Krystal, and R. K. Humphries. 1998. Targeted disruption of SHIP leads to hemopoietic perturbations, lung pathology, and a shortened life span. *Genes Dev.* 12: 1610–1620.
54. Nguyen, N. Y., M. J. Maxwell, L. M. Ooms, E. M. Davies, A. A. Hilton, J. E. Collinge, D. J. Hilton, B. T. Kile, C. A. Mitchell, M. L. Hibbs, et al. 2011. An ENU-induced mouse mutant of SHIP1 reveals a critical role of the stem cell isoform for suppression of macrophage activation. *Blood* 117: 5362–5371.
55. Kerr, W. G., M. Y. Park, M. Maubert, and R. W. Engelman. 2011. SHIP deficiency causes Crohn's disease-like ileitis. *Gut* 60: 177–188.
56. Zhou, P., H. Kitaura, S. L. Teitelbaum, G. Krystal, F. P. Ross, and S. Takeshita. 2006. SHIP1 negatively regulates proliferation of osteoclast precursors via Akt-dependent alterations in D-type cyclins and p27. *J. Immunol.* 177: 8777–8784.
57. Sly, L. M., M. J. Rauh, J. Kalesnikoff, C. H. Song, and G. Krystal. 2004. LPS-induced upregulation of SHIP is essential for endotoxin tolerance. *Immunity* 21: 227–239.
58. Lu, J., K. D. Marjon, C. Mold, T. W. Du Clos, and P. D. Sun. 2012. Pentraxins and Fc receptors. *Immunol. Rev.* 250: 230–238.
59. Futosi, K., S. Fodor, and A. Mócsai. 2013. Neutrophil cell surface receptors and their intracellular signal transduction pathways. *Int. Immunopharmacol.* 17: 638–650.

Supplemental figures and tables

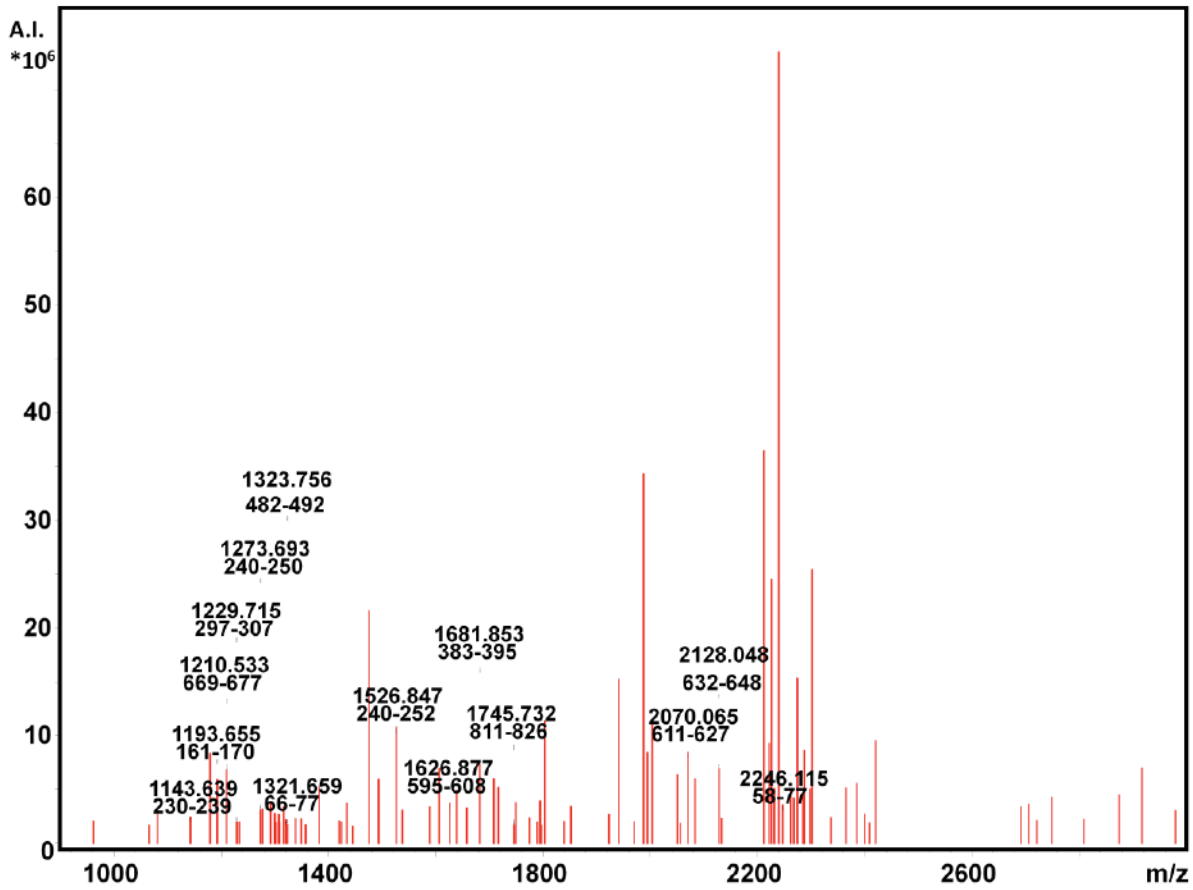

Supplemental figure 1. MALDI FT-ICR MS spectrum of Proline-serine-threonine phosphatase-interacting protein 2 tryptic peptides. The position in the protein sequence and experimental mass are shown

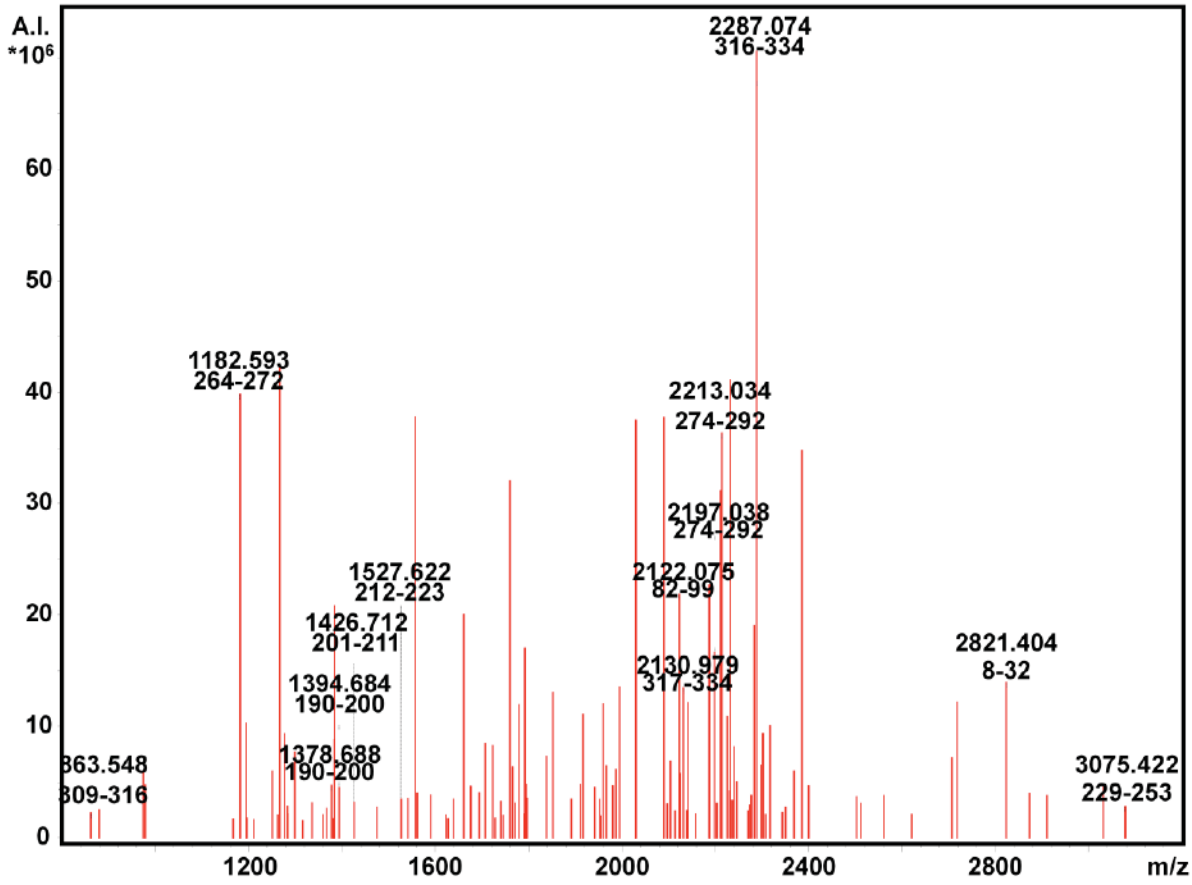

Supplemental figure 2. MALDI FT-ICR MS spectrum of Phosphatidylinositol 3,4,5-trisphosphate 5-phosphatase 1 tryptic peptides. The position in the protein sequence and experimental mass are shown.

Mutation	expression	Csk binding	PEST-PTPs binding	SHIP1 binding	Tyr-P
Y21F + W232A	expressed	no effect			
Y52F + W232A	expressed	no effect			
Y144F + W232A	expressed	no effect			
Y191F + W232A	expressed	no effect			
Y249F	expressed	no effect	reduced		
Y249F + W232A	expressed	no effect	abolished		
Y249,267F + W232A	expressed	no effect			
Y284F	expressed	no effect			
Y284,288F + W232A	expressed	no effect			
Y323,329,333F	expressed	no effect		abolished	abolished
W232A	expressed	reduced	abolished	slightly increased	
P278A + P279,281G	not expressed				
Deletion 278-281	not expressed				
Deletion 166-295	very low expression				
Deletion 296-334	expressed	no effect			abolished
All Y to F	not expressed				

Supplemental table 1. Effecs of PSTPIP2 mutations on PSTPIP2 expression, on PSTPIP2 binding to PEST-PTPs, Csk and SHIP1, and on PSTPIP2 tyrosine phosphorylation. Empty fields = not tested.

Dysregulated ROS production by neutrophil NADPH oxidase promotes bone damage in autoinflammatory osteomyelitis

Jarmila Kralova,[1,2,6] Ales Drobek,[1,3,6] Jan Prochazka,[4,5,6] Frantisek Spoutil,[5] Daniela Glatzova,[1,2] Simon Borna,[1] Jana Pokorna,[1] Tereza Skopcova,[1] Pavla Angelisova,[1] Radislav Sedlacek,[4,5] and Tomas Brdicka[1,7,*]

[1]Laboratory of Leukocyte Signalling, Institute of Molecular Genetics of the ASCR, 14220, Prague, Czech Republic

[2]Faculty of Science, Charles University, 12843, Prague, Czech Republic

[3]Laboratory of Adaptive Immunity, Institute of Molecular Genetics of the ASCR, 14220, Prague, Czech Republic

[4]Laboratory of Transgenic Models of Diseases, Institute of Molecular Genetics of the ASCR, 25242, Vestec, Czech Republic

[5]Czech Centre for Phenogenomics, Institute of Molecular Genetics of the ASCR, 25242, Vestec, Czech Republic

[6]These authors contributed equally to this work

[7]Lead contact

*Correspondence: tomas.brdicka@img.cas.cz

Summary

Autoinflammatory diseases are characterized by dysregulation of the innate immune system leading to spontaneous inflammation. Some of these diseases result in serious inflammatory bone damage. *Pstpip2*^{cmo} mouse strain is a well-characterized model of this class of disorders. Due to the mutation in the gene coding for adaptor protein PSTPIP2 these animals suffer from autoinflammatory chronic multifocal osteomyelitis similar to several human syndromes. Current evidence suggests that it is driven mainly by hyperproduction of IL-1β by neutrophil granulocytes. Here we show that neutrophils from these mice display highly elevated NADPH oxidase-dependent ROS production in response to a wide range of stimuli. Our analysis of NADPH oxidase-deficient *Pstpip2*^{cmo} mice shows that while IL-1β levels are unaffected and the autoinflammatory process is initiated with similar kinetics in these mice, bone damage is almost completely alleviated, suggesting that dysregulated NADPH oxidase activity is a critical part of the mechanism targeting autoinflammation to the bone.

Keywords

Inflammation, Reactive oxygen species, Inflammatory bone damage, Chronic multifocal osteomyelitis, PSTPIP2, NADPH oxidase, gp91phox

Introduction

Autoinflammatory diseases represent a distinct class of disorders of the innate immune system. They are characterized by a pathological inflammation that typically arises spontaneously without detectable extrinsic cause and in the absence of autoantibodies or auto-reactive T cells. The symptoms are rather diverse. The most characteristic include periodic fever attacks, skin rashes, arthralgia, myalgia, abdominal pain, arthritis, osteomyelitis, and other signs of systemic or organ specific inflammation (de Jesus et al., 2015; Manthiram et al., 2017; Masters et al., 2009). A number of these diseases are heritable syndromes caused by mutations in single genes. A significant proportion of these mutations affects inflammasomes or other components of the IL-1β pathway (de Jesus et al., 2015; Manthiram et al., 2017). However, the role of cellular stress is also being increasingly appreciated and some of the genetic defects behind autoinflammation are thought to act via triggering an inflammatory response to cellular stress or perturbations in cell homeostasis (de Jesus et al., 2015; Liston and Masters, 2017; Park et al., 2012; Varga et al., 2015).

The inflammatory response to stress and IL-1β pathway are interconnected since multiple stress factors can trigger inflammasome activation. A key role is played mainly by NLRP3 inflammasome, which is activated by aberrant ion fluxes, lysosomal damage by crystalline matter, such as silica or monosodium urate crystals, mitochondrial damage, presence of reactive oxygen species (ROS), as well as various PAMPs and DAMPs (Broz and Dixit, 2016; Gong et al., 2018; Hughes and O'Neill, 2018; Lawlor and Vince, 2014; Rubartelli, 2012). Several unifying mechanisms enabling recognition of such a variety of stress agents by a single type of inflammasome have been suggested, but none of them has yet gained universal acceptance (Broz and Dixit, 2016; Gong et al., 2018; Hughes and O'Neill, 2018; Lawlor and Vince, 2014). Production of ROS represents one such a mechanism that could connect cellular stress to NLRP3 inflammasome activation (for review see (Abais et al., 2015; Rubartelli, 2012)). In most of the cell types, there appear to be at least two main sources of ROS, NADPH oxidases and mitochondria (Holmström and Finkel, 2014). In phagocytes, NADPH oxidase is activated downstream of PAMPs, DAMPs and other pro-inflammatory stimuli and its products are toxic to microorganisms. Various NADPH oxidases are also part of a broad array of signaling pathways in multiple cell types (Brandes et al., 2014; Sumimoto, 2008). Mitochondrial ROS are produced mainly as a result of respiratory chain activity and their generation can be enhanced by stress or mitochondrial damage (Brookes et al., 2004; West et al., 2011; Zhou et al., 2011).

Several studies have shown increased production of ROS in monocytes from autoinflammatory disease patients (Borghini et al., 2011; Bulua et al., 2011; Carta et al., 2015; Carta et al., 2012; Omenetti et al., 2014; Tassi et al., 2010; van der Burgh et al., 2014). In some of these works it has been proposed that these ROS are of mitochondrial origin (Bulua et al., 2011; Carta et al., 2012), but there are only limited options how to study this aspect in patients.

The effects of increased ROS production, whether of mitochondrial or NADPH oxidase origin, on the development and/or severity of autoinflammatory diseases is currently unknown.

There are relatively few mouse models of autoinflammatory diseases. One of the best characterized is *Pstpip2*^{cmo} mouse strain which spontaneously develops severe bone and soft tissue inflammation mainly in hind paws and tail. In several aspects, the disease resembles a human condition known as chronic recurrent multifocal osteomyelitis (CRMO) and was thus termed chronic multifocal osteomyelitis (CMO). From there the strain derives its name *Pstpip2*^{cmo} (Byrd et al., 1991). The disease is caused by a point mutation in the gene coding for the adaptor protein PSTPIP2 (Ferguson et al., 2006). As a result, no PSTPIP2 is detectable in these mice at the protein level (Chitu et al., 2009). The mechanism of how PSTPIP2 deficiency leads to CMO disease is only partially understood. It binds several inhibitory molecules, including PEST-family protein tyrosine phosphatases, phosphoinositide phosphatase SHIP1 and inhibitory kinase Csk, which likely mediate its negative regulatory effect on the inflammatory response (Drobek et al., 2015; Wu et al., 1998). In addition, it has been reported that osteomyelitis in *Pstpip2*^{cmo} mice is completely dependent on excessive IL-1β production by neutrophilic granulocytes (Cassel et al., 2014; Lukens et al., 2014a; Lukens et al., 2014b). Genetic studies suggest a combined involvement of the NLRP3 inflammasome and a poorly characterized mechanism dependent on caspase-8. A relatively limited role of neutrophil proteases has also been demonstrated (Gurung et al., 2016; Lukens et al., 2014b). The involvement of NLRP3 inflammasome suggests that cellular stress and ROS might be involved in CMO disease pathology, especially, when we consider the fact that neutrophils are very potent producers of NADPH-oxidase-derived ROS. Here we show that in *Pstpip2*^{cmo} neutrophils, this process is dysregulated and these cells produce substantially increased amounts of ROS in response to variety of stimuli. Strikingly, the dysregulated ROS production by these neutrophils does not have a strong effect on IL-1β production, and soft tissue inflammation, but rather on the bone inflammation and subsequent bone damage, suggesting that the role of NADPH-oxidase-derived ROS is not in triggering the CMO, but rather in directing the damage accompanying this disease to the bones.

Results

Pstpip2^{cmo} neutrophils produce substantially more ROS in response to inflammasome activator silica than wild-type neutrophils.

Disease development in *Pstpip2*^{cmo} mice is, in part, dependent on NLRP3 inflammasome (Gurung et al., 2016). Since ROS are involved in the NLRP3 inflammasome regulation, we tested if their production was dysregulated in *Pstpip2*^{cmo} bone marrow (BM) cells. We isolated these cells from wild-type C57Bl/6 (WT) and *Pstpip2*^{cmo} mice (backcrossed to the same genetic background) and stimulated these cells with silica particles, a well established activator of NLRP3 inflammasome (Cassel et al., 2008) employed in previous studies of *Pstpip2*^{cmo} mice (Cassel et al., 2014; Drobek et al., 2015; Lukens et al., 2014b). Strikingly, this stimulation led to a substantially stronger ROS response in *Pstpip2*^{cmo} cells, when compared to their WT counterparts (Figure 1A). Since ROS production is predominantly characteristic of neutrophils, which form a large fraction of bone marrow leukocytes (Figure 1B), we have isolated these cells for further testing. Silica stimulation of untouched neutrophils, isolated by negative selection, led to even higher production of ROS when compared to full bone marrow. Moreover, the difference between WT and *Pstpip2*^{cmo} cells was still preserved (Figure 1C). In our experiments, negatively selected neutrophils were typically more than 90% pure. However, large fraction of the contaminating cells were monocytes. Since these cells are also known to respond by ROS production to a variety of stimuli we have analyzed ROS generation by purified monocytes. In order to determine the impact of these cells on our results we have adjusted the quantity of monocytes to 10% of the neutrophil numbers, which is similar to the amount of monocytes contaminating our neutrophil samples prepared by negative selection. We compared the response of these monocytes with the ROS production by neutrophils isolated by positive selection on Ly6G. This purification resulted in virtually pure (more than 99%) neutrophils. The response of purified monocytes was almost two orders of magnitude lower than that of purified neutrophils, and there was no significant difference between WT and *Pstpip2*^{cmo} cells (Figure 1D). These data demonstrated that in the neutrophil samples prepared by negative selection, the monocyte contribution to the measured ROS production is negligible. They also lead to the conclusion that even in non-separated bone marrow the vast majority of ROS originated from neutrophils, and that neutrophils are responsible for enhanced ROS production by *Pstpip2*^{cmo} bone marrow cells.

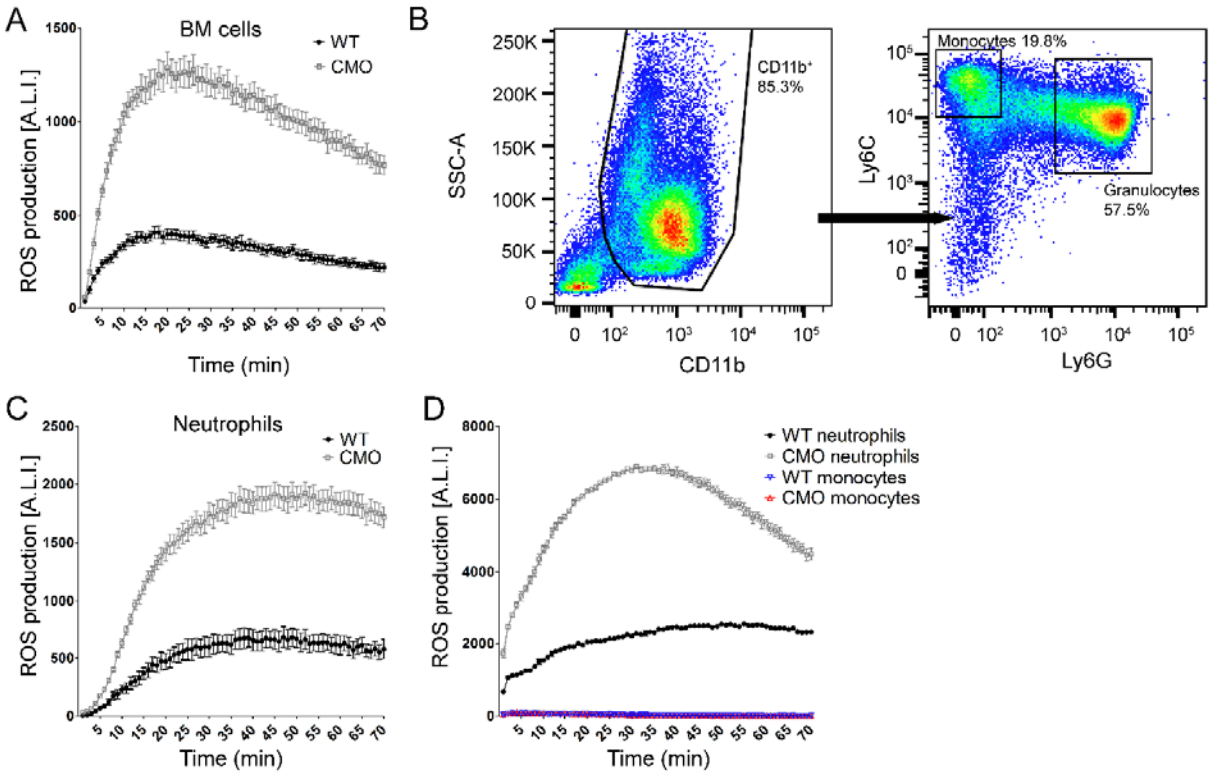

Figure 1. *Pstpip2^{cmo}* neutrophils produce higher amounts of ROS.

(A) ROS production by *Pstpip2^{cmo}* (CMO) and wild-type (WT) bone marrow cells. BM cells (10^6 cells per well) were treated in a 96-well plate with silica particles in the presence of 100 µM luminol. ROS-induced luminescence was measured in 1 min intervals.

(B) Representative flow cytometry dot plot showing percentages of monocytes and neutrophils in *Pstpip2^{cmo}* BM. N > 5.

(C) Similar experiment as in (A) performed on neutrophils purified by negative selection (10^6 cells per well)

(D) Similar experiment as in (A) performed on neutrophils purified by positive selection (10^6 cells per well). The response is compared to ROS production by FACS-sorted ($Ly6C^+$, $Ly6G^-$) monocytes (1×10^5 per well). N = 3.

Representative plots are shown. In panels A, C, D, individual points and error bars represent mean ± SEM values obtained from 2-8 technical replicates. Quantification based on multiple biological replicates is shown in Figure 2 below. A.L.I. stands for Arbitrary Luminescence Intensity.

Higher ROS production by *Pstpip2*^{cmo} neutrophils is observed across a range of conditions

To find out how universal the ROS overproduction in *Pstpip2*^{cmo} neutrophils is, we treated either BM cells or purified neutrophils with silica, PMA, live *E.coli* bacteria, heat-aggregated mouse IgG (as a model of immunocomplexes), TNF-α, LPS or fMLP. All these experiments demonstrated dysregulated ROS production in *Pstpip2*^{cmo} BM cells (Figure 2A-D) and purified neutrophils (Figure 2B, C, E). The same dysregulation was also observed in the bone marrow cells with *Pstpip2*^{cmo} mutation on Balb/c genetic background (Figure S1). These results show that PSTPIP2 deficiency renders neutrophils more sensitive and prone to produce more ROS than WT cells. Interestingly, unstimulated BM cells from *Pstpip2*^{cmo} mice produced low but detectable levels of ROS even in the absence of any stimulus. This constitutive production has not been observed in WT BM (Figure 2A, F).

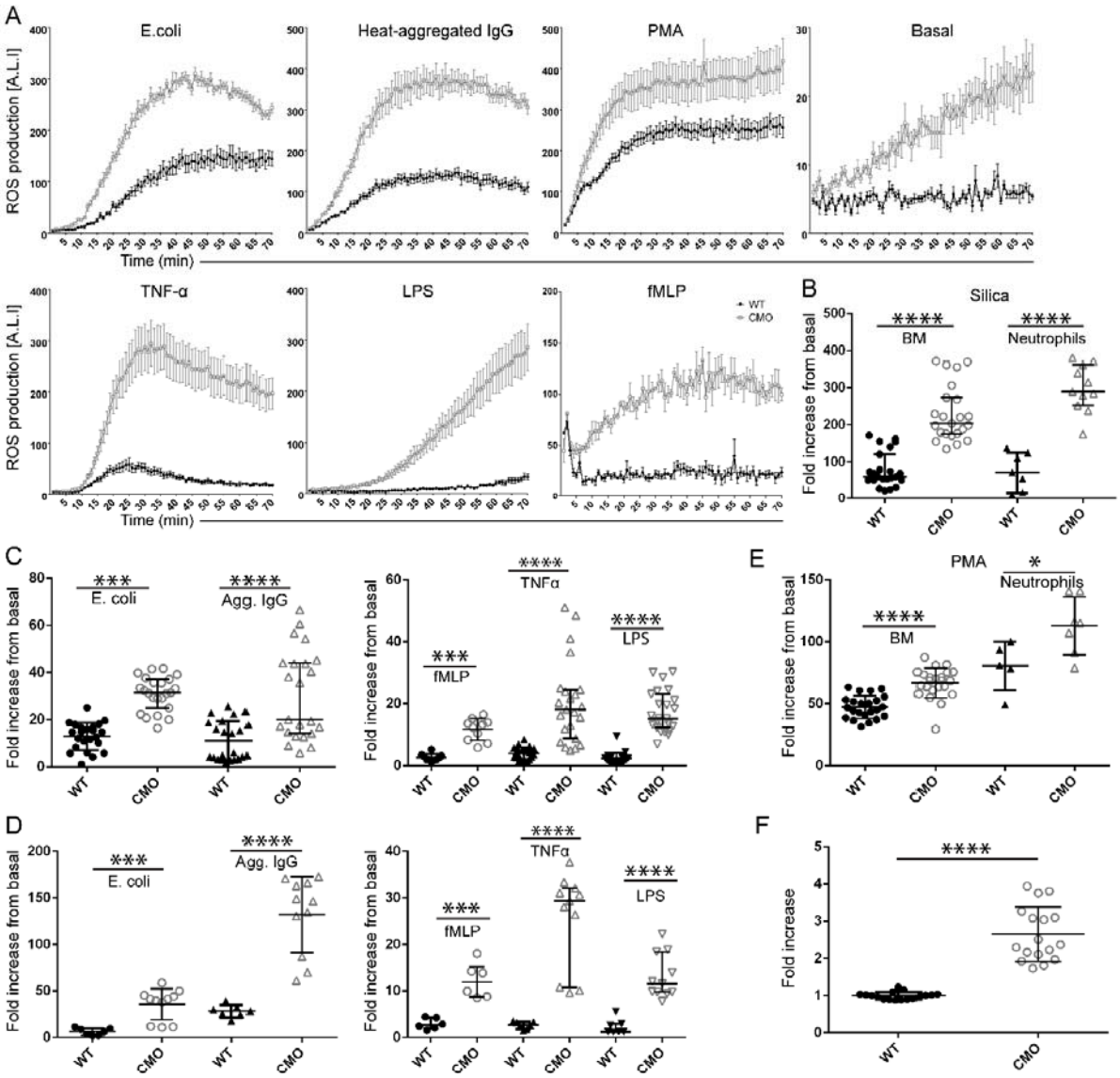

Figure 2. Increased ROS production by *Pstpip2^{cmo}* neutrophils is triggered by a variety of stimuli.

(A) ROS production by *Pstpip2^{cmo}* (CMO) and wild-type (WT) bone marrow cells treated with indicated agents (E.coli culture OD600 = 0.8, diluted 1:5; 300 µg/ml heat-agregated murine IgG (Agg. IgG); 100 ng/ml PMA; 10 ng/ml TNFα; 100 ng/ml LPS; 1 µg/ml fMLP). Graphs from representative experiments are shown with the data depicted as mean ± SEM from 2-3 technical replicates.

(B) Quantification of ROS production by BM cells and neutrophils after silica treatment.

(C) Quantification of ROS production by BM cells treated with live E.coli bacteria (E.coli), mouse aggregated IgG (IC), fMLP, TNFα, and LPS.

(D) Similar analysis as in (C), performed on neutrophils purified by negative selection.

(E) Quantification of ROS production by BM cells and neutrophils after treatment with PMA.

(F) Quantification of basal ROS production by non-stimulated BM cells.

Fold increase (B-E) was calculated as a ratio between maximum response after stimulation and basal ROS production of unstimulated cells in each experiment. In (F), fold increase is calculated as a ratio of maximum response and mean ROS production by WT cells. In (B-F), data points represent results from biological replicates, each of them mean of 2-3 technical replicates. See also Figure S1.

Excessive ROS production by *Pstpip2^{cmo}* neutrophils is not a consequence of ongoing inflammation

Higher ROS production under resting conditions and after activation with a wide range of stimuli demonstrates general dysregulation of pathways leading to ROS production in *Pstpip2^{cmo}* neutrophils. This dysregulation could be cell intrinsic due to PSTPIP2 deficiency or a side effect of ongoing bone inflammation, which could prime bone marrow neutrophils located in the proximity of the inflamed tissue. It has previously been reported that autoinflammation in *Pstpip2^{cmo}* mice is completely dependent on IL-1β and its receptor (Cassel et al., 2014; Lukens et al., 2014a). Signaling through this receptor is critically dependent on MyD88 adaptor protein (Adachi et al., 1998). In order to determine whether the observed overproduction of ROS in *Pstpip2^{cmo}* neutrophils is not just the effect of ongoing inflammation, we crossed *Pstpip2^{cmo}* mice with MyD88-deficient strain to block IL-1β signaling. As expected, *Pstpip2^{cmo}* mice were in the absence of MyD88 completely protected from the disease development as determined by visual inspection (Figure 3A) and X-ray micro computed tomography (X-ray μCT) of hind paws (Figure 3B). MyD88-deficient *Pstpip2^{cmo}* bone marrow cells displayed the same dysregulation in ROS production triggered by a variety of stimuli as *Pstpip2^{cmo}* cells. Treatments with LPS or *E.coli* were the only exceptions where the response was lower in both *Pstpip2^{cmo}/MyD88$^{-/-}$* and *MyD88$^{-/-}$* cells, probably due to the higher dependence of signaling triggered by these activators on the TLR/MyD88 pathway. On the other hand, even in *MyD88*-deficient cells the *cmo* mutation gave rise to a stronger response to these two stimuli when compared to *MyD88* deficient cells without the *cmo* mutation (Figure 3C). These results demonstrate the cell intrinsic dysregulation of NADPH oxidase machinery that is not caused by chronic exposure to the inflammatory environment.

Autoinflammation in *Pstpip2^{cmo}* mice is independent of MyD88 expression in hematopoietic cells

It has been previously reported that alterations in gut microbiota composition play a critical role in autoinflammatory disease development in *Pstpip2^{cmo}* mice leading to the conclusion that response to microbiota alterations by innate immune cells is a part of the disease etiology (Lukens et al., 2014b; Phillips et al., 2016). The TLR/MyD88 pathway is a key component of the microorganism recognition machinery employed by the innate immune system (O'Neill and Bowie, 2007). Having obtained *Pstpip2^{cmo}/MyD88* double-deficient mice, we could test the idea that sensing the gut microbiota by leukocyte TLR/MyD88 pathway could play a role in disease development. To analyze how significant the contribution of TLR/MyD88 signaling on leukocytes to the disease development was, we performed BM transplantation from young asymptomatic *Pstpip2^{cmo}* or *Pstpip2^{cmo}/MyD88$^{-/-}$* donors into lethally irradiated WT recipients. Unexpectedly, we observed complete disease development without any delay in

disease progression, regardless of the donor cell origin (Figure 3D). These data suggest that priming of leukocytes through TLR/MyD88 signaling does not play any major role in CMO development since even *MyD88*-deficient *Pstpip2*^{cmo} hematopoietic cells were fully capable of driving the inflammatory disease in wild-type mice. This result also confirmed the earlier finding that IL-1 receptor on hematopoietic cells is dispensable for CMO development (Gurung et al., 2016).

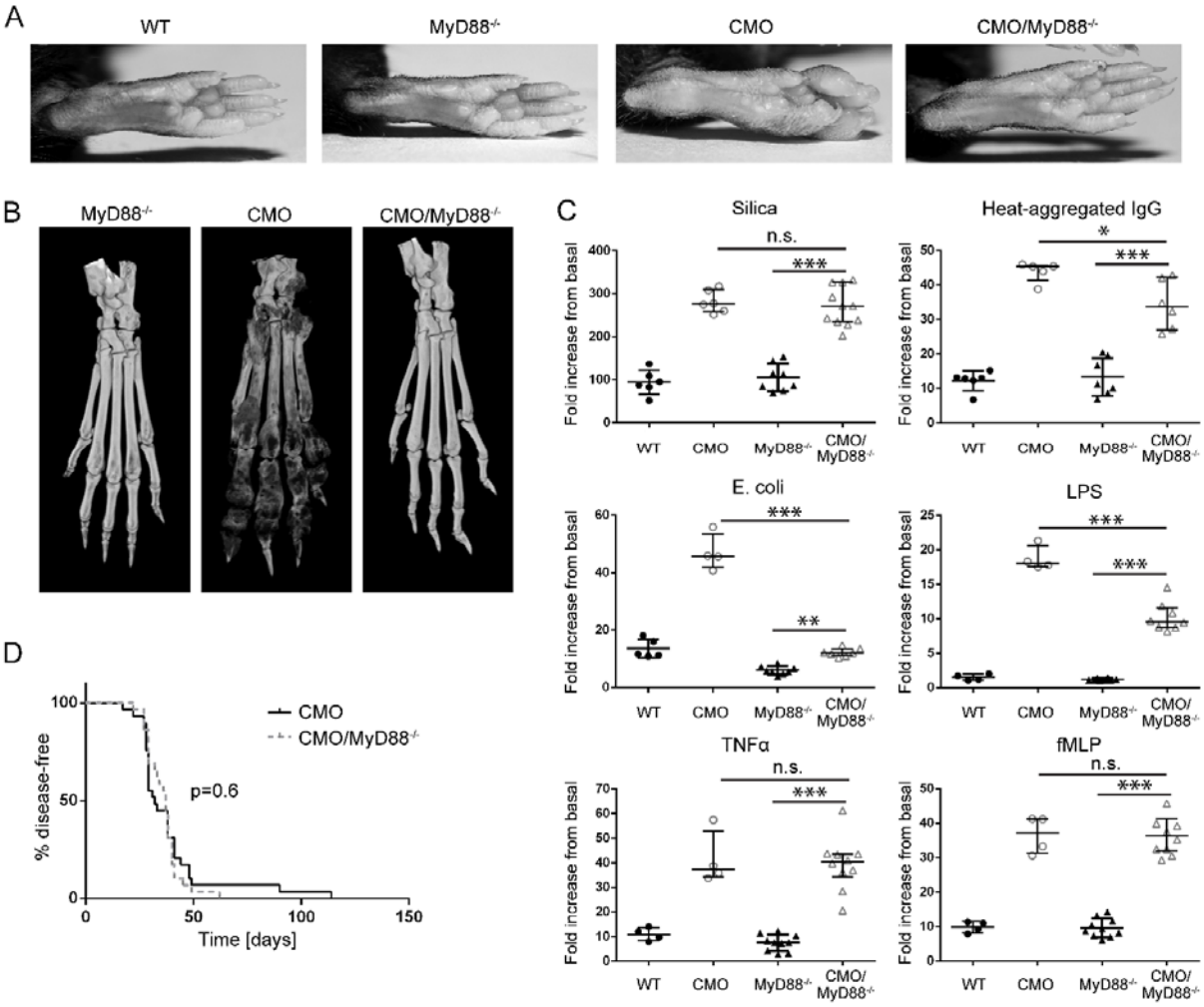

Figure 3. Overproduction of ROS is not triggered by ongoing inflammation

(A) Representative hind paw photographs of 23 - 26 week old WT, *MyD88*$^{-/-}$, *Pstpip2*^{cmo} (CMO) and *Pstpip2*^{cmo}*/MyD88*$^{-/-}$ (CMO/MyD88$^{-/-}$) mice. For *Pstpip2*^{cmo}*/MyD88*$^{-/-}$, 24 animals between 13 and 34 weeks of age were photographed, none of which showed any symptom of CMO disease.

(B) Representative X-ray µCT scans of hind paws from *MyD88*$^{-/-}$, *Pstpip2*^{cmo} and *Pstpip2*^{cmo}*/MyD88*$^{-/-}$ mice, 14 weeks old. N = 5 for *Pstpip2*^{cmo}*/MyD88*$^{-/-}$ and N = 3 for *MyD88*$^{-/-}$

(C) Quantification of ROS production by BM cells isolated from WT, *MyD88*$^{-/-}$, *Pstpip2*^{cmo} and *Pstpip2*^{cmo}*/MyD88*$^{-/-}$ mice and treated with indicated stimuli. Fold increase was calculated as a ratio between maximum response after stimulation and basal ROS production of unstimulated cells in each experiment. Data points represent results from biological replicates (individual mice), each of them mean of 2-3 technical replicates.

(D) BM from *Pstpip2*^{cmo} or *Pstpip2*^{cmo}*/MyD88*$^{-/-}$ mice was transplanted into lethally irradiated CD45.1 wild-type recipients. Development of visible symptoms of disease was evaluated twice a week.

ROS hyperproduction in *Pstpip2*^{cmo} neutrophils is suppressed by PSTPIP2 binding partners and is accompanied by hyperphosphorylation of p47-phox.

To elucidate the mechanism of how of PSTPIP2 suppresses ROS production, we employed conditionally immortalized *Pstpip2*^{cmo} granulocyte progenitors (Wang et al., 2006) we have

established previously (Drobek et al., 2015) and reconstituted these cells with doxycycline-inducible retroviral constructs coding for WT PSTPIP2 and its mutated versions unable to bind PEST-family phosphatases (W232A) and SHIP1 (3YF) (Drobek et al., 2015; Wu et al., 1998). After maturation of these progenitors into neutrophils and induction of PSTPIP2 expression with doxycycline, we treated these cells with silica and measured ROS response. We observed around 50% reduction of ROS response in cells expressing WT PSTPIP2. In contrast, both mutated versions of PSTPIP2 were unable to substantially inhibit silica-induced ROS generation, despite similar expression levels of these constructs (Figures 4A and S2).

To analyze subcellular localization of PSTPIP2 during silica stimulation we isolated bone marrow progenitors from *Pstpip2*^{cmo} mice and transduced these cells with retroviral construct coding for PSTPIP2 fused to EGFP. Next, we transplanted these cells into lethally irradiated mice and after 2 weeks we collected neutrophils expressing PSTPIP2-EGFP for microscopy analysis. In neutrophils, PSTPIP2 showed diffuse distribution throughout the cytoplasm with occasional formation of speckles in a small fraction of cells (Figure 4B, left panel, see an arrowhead). After addition of fluorescently labelled silica particles, neutrophils interacted with these particles and phagocytosed some of them (Figure 4B, right panel, see an arrowhead). However, we did not observe any changes in PSTPIP2 subcellular localization during this process (Figure 4B). This result suggests that large-scale redistribution of PSTPIP2 inside the cells is not part of the mechanism of how PSTPIP2 controls neutrophil activity during the treatment with silica.

In order to identify the dysregulated process leading to ROS overproduction at the biochemical level, we measured the calcium response in WT and *Pstpip2*^{cmo} BM cells. Cells were loaded with Fura Red dye and stimulated with silica particles. We observed the same calcium response in both WT and *Pstpip2*^{cmo} cells (Figure 4C) indicating that proximal signaling steps leading to calcium response are not responsible for increased ROS production in *Pstpip2*^{cmo} cells.

One of the major events further downstream is phosphorylation of NADPH oxidase cytosolic subunits by members of protein kinase C (PKC) family, including phosphorylation of p47phox, which then serves as an assembly hub for building the active NADPH oxidase complex (Brandes et al., 2014). To detect p47phox phosphorylation we isolated phosphoproteins from untreated and silica treated BM cells or purified neutrophils and detected p47phox in the isolated material by immunoblotting. In both *Pstpip2*^{cmo} BM cells and neutrophils we found substantially stronger phosphorylation of p47phox when compared to WT cells (Figure 4D).

In addition to the PKCs, p47-phox can also be phosphorylated by other kinases, such as Erk, which is dysregulated in silica-treated CMO neutrophils (Dang et al., 2006; Drobek et al., 2015). To identify the kinases involved in the observed hyperphosphorylation of p47phox, we treated *Pstpip2^{cmo}* neutrophils either with PKC inhibitor Gö6976 or MEK1/MEK2 inhibitor U0126 prior to activation with silica. Only the treatment with PKC inhibitor led to specific block of p47-phox phospholylation (Figure 4E).

Small G-protein RAC is another critical component of active NADPH oxidase. We have tested the activation status of RAC after silica treatment of bone marrow cells, but no difference between WT and *Pstpip2^{cmo}* cells has been observed (Figure 4F)

Collectively these data suggest that PSTPIP2 via its binding partners, suppresses pathways leading to PKC-mediated p47-phox phosphorylation and that this is the mechanism how PSTPIP2 attenuates NADPH oxidase activity and ROS production.

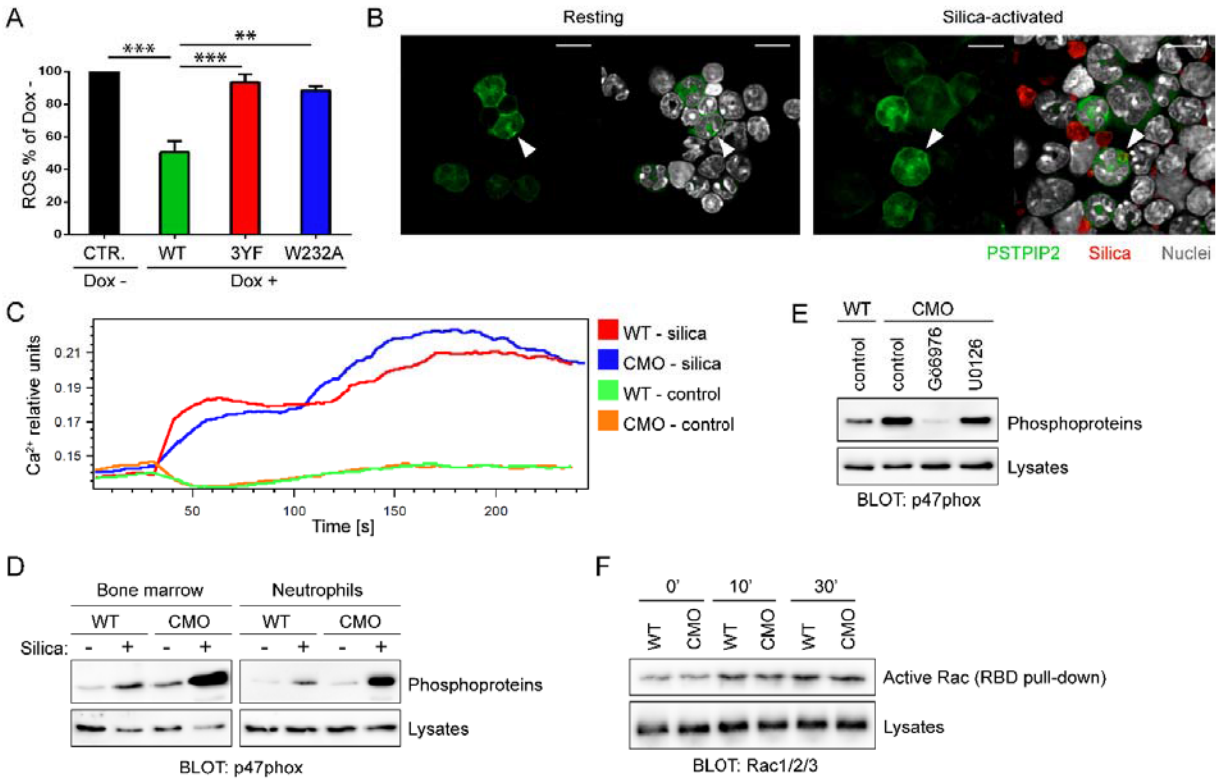

Figure 4. PSTPIP2-mediated suppression of ROS production in neutrophils is dependent on PSTPIP2 binding partners and involves negative regulation of p47phox phosphorylation.

(A) Suppression of ROS production by wild-type and mutant PSTPIP2 in mature granulocytes differentiated from conditionally immortalized granulocyte progenitors transduced with inducible PSTPIP2 constructs. Expression of PSTPIP2 was triggered by overnight incubation with doxycycline. On the vertical axis percentage of ROS response by Dox treated cells when compared to Dox non-treated cells is shown. Error bars represent SEM of 3 biological replicates. Only significant differences are highlighted with asterisks.

(B) Subcellular localization of PSTPIP2 in resting and silica-activated neutrophils differentiated *in vivo* from bone marrow cells transduced with retroviral PSTPIP2-EGFP construct. Bar = 10 µm. N = 4.

(C) Calcium response of WT and *Pstpip2^{cmo}* neutrophils (gated from full BM) after silica treatment. N = 3
(D) Phosphorylation of p47phox in WT and *Pstpip2^{cmo}* neutrophils after 30 min incubation with silica. To detect p47phox phosphorylation, total phosphoproteins were isolated from neutrophil lysates followed by p47phox detection by immunoblotting. N = 3
(E) Phosphorylation of p47phox in *Pstpip2^{cmo}* neutrophils treated for 30 min with silica together with PKC inhibitor Gö6976 or MEK inhibitor U0126. Phosphorylation of p47phox was detected as in (D). N = 4 for Gö6976 and N = 2 for U0126.
(F) RAC activation in WT and *Pstpip2^{cmo}* neutrophils. Active RAC was isolated using PAK1-RBD-GST and Glutathion-Sepharose and detected by immunoblotting with antibody to all three RAC proteins (RAC1/2/3). N = 2.

Unprovoked ROS production in vivo precedes the onset of the disease

To analyze the ROS production in vivo during the disease development we used luminol derivative L-012 to visualize ROS generation in living anesthetized mice. Very interestingly, we observed a strong luminescent signal already in freshly weaned 3 week old mice that were otherwise asymptomatic (Figure S3). The signal was mostly localized along the tail and with weaker intensity also in the hind paws. Visualization at later time points revealed that at 4 weeks of age the ROS production was equally intensive in the tail and paws (Figure 5A, B) and gradually moved to the hind paws during the weeks 6-8. At this age, ROS production became predominant in hind paws with more restricted focal localization (Figures 5B and S3).

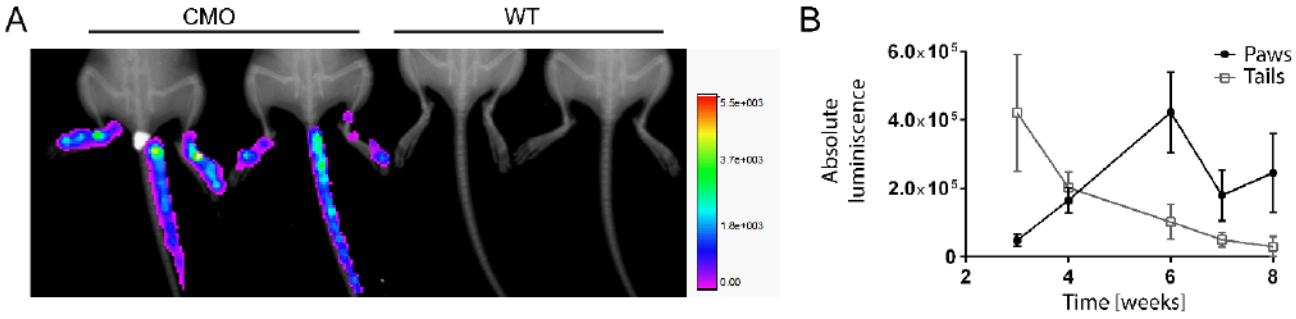

Figure 5. ROS production in vivo precedes the onset of the disease
(A) Representative *in vivo* measurement of ROS in 4 week old anesthetized WT and *Pstpip2^{cmo}* (CMO) mice. Mice were injected intraperitoneally with L-012 (75 mg/kg) and ROS-induced luminescence was measured in the whole body imager. The luminescence is shown as a heat-map in artificial colors on the background of an X-ray image.
(B) Time course quantification of absolute L-012 luminescence driven by *in vivo* ROS production in Pstpip2^{cmo} mice. The luminescence was quantified separately for paws and tails. N = 6 per time point.
See also Figure S3.

ROS deficiency has specific effects on bone destruction

Strong unprovoked production of ROS in very young mice preceding visible symptoms weeks before their demonstration suggested that ROS may act upstream of IL-1β in osteomyelitis development. To determine the contribution of high *in vivo* ROS generation to disease development, we crossed *Pstpip2^{cmo}* mice to gp91phox-deficient mouse strain. In the absence of gp91phox, we were unable to detect any ROS production even in *Pstpip2^{cmo}* cells (Figures 6A and S4). These data confirm that NADPH oxidase was responsible for the dysregulated ROS production in *Pstpip2^{cmo}* neutrophils. Surprisingly, *Pstpip2^{cmo}* mice lacking gp91phox developed similar disease symptoms like *Pstpip2^{cmo}* mice (Figure 6B) and with similar, only slightly delayed, kinetics (Figure 6C). Blind scoring of the disease severity by visual inspection of hind paw photographs collected throughout various experiments revealed that the symptoms of the disease are only partially alleviated in gp91phox-deficient animals, approximately by 1-2 points on 8-point scale (Figure 6D). Moreover, ELISA analysis detected comparable amount of IL-1β in hind paw extracts from *Pstpip2^{cmo}* and *Pstpip2^{cmo}/gp91phox$^{-/-}$* animals (Figure 6E) and similar amount of processed IL-1β p17 was found in the lysates of silica-stimulated bone marrow cells by immunoblot (Figure 6F). These data demonstrated that the phagocyte NADPH-oxidase is dispensable for autoinflammatory disease initiation, but it affects the severity of the disease. We also noticed that the character of the hind paw edema was somewhat different in *Pstpip2^{cmo}/gp91phox$^{-/-}$* mice. Typically, the swelling was most serious at the distal part of phalanges and only rarely affected metatarsal area in *Pstpip2^{cmo}/gp91phox$^{-/-}$* animals, while in *Pstpip2^{cmo}* mice metatarsi were frequently enlarged and the phalanges were often most seriously affected in their central parts (Figure 6B).

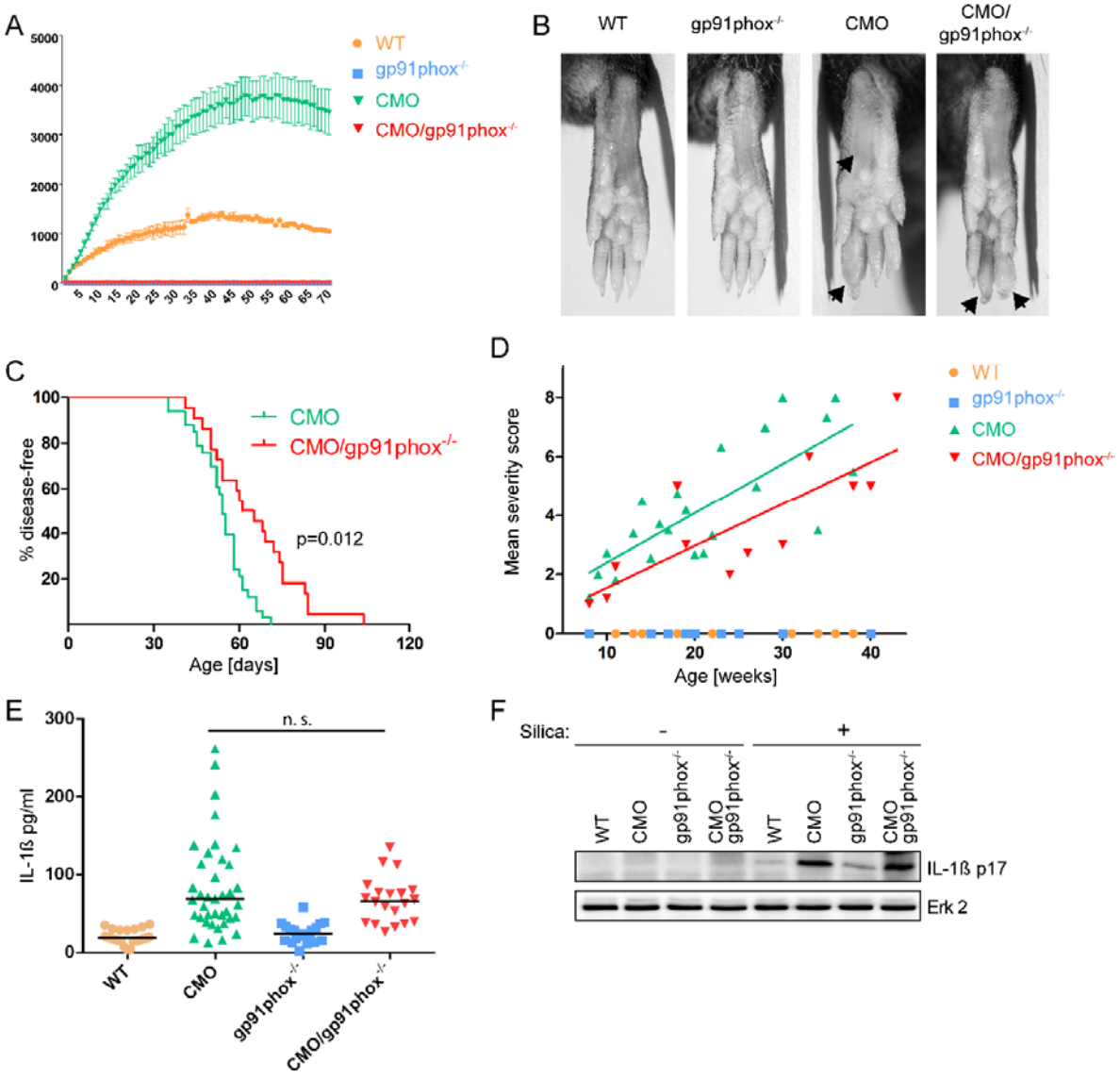

Figure 6. Limited effect of gp91phox deficiency on visible symptom development and IL-1β production

(A) In vitro ROS response induced by silica treatment in BM cells from WT, *Pstpip2^{cmo}*, *gp91phox$^{-/-}$* and *Pstpip2^{cmo}/gp91phox$^{-/-}$* mice.

(B) Representative photographs of hind paws of 18-19 week old WT, *Pstpip2^{cmo}*, *gp91phox$^{-/-}$* and *Pstpip2^{cmo}/gp91phox$^{-/-}$* mice.

(C) Disease-free curve comparing the time of disease appearance in *Pstpip2^{cmo}* and *Pstpip2^{cmo}/gp91phox$^{-/-}$* mice. Development of visible symptoms was evaluated 2-3 times per week.

(D) Disease severity was scored (scale from 0 to 8) by visual inspection of photographs of the hind paws collected over the course of this study. Each point represents mean value for the mice of the same age and genotype. Lines were generated using linear regression.

(E) ELISA analysis of IL-1β from hind paw lysates. Samples were adjusted to the same protein concentration before analysis.

(F) Presence of processed IL-1β in the lysates from bone marrow cells treated for 60 min (or not) with silica was detected by immunoblotting. N = 4. See also Figure S4.

In order to find out if these differences were caused by different character of bone inflammation we performed X-ray µCT analysis of *Pstpip2^{cmo}* and *Pstpip2^{cmo}/gp91phox$^{-/-}$* mice. Very surprisingly, bone destruction in *Pstpip2^{cmo}/gp91phox$^{-/-}$* animals was almost entirely missing, while in *Pstpip2^{cmo}* mice substantial bone damage could be observed (Figure 7A). To support this observation with a quantitative analysis, we calculated bone surface to volume ratio and bone fragmentation from the X-ray µCT data. *Pstpip2^{cmo}*/gp91phox$^{-/-}$ mice showed similar values to WT, while values for *Pstpip2^{cmo}* mice were substantially higher (Figure 7B). Timeline X-ray µCT scans of hind paws revealed progressive bone lesion formation in *Pstpip2^{cmo}* mice while *Pstpip2^{cmo} gp91phox$^{-/-}$* littermates remained largely protected (Figure S5).

The lack of bone damage can also be demonstrated on tissue sections from tarsal area of hind paws (Figure 7C). The CMO mice show very high level of osteolysis of tarsal bones with almost missing joint cartilages due to arthritic changes accompanied with robust granulomatous infiltration. The WT mice have normally developed and structurally well-defined tarsal bones with undamaged joint cartilages with no infiltration of immune cells and no adverse changes in the bone marrow. The *Pstpip2^{cmo}/gp91phox$^{-/-}$* mice showed rescue effect in ossified parts of tarsal bones with no or minimal signs of bone damage by immune cells, the soft tissue infiltration is in metatarsal area minimal compared to CMO mice. The cartilages are also well shaped and are covering the joint areas comparably with WT animals. The difference from WT animals is in hypercellular structure of bone marrow resulting in decreased volume of ossified tissue.

To address protection potential of gp91phox deficiency in old *Pstpip2^{cmo}* mice we performed X-ray µCT scans on 7 month old mice. Old *Pstpip2^{cmo}* mice suffered from strong bone destruction and remodeling but *Pstpip2^{cmo}/gp91phox$^{-/-}$* mice were still protected from adverse effects of osteomyelitis (Figure S5). To gain a quantitative insight into the level of soft tissue inflammation we have performed computational reconstruction of soft tissues from X-ray µCT scans described above in Figure 7B and calculated soft tissue volume. This measurement revealed that soft tissues in *Pstpip2^{cmo}/gp91phox$^{-/-}$* hind paws were significantly enlarged, albeit not to the same extent as in *Pstpip2^{cmo}* mice (Figure 7D). Collectively, these data demonstrate that despite significant swelling that can be detected in the hind paw soft tissues of *Pstpip2^{cmo}/gp91phox$^{-/-}$* mice, bones remain largely protected in the absence of NADPH oxidase activity.

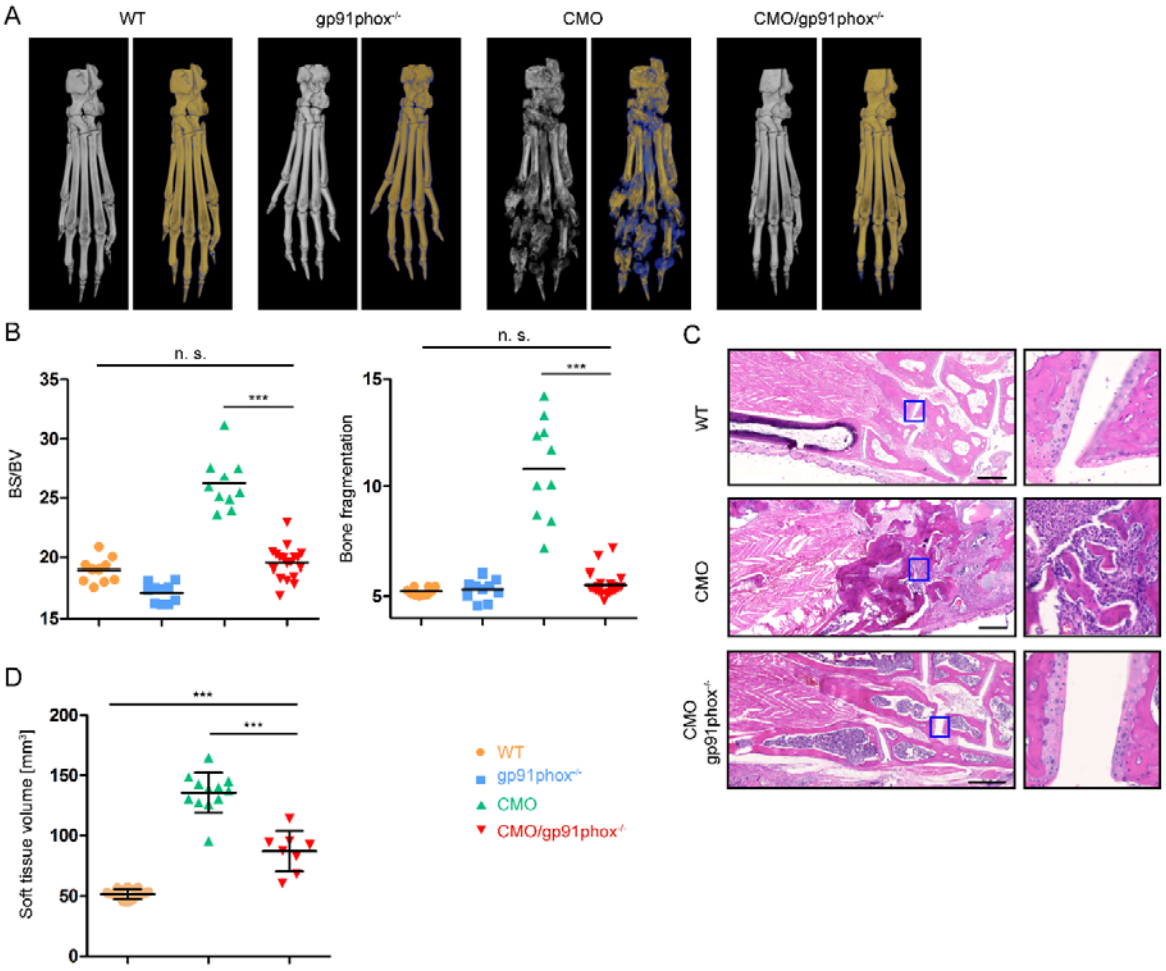

Figure 7. Almost complete absence of bone damage in gp91phox-deficient *PSTPIP2^{cmo}* mice.
(A) Representative X-ray µCT scans of bones from 14 week old mice. Grey images represent visualization of total bone tissue. Pseudocolor images distinguish between old (in yellow) and newly formed (in blue) bone mass.
(B) Quantification of bone surface/bone volume ratio (BS/BV) and bone fragmentation in paw bones of 14 weeks old mice.
(C) Sections of paraffin embedded tissue from tarsal area of hind paw stained with hematoxylin-eosin.
(D) Volume of soft tissue in hind paws calculated as a total paw volume from which the bone volume has been subtracted. Values were calculated from X-ray µCT data.
See also Figure S5.

Discussion

Monogenic autoinflammatory diseases develop as a result of dysregulation of the innate immune system. Although the specificity of this branch of the immune system is relatively limited, these diseases still show tissue and organ selectivity. The mechanisms of this selectivity are often poorly understood (de Jesus et al., 2015). *Pstpip2^{cmo}* mice represent an important model of tissue-selective autoinflammatory disease that affects mainly bones and surrounding tissue in hind paws and tails (Byrd et al., 1991; Chitu et al., 2009; Ferguson et al., 2006). Our current studies demonstrate that in these animals ROS production by neutrophil NADPH oxidase is substantially enhanced and suggest that dysregulated ROS production is a critical part of the selectivity mechanisms governing specific damage to the bones.

We found that increased ROS production was associated with p47phox hyperphosphorylation. This phosphorylation could be almost completely abolished by inhibition of Protein kinases C (PKC). These kinases are known to be activated by calcium ions and diacylglycerol, which are both produced as a result of phospholipase C (PLC) activity (Kadamur and Ross, 2013; Lipp and Reither, 2011). The calcium response, which is a hallmark of PLC activity appeared normal in silica-stimulated *Pstpip2^{cmo}* neutrophils, where the scale of ROS dysregulation was largest. Therefore, we assume that the signaling is altered either at the level of PKC regulation that is independent of PLC activity, or that PSTPIP2 controls an unknown negative regulator of p47phox phosphorylation (e.g. a phosphatase) that is independent of PKCs. Further experiments are needed to clarify this issue and determine individual components of the pathway connecting PSTPIP2 to p47phox phosphorylation.

Our data are in agreement with several other reports that disprove the role of NADPH oxidase-generated ROS in IL-1β processing by inflammasome. They are mainly based on analyses of monocytes and macrophages from NADPH-oxidase-deficient patients and mice, where IL-1β production is not altered or it is even enhanced (Meissner et al., 2008; Meissner et al., 2010; van Bruggen et al., 2010; van de Veerdonk et al., 2010). In a single study on human neutrophils, NADPH oxidase deficiency also did not lead to reduction of NLRP3 inflammasome activity (Gabelloni et al., 2013). On the other hand, inhibition of mitochondrial ROS production in monocytes/macrophages results in an impairment of IL-1β production in these cells (Nakahira et al., 2011; Zhou et al., 2011), suggesting that the majority of ROS supporting inflammasome activation in these cell types is generated by mitochondria.

The roles of IL-1β and ROS in CMO pathophysiology appear to be different form each other. While dysregulated IL-1β production is a critical trigger of the disease development, enhanced ROS production modifies the outcome. However, ROS are not able to initiate the disease on their own in the absence of IL-1β signaling. It is documented by our experiments with *MyD88*-deficient *Pstpip2^{cmo}* mice, which displayed the same ROS dysregulation as *Pstpip2^{cmo}* mice and yet they did not develop any symptoms of autoinflammation. These data

also demonstrate that enhanced ROS production is not downstream of IL-1β, since MyD88 is critical for signaling by IL-1 receptor (Deguine and Barton, 2014).

The observation of hyperproduction of ROS *in vivo* during the very early stages of the disease, well before any visible symptoms can be detected, suggests that the disease development is triggered earlier than thought and that ROS production is involved very early in the process. However, the precise stimulus, receptor or pathway that triggers deregulated production of IL-1β by neutrophils and initiate the disease are currently unknown. Previously published data suggest that altered response to gut microbiota might be at the root of CMO initiation (Lukens et al., 2014b). Toll-like receptors were among the best candidates for triggering such a response. In addition, they are also responsible for detecting various damage-associated molecular patterns (DAMP) (Schaefer, 2014), which can also be suspected of the involvement in the disease initiation. Signaling through majority of these receptors is critically dependent on adaptor protein MyD88 (Kawai et al., 1999; O'Neill and Bowie, 2007; Takeuchi et al., 2000). This adaptor is also critical for signal transduction downstream of IL-1 receptor (Deguine and Barton, 2014). IL-1 receptor presence on hematopoietic cells was shown to be dispensable for CMO development (Gurung et al., 2016). However, the role of TLRs has not been studied in the context of CMO. Surprisingly, our results revealed that MyD88-deficient *Pstpip2*^{cmo} hematopoietic cells were fully capable of triggering the disease when transplanted into wild-type mice, demonstrating that CMO is independent of MyD88 signaling in hematopoietic cells. Although signaling by majority of TLRs is severely compromised in the absence of MyD88, limited number of signaling pathways governed by adaptor TRIF are still preserved downstream of some TLR family members (O'Neill and Bowie, 2007). There also is a number of other pattern recognition receptors on hematopoietic cells that do not use MyD88 for signaling. Thus, it still remains unclear, which pathways trigger deregulated IL-1β production by neutrophils and the disease development. However, it clearly must be pathways that are independent of MyD88.

ROS are known to play a key role in differentiation and activity of osteoclasts. These cells are responsible for physiological bone resorption during bone remodeling processes. They are also involved in pathological bone damage in a number of disease states (Okamoto et al., 2017). *Pstpip2*^{cmo} mice exhibited increased osteoclastogenesis and osteoclast hyperactivity suggesting that osteoclasts are responsible for inflammatory bone damage in these mice (Chitu et al., 2012). Our data show that the bone damage can be almost completely abolished when phagocyte NADPH oxidase is inactivated by deletion of its gp91phox subunit. One possibility is that deficiency in osteoclast gp91phox results in defects in their differentiation and activity and reduced bone damage. However, in *gp91phox*$^{-/-}$ mice no bone abnormalities have been observed. In addition, gp91phox-deficient osteoclasts differentiate normally and have normal bone resorption activity (Lee et al., 2005; Sasaki et al., 2009; Yang et al., 2001). These results show that gp91phox expressed in osteoclasts is dispensable for differentiation and activity of

these cells. In fact, other NADPH oxidases were shown to be more important for their function (Goettsch et al., 2013; Lee et al., 2005). Our data together with published results thus favor the explanation that exogenous ROS originating from hyperactive neutrophils, lead either directly or indirectly to increased differentiation and/or activity of osteoclasts and resulting bone damage.

PSTPIP2 mutations in humans have not yet been described. However, PSTPIP2 gene has been sequenced only in a limited number of CRMO patients and patients with closely related SAPHO syndrome (Ferguson et al., 2008; Hurtado-Nedelec et al., 2010; Jansson et al., 2007). CRMO and SAPHO form a rather heterogeneous disease spectrum, which may in fact represent a number of distinct disorders where various defects at the molecular level may lead to similar outcome, and so PSTPIP2 mutations in some of these patients may still be discovered in the future. The data on ROS production in these diseases are also largely missing. We are aware of only a single study where the ROS production by neutrophils was analyzed in two SAPHO patients from a single family without any mutations in PSTPIP2 gene (Ferguson et al., 2008). These data showed reduced ROS response after activation with multiple activators, including PMA, fMLP and TNFα when compared to healthy controls. However, from the information provided it was unclear whether the patients were undergoing anti-inflammatory treatment that could suppress the response at the time of analysis. Further studies are needed to fully understand the role of PSTPIP2 and ROS in CRMO, SAPHO and other inflammatory bone diseases in humans.

Inflammatory bone damage is a serious problem accompanying a number of human disorders. Full understanding of possible mechanisms that can govern its development is critical for designing successful therapeutic interventions. Our data reveal how dysregulated ROS production results in bone damage in the specific case of CMO. However, these findings may represent a more general mechanism with broader validity for other syndromes where inflammatory bone damage is involved and analysis of ROS production in other instances of inflammatory bone damage may prove beneficial.

Acknowledgements

This work was supported by Czech Science Foundation (project 17-07155S), by institutional funding from the Institute of Molecular Genetics, Academy of Sciences of the Czech Republic (RVO 68378050), and by the Czech Centre for Phenogenomics (CCP, project no. LM2015040) and OP RDI CZ.1.05/2.1.00/19.0395 (Higher quality and capacity for transgenic models). We also acknowledge Light Microscopy Core Facility, IMG ASCR, Prague, Czech Republic, supported by MEYS (LM2015062), OPPK (CZ.2.16/3.1.00/21547) and NPU I (LO1419). JK and DG received additional support from Charles University Grant Agency (GAUK) (project number 923116).

Author contributions

J.K., A.D., and J.P. designed and conducted majority of experiments and wrote part of the paper. F.S. contributed to in vivo imaging analysis and analysis of corresponding data, D.G. with contribution from S.B. generated microscopy images. S.B. was also involved in signaling pathway analysis. P.A. and J.P. produced and tested PSTPIP2 antibodies. J.P. also collected data for majority of disease-free curves. T.S. performed genotyping and part of the biochemistry experiments. R.S. contributed to conceptualizing and designing in vivo imaging experiments. T.B. conceptualized the project, designed experiments, performed signaling pathway analyses and wrote part of the paper.

Materials and methods

Antibodies

Antibodies to the following murine antigens were used: RAC1/2/3 (Cell Signaling Technology, Danvers, MA); p47, Erk2 (Santa Cruz Biotechnology, Dallas, TX); B220-biotin, TER119-biotin, c-Kit- biotin, CD3ε-biotin, Ly6G-biotin, CD115-biotin, CD11b-APC, CD11b-FITC, B220-FITC, Ly6C-PE-Cy7, Ly6C-FITC, Ly6G-FITC, Ly6G-APC, c-Kit-PE, Sca-1-APC, CD16/32-PE/Cy7 (Biolegend, San Diego, CA); CD34-FITC, DX5-biotin, F4/80-biotin, Thy1.2-FITC (eBioscience, ThermoFisher, Waltham, MA); Fc Bloc (2.4G2) (BD Biosciences, San Jose, CA); HRP-conjugated goat anti-mouse IgG (Sigma), HRP-goat anti-rabbit (Bio-Rad, Hercules, CA). The mouse mAb that recognizes murine PSTPIP2 has been described earlier (Drobek et al., 2015). Heat aggregated IgG was prepared as follows: IgG was purified from mouse serum (Sigma-Aldrich) on protein A-Sepharose (GE Healthcare, Uppsala, Sweden), transferred to PBS, and concentrated to 30 mg/ml on an Amicon Ultracel–30K unit (Millipore, Merck, Darmstadt, Germany). The aggregation was induced by heating to 63˚C for 30 min.

Other reagents

In this study we also used Luminol, Lipopolysaccharides from Escherichia coli O127:B8, fMLP, PMA (all from Sigma-Aldrich), L-012 (Wako Chemicals, USA), TNFα, G-CSF (Peprotech, Rocky Hill, NJ), U0126 (Cell Signalling Technology), Gö6976 (Calbiochem, Merck). Silica (silicon dioxide crystals) was obtained from Sigma. To enable fluorescent labelling for microscopy, 5 mg/ml silica particles were first coated with non-fat dry milk (2% in PBS, 1 h at room temperature) and then labelled with 5 µM Cell Proliferation Dye eFluor 670 (eBioscience), 30 min at 37˚C.

Mice

Pstpip2^{cmo} mouse strain (C.C*g*-*Pstpip2*^{cmo}/J, JAX stock #002864) carrying the c.293T→C mutation in the Pstpip2 gene (on Balb/C genetic background) resulting in an L98P change in

the PSTPIP2 protein (Byrd et al., 1991; Ferguson et al., 2006), B6.129S-*Cybb*^{tm1Din}/J lacking NADPH subunit gp91phox, JAX stock #002365 (Pollock et al., 1995), and Myd88-deficient mouse strain (B6.129P2(SJL)-*Myd88*$^{tm1.1Defr}$/J, JAX stock #009088) derived from *MyD88*^{fl} mice (Hou et al., 2008) and B6.SJL-Ptprca Pepcb/BoyJ (CD45.1^{+}) congenic strain (Shen et al., 1985), JAX stock #002014, were obtained from The Jackson Laboratory (Bar Harbor, ME). *Pstpip2*^{cmo} mouse strain was backcrossed on C57Bl/6J background for at least 10 generations and then used in the majority of experiments with the exception of experiments in Figure 1D and 4A, D, E, F, and S1. For these experiments the original *Pstpip2*^{cmo} strain on Balb/c genetic background has been selected due to the higher number of neutrophils that could be obtained by the negative selection method and due to the better quality of immortalized granulocyte progenitors derived from this strain. Both genetic backgrounds showed similar disease symptoms and similar dysregulation in ROS production. The BALB/c and C57Bl/6J inbred strains were obtained from the animal facility of Institute of Molecular Genetics, Academy of Sciences of the Czech Republic (Prague, Czech Republic). Experiments in this work that were conducted on animals were approved by the Expert Committee on the Welfare of Experimental Animals of the Institute of Molecular Genetics and by the Academy of Sciences of the Czech Republic and were in agreement with local legal requirements and ethical guidelines.

Primary Cells and Cell Lines

All primary cells and cell lines were cultured at 37°C with 5% CO_2 in Iscove's Modified Dulbecco's Media (IMDM) supplemented with 10% fetal calf serum (FCS) and antibiotics. For bone marrow (BM) cell isolation, mice were sacrificed by cervical dislocation, BM was flushed with PBS supplemented with 2% FCS and erythrocytes were lysed in an ACK buffer (150 mM NH_4Cl, 0.1 mM EDTA (disodium salt), 1 mM $KHCO_3$). Murine neutrophils were isolated from BM cells using anti-biotin MicroBeads, and LS magnetic columns (Miltenyi Biotec, Bergisch Gladbach, Germany). For negative selection cells were labeled with biotinylated antibodies to B220, F4/80, DX5, c-Kit, CD3ε, CD115, and Ter119 prior to magnetic bead purification. For positive selection only anti-Ly6G-biotin was used. The purity of isolated cells was determined by flow cytometry. Primary murine monocytes were sorted from BM cells as Ly6G negative, Ly6C highly positive and Side-Scatter low cells using BD Influx sorter (BD Biosciences). The following cell lines were used in this study: HEK293FT cells (Invitrogen), Platimun Eco cells (Plat-E cells, Cell Biolabs, San Diego, CA), and immortalized granulocyte progenitors. For preparation of immortalized granulocyte progenitors we used a modified version of the protocol for generation of immortalized macrophage progenitors (Wang et al., 2006). The progenitors were first enriched by the depletion of Mac-1^{+}, B220^{+}, and Thy1.2^{+} from mouse BM cells and cultured in the presence of IL-3, IL-6, and SCF (supplied as culture supernatants from HEK293FT cells transfected with constructs coding for respective cytokines) for 2 days.

Next, progenitors were transduced with ER-HoxB8 construct. The transduced cells were enriched for the GMP progenitor population by FACS (Lin^-, $Sca\text{-}1^-$, $c\text{-}Kit^+$, $Fc\gamma R^+$, $CD34^+$) and propagated in a media containing 1 µM β-estradiol and 1% SCF-containing supernatant. Granulocyte differentiation was induced by β-estradiol withdrawal or by the β-estradiol withdrawal and replacement of SCF for G-CSF (50 ng/ml).

Flow cytometry

Single cell suspensions of bone marrow cells were incubatecd with Fc-bloc and fluorophore-conjugated antibodies and analyzed on BD LSRII flow cytometer. For calcium response measurement, single cell suspensions of bone marrows from 6-8 week old mice were loaded with 2 µM calcium indicator Fura Red (Invitrogen). Samples were analyzed using a BD LSRII flow cytometer for 30 s at rest and then another 210 s after activation (either with fMLP, Silica or E.coli with OD=0.8). The relative calcium concentration was measured as a ratio of the Fura Red fluorescence intensity elicited by excitation wavelengths of 405 nm (emission measured at 635–720 nm) and 488 nm (emission measured at 655–695 nm). The data were analyzed with FlowJo software (TreeStar, Ashland, OR). Granulocytes were gated according to forward and side scatter properties.

ROS meassurement

ROS production *in vitro* was assessed by luminol-based chemiluminescence assay as published previously (Goodridge et al., 2011). BM cells or purified murine neutrophils in IMDM supplemented with 0.2% FCS were plated in density of 10^6 cells per well into a black 96-well plate (SPL Life Sciences, Naechon-Myeon, Korea). Cells were rested for 30 minutes at 37°C and 5% CO_2. Then, luminol at final concentration 100 µM and stimuli (100 ng/ml LPS, fMLP 1 µg/ml, TNFα 10 ng/ml, E.coli OD_{600} ~ 0.8 – 5× diluted, Silica 50 µg/cm^2, heat-agregated murine IgG 300 µg/ml, PMA 100 ng/ml) were added. Luminiscence was measured immediately on EnVison plate reader (Perkin Elmer, Waltham, MA); each well was scanned every minute for 70 minutes.

To assess ROS production *in vivo*, mice were intraperitoneally injected with luminescence reporter LC-012 in final concentration 75mg/kg (1,8mg/25g mouse) dissolved in PBS as described by (Kielland et al., 2009). Luminiscence signal was acquired by Xtreme whole body imager (Bruker, Billerica, MA), with the following settings: binning 8x8, exposure time: 5 min. The quantification of photon counts was performed in Molecular Imaging Software (Bruker).

Bone Marrow Transplantations

In bone marrow transplantation experiments congenic C57Bl/6 ($CD45.1^+$) recipient mice were lethally irradiated with a single dose of 7 Gy. After 6 hours, mice were injected with 2×10^6 bone marrow cells from *Pstpip2^{cmo}* or *Pstpip2^{cmo}/MyD88$^{-/-}$* mice (both on $CD45.2^+$,

C57Bl/6 genetic background) into tail vein. Mice were monitored for the presence of paw swelling and inflammation twice a week.

DNA constructs

Generation of MSCV-PSTPIP2-EGFP construct. The coding sequence of mouse PSTPIP2 was amplified from cDNA of mouse myeloid progenitors (CMPs) and subcloned into pXJ41-EGFP cloning vector (Chum et al. 2016). IRES and Thy1.1 coding sequence was removed from MSCV-IRES-Thy1.1 retroviral vector (Clontech, Mountain View, CA) by digestion with EcoRI and ClaI followed by blunt ligation. PSTPIP2-EGFP coding sequence was then subcloned into modified MSCV vector using BglII and XhoI restriction sites to generate MSCV-PSTPIP2-EGFP.

Generation of MSCV-mPSTPIP2-TetOn inducible constructs. WT and mutated sequences (W232A or 3YF) of mouse PSTPIP2 described earlier (Drobek et al., 2015) were fused to C-terminal EGFP by PCR using P2A sequence as a linker. Fusion constructs were cloned into pLVX-Tet3G doxycycline inducible vector (Clontech) using AgeI and BamHI restriction sites. Resulting vectors were used as templates to amplify sequence spanning Tet-On 3G and TRE3G regulation/inducible elements together with PSTPIP2 by PCR and the resulting product was cloned it into MSCV-IRES-EGFP vector using ClaI and BglII restriction sites.

Retroviral transduction.

For confocal microscopy, c-kit+ stem and progenitor cells were obtained from BM of *Pstpip2*^{cmo} (C57Bl/6J) mice using magnetic purification (c-kit-biotin antibody, Anti-biotin mircobeads). Cells were expanded in IL-3, IL-6 and SCF supplemented media for 20h, then infected with PSTPIP2-EGFP retroviral construct. For the production of replication incompetent retrovirus, ecotropic packaging cells (Plat-E) were plated in 10 cm dish and transfected with 24 µg of plasmid DNA using Lipofectamine 2000 Reagent (Life Technologies) according to the manufacturer's instructions. Virus containing supernatant was collected, concentrated with Amicon Ultra centrifugal filters with molecular weight cut-off 100 kDa (Merck Millipore) and immediately used to infect the cytokine expanded c-kit+ bone marrow cells. These cells were centrifuged with 150 µl of concentrated virus supernatant and 2.4 µl of Lipofectamine 2000 reagent (Sigma-Aldrich) at 1250 × g for 90 min at 30 °C and then incubated for another 4h at 37°C in 5% CO_2 in a humidified incubator before the exchange of the media. Immortalized granulocyte progenitors were propagated in IMDM with 1 µM β-estradiol and 1% SCF-containing supernatant and then infected with PSTPIP2 mutant constructs using the same procedure described above.

Microscopy

One day after infection, EGFP positive cells were sorted on Influx sorter and injected into sub-lethally irradiated (6 Gy in a single dose) CD45.1^{+} recipient mice. After 2 weeks, mice were sacrificed, BM cells isolated and resuspended in IMDM with 0.1% FCS. The cells were activated by 50 µg/cm^2 fluorescent silica (see above) in a 96-well plate for 10 min. The cells were transferred to 4% paraformaldehyde in PBS and fixed at room temperature for 20 min. Cell nuclei were stained with 10 µg/ml Hoechst 33258 (Sigma) for 15 min. Cells were than washed 2x with PBS, resuspended in 150 µl of ddH2O and centrifuged on glass slide at 30 × g for 5min using Centurion Scientific K3 cytospin centrifuge (Centurion Scientific, Stoughton, U.K.). Cell samples were than mounted in 10 µl of DABCO mounting reagent (Sigma-Aldrich) and covered with glass coverslip (Zeiss, Oberkochen, Germany). Microscope setup: sequential 2-colour imaging was performed using a Leica TCS SP8 laser scanning confocal microscope (Leica, Wetzlar, Germany) with a 63×1.4 NA oil-immersion objective. Acquired images were manually thresholded to remove signal noise detected outside of the cell using ImageJ software.

Cell activation, lysis, and immunoprecipitation

For Western blotting, the cells were washed and resuspended in IMDM with 0.1% FCS at a concentration of 1–4 × 10^7 cells/ml. Subsequently, the cells were stimulated as indicated at 37°C. The activation of cells was stopped by the addition of an equal volume of a 2 × concentrated SDS-PAGE sample buffer (128 mM Tris pH 6.8, 10% glycerol, 4% SDS) followed by the sonication and heating of the samples (99°C for 2 min). The samples were analyzed by SDS-PAGE followed by Western blotting. For detection of p47 phosphorylation, phosphoproteins were isolated from bone marrow cells using PhosphoProtein purification Kit (Qiagen, Hilden, Germany) according to manufacturer's instructions, followed by detection of p47 by immunoblotting.

RAC activity assay

2 × 10^7 neutrophils (silica activated or not) were lysed in 1 mL Lysis buffer (25 mM HEPES pH 7.2, 150 mM NaCl, 10 mM $MgCl_2$, 1 mM EDTA, 1% NP-40, 10% glycerol, 100 × diluted Protease Inhibitor Cocktail Set III (Calbiochem, Merck)) containing 5 µg PAK-RBD-GST (RAC-binding domain from PAK1 fused to GST, isolated from E.coli strain BL21 transformed with corresponding expression plasmid). After preclearing the lysate by centrifugation the complexes of active RAC and PAK-RBD-GST were isolated on Glutathion-Sepharose (GE Healthcare). RAC was then detected by immunoblotting.

Anaesthesia

Mice for in-vivo imaging were anaesthetized by intra muscular injection of Zoletil (20mg/ml) – Xylazine (1mg/ml) solution with Zoletil dose 100mg/kg and Xylazine dose 1mg/kg.

X-ray micro-computerized tomography

Hind paws were scanned in *in-vivo* X-ray µCT Skyscan 1176 (Bruker). Scanning parameters were: voltage: 50 kV, current: 250 µA, filter: 0.5 mm aluminium, voxel size: 8.67 µm, exposure time: 2 s, rotation step: 0.3° for 180° total, object to source distance: 119.271 mm, and camera to source distance: 171.987 mm with time of scanning: 30 min. Reconstruction of virtual slices was performed in NRecon software 1.6.10 (Bruker) with set-up for smoothing = 3, ring artifact correction = 4, and beam hardening correction = 36%. Intensities of interest for reconstruction were in the range from 0.0045 to 0.0900. For reorientation of virtual slices to the same orientation the DataViewer 1.5.2 software (Bruker) was used.

For µCT data analysis CT Analyser 1.16.4.1 (Bruker) was used. The volume of interest (VOI) was chosen there containing the distal part of hind paw starting from the half of metatarsus. Based on differences of X-ray absorption three parts were analyzed separately: the whole VOI, the newly formed bone connected mostly with arthritis, and the area inhabited by the original bone of phalanges and metatarsi. The total volume was recorded for all three parts. For original and new bone other parameters from 2D and 3D analysis were recoded to describe changes in the structure, namely: surface of the bone, surface-volume ratio, number of objects, closed porosity, mean fractal dimension, mean number of objects per slice, mean closed porosity per slice, and mean fractal dimension per slice. Scans with technical artifacts caused by spontaneous movements of animals were excluded from the analysis.

Cytokine detection

Murine paws were homogenized in 1 mL RIPA lysis buffer (20 mM TRIS pH7.5, 150 mM NaCl, 1% NP-40, 1% Sodium deoxycholate, 0.1% SDS) containing 5 mM iodoacetamide (Sigma) and 100 × diluted Protease Inhibitor Cocktail Set III (Calbiochem, Merck) using Avans AHM1 Homogenizer (30s, speed 25). Any insoluble material was removed by centrifugation (20 000 × g, 5 min, 2°C). Concentrations of IL-1β in the samples were determined by Ready-SET-Go!® ELISA kits from eBioscience according to the instructions of the manufacturer.

Histology

The paws were fixed in 10% formol solution for 24h and decalcified in Osteosoft® (Merck) solution for 1 week, followed by paraffin embedding and histological cutting. The slides were stained in automatic system Ventana Symphony (Roche) and slides were scanned in Axio Scan.Z1 (Zeiss). The image postprocessing and analysis was done in Zen software (Zeiss).

Statistical analysis

P values were calculated in GraphPad Prism software (GraphPad Software, La Jolla, CA) using unpaired t test (two-tailed) for data in Figure 2B-F, one-way ANOVA with Tukey-Kramer multiple comparison post test for data in Figure 3C, 4A, 6E, 7B, 7D, and Gehan-Breslow-Wilcoxon test for disease-free curves in Figure 3D and 6C. Symbol meanings: n.s. $P > 0.05$; * $P \leq 0.05$; ** $P \leq 0.01$; *** $P \leq 0.001$; **** $P \leq 0.0001$. N numbers in figure legends represent number of biological replicates (in most cases animals).

Abais, J.M., Xia, M., Zhang, Y., Boini, K.M., and Li, P.L. (2015). Redox regulation of NLRP3 inflammasomes: ROS as trigger or effector? Antioxid. Redox. Signal. *22*, 1111-1129.

Adachi, O., Kawai, T., Takeda, K., Matsumoto, M., Tsutsui, H., Sakagami, M., Nakanishi, K., and Akira, S. (1998). Targeted disruption of the MyD88 gene results in loss of IL-1- and IL-18-mediated function. Immunity *9*, 143-150.

Borghini, S., Tassi, S., Chiesa, S., Caroli, F., Carta, S., Caorsi, R., Fiore, M., Delfino, L., Lasiglie, D., Ferraris, C.*, et al.* (2011). Clinical presentation and pathogenesis of cold-induced autoinflammatory disease in a family with recurrence of an NLRP12 mutation. Arthritis. Rheum. *63*, 830-839.

Brandes, R.P., Weissmann, N., and Schroder, K. (2014). Nox family NADPH oxidases: Molecular mechanisms of activation. Free. Radic. Biol. Med. *76*, 208-226.

Brookes, P.S., Yoon, Y., Robotham, J.L., Anders, M.W., and Sheu, S.-S. (2004). Calcium, ATP, and ROS: a mitochondrial love-hate triangle. Am. J. Physiol. Cell Physiol. *287*, C817-C833.

Broz, P., and Dixit, V.M. (2016). Inflammasomes: mechanism of assembly, regulation and signalling. Nat. Rev. Immunol. *16*, 407.

Bulua, A.C., Simon, A., Maddipati, R., Pelletier, M., Park, H., Kim, K.Y., Sack, M.N., Kastner, D.L., and Siegel, R.M. (2011). Mitochondrial reactive oxygen species promote production of proinflammatory cytokines and are elevated in TNFR1-associated periodic syndrome (TRAPS). J. Exp. Med. *208*, 519-533.

Byrd, L., Grossmann, M., Potter, M., and Shen-Ong, G.L. (1991). Chronic multifocal osteomyelitis, a new recessive mutation on chromosome 18 of the mouse. Genomics *11*, 794-798.

Carta, S., Penco, F., Lavieri, R., Martini, A., Dinarello, C.A., Gattorno, M., and Rubartelli, A. (2015). Cell stress increases ATP release in NLRP3 inflammasome-mediated autoinflammatory diseases, resulting in cytokine imbalance. Proc. Natl. Acad. Sci. U. S. A. *112*, 2835-2840.

Carta, S., Tassi, S., Delfino, L., Omenetti, A., Raffa, S., Torrisi, M.R., Martini, A., Gattorno, M., and Rubartelli, A. (2012). Deficient production of IL-1 receptor antagonist and IL-6 coupled to oxidative stress in cryopyrin-associated periodic syndrome monocytes. Ann. Rheum. Dis. *71*, 1577-1581.

Cassel, S.L., Eisenbarth, S.C., Iyer, S.S., Sadler, J.J., Colegio, O.R., Tephly, L.A., Carter, A.B., Rothman, P.B., Flavell, R.A., and Sutterwala, F.S. (2008). The Nalp3 inflammasome is essential for the development of silicosis. Proc. Natl. Acad. Sci. U. S. A. *105*, 9035-9040.

Cassel, S.L., Janczy, J.R., Bing, X., Wilson, S.P., Olivier, A.K., Otero, J.E., Iwakura, Y., Shayakhmetov, D.M., Bassuk, A.G., Abu-Amer, Y., *et al.* (2014). Inflammasome-independent IL-1beta mediates autoinflammatory disease in Pstpip2-deficient mice. Proc. Natl. Acad. Sci. U. S. A. *111*, 1072-1077.

Chitu, V., Ferguson, P.J., de Bruijn, R., Schlueter, A.J., Ochoa, L.A., Waldschmidt, T.J., Yeung, Y.G., and Stanley, E.R. (2009). Primed innate immunity leads to autoinflammatory disease in PSTPIP2-deficient cmo mice. Blood *114*, 2497-2505.

Chitu, V., Nacu, V., Charles, J.F., Henne, W.M., McMahon, H.T., Nandi, S., Ketchum, H., Harris, R., Nakamura, M.C., and Stanley, E.R. (2012). PSTPIP2 deficiency in mice causes osteopenia and increased differentiation of multipotent myeloid precursors into osteoclasts. Blood *120*, 3126-3135.

Dang, P.M., Stensballe, A., Boussetta, T., Raad, H., Dewas, C., Kroviarski, Y., Hayem, G., Jensen, O.N., Gougerot-Pocidalo, M.A., and El-Benna, J. (2006). A specific p47phox -serine phosphorylated by convergent MAPKs mediates neutrophil NADPH oxidase priming at inflammatory sites. J. Clin. Invest. *116*, 2033-2043.

de Jesus, A.A., Canna, S.W., Liu, Y., and Goldbach-Mansky, R. (2015). Molecular mechanisms in genetically defined autoinflammatory diseases: disorders of amplified danger signaling. Annu. Rev. Immunol. *33*, 823-874.

Deguine, J., and Barton, G.M. (2014). MyD88: a central player in innate immune signaling. F1000prime rep. *6*, 97.

Drobek, A., Kralova, J., Skopcova, T., Kucova, M., Novak, P., Angelisova, P., Otahal, P., Alberich-Jorda, M., and Brdicka, T. (2015). PSTPIP2, a Protein Associated with Autoinflammatory Disease, Interacts with Inhibitory Enzymes SHIP1 and Csk. J. Immunol. *195*, 3416-3426.

Ferguson, P.J., Bing, X., Vasef, M.A., Ochoa, L.A., Mahgoub, A., Waldschmidt, T.J., Tygrett, L.T., Schlueter, A.J., and El-Shanti, H. (2006). A missense mutation in pstpip2 is associated with the murine autoinflammatory disorder chronic multifocal osteomyelitis. Bone *38*, 41-47.

Ferguson, P.J., Lokuta, M.A., El-Shanti, H.I., Muhle, L., Bing, X., and Huttenlocher, A. (2008). Neutrophil dysfunction in a family with a SAPHO syndrome-like phenotype. Arthritis. Rheum. *58*, 3264-3269.

Gabelloni, M.L., Sabbione, F., Jancic, C., Bass, J.F., Keitelman, I., Iula, L., Oleastro, M., Geffner, J.R., and Trevani, A.S. (2013). NADPH oxidase derived reactive oxygen species are involved in human neutrophil IL-1β secretion but not in inflammasome activation. Eur. J. Immunol. *43*, 3324-3335.

Goettsch, C., Babelova, A., Trummer, O., Erben, R.G., Rauner, M., Rammelt, S., Weissmann, N., Weinberger, V., Benkhoff, S., Kampschulte, M., *et al.* (2013). NADPH oxidase 4 limits bone mass by promoting osteoclastogenesis. J. Clin. Invest. *123*, 4731-4738.

Gong, T., Yang, Y., Jin, T., Jiang, W., and Zhou, R. (2018). Orchestration of NLRP3 Inflammasome Activation by Ion Fluxes. Trends Immunol.

Goodridge, H.S., Reyes, C.N., Becker, C.A., Katsumoto, T.R., Ma, J., Wolf, A.J., Bose, N., Chan, A.S., Magee, A.S., Danielson, M.E., *et al.* (2011). Activation of the innate immune receptor Dectin-1 upon formation of a 'phagocytic synapse'. Nature *472*, 471-475.

Gurung, P., Burton, A., and Kanneganti, T.D. (2016). NLRP3 inflammasome plays a redundant role with caspase 8 to promote IL-1beta-mediated osteomyelitis. Proc. Natl. Acad. Sci. U. S. A. *113*, 4452-4457.

Holmström, K.M., and Finkel, T. (2014). Cellular mechanisms and physiological consequences of redox-dependent signalling. Nat. Rev. Mol. Cell Biol. *15*, 411.

Hou, B., Reizis, B., and DeFranco, A.L. (2008). Toll-like receptors activate innate and adaptive immunity by using dendritic cell-intrinsic and -extrinsic mechanisms. Immunity *29*, 272-282.

Hughes, M.M., and O'Neill, L.A.J. (2018). Metabolic regulation of NLRP3. Immunol. Rev. *281*, 88-98.

Hurtado-Nedelec, M., Chollet-Martin, S., Chapeton, D., Hugot, J.P., Hayem, G., and Gerard, B. (2010). Genetic susceptibility factors in a cohort of 38 patients with SAPHO syndrome: a study of PSTPIP2, NOD2, and LPIN2 genes. J. Rheumatol. *37*, 401-409.

Jansson, A., Renner, E.D., Ramser, J., Mayer, A., Haban, M., Meindl, A., Grote, V., Diebold, J., Jansson, V., Schneider, K., and Belohradsky, B.H. (2007). Classification of non-bacterial osteitis: retrospective study of clinical, immunological and genetic aspects in 89 patients. Rheumatology (Oxford, England) *46*, 154-160.

Kadamur, G., and Ross, E.M. (2013). Mammalian phospholipase C. Annu. Rev. Physiol. *75*, 127-154.

Kawai, T., Adachi, O., Ogawa, T., Takeda, K., and Akira, S. (1999). Unresponsiveness of MyD88-deficient mice to endotoxin. Immunity *11*, 115-122.

Kielland, A., Blom, T., Nandakumar, K.S., Holmdahl, R., Blomhoff, R., and Carlsen, H. (2009). In vivo imaging of reactive oxygen and nitrogen species in inflammation using the luminescent probe L-012. Free Radic. Biol. Med. *47*, 760-766.

Lawlor, K.E., and Vince, J.E. (2014). Ambiguities in NLRP3 inflammasome regulation: Is there a role for mitochondria? Biochim. Biophys. Acta. General Subjects *1840*, 1433-1440.

Lee, N.K., Choi, Y.G., Baik, J.Y., Han, S.Y., Jeong, D.W., Bae, Y.S., Kim, N., and Lee, S.Y. (2005). A crucial role for reactive oxygen species in RANKL-induced osteoclast differentiation. Blood *106*, 852-859.

Lipp, P., and Reither, G. (2011). Protein kinase C: the "masters" of calcium and lipid. Cold Spring Harb. Perspect. Biol. *3*.

Liston, A., and Masters, S.L. (2017). Homeostasis-altering molecular processes as mechanisms of inflammasome activation. Nat. Rev. Immunol. *17*, 208.

Lukens, J.R., Gross, J.M., Calabrese, C., Iwakura, Y., Lamkanfi, M., Vogel, P., and Kanneganti, T.D. (2014a). Critical role for inflammasome-independent IL-1beta production in osteomyelitis. Proc. Natl. Acad. Sci. U. S. A. *111*, 1066-1071.

Lukens, J.R., Gurung, P., Vogel, P., Johnson, G.R., Carter, R.A., McGoldrick, D.J., Bandi, S.R., Calabrese, C.R., Walle, L.V., Lamkanfi, M., and Kanneganti, T.-D. (2014b). Dietary modulation of the microbiome affects autoinflammatory disease. Nature *516*, 246-249.

Manthiram, K., Zhou, Q., Aksentijevich, I., and Kastner, D.L. (2017). The monogenic autoinflammatory diseases define new pathways in human innate immunity and inflammation. Nat. Immunol. *18*, 832.

Masters, S.L., Simon, A., Aksentijevich, I., and Kastner, D.L. (2009). Horror autoinflammaticus: the molecular pathophysiology of autoinflammatory disease (*). Annu. Rev. Immunol. *27*, 621-668.

Meissner, F., Molawi, K., and Zychlinsky, A. (2008). Superoxide dismutase 1 regulates caspase-1 and endotoxic shock. Nat. Immunol. *9*, 866-872.

Meissner, F., Seger, R.A., Moshous, D., Fischer, A., Reichenbach, J., and Zychlinsky, A. (2010). Inflammasome activation in NADPH oxidase defective mononuclear phagocytes from patients with chronic granulomatous disease. Blood *116*, 1570-1573.

Nakahira, K., Haspel, J.A., Rathinam, V.A., Lee, S.J., Dolinay, T., Lam, H.C., Englert, J.A., Rabinovitch, M., Cernadas, M., Kim, H.P., *et al.* (2011). Autophagy proteins regulate innate immune responses by inhibiting the release of mitochondrial DNA mediated by the NALP3 inflammasome. Nat. Immunol. *12*, 222-230.

O'Neill, L.A., and Bowie, A.G. (2007). The family of five: TIR-domain-containing adaptors in Toll-like receptor signalling. Nat. Rev. Immunol. *7*, 353-364.

Okamoto, K., Nakashima, T., Shinohara, M., Negishi-Koga, T., Komatsu, N., Terashima, A., Sawa, S., Nitta, T., and Takayanagi, H. (2017). Osteoimmunology: The Conceptual Framework Unifying the Immune and Skeletal Systems. Physiol. Rev. *97*, 1295-1349.

Omenetti, A., Carta, S., Delfino, L., Martini, A., Gattorno, M., and Rubartelli, A. (2014). Increased NLRP3-dependent interleukin 1beta secretion in patients with familial Mediterranean fever: correlation with MEFV genotype. An. Rheum. Dis. *73*, 462-469.

Park, H., Bourla, A.B., Kastner, D.L., Colbert, R.A., and Siegel, R.M. (2012). Lighting the fires within: the cell biology of autoinflammatory diseases. Nat. Rev. Immunol. *12*, 570.

Phillips, F.C., Gurung, P., and Kanneganti, T.D. (2016). Microbiota and caspase-1/caspase-8 regulate IL-1beta-mediated bone disease. Gut microbes *7*, 334-341.

Pollock, J.D., Williams, D.A., Gifford, M.A., Li, L.L., Du, X., Fisherman, J., Orkin, S.H., Doerschuk, C.M., and Dinauer, M.C. (1995). Mouse model of X-linked chronic granulomatous disease, an inherited defect in phagocyte superoxide production. Nat. Genet. *9*, 202-209.

Rubartelli, A. (2012). Redox control of NLRP3 inflammasome activation in health and disease. J. Leukoc. Biol. *92*, 951-958.

Sasaki, H., Yamamoto, H., Tominaga, K., Masuda, K., Kawai, T., Teshima-Kondo, S., Matsuno, K., Yabe-Nishimura, C., and Rokutan, K. (2009). Receptor activator of nuclear factor-kappaB ligand-induced mouse osteoclast differentiation is associated with switching between NADPH oxidase homologues. Free Radic. Biol. Med. *47*, 189-199.

Schaefer, L. (2014). Complexity of danger: the diverse nature of damage-associated molecular patterns. J. Biol. Chem. *289*, 35237-35245.

Shen, F.W., Saga, Y., Litman, G., Freeman, G., Tung, J.S., Cantor, H., and Boyse, E.A. (1985). Cloning of Ly-5 cDNA. Proc. Natl. Acad. Sci. U. S. A. *82*, 7360-7363.

Sumimoto, H. (2008). Structure, regulation and evolution of Nox-family NADPH oxidases that produce reactive oxygen species. FEBS J. *275*, 3249-3277.

Takeuchi, O., Takeda, K., Hoshino, K., Adachi, O., Ogawa, T., and Akira, S. (2000). Cellular responses to bacterial cell wall components are mediated through MyD88-dependent signaling cascades. Int. Immunol. *12*, 113-117.

Tassi, S., Carta, S., Delfino, L., Caorsi, R., Martini, A., Gattorno, M., and Rubartelli, A. (2010). Altered redox state of monocytes from cryopyrin-associated periodic syndromes causes accelerated IL-1beta secretion. Proc. Natl. Acad. Sci. U. S. A. *107*, 9789-9794.

van Bruggen, R., Koker, M.Y., Jansen, M., van Houdt, M., Roos, D., Kuijpers, T.W., and van den Berg, T.K. (2010). Human NLRP3 inflammasome activation is Nox1-4 independent. Blood *115*, 5398-5400.

van de Veerdonk, F.L., Smeekens, S.P., Joosten, L.A., Kullberg, B.J., Dinarello, C.A., van der Meer, J.W., and Netea, M.G. (2010). Reactive oxygen species-independent activation of the IL-1beta inflammasome in cells from patients with chronic granulomatous disease. Proc. Natl. Acad. Sci. U. S. A.*107*, 3030-3033.

van der Burgh, R., Nijhuis, L., Pervolaraki, K., Compeer, E.B., Jongeneel, L.H., van Gijn, M., Coffer, P.J., Murphy, M.P., Mastroberardino, P.G., Frenkel, J., and Boes, M. (2014). Defects in mitochondrial clearance predispose human monocytes to interleukin-1beta hypersecretion. J. Biol. Chem. *289*, 5000-5012.

Varga, G., Gattorno, M., Foell, D., and Rubartelli, A. (2015). Redox distress and genetic defects conspire in systemic autoinflammatory diseases. Nat. Rev. Rheumatol. *11*, 670-680.

Wang, G.G., Calvo, K.R., Pasillas, M.P., Sykes, D.B., Hacker, H., and Kamps, M.P. (2006). Quantitative production of macrophages or neutrophils ex vivo using conditional Hoxb8. Nat. Methods *3*, 287-293.

West, A.P., Shadel, G.S., and Ghosh, S. (2011). Mitochondria in innate immune responses. Nat. Rev. Immunol. *11*, 389.

Wu, Y., Dowbenko, D., and Lasky, L.A. (1998). PSTPIP 2, a second tyrosine phosphorylated, cytoskeletal-associated protein that binds a PEST-type protein-tyrosine phosphatase. J. Biol. Chem. *273*, 30487-30496.

Yang, S., Madyastha, P., Bingel, S., Ries, W., and Key, L. (2001). A new superoxide-generating oxidase in murine osteoclasts. J. Biol. Chem. *276*, 5452-5458.

Zhou, R., Yazdi, A.S., Menu, P., and Tschopp, J. (2011). A role for mitochondria in NLRP3 inflammasome activation. Nature *469*, 221-225.

Supplementary figures

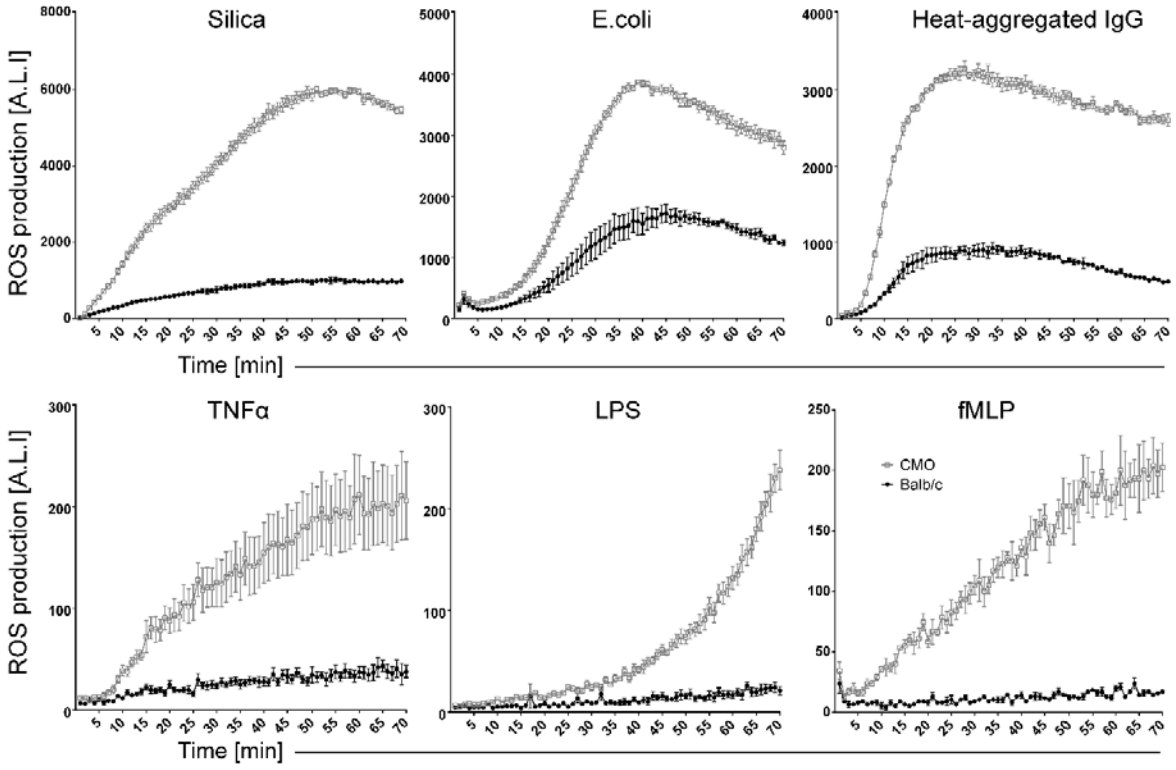

Figure S1. Related to Figure 2. Dysregulated ROS production by bone marrow cells from *Pstpip2*^{cmo} mice of Balb/c genetic background. ROS production was detected by Luminol-based assay, exactly as described in Figure 2A.

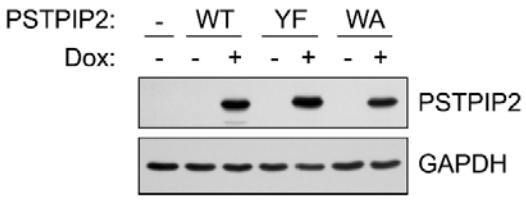

Figure S2. Related to Figure 4. Verification of the expression of inducible PSTPIP2 constructs.

Pstpip2^{cmo} neutrophils differentiated from immortalized neutrophil progenitors retrovirally transduced with inducible expression constructs coding for PSTPIP2 wild-type (WT), PSTPIP2 W232A (WA), and PSTPIP2 Y323/329/333F (YF) were treated (or not) with Doxycycline (Dox) overnight and expression of PSTPIP2 was analyzed by immunoblotting. GAPDH was used as a loading control.

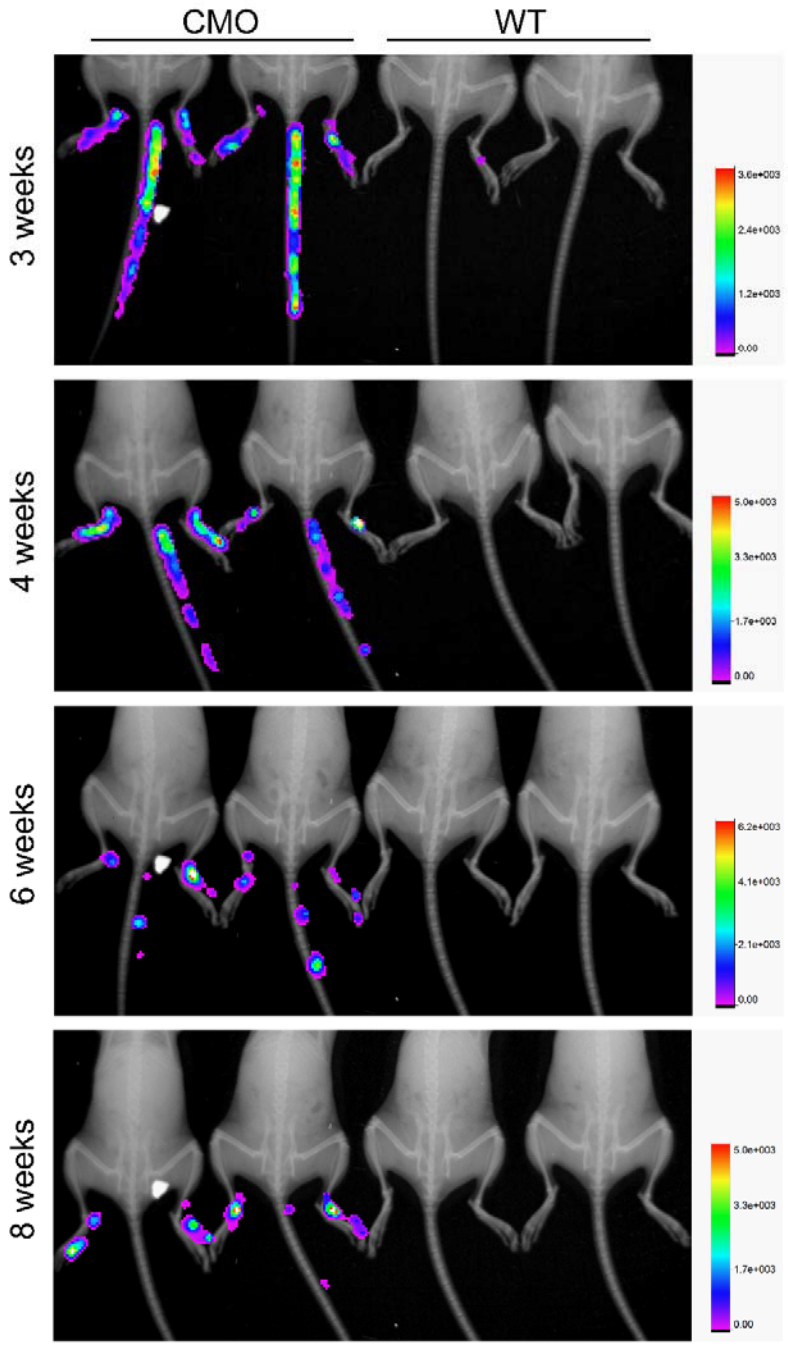

Figure S3. Related to Figure 5. In vivo ROS production in WT and *Pstpip2*^{cmo} (CMO) mice of various ages: representative images of the animals that were part of the analysis in Figure 5B.

Mice at 3, 4, 6, and 8 weeks of age were anesthetized, injected intraperitoneally with L-012 (75 mg/kg) and the ROS-dependent luminescence was measured in the whole body imager.

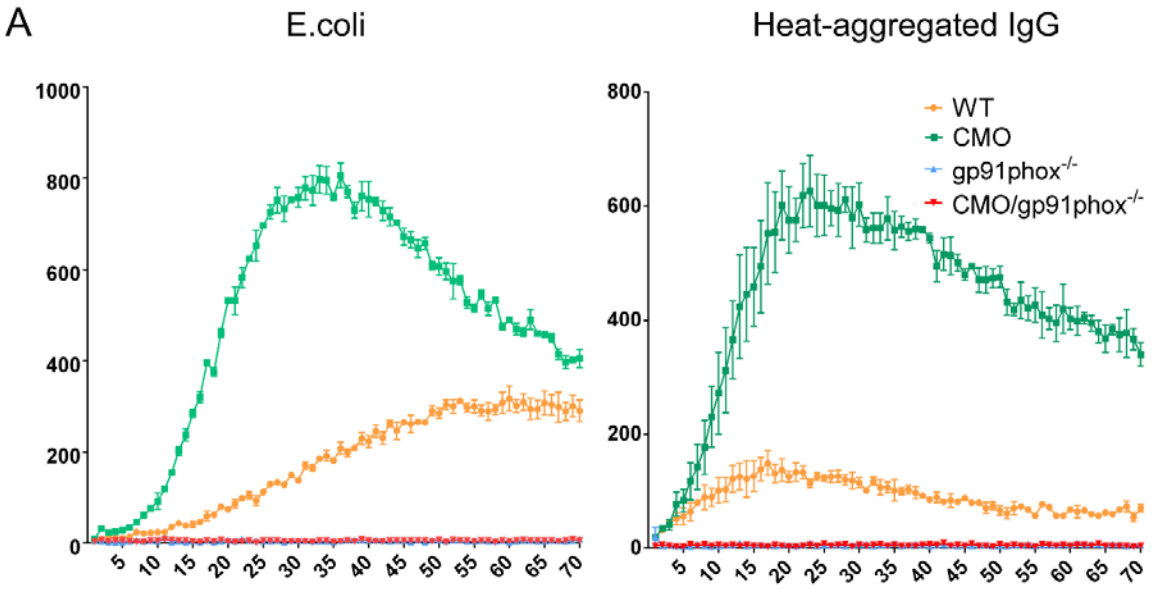

Figure S4. Related to Figure 6. Absence of ROS production in bone marrow cells from *gp91phox*$^{-/-}$ and *Pstpip2*^{cmo}*/gp91phox*$^{-/-}$ mice.

BM cells from mice of indicated genotypes were activated by live E.coli bacteria or heat-aggregated IgG in the presence of luminol and ROS-dependent luminescence was quantified in 1 min intervals.

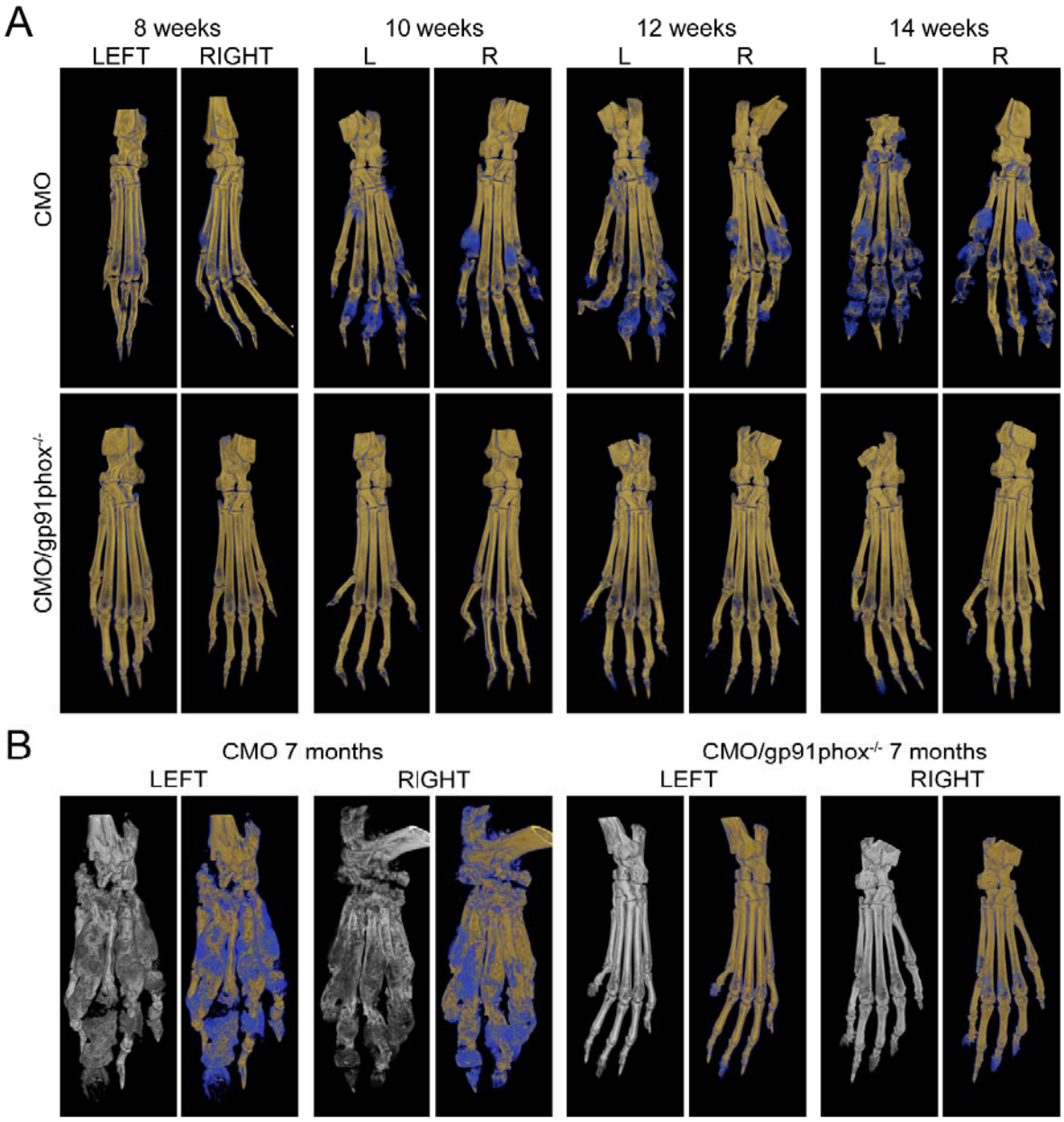

Figure S5. Related to Figure 7. Time course of bone damage development in *Pstpip2^{cmo}* and *Pstpip2^{cmo}/gp91phox$^{-/-}$* mice.

(A) Mice at 8, 10, 12, and 14 weeks of age were anesthetized and their hind paw bones were imaged on X-ray µCT scanner.

(B) The same analysis performed on 7 months old animals.

Grey images represent visualization of total bone tissue. Pseudocolor images distinguish between old (in yellow) and newly formed (in blue) bone mass.